CCSP Synthesis and Assessment Report 3.1

Climate Models: An Assessment of Strengths and Limitations for User Applications

Public Review Draft

May 15, 2007

Executive Summary

The goal of simulating the Earth's climate with mathematical models, using the most powerful computers available, is valid scientifically and fully consistent with the approaches being taken in many other fields of science dealing with very complex systems. These climate simulations provide the frame within which improved understanding of climate-relevant processes and improved observations are naturally merged into coherent projections of future climate change.

The science of climate models has matured to the point that many aspects of current climate models and simulations are very convincing. These form a growing set that intersects significantly with, but does not completely cover, the set of processes that are centrally important for the attribution of past climate changes and the projection of future climate.

The set of the most recent climate simulations, referred to as the CMIP3 models and utilized heavily in the Working Group 1 and 2 reports of the 4th IPCC Assessment, have received unprecedented scrutiny by hundreds of investigators with differing areas of expertise. While there are a number of systematic biases across the set of models, more generally the strengths and weaknesses of the simulations, when compared against the current climate, vary substantially from model to model. It is clear from many perspectives that an average over the set of models provides a superior climate simulation than any individual model, justifying the multi-model approach taken in many recent attribution and climate projection studies.

The pace of climate model improvement has been steady over the past several decades, but the improvement has understandably been uneven, because several important aspects of the climate system present especially severe challenges to the goal of simulation.

Climate models are compared to observations of the mean climate in a multitude of ways, and their ability to simulate observed climate changes, particularly those of the past century, have been examined extensively. However, it has proven difficult to measure the quality of climate models in such a way that the metric used is directly relevant to our confidence in the models' projections of

future climate. The most appropriate ways of translating the strengths and weaknesses of the simulations into confidence in climate projections remains a subject of active research.

The climate models developed in the US and around the world show many consistent features in their simulations and projections for the future. However, they have not fully converged, since different groups approach uncertain aspects of the models in distinctive ways. This absence of convergence is one useful measure of the state of the science of climate simulation; convergence is to be expected once all climate-relevant processes are simulated in a convincing physically-based manner.

.

Climate Sensitivity

The response of global mean temperature to a doubling of carbon dioxide remains a useful measure of climate sensitivity. The equilibrium response, the response expected if one waits long enough (many hundreds of years) for the system to re-equilibrate, is the most commonly quoted measure. The range of equilibrium climate sensitivity obtained from models has remained robust for three decades, and roughly consistent with estimates from the observations of recent climates and those from the more distant past. The canonical three-fold range of uncertainty, 1.5-4.5 degrees Centigrade, has evolved very slowly. The lower limit has been particularly robust over time, with very few recent models below 2 degrees. The difficulty in simulating the Earth's clouds and their response to climate change are the fundamental reason why it has proven difficult to reduce the range of uncertainty in model-generated climate sensitivity.

Other common measures of climate sensitivity are of more relevance to the response on time scales shorter than 100 years. By these measures there is considerably less spread among the models -- roughly a factor of two rather than three. Uncertainty still remains considerable and is not decreasing rapidly, due in part to the difficulty of cloud simulation but also to uncertainty in the rate

of heat uptake by the oceans which rises in importance when considering the responses on these shorter time scales.

Improvements in our confidence in estimates of the sensitivity of climate are most likely to arise from new data streams, such as satellite platforms that are now providing a first look at the 3-dimensional global distributions of clouds, and new, very computationally intensive, climate modeling strategies that explicitly resolve some of the smaller scales of motion that help control cloud cover and cloud radiative properties.

Regional modeling and downscaling

Simulations by limited-area models, stretched grid models and uniformly high-resolution atmospheric models forced by specified oceanic and sea ice conditions are all capable of resolving phenomena too fine for standard atmosphere-ocean GCMs, such as precipitation influenced by mountains and ocean-land interaction in coastal zones. These dynamical downscaling strategies are beneficial when supplied with appropriate sea-surface and atmospheric boundary conditions, but their value is limited by uncertainties in the information supplied by the global models. Given the value of multi-model ensembles for larger-scale climate prediction, it is clear that downscaling must presently be performed in a coordinated fashion with a representative set of global model simulations as input, rather than focusing on the results from one or two models. Relatively few such multi-model dynamical downscaling studies have been performed to date.

Statistical techniques to produce appropriate small-scale structures from climate simulations, referred to as “statistical downscaling”, can be as effective as high-resolution numerical simulations in providing climate change information to regions unresolved by most current global models, and because of their computational efficiency they can much more easily utilize a full suite of multi-model ensembles. However, the statistical methods are completely dependent on the accuracy of the regional circulation patterns produced by the global models, whereas regional models, through higher resolution and/or better representation of important physical processes, can often improve the

physical realism of the simulated regional circulation. Thus, the strengths and weaknesses of the regional modeling and statistical methods are often complimentary.

The quality of climate simulations

Accurate simulation of the present-day climatology for near-surface temperature and precipitation is necessary for most practical applications of climate modeling. The seasonal cycle and large-scale geographical variations of near-surface temperature are indeed well simulated in recent models, with typical correlations between models and observations of 95% or better.

AOGCM simulation of precipitation has improved over time but is still problematic. The correlation between models and observations is 50-60% for seasonal means on scales of a few hundred kilometers. Comparing simulated and observed latitude-longitude maps of precipitation reveals similarity of magnitudes and patterns in most regions of the globe with the most striking disagreements occurring in the tropics. In most models, the appearance of the Inter-tropical Convergence Zone of cloudiness and rainfall in the equatorial Pacific is distorted, and rainfall in the Amazon Basin is substantially underestimated. These errors may prove consequential for a number of model predictions, such as forest uptake of atmospheric CO2.

The simulation of the storms and jet streams in middle latitudes are considered one of the strengths of atmospheric models because the dominant scales involved are reasonably well-resolved. As a consequence, there is relatively high confidence in models' ability to simulate the changes in these extratropical storms and jet streams as the climate changes. The deficiencies that still exist may be partly due to insufficient resolution to resolve features such as fronts or to inadequacies in the simulated interactions between the tropics and midlatitudes or between the stratosphere and the troposphere. These deficiencies are still large enough to impact the ocean circulation and some regional climate simulations and projections.

A dominant mode of low-frequency variability in the atmosphere known as the northern and southern annular modes, are very well captured in current models. These modes involve north/south displacements of the extratropical storm track and dominate the observed trends in atmospheric circulation in recent decades.Because of their ability to simulate the annular modes, global climate models simulate fairly well the interannual variability in the polar regions of both hemispheres. They are less successful at simulating daily polar-weather variability, though finer scale regional simulations do simulate polar weather well, thus showing promise for improved global-model simulations as their resolution increases.

In the tropics, simulations in current models are less credible. The Madden-Julian oscillation, a feature of the tropics in which the precipitation is organized by large-scale eastward propagating features with periods of roughly 30-60 days, is a useful test of simulation credibility in the tropics. Model performance using this measure is still unsatisfactory. The “double ITCZ-cold tongue bias”, in which water is excessively cold near the equator and precipitation splits artificially into two zones straddling the equator, remains as a persistent bias in current coupled atmosphere-ocean models. Projections of tropical climate change are adversely affected by these deficiencies in simulations of the organization of tropical convection. Models typically overpredict light precipitation and underpredict heavy precipitation in both the tropics and middle latitudes, creating potential biases when studying extreme events.

Tropical cyclones are poorly resolved by the present generation of global models, but recent results with high resolution atmosphere-only models and dynamical downscaling provide optimism that the simulation of tropical cyclone climatology will advance rapidly in the coming years, as will our understanding of observed variations and trends.

Land surface modeling for climate simulation has increased markedly in sophistication over the past 25 years, with increasing detail and range of processes included in the biological, chemical and physical behavior simulated in the terrestrial portion of the climate system. Systematic programs comparing land models have gradually led to greater agreement between land models and observations, in part because a greater variety of observations have been used to understand and constrain their behavior.

Land models that predict vegetation patterns are being actively developed, but the demands that these models make on the quality of the simulated precipitation patterns ensures that the their evolution will be gradual and tied to improvements in the regional climate simulations.

The quality of ocean climate simulations has improved steadily in recent years, owing to improved numerical algorithms and more realistic assumptions concerning the mixing occurring on scales smaller than the models' grid. Many of the CMIP3 class of models are able to maintain an overturning circulation in the Atlantic with approximately the observed strength without the artificial correction to the air-sea fluxes commonly in use in previous generations of models, providing a much better foundation for analysis of the stability of this circulation.

The circulation in the Southern Oceans, thought to be of vital importance for the oceanic uptake of carbon dioxide from the atmosphere, is sensitive to deficiencies in the simulated winds and salinities, but a subset of the models are producing realistic circulation in the Southern Ocean as well

Simulations of El Nino oscillations provide a significant success story for climate models, as these have improved substantially in recent years. Most current models spontaneously generate El Nino-Southern Oscillation variability, albeit with varying degrees of realism. The spatial structure and period of the oscillations is impressive in a subset of the models, but with a tendency towards too short a period. The bias in the intertropical convergence zone in the coupled models is a major factor preventing further improvement in these models. Projections for the future of El-Nino variability and the state of the Pacific Ocean are of central importance for regional climate change projections throughout the tropics and in North America.

The quality of simulations of low frequency variability on decadal to multi-decadal time scales varies regionally and also varies substantially from model to model. On average, the models do reasonably well in the North Pacific and North Atlantic. In other oceanic regions, data paucity contributes to the uncertainty in the estimation of the quality of the simulations at these low frequencies.

The ocean components of current climate models do not directly simulate the very energetic motions in the oceans referred to as “meso-scale eddies” . The simulation of these small scale flow patterns requires horizontal grid sizes of 10km or smaller. Current oceanic components of climate models are effectively laminar rather than turbulent, and the effects of these eddies must be approximated by imperfect theories. As computer power increases, new models that resolve these eddies will be incorporated into climate models to explore their impact on decadal variability, as well as heat and carbon uptake.

Models of glacial ice are in their infancy. Glacial models directly coupled to atmosphere-ocean models typically only account for direct melting and accumulation at the surface of the ice-sheets and not the dynamic discharge due to glacial flow. More detailed current models that incorporate this discharge typically generate discharges that change only over centuries and millennia. Recent evidence for rapid variations in this glacial outflow indicates that more realistic glacial models are needed to estimate the evolution of future sea level.

Simulation of 20th century trends

Models forced by the observed well-mixed greenhouse gas concentrations, volcanic aerosols, as well as estimates of variations in the solar energy incident on the Earth and anthropogenic aerosol concentrations, are able to simulate the 20th century global mean temperature record in a plausible way. Solar variations are known by direct satellite measurements for the last few decades and do not contribute significantly to the warming during that period. Solar variations earlier in the 20th century are much less certain, but are thought to a potential contributor to the warming in the early part of the century,

Uncertainties in the climatic effects of man-made aerosols (liquid and solid particles suspended in the atmosphere) are a major stumbling block in quantitative attribution studies and in attempts to use the observational record to constrain climate sensitivity. We do not know how much warming due to greenhouse gases has been cancelled by cooling due to aerosols. Uncertainties related to clouds increase the difficulty in simulating the climatic effects of aerosols, since these aerosols are known to interact with clouds and potentially change cloud radiative properties and cloud cover.

The possibility that natural variability has been a significant contributor to the detailed time evolution seen in the global temperature record is plausible, but still difficult to address with models given the large differences between models in the characteristics of the natural decadal variability that they generate. While natural variability may very well be relevant to observed variations on the scale of 10-30 years, no models show any hint of generating large enough natural, unforced variability on the 100 year time scale that would compete with explanations of the observed century-long warming trend as being predominantly forced.

The observed southward displacement of the Southern hemisphere storm track and jet stream in recent decades is reasonably well simulated in current models, which show that it is partly due to greenhouse gases but also partly due to the presence of the ozone hole in the stratosphere. Northern Hemisphere circulation changes over the past decades have proven more difficult to capture in current models, perhaps due to the more complex interactions between the stratosphere and the troposphere in the Northern Hemisphere.

Observations of ocean heat uptake are beginning to provide a direct test of aspects of the ocean circulation directly relevant to climate change simulations. Coupled models provide reasonable simulations of the observed heat uptake in the oceans, but underestimate the observed sea level rise over the past decades.

Model simulations of trends in extreme weather typically produce global increases in extreme precipitation and severe drought, and decreases in extreme minimum temperatures and frost days, in general agreement with observations.

Regional trends in extreme events are not always captured by current models , but it is difficult to assess the significance of these discrepancies, and to distinguish between model deficiencies and natural variability.

The use of climate model results to assess economic, social, and environmental impacts is becoming more sophisticated, albeit slowly. Simple methods requiring only mean changes in temperature and

precipitation to estimate impacts remain popular, but an increasing number of studies are utilizing more detailed information, such as the entire distribution of daily or monthly values and extreme outcomes. The mismatch between the spatial resolution of models and the scale of impacts-relevant climate features and of impacts models remains an impediment for certain applications.

Chapter I – Introduction

The use of computers to simulate complex systems has grown in the past few decades to play a central role in many areas of science. Climate modeling is one of the best examples of this trend and one of the great success stories of scientific simulation. It is impossible to build a laboratory analog of the Earth's climate system with all of its complexity. The successes of climate modeling allow us to address many questions about the climate by experimenting instead with simulations —that is, with mathematical models of the climate system.

Despite the success of the climate modeling enterprise, the complexity of our Earth imposes important limitations on existing climate models. It is the purpose of this report to help the reader understand the valid uses, as well as the limitations, of current climate models.

Climate modeling and forecasting grew out of the desire to predict weather. The distinction between climate and weather is not sharp. Operational weather forecasting has historically focused on times scales of a few days but has more recently been extended to monthly and seasonal time scales, for example, in attempts to predict the evolution of El Niño episodes. The goal of climate modeling can be thought of as the extension of forecasting to longer and longer time scales, with a focus not on individual weather events, which are unpredictable on these long time scales, but on the statistics of these events as well as on the slow evolution of the oceans and ice sheets. Whether one considers the forecasting of individual El Niño episodes as weather or climate forecasting is a matter of convention. For the purpose of this report, we will consider El Nino forecasting with weather, and will not address it directly. On the climate side we are concerned, for example, with the ability of models to simulate the statistical characteristics of El Niño variability, or extratropical storms, or Atlantic hurricanes, with an eye toward assessing the ability of these models to predict how this variability might change as the climate evolves in the coming decades and centuries.

An important constraint required of climate models that is not imposed on weather forecast models is the requirement that the global system precisely and accurately maintain the global energy balance over very long time periods. Energy balance (or "budget") is defined as the difference between absorbed solar energy and emitted infrared radiation. It is affected by a number of things including human production of greenhouse gases like carbon dioxide. The decadal to century-scale

changes in the Earth's energy budget that are manifested as climate change are just a few per cent of the average values of the largest terms in that budget. Many of the decisions about model construction described in Chapter II are based on the need to properly and accurately simulate the long term energy balance.

This report will focus primarily on the most advanced physical climate models that were used for the most recent international Coupled Model Intercomparison Project's (CMIP) coordinated experiments (Meehl, *et al*., 2006), sponsored by the World Climate Research Programme (WCRP). These coupled Atmosphere–Ocean General Circulation Models (AOGCMs) incorporate detailed representations of the atmosphere, land surface, oceans, and sea ice. Where practical, we will emphasize and highlight the results from the three US modeling projects that participated in the CMIP experiments. Additionally, this report examines the use of Regional Climate Models used for obtaining higher resolution details from AOGCM simulations over smaller regions. Nevertheless, it must be noted that there are other types of climate models being developed and applied to climate simulation. More complete Earth systems models build carbon cycle and ecosystems processes on top of the AOGCMs, but are employed more for studies of future climate change and paleoclimatology, neither of which is directly relevant to this report. Another class of models not discussed here, but used extensively, particularly when computer resources are limited, are Earth-system Models of Intermediate Complexity (EMICs). Although these models have many more assumptions and simplifications than are found in the CMIP models (Claussen *et a*l., 2002), they are particularly useful in exploring a wide range of mechanisms and obtaining broad estimates of future climate change projections that can be further refined with AOGCM experiments.

Brief History of Climate Model Development

As the possibility of numerical weather prediction developed in the 1950's as one of the first applications of computers, it became evident almost immediately that the numerical simulation approach could also be used to study the climate. In 1955, Joseph Smagorinsky started a program in climate modeling that ultimately became one of the most vigorous and longest-lived General Circulation Model (GCM) development programs at NOAA's Geophysical Fluid Dynamics Laboratory (GFDL) at Princeton University. The feasibility of generating stable integrations of the

atmospheric equations for arbitrarily long time periods was demonstrated by Norman Phillips in 1956. The University of California at Los Angeles began producing Atmospheric General Circulation Models (AGCMs) beginning in 1961 under the leadership of Yale Mintz and Akio Arakawa. This program influenced others in the 1960's and 1970's, leading to modeling programs found today at NASA laboratories and several universities. At Lawrence Livermore National Laboratory, Cecil E. Leith developed an AGCM in the early and mid-1960's. The U.S. National Center for Atmospheric Research (NCAR) initiated AGCM development in 1964 under Akira Kasahara and Warren Washington, an effort that ultimately evolved into the construction of the Community Climate Model, a predecessor to the present Community Climate System Model. Also in the 1960's and 70's, efforts in climate simulations developed throughout the world, with major centers emerging in Europe and Asia.

Additions to the original atmospheric general circulation models used for weather analysis and prediction were needed to improve weather simulations and forecasts as well as to make climate simulations possible. The early weather models focused on fluid dynamics rather than on radiative transfer and the atmosphere's energy budget, which are of central importance for climate simulations. Furthermore, as one focuses on time scales longer than a season, the oceans and sea ice must be coupled to the more rapidly evolving atmosphere. Thus, ocean and ice models have been coupled with atmospheric models. The first ocean general circulation models were developed at GFDL by Bryan and Cox in the 1960's, and then coupled with the atmosphere by Manabe and Bryan in the 1970's.

Climate models began to be used in research on carbon dioxide and climate in the mid-1970's. Two important studies, the *Study of Critical Environmental Problems* and the *Study of Man's Impact on Climate*, both endorsed the use of GCM-based climate models to study the possibility of anthropogenic climate change. Beginning in the late 1980's, several national and international organizations were formed with the purpose of assessing and expanding scientific research related to global climate change. These developments spurred interest in developing and improving climate models. The work of the Intergovernmental Panel on Climate Change (IPCC), beginning in 1987, had as a primary focus of Working Group 1 scientific inquiry into atmospheric processes governing climate change. The **IPCC**,1990: *Scientific Assessment* (Houghton *et al*., 1990) stated, "Improved

prediction of climate change depends on the development of climate models, which is the objective of the climate modeling programme of the World Climate Research Programme (WCRP)." The United States Global Change Research Program (USGCRP), established in 1989, designated Climate Modeling and Prediction as one of the four high-priority integrating themes of the program (CEES, 1991). The combination of steadily increasing computer power and research spurred by the WCRP and USGCRP has led to a steady improvement in the completeness, accuracy and resolution of AOGCMS used for climate simulation and prediction. A classic figure from the Third IPCC Working Group I Scientific Assessment of Climate Change in 2001 depicts this evolution in **Figure I.A.** The comprehensive climate models that contributed results to the Third Climate Model Intercomparison Project (CMIP3) that was utilized by the Fourth IPCC Assessment were generated by 3 groups in the US (GFDL, NCAR, and the NASA Goddard Institute for Space Studies (GISS)), and groups in the U.K., Germany, France, Japan, Australia, Canada, Russia, China, Korea, and Norway.

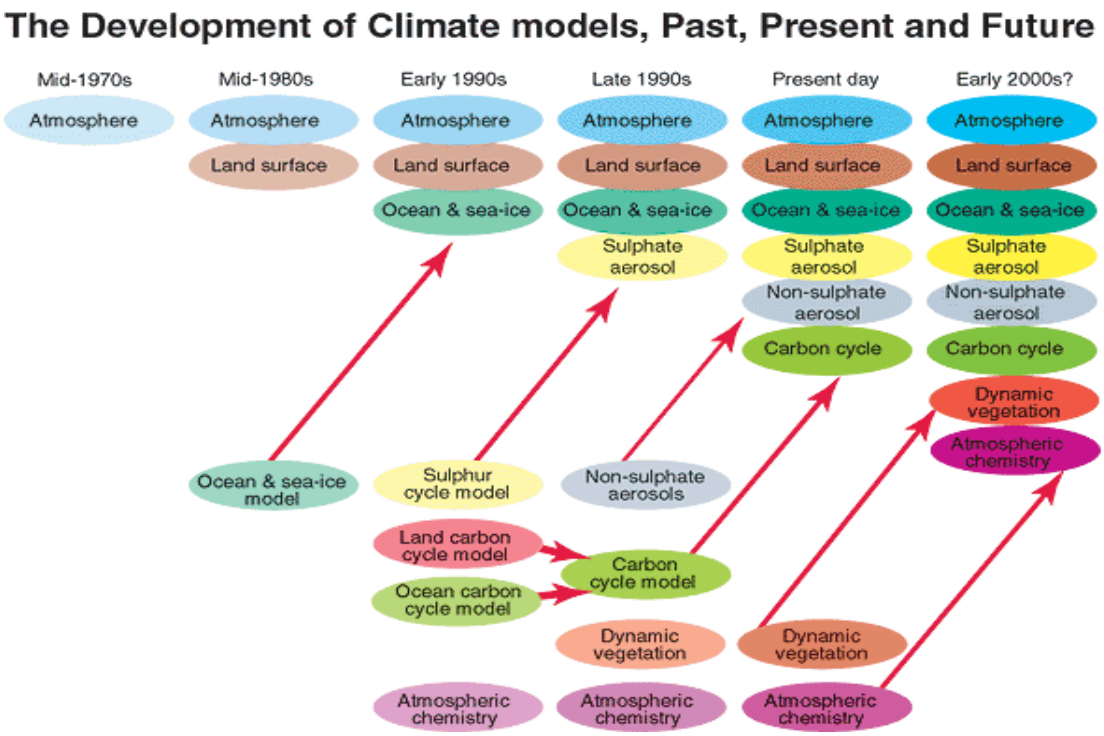

Source: IPCC 2001

Figure.I.A Historical development of climate models (From IPCC, 2001).

Climate model construction

Comprehensive climate models are constructed using expert judgments to satisfy many constraints and requirements. The overarching considerations are the determination of the most important climate features that should be accurately simulated and the scientific understanding of these features that guide one towards the most powerful simulation strategies and algorithms. Typically, the basic requirement is that models should simulate features that are important to humans, particularly surface variables, such as temperature, precipitation, windiness, and storminess. This is a less straightforward requirement than it seems, since a physically-based climate model must also simulate all of the complex interactions in the coupled atmosphere–ocean–land surface–ice system that are manifested as the climate variables of interest. For example, jet streams at altitudes of 10 kilometers above the surface must be accurately simulated if the models are to generate midlatitude weather with realistic characteristics, since the midlatitude highs and lows that we see on surface

weather maps are intimately associated with these high-altitude wind patterns. As another example, one cannot simulate the basic temperature decrease from the equator to the poles without taking into account the poleward transport of heat in the oceans, some of this heat being carried by currents 2 or 3 kms deep in the oceanic interior. Our models should correctly produce not just the means of variables of interest, but also extremes and other measures of natural variability. Finally, they should be capable of simulating the changes in those statistics that result from the relatively small changes in the Earth's energy budget that result from natural and human actions.

Climate processes operate on time scales ranging from several hours to millennia, and spatial scales ranging from a few centimeters to thousands of kilometers. Principles of scale analysis, fluid dynamical filtering, and numerical analysis are used to make intelligent compromises and approximations to simplify the system sufficiently to make it tractable to formulate mathematical representations of the processes and their interactions. These mathematical models are then translated into computer codes, which are executed on some of the most powerful computers in the world. Available computer power helps determine the types of approximations required; as a general rule, increasing computational resources allows modelers to formulate algorithms that are less dependent on relatively uncertain methods (referred to as "closure" or "parameterization" schemes) for taking into account unresolved motions and processes, thereby producing simulations that are more solidly founded on established physical principles. Climate simulations must always be designed so that they can be completed and analyzed by scientists in a timely manner.

Climate models have shown steady improvement over time as computer power has increased, as our understanding of physical processes of climatic relevance has increased, as data sets useful for model evaluation have been developed, and as our computational algorithms have improved. **Figure I.B** shows one attempt at quantifying this improvement. It compares a particular metric of climate model performance among the CMIP1 (1995), CMIP2 (1997) and CMIP3 (2004) ensembles of AOGCMs. This particular metric assesses the performance of the models in simulating the mean climate of the late 20th century as measured by a basket of indicators, focusing on aspects of the atmospheric climate for which observational counterparts are deemed adequate for this purpose. The ranking of models according to individual members of this basket of indicators varies greatly, so this aggregate ranking is dependent on how one weights the relative importance of different

indicators. But the general conclusion of an improvement in climate simulation quality is robust to these changes in weighting factors. The construction of metrics for evaluating climate models is itself a subject of intensive research and will be covered in more detail in Chapter II.

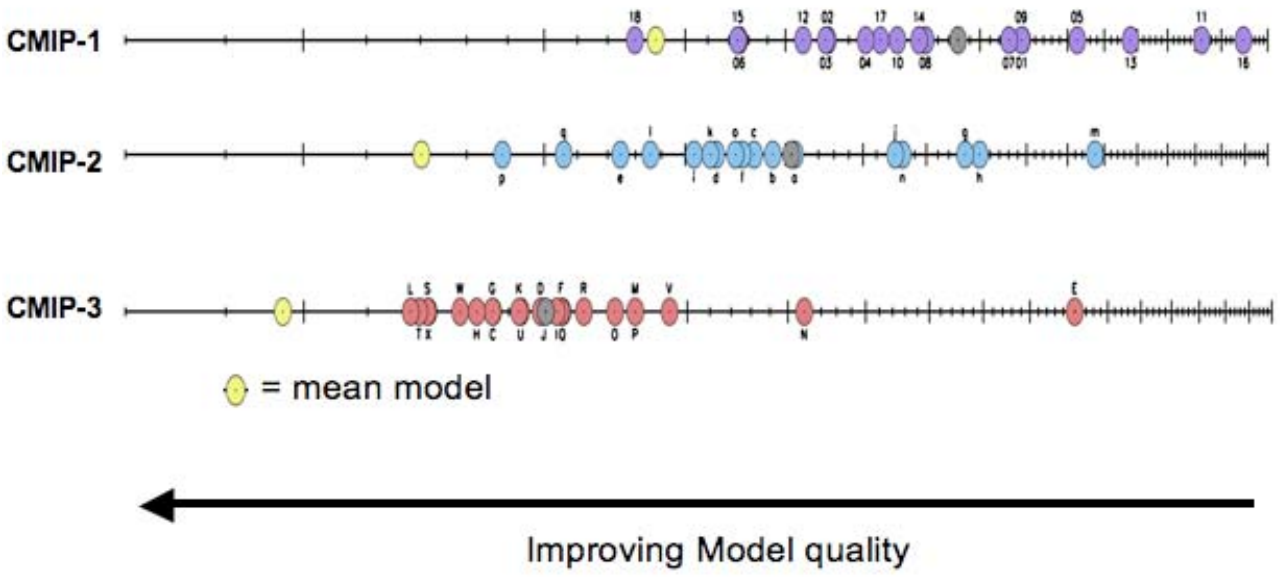

Figure.I.B One possible composite metric for the evaluation of climate models, focusing primarily on the atmospheric circulation (Kim and Riechler, 2007,, baased on PCMDI CMIP-1, CMIP-2, and CMIP-3 archives Each oval corresponds to a single model, with model quality improving towards the left. Yellow ovals mark the quality of the climate obtained by averaging all of the available models. The CMIP-1 model archive was generated from models available around1995, the CMIP-2 models around 2000, and the CMIP-3 models around 2005.

Also, shown in **Figure I.B** is the same metric evaluated from the climate obtained by averaging over all of the AOGCMs in the CMIP1, CMIP2, and CMIP3 archives. The CMIP3 "ensemble-mean" model performs better than any individual model by this metric, and by many others. This kind of result has convinced the community of the value, at this point in time, of a multi-model approach to climate change projection, in which a number of modeling centers work on their own distinctive approaches to the fundamental fluid dynamical simulation problem as well as the many issues related to the parameterization of unresolved processes. Our understanding of climate is still insufficient to justify the construction or identification of a single model that we can confidently judge to be the best possible model. It is generally felt to be more appropriate, in any assessments focusing on adaptation or mitigation strategies, to take into account, in an appropriately informed manner, the attempts at climate simulation underway around the world.

The remaining sections of this report describe climate model development, evaluation and applications in more detail. Chapter II describe the development and construction of models and how they are employed for climate research. Chapter III discusses Regional Climate Models and their use in "downscaling" global model results to specific geographic regions, particularly North America. The concept of climate sensitivity, which is the response of a surface temperature to a specified change in the energy budget at the top of the model's atmosphere, is described in Chapter IV. A survey of how well important climate features are simulated by modern models is found in Chapter V, while Chapter VI depicts the near-term development priorities for future model development. Finally, Chapter VII illustrates a few examples of how climate model simulations are used for practical applications. A detailed References section follows Chapter VII.

Chapter II - Description of Global Climate System Models

Modern climate models are comprised of a system of model components, each of which simulates a different part of the climate system, and usually can be run independently for certain applications. Nearly all of the CMIP3 class of models are composed of four primary components, the atmosphere, land surface, the ocean and sea ice. The atmospheric and ocean components are known as “general circulation models” or GCMs, because they explicitly simulate the large scale global circulation of the atmodphere and ocean. Sometimes, climate models are referred to as coupled atmosphere-ocean GCMs, which may be misleading, because a coupled GCM model can be employed to simulate aspects of weather and ocean dynamics, without being a climate model. What follows in this chapter is a description of the major components of a modern climate model, and how they are coupled together and tested for climate simulation.

Atmospheric General Circulation Models

Atmospheric general circulation models (AGCMs) are numerical programs that calculate the state variables of the atmosphere, such as temperature, pressure, humidity, kinetic energy, etc, as a function of space and time. . The set of model equations is formulated by using geophysical fluid dynamics theory and physical laws governing the exchanges of the mass and energy. because of the various assumptions and approximations that are made to more complete equations of classical fluid dynamics. The atmosphere can be thought of as a thin spherical shell of air that envelopes the earth. For climate simulation, typically only the lowest 20-30 km or so of the atmosphere, the troposphere and part of the stratosphere, are explicitly simulated. Within this volume all weather occurs because it contains over 95 % of the mass and virtually all of the water vapor. Because of disparity between the scales of the horizontal and vertical motions resolved in tyrpical global models, the horizontal motions are treated differently than vertical motions.by the model algorithms. The resulting basic set of equations is often referred to collectively as the primitive equations (Haltiner and Williams, 1980),

Although nearly all AGCMs use the same primitive dynamical equations, they use different numerical algorithms to solve.them. In all cases, the atmosphere is divided into discrete vertical layers, which are then overlaid with a two dimensional horizontal grid, producing a three dimensional mesh of grid elements. The set of primitive equations is then solved as a function of space and time on this mesh. The portion of the model code governing the fluid dynamics explicitly simulated on this mesh is often referred to as the model's "dynamics." Computational solutions of the model dynamics can be grouped into four categories: spectral methods, finite difference methods, semi-Lagrangian methods, (Washington and Parkinson, 2005) and finite volume methods (Lin and Rood, 1996). The majority of the climate models use the first two approaches, Even with the same numerical approach, AGCMs differ in spatial resolutions and configuration of model grids. Some models have few layers above the troposphere (the moving boundary between the troposphere and stratosphere), while others could have as many layers above the troposphere as in it. AGCMs all use transformed equations to treat the Earth's surface as a constant coordinate surface so that the specification of heat, moistrure, trace substances and momentum exchanges between the earth's surface and the atmosphere can be simplified. Numerical algorithms of AGCMs should preserve the basic conservation of mass and energy of the atmosphere. Typical AGCMs have spatial resolution of 200 kilometers in the horizontal and 20 levels below the altitude of 15 km. Because numerical errors often depend on flow patterns, there are no simple ways to assess the accuracy of numerical discretization of AGCMs. Therefore, AGCMs are tested using a series of both idealized and realistic test cases (e.g. Held and Suarez ,1994) before being included in a climate model. Table 1 lists the specifications of numerical approaches and resolutions of some AGCMs.

All GCMs use parameterizations, or approximate sub-models, to simulate many processes that are too small, or operate on time scales too fast, to be resolved on the grid of the model dynamics. Some of the most important parameterizations are those that calculate radiant energy (or "radiative") transfer, cloud formation and dissipation, the vertical motions on small scales caused by thunderstorm clouds (cumulus convection), and turbulence and subgrid scale mixing. The radiative transfer code computes the absorption and emission of electrcomagnetic waves by air molecules and atmospheric particles. Most atmospheric gases absorb and emit radiation at discrete wavelengths, but the computational costs are too high to perform this calculation at individual wavelengths.

AGCMs use approximations, which differ among models, to group bands of wavelengths together in a single calculation. Most models have separate radiation codes to treat solar or visible, radiation differently from the much longer wavelength terrestrial, or infrared, radiation. The radiation calculation includes the effects of water vapor, carbon dioxide, ozone, and clouds. Many models also include aerosols and trace gases such as methane. Validation of the AGCM radiation codes is often done offline against resolved wavelength model calculations which, in turn, are compared against laboratory and field observations

For cloud calculations, AGCMs treat ice and liquid water as part of the atmospheric state variables. Some models also separate cloud particles into ice crystals, snow, graupel, cloud water, and rainwater. Empirical relationships are used to calculate conversions between different particle types. The representation of these processes on the scale of model grids is particularly difficult. It relies heavily on empirical formulations because of the lack of sub-grid scale information. This includes the calculation of cloud amount, which greatly affects radiative transfer and model sensitivity. Current models use one of the following two methods to calculate cloud amount: statistical distribution of thermodynamic and hydrological variables within a grid box, or prognostic cloud amount calculation. The statistical method may use simple model diagnostics, such as relative humidity, or more sophisticated calculations with higher order of moments of moisture contents. A sample of cloud schemes used in AGCMs is listed in Table II 1. None of the current AGCMs calculates size-resolved cloud particles nor do they treat the effects of and non-spherical ice particles.

Cumulus convective transports, which are important in the atmosphere but cannot be explicitly resolved at GCM scale, are calculated using convective parameterization algorithms. Most current models utilze a cumulus mass flux scheme patterned after that proposed by Arakawa and Schubert (1974), in which the upward motion is the convection is envisioned as occurring in very narrow plumes that takes up a negligible fraction of the area of a grid box. Schemes differ in the techniques used to determined the amount of mass flowing through these plumes, and the manner in which air is entrained and detrained by the plume as it rises. Most models do not separately calculate the area and vertical velocity of convection, but try to predict only the product of the mass and the area, or the covnective mass flux. Most current schemes do not account for the differences of convection

between organized mesoscale systems and simple plumes. The turbulent mixing rate of updrafts and downdrafts with the environments, and the phase changes of water vapor within the convective systems with a mix of empiricism and constraints due to the moist thermodynamics of rising air parcels.. Some models also include a separate calculation of shallow, non-preciiptiating convection (or “fair-weather cumulus cloud) with different assumptions from those for deep convections. . Cloud genrated by cumulus convection should therefore be thought as based in large-part on empirical relationships. Convection schemes used in AGCMs are listed in Table II 1.

All AGCMs compute turbulent transport of momentum, moisture, and energy in the atmospheric boundary layer (ABL) near the surface. A long-standing theoretical framework, “Monin-Obukhov Similarity theory” is used to calculate the vertical distribution of turbulent fluxes and state variables in a thin air layer of tens of meters adjacent to the surface. Above that, turbulent fluxes are calculated based on covariances and closure assumptions for the ABL which differ among AGCMs. Some models use high order closures in which the fluxes or second order moments are prognostically calculated. Other models calculate the fluxes diagnostically. Turbulent ABL fluxes heavily depend on surface conditions such as roughness, soil moisture, and vegetation. Besides explicit calculation of boundary layer turbulence, all models use additional diffusion schemes to either calculate the impact of “clear air turbulence”, or to damp artificial numerical modes introduced in the discretization of the model. Table II.A lists turbulent schemes in AGCMs.

Table II. 1. Physical parameterization schemes in a sample of AGCMs.

	Resolution	Convection	ABL	Stratiform Clouds	Convective Clouds	Cloud Microphysics
CAM3	T85L26 (1.4^ox1.4^o) Spectral	Mass Flux [Hack 1994; Zhang and McFarlane, 1995]	1st order non-local [Holtslag and Boville, 1993]	Diagnostic (RH based) [Kiehl *et al*., 1996]	Diagnostic [Rasch and Kristjansson, 1998]	Rasch and Kristjánsson [1998]
GFDL	2.5^ox2.0^oL24 Finite Difference	Mass flux (RAS) [Moorthi and Suarez, 1992]	Cloud entrainments [Lock *et al*., 2000; GFDL GAMDT, 2004]	Prognostic [Tiedtke, 1993; GFDL GAMDT, 2004]	Prognostic [Tiedtke, 1993; GFDL GAMDT, 2004]	Rotstayn [1997], GFDL GAMDT [2004]
GISS	4^ox5^o L12 Finite Difference	Mass flux [Del Genio and Yao, 1993]	2nd order [Cheng *et al*., 2002]	Diagnostic (RH based) [Del Genio et al., 2004]	Diagnostic [Del Genio *et al*., 2004]	Del Genio *et al*. [2004]
GSFC	2.5^ox2^o L40 Finite Volume	Mass flux (RAS) [Moorthi and Suarez, 1992]	2.5 order [Helfand and Labraga, 1988]	Diagnostic (RH based) [Del Genio *et al*., 2004]	Diagnostic [Del Genio *et al*., 1996]	Del Genio et al. [1996], Sud and Walker [1999]
HadAM4	3.75^ox2.5^oL30 Finite Difference	Mass flux [Gregory and Rowntree, 1990; Gregory and Allen, 1991]	1st order with cloud entrainment [Lock *et al*., 2000; Martin et al., 2000]	Diagnostic statistical [Smith, 1990; Pope et al.].	Diagnostic [Gregory and Rowntree, 1990]	Wilson and Ballard [1999]
ECHAM5	T63L31 (1.9^ox1.9^o) Spectral	Mass flux [Tiedtke, 1989; Nordeng, 1994]	1st order, [Brinkop and Roeckner, 1995]	Prognostic statistical [Tompkins, 2002],	Diagnostic [Roeckner *et al*., 1996]	Lohmann and Roeckner [1996]
LMD	3.75^ox2.5^oL19	Emanuel	1st order [Li,	Statistical	Statistical	Le Treut and Li

	Finite Difference	[1991]	1999]	[Le Treut and Li, 1991]	[Bony and Emanuel, 2001]	[1991]

1

Ocean General Circulation Models

General overview: The ocean (Ocean General Circulation Models: OGCM) component of the current generation of climate models can be placed into one of two general categories. All the models are fully four dimensional primitive equation models and are coupled to the atmosphere and ice models through the exchange of fluxes of heat, temperature, and momentum at the boundary between components.. TableII 2 gives a brief summary of the major differences between the models described in the next paragraphs. Like the atmosphere, the horizontal dimensions of the ocean are much larger than the vertical dimension, again resulting in separating the processes that occur in the vertical from those that occur in the horizontal. Unlike the atmosphere, which only has to deal with terrain differences at the lower boundary, the ocean has a much more complex, three-dimensional boundary, with continents and submarine basins and ridges. Further, the fluid behavior of sea water is very different than that of air, resulting in a slightly different set of equations controlling ocean fluid dynamics.

The models utilized by the three US climate modeling groups that contributed models to the CMIP3 archive are used here to illustrate some of the choices made by ocean modelers.

An important category of OGCMs are referred to as Z-level models in which the model's vertical levels are calculated at fixed distances below the surface. (Many of these models are based on the early efforts of Bryan and Cox (1967) and Bryan (1969a, b). The GFDL and CCSM ocean components fall into this category (Griffies *et al*., 2005, Smith and Gent, 2002The models are similar in that the fundamental physical quantities advancing in time are the same. These quantities are velocity, potential temperature, salinity, sea surface height, and any number of specific passive tracers that maybe included for a given simulation. The two modeling efforts use similar horizontal resolution at about the same order: 1 degree or 110 km for most of the Earth and about 1/3 of a degree at the equator. Usually the models have increasing resolution between 5°N and 5°S to increase their ability to simulate important equatorial processes.

The vertical and horizontal structure of the models can also differ and are listed in TableII 2. The CCSM OGCM's horizontal grid has its north pole displaced onto a land coordinate (a so-called stretched grid) and the GFDL models use a grid that has three poles (Murray, 1996). There is an explicit treatment of the bottom boundary and overflow regions in the GFDL models (Beckman and Doscher, 1997) to improve the down-slope flow of water. Such treatment of the overflows should improve the representation of deep ocean waters (Roberts and Wood, 1997), but problems remain (Griffies *et al*., 2005).

The second category of OGCMs includes those developed by GISS. There are two different ocean models that are used in the GISS simulations: the "Russell Ocean" (GISS-ModelE-R and GISS-AOM: Russell *et al*., 1995, Russell *et al*., 2000) and the "HYCOM Ocean" (GISS-ModelE-H: Sun and Bleck, 2001; Bleck 2002; Sun and Hansen, 2003; **Hy**brid **C**oordinate **O**cean **M**odel). The fundamental (prognostic) variables for the E-R and AOM simulations are potential enthalpy (rather than potential temperature), salt, mass, vertical gradients of potential enthalpy and salt, in addition to velocity. At this time, these models are run at a resolution much lower than the models of the first category (see Table 2 The vertical coordinate is defined in units of mass/unit area (while in category 1, the unit is meters).

The HYCOM OGCM (GISS-EH) fundamental variables include temperature, salinity, layer thickness, and velocity,. The horizontal grid is different from the others described. It is two grids, with one a Mercator grid to 60°N with a resolution of 2°and it is patched (i.e. boundary values exchanged at each time step) to a North Pole grid defined as 1° at 60°N to 0.5° at the North Pole. The vertical grid is a complex or "hybrid" with a z-level grid (units meters) to represent the mixed upper ocean and layers below represented as density layers (Bleck, 2002).

The analyses of the simulations, in most cases, are performed on the model fields that are interpolated to a common grid. This interpolation may introduce small inaccuracies (AchutaRao *et al.*, 2006) in the results of analyses of a model, but is not considered significant. For example, no more than 3% of heat content change can be associated with regridding errors at the end of a simulation.

1 Table II 2 Ocean CGM Characteristics

Model	Resolution Long x Lat L = Levels	Diabatic Mixing	Adiabatic Mixing	Primary Variables	Other Comments
CCSM3 POP	320x395 L40	KPP	GM	Velocity, T, S, SSH, ideal age	z-level vertical coordinate
GFDL: CM2: OM3	360x200 L50	KPP	GM	Velocity, T, S, SSH, ideal age	z-level vertical coordinate
GISS: AOM	90x60 L16	KPP	none	Potential Enthalpy, velocity, salt, mass	z*vertical coordinate
GISS: ER	72x46 L16	KPP	GM	See AOM	See AOM
GISS EH:	180x90	Kraus-Turner	No special treatment	T, S, SSH, mass flux, velocity	Isopycnal Vertical coordinate

2

Parameterization

Ocean Mixing: At the interface of the atmosphere and the ocean, the sea surface temperature plays a critical role in the climate problem. Processes that control mixing in the ocean are complicated and take place on small scales (order of centimeters) in the turbulent regime near the surface (the mixed layer). Within the stratified, adiabatic interior of the ocean, mixing is influenced by the exchange of water on scales on the order of meters to kilometers (**Figure II.A**). The current ocean components of climate models are at resolutions that are greater than either of these scales. The mixing of the ocean contributes to the ocean's stratification and heat uptake. This stratification, in turn, affects the circulation patterns on temporal scales of decades and longer. It is also generally felt (Schopf *et al.*, 2003) that the mixing schemes in the ocean modeling components contribute significantly to the uncertainty in the estimates of the ocean's contribution to the predictions of climate change.

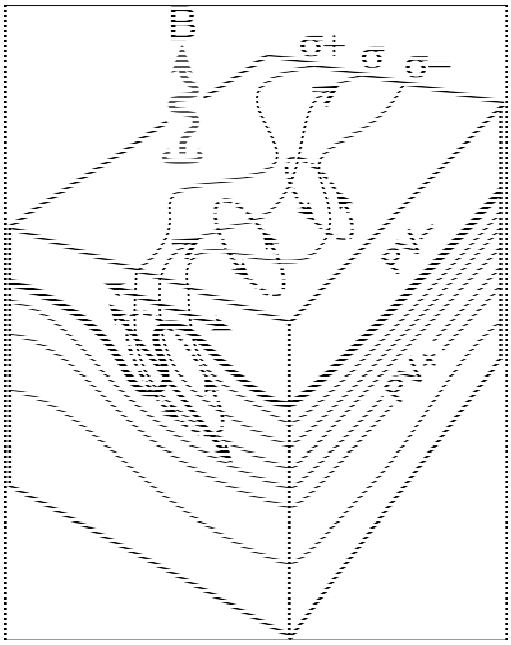

Figure II.A. Schematic showing the interaction of a mixed layer (low Potential Vorticity: PV) with the stratified interior (high PV) in a strong frontal region with outcropping isopycnal surfaces, , undergoing cooling, “B” indicates where eddies forming along the front play a central role in controlling horizontal fluxes through the mixed layer and quasi-adiabatic exchange between the mixed layer and the interior. This process is poorly observed, understood and modeled and must be parameterized in large-scale models. (from *Coupling Process and Model Studies of Ocean Mixing to Improve Climate Models - A Pilot Climate Process Modeling and Science Team*, a US CLIVAR white paper by Schopf, Gregg, Ferrari, *et al*., (2003).

For turbulent mixing of the upper ocean at the boundary with the atmosphere, the current generation of climate models (resolutions on the order of degrees) parameterizes the processes primarily through the use of several different approaches. Large *et al*., (1994) also provides a more complete comparison of these mixing schemes. While not all international AOGCMs use the K-profile Parameterization (KPP; Large *et al*., 1994) scheme, most of the major US climate models incorporate a version of the scheme. Li *et al*., (2001) showed that in the tropical Pacific, the use of the KPP scheme for handling the mixed layer of the upper ocean reduced the error in the simulation as compared to observations over a simulation that used a more simplified method (Pacanowski and Philander, 1981).

The adiabatic mixing, related to the interactions of eddy motions, generally is handled through the incorporation of the methods of Gent and McWilliams (GM) (1990) and Griffies (1998). Eddies will generally mix the ocean on constant density surface. The GM method incorporates various separate parameters that include the scale of the process to be considered and a parameter related to the ability of a parcel to move up and down. For any model the parameters are set so that coefficient related to diffusivity is high in the boundary currents and low in the interior of the ocean (Griffies *et al*., 2006). The ocean's flow is effected by the eddies, leading to adjustments in how much heat is moved through the oceans, and thus impacts the climate characteristics of the ocean.

To accurately represent ocean mixing at scales important to climate, other processes may need to be represented explicitly or parameterized in the model. These include incorporation of tidal mixing and more accurate representation of interactions with the ocean's bottom. Some of the models also include a scheme for handling tidal mixing (Lee *et al*., 2005). The limited study of *Lee et al.* (2005) shows that the tidal mixing enhanced the ventilation of the surface waters and increased the formation of deep water in the Labrador Sea by homogenizing the salinity distribution but did not have a major effect on the overturning circulation. It is still an open discussion on the importance of tidal mixing in ocean in relationship other larger scale changes occurring in the ocean related to climate. A few OGCMs also explicitly treat the bottom boundary and sill overflows (Beckman and Dosher, 1997).

***Other parameterizations*:** Another aspect of the model that is available to climate modelers when running the simulations is the explicit treatment for handling the penetration of sunlight (and thus, affecting chlorophyll distributions) into the upper ocean (e.g.. Paulson and Simpson, 1977: Morel and Antoine, 1994: Ohlmann, 2003). All of the US models include such capability. The inclusion of river input (which, in turn, effects ocean mixing locally) in OGCMs is also handled by the models in a variety of ways. The models' low resolution results in the smaller seas of the Earth being isolated from the large ocean basins. This requires that there be a method to exchange water between an isolated sea and the ocean to simulate what in nature involves a channel or strait. The various modeling groups have chosen different methods to handle the mixing of the water between these seas and the larger ocean basins, and is one potential source of model differences in climate simulations.

Evaluation of OGCMs: Like the atmosphere, ocean components of climate models are separately evaluated, in addition to the evaluation of coupled ocean-atmosphere GCMs discussed in Chapter V below. Ocean model evaluation requires specification (as input to the computer models) of boundary conditions at the air-sea interface. Typically, these are specified to match observations of the recent decades, and the OGCM simulation is then evaluated by comparison with observations of the ocean from the same time period. OGCM experiments with specified sea surface boundary conditions are at present less robost and generally exhibit more uncertainty in model performance than similar experiments for the atmosphere.

Land Surface Models

The interaction of the Earth's surface with the atmosphere is an integral aspect of the climate system. At the interface, there are exchanges (fluxes) of mass and energy, notably heat, water vapor, and momentum. Feedbacks between the atmosphere and the surface affecting these fluxes have important effects on the climate system (Seneviratne *et al*., 2006). Modeling the processes over land is particularly challenging because the land surface is very heterogeneous and biological mechanisms in plants are important. Climate model simulations are very sensitive to the choice of land parameterizations (Irannejad *et al*., 2003).

In the earliest global climate models, the land surface modeling occurred in large measure to provide a lower boundary to the atmosphere that was consistent with energy, momentum and moisture balances (e.g., Manabe 1969). The land surface was represented by a balance among incoming and outgoing energy fluxes and a "bucket" that received precipitation from the atmosphere and evaporated moisture into the atmosphere, with a portion of the bucket's water draining away from the model as a type of runoff. The bucket's depth equaled soil field capacity. There was little attention given to the detailed set of biological, chemical and physical processes linked together in the terrestrial portion of the climate system. From this simple starting point, land surface modeling for climate simulation has increased markedly in sophistication, with increasing realism and inclusiveness of terrestrial surface and subsurface processes.

Although these developments have increased the physical basis of land modeling, the greater complexity has at times contributed to greater differences between climate models (Gates *et al*., 1995). However, the advent of systematic programs comparing land models, such as the Project for Intercomparison of Land Surface Parameterization Schemes (PILPS; Henderson-Sellers *et al*., 1995; Henderson-Sellers, 2006) has gradually led to greater agreement with observations and among land models (Overgaard *et al*. 2006), in part because more observations have been used to constrain their behavior. However, choices for adding processes and increasing realism have varied between land-surface models (e.g., Randall et al. 2007), so convergence of simulations by current models should not be expected. This section reviews the range of developments that have led to contemporary simulation of land processes in climate models.

Figure II. B shows schematically the types of physical processes included in typical land models. It is noteworthy that the schematic in Figure II. B describes a land model used for both weather forecasting and climate simulation, an indication of the increasing sophistication demanded by both. The figure also hints at important biophysical and biogeochemical processes that have gradually been added to land models used for climate simulation (and continue to be added), such as biophysical controls on transpiration and carbon uptake.

Figure II. B. Schematic of physical processes in a contemporary land model (from Chen and Dudhia, 2001).

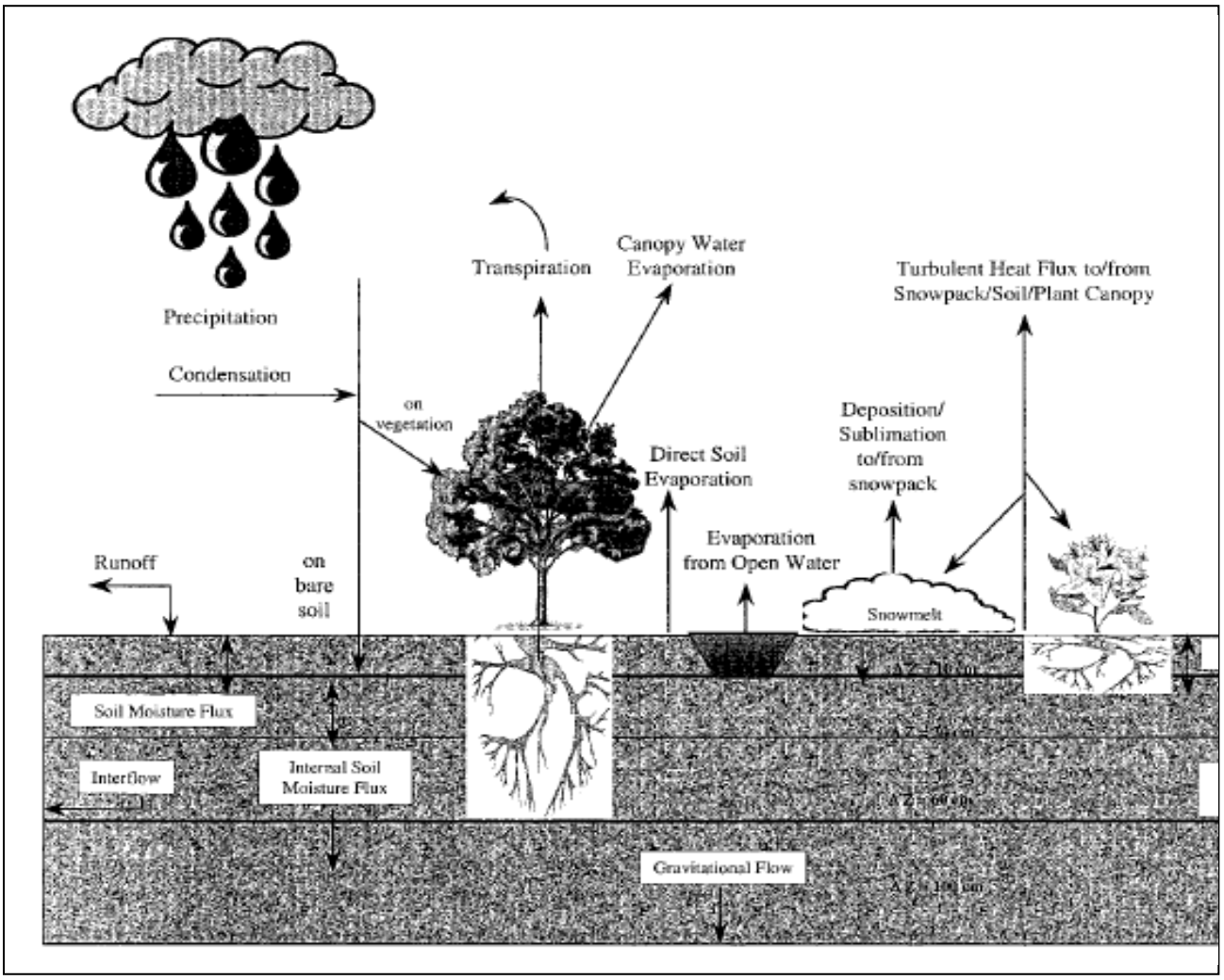

***Vegetation*:** Some of the most extensive increases in complexity and sophistication have occurred with vegetation modeling in land models. An early generation of land models (Wilson *et al*., 1987; Sellers *et al*., 1986) introduced biophysical controls on plant transpiration by adding a vegetation canopy over the surface, thereby implementing vegetative control on the terrestrial water cycle. These models included exchanges of energy and moisture between the surface, canopy and atmosphere, along with momentum loss to the surface. Further developments included improved plant physiology that allowed simulation of carbon dioxide fluxes (e.g., Bonan 1995; Sellers *et al*., 1996), which lets the model treat the flow of water and carbon dioxide as an optimization problem balancing carbon uptake for photosynthesis against water loss through transpiration. Improvements also included implementation of model parameters that could be calibrated with satellite observation (Sellers *et al*., 1996), thereby allowing global-scale calibration.

Continued development has included more realistic parameterization of roots (Arora and Boer, 2003; Kleidon, 2004) and adding multiple canopy layers (e.g., Gu *et al*., 1999; Baldocchi and Harley, 1995; Wilson *et al*., 2003). However, the latter has not been used in climate models as the added complexity of multi-canopy models renders unambiguous calibration very difficult. An important ongoing advance is the incorporation of biological processes that produce carbon sources and sinks through vegetation growth and decay and cycling of carbon in the soil (e.g., Li *et al*., 2006), although considerable work is needed to determine observed magnitudes of carbon uptake and depletion.

Soils: The spatial distribution of soils, at least for the contiguous U.S. appears to be fairly well mapped (Miller and White 1998). Most land models include only inorganic soils, generally composed of mixtures of loam, sand and clay. However, high-latitude regions may have extensive zones of organic soils (peat bogs), and some models have included organic soils topped by mosses, which has led to decreased soil heat flux and increased surface sensible and latent heat fluxes (Berringer et *al*., 2001).

Snow and ice: Climate models initially treated snow as a single layer that could grow through snow fall or deplete though melt (e.g., Dickinson et *al*., 1993). More recent land models for climate

simulation include sub-grid distributions of snow depth (Liston, 2004) and blowing of snow (Essery and Pomeroy, 2004). Snow models now may use multiple layers to represent fluxes through the snow (Oleson *et al*., 2004). Effort has also gone into including and improving effects of soil freezing and thawing (Koren *et al*., 1999; Boone *et al*, 2000; Warrach *et al*., 2001; Li and Koike, 2003; Boisserie *et al*., 2006) though permafrost modeling is more limited (Malevsky-Malevich *et al*., 1999; Yamaguchi *et al*., 2005).

Vegetation interacts with snow by covering it, thereby masking snow's higher albedo (Betts and Ball, 1997) and retarding spring snowmelt (Sturm et al., 2005). The net effect is to maintain warmer temperatures than would occur without vegetation masking (Bonan et al., 1992). Vegetation also traps drifting snow (Sturm et al., 2001), insulating the soil from subfreezing winter air temperatures and potentially increasing nutrient release and enhancing vegetation growth (Sturm et al., 2001). The albedo masking is included in some land surface models, but it requires accurate simulations of snow depth to produce accurate simulation of surface-atmosphere energy exchanges (Strack et al., 2003).

Ice Sheets Global sea level is rising at a rate of 30 cm/century, thanks to a combination of ocean thermal expansion, melting of mountain glaciers and small ice caps, and retreat of the large ice sheets of Greenland and Antarctica (Cazenave and Nerem, 2004; Church and White 2006). The rise in sea level provides a common disruption and challenge to nearly every country, and the 400 million inhabitants who live within roughly 20 meters of elevation above sea level (Small et *al.*, 2000). By far the greatest uncertainty in sea level rise is associated with ice sheets. Complete melting of the Greenland and West Antarctic ice sheets, which are believed vulnerable to climate warming, would raise sea level by about 7 m and 5 m, respectively. During the last interglacial period, roughly 125,000 years ago, these ice sheets were smaller and sea level was a few meters higher than its present-day value (McCulloch and Ezat 2000, Siddall et *al.* 2003). Given the potentially catastrophic impacts of sea level rise, it is essential to be able to predict how fast ice sheets will melt and whether that melting, once begun, can be reversed. This is not yet possible because key ice sheet dynamical processes are poorly understood and are not included in current climate models. The recent IPCC assessment report (IPCC, 2007) underscores the need for improved ice sheet models, but because of the early stage of model development, specifically excluded rapid changes in ice flow from its 21st century sea level projections.

Ice sheets were once thought to be too sluggish to respond to climate change on time scales of less than a century. However, analysis of coral reefs at several locations indicate periods, including around 14,000 years ago, when sea level rose by as much as a few meters per century (Bard *et al.*, 1990). Recent observations suggest that ice sheets are already responding to warming. Outlet glaciers in Greenland have accelerated and thinned (Rignot and Kanagaratnam, 2006), driven by ocean warming and possibly by increased basal sliding. Ice shelves in the Amundsen Sea embayment of West Antarctica have thinned and retreated, giving rise to acceleration of glaciers tens of km upstream (Payne et *al*., 2004). Satellites provide near-complete spatial coverage and recent instruments have measured changes in total ice volume with precision that is unprecedented. Surface altimetry and synthetic aperture radar interferometry measure the height of the ice surface, and can be used to estimate changes in ice volume with additional information or assumptions about depth (Rignot and Kanagaratnam, 2006). Surveys of the changing gravitational field provide direct measurements of ice mass (Velicogna and Wahr 2006). Both indicate that the Greenland and Antarctic ice sheets are losing mass. Shepherd and Wingham (2007) estimate a net loss of about 125 Gt/yr (which includes losses of 100 Gt/yr for Greenland and 50 Gy/yr for West Antarctica, offset by a gain of 25 Gt/yr from increased snowfall in East Antarctica). The resulting contribution to sea level rise is currently a modest 3.5 cm/century, but this contribution will likely increase in a warming climate.

Most global climate models to date have been run with prescribed, immovable ice sheets, but several modeling groups are now incorporating dynamic ice sheet models. Scientists are coupling GLIMMER, an ice sheet model originally developed at the University of Bristol, to the Community Climate System Model. GLIMMER will be forced with temperature, precipitation, and other climate fields, and will return a modified surface elevation profile along with meltwater *freshwater* fluxes. As the ice sheet thins, melting will likely increase because the surface descends to a lower elevation where the temperature is higher *temperature-elevation feedback*. Meanwhile, meltwater *freshwater fluxes* will freshen the upper ocean and possible modify the thermohaline circulation. GLIMMER will initially be used to model the Greenland ice sheet and later will be used for simulations of the Antarctic ice sheet as well as paleo ice sheets (e.g., the Laurentide ice sheet that covered much of North America during the last glacial period).

Like most current-generation models, GLIMMER is based on the shallow-ice approximation, which assumes that ice flow is dominated by vertical shear. This approximation is valid in slow-moving ice sheet interiors but is insufficient to model fast dynamic changes near the ice sheet margin. A number of physical, numerical and computational improvements are needed to provide realistic projections of 21st century ice sheet changes. Among the major challenges are the following.

- Incorporate a unified treatment of stresses: both the vertical shear stresses that dominate in the ice sheet interior and the longitudinal stresses that are important in ice shelves and ice streams.
- Decrease grid spacing to 5 km or less to resolve small-scale features such as ice streams and outlet glaciers. This may require nested or unstructured grids, as well as parallel codes that scale efficiently with large numbers of processors.
- Develop improved methods of downscaling atmospheric fields, which are typically at a grid spacing of 100 km or more, to the finer ice sheet grid, making sure that energy is conserved in the process.
- Develop realistic parameterizations of surface and subglacial hydrology. Fast dynamic processes are largely controlled by the pressure and extent of water at the base of the ice sheet.
- Model the interaction of ice shelves with the ocean circulation. Ocean models, which usually assumed fixed topography, must be modified to include flow beneath advancing and retreating ice.

Meeting these challenges will require increased interaction between the glaciological and climate modeling communities, which until recently have been largely isolated from one another.

Hydrology: The initial focus of land models was vertical coupling of the surface with the overlying atmosphere. However, horizontal water flow through river routing has been available in some models for some time (e.g., Sausen *et al*., 1994; Hagemann and Dümenil, 1998), with spatial resolution of routing in climate models increasing in more recent versions (Ducharne *et al*., 2003).

However, freezing soil poses additional challenges for modeling runoff (Pitman *et al*., 1999), with more recent work showing some skill in representing its effects (Luo *et al*., 2003; Rawlins *et al*., 2003; Niu and Yang, 2006).

Work is also underway to couple ground-water models into land models (e.g., Gutowski *et al*., 2002; York *et al*., 2002; Liang *et al*., 2003; Maxwell and Miller, 2005; Yeh and Eltahir, 2005). Ground water potentially introduces longer time scales of interaction in the climate system in places where it has contact with vegetation roots or emerges through the surface.

Scale considerations: Land models encompass spatial scales ranging from the size of the model grid box down to biophysical and turbulence processes operating on scales the size of leaves. Explicit representation of all these scales in a climate model is beyond the scope of current computing systems as well as observing systems that would be needed to provide adequate model calibration for global and regional climate. As indicated above, land models have been developed to increase the sophistication of their climate-system simulation without becoming so complex as to be intractable. Thus, for example, typical land models in climate simulation do not represent individual leaves but the collective behavior of a canopy of leaves, and multiple canopy layers are generally represented by a single, effective canopy.

Although model fluxes are primarily in the vertical direction, they do not represent a single point but behavior in a grid box that may be many tens or hundreds of kilometers across. Initially, these grid boxes were treated as homogeneous units, but starting with the pioneering work of Avissar and Pielke (1989), many land models have tiled a grid box with patches of different land-use and vegetation types. Although these patches may not interact directly with their neighbors, they are linked by their coupling to the grid box's atmospheric column. This coupling does not allow possible small-scale circulations that might occur because of differences in surface-atmosphere energy exchanges between patches (Segal and Arritt, 1992; Segal *et al*., 1997), but under most conditions, the imprint of such spatial heterogeneity on the overlying atmospheric column appears to be limited to a few meters above the surface (e.g., Gutowski *et al*.,1998).

Vertical fluxes linking the surface, canopy and near-surface atmosphere generally assume some form of down-gradient diffusion, though counter-gradient fluxes can exist in this region much like in the overlying atmospheric boundary layer, so there has been some attempt to replace diffusion with more advanced, Lagrangian random-walk approaches (Gu *et al*., 1999; Baldocchi and Harley, 1995; Wilson *et al*., 2003).

Digital Elevation Models: Topographic variation within a grid box is usually ignored in land modeling. However, implementing detailed river-routing schemes will require accurate digital elevation models (e.g., Hirano *et al*., 2003; Saraf *et al*., 2005). In addition, some soil water schemes also include effects of land slope on water distribution (Choi *et al*., 2007) and surface radiative fluxes (Zhang *et al*., 2006).

Validation: Validation of land models, especially globally, remains a problem, due to lack of measurements for relevant quantities such as soil moisture and energy, momentum, moisture and carbon fluxes. PILPS (Henderson-Seller *et al*., 1995) has provided opportunity to make detailed comparisons of multiple models with observations at point locations around the world with differing climates, thus providing some constraint on the behavior of land models. Global participation in PILPS has led to a greater understanding of differences among schemes and improvements. The latest generation of land surface models exhibit relatively smaller differences (Henderson-Sellers *et al*., 2003) compared to previous generations. River routing can provide a diagnosis versus observations of the spatially distributed behavior of a land model (Kattsov *et al*., 2000). Remote sensing has been useful for calibration of models developed to exploit it, but it has not generally been used for model validation. The development of regional observing networks that aspire to give Earth-system observations, such as some of the mesonets in the United States, offers promise of spatially distributed observations of important fields for land models that resolve some of the spatial variability of land behavior.

Future: Land modeling has developed in other disciplines roughly concurrently with the advances implemented in climate models. Applications are wide ranging and include detailed models used for water resource planning (Andersson *et al*. 2006), managing ecosystems (e.g., Tenhunen *et al*., 1999), estimating crop yields (e.g., Jones and Kiniry, 1986; Hoogenboom *et al*.; 1992), simulating

ice sheet behavior (Peltier, 2004), and projecting land-use, such as for transportation planning (e.g., Schweitzer; 2006). As suggested by this list, there are widely disparate applications, which have developed from differing scales of interest and focus processes. Land-model development in some of these other applications has informed advances in land models for climate simulation, as in representation of vegetation and hydrologic processes. Because land models do not include all climate system processes, they can be expected in the future to engage other disciplines and encompass a wider range of processes, especially as resolution increases.

Sea Ice Models, including parameterizations and evaluation

General overview: All the considered climate models have sea ice components that are both dynamic and thermodynamic. That is, the models include the physics for ice movement as well as the physics that is related to energy and heat within the ice. The differences in the various models relate primarily to how complex the code for the dynamics is in determining the representation of ice rheology and their use of parameters.

Two dynamical codes are in common use in ice models, the standard Hibler viscous-plastic (VP) rheology (Hibler, 1979; Zhang and Rothrock, 2000) and the more complex elastic-viscous-plastic (EVP) rheology of Hunke and Dukowicz (1997). The EVP method explicitly solves for the ice stress tensor, while the VP solution uses an implicit iterative approach. The solutions are similar (Hunke and Zhang, 1997). The NOAA-GFDL models [Delworth *et al*., 2005] and the NCAR-CCSM3 (Collins *et al*., 2005) use the EVP rheology, while the NASA-GISS models use the VP implementation. The EVP is more efficient, especially when using multiple processors.

The thermodynamics portions of the codes also vary in their implementation. Previous climate models generally used the thermodynamics code of Semtner (1976). This classic sea ice model includes one snow layer and two ice layers with constant heat conductivities and a simple parameterization of the brine (salt) content. The NOAA-GFDL models continue to use the Semtner structure with three layers but extend the code relating to brine content in the upper ice layer to be represented by variable heat capacity (Winton, 2000). The NCAR-CCSM3 and NASA-GISS models use variations of the Bitz and Lipscomb (1999) thermodynamics (Briegleb *et al*., 2002).

The code accounts for more of the physical processes within the ice, including the melting of internal brine regions and conserves energy.

The prognostic variables of the sea ice components of the separate climate models are similar to their ocean counterpart, that is the NOAA-GFDL and NCAR-CCSM use velocity, temperature and volume while the NASA-GISS models use velocity, enthalpy, and mass. The amounts of snow and ice for the layers are also computed with each model defining the number of ice layers and ice categories differently. The NOAA-GFDL models use a snow layer, two ice layers and five ice-thickness categories. The NCAR-CCSM3 model has a snow layer, four ice layers, and six ice categories. The NASA-GISS model includes one snow layer, three ice layers, and two ice categories. There is variation among the models on how ice categories are defined, but all include a "no ice" category. The resolution of the sea-ice component is the same as the ocean components of a specific climate model: NASA-GISS is at a relatively low resolution of 4°x5°, while the NOAA-GFDL and NCAR-CCSM models are on the order of 1°.

Parameterizations

Albedo: As an important feedback to the atmosphere, the albedo (the proportion of incident radiation reflected off a surface) of the snow and ice plays a significant role in the climate system. All the sea ice component models parameterize the albedo to some extent. Figure II. C from Curry *et al*. (1995**)** illustrates the interrelations of the sea-ice system and how the albedo is a function of the snow or ice thickness, ice extent, open water, and the surface temperature, along with other factors, including the spectral band of the radiance. The various models treat the different contributions to the total albedo in similar ways, but vary on the details. For example, the NCAR-CCSM3 sea-ice component does not include dependence on the solar elevation angle (Briegleb *et al.*, 2002), while the NASA-GISS model does (Schmidt *et al*., 2006). Both of these models include the contribution of melt ponds (Ebert and Curry, 1993; Schramm *et al*., 1997) The NOAA-GFDL model follows Briegleb *et al*. (2002), but accounts for the differences in spectral contributions using fixed ratios (Delworth *et al.* 2006).

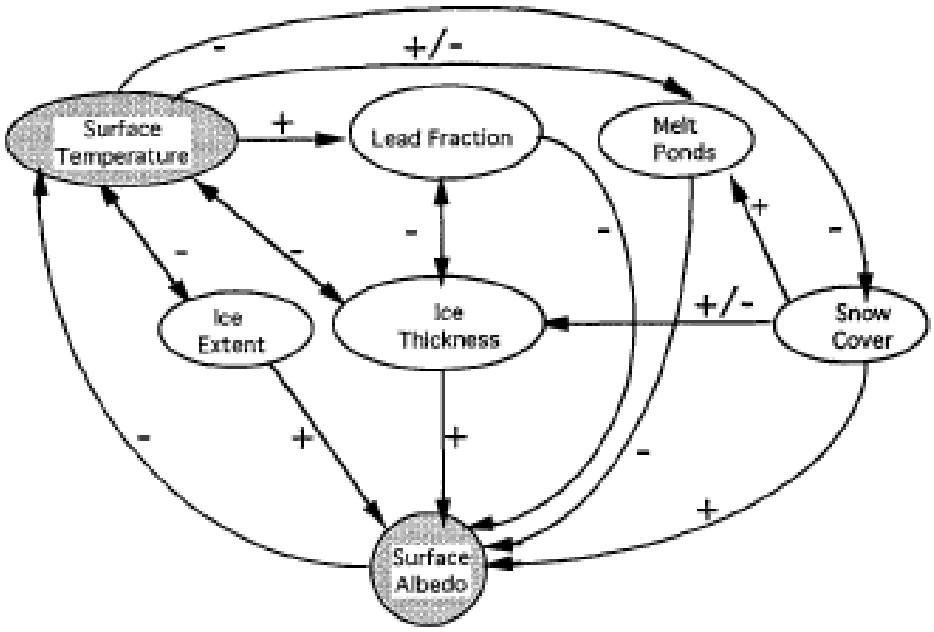

FIG. 6. Schematic diagram of the sea ice–albedo feedback mechanism. The direction of the arrow indicates the direction of the interaction. A "+" indicates a positive interaction (an increase in the first quantity leads to an increase in the second quantity) and a "−" indicates a negative interaction (an increase in the first quantity leads to a decrease in the second quantity). A "±" indicates either that the sign of the interaction is uncertain or that the sign changes over the annual cycle.

1

2 Figure II. C (from Curry *et al*. (1995)).

Other parameterizations: Additional parameters include reference values for defining ice salinities, strengths, roughness, and drag coefficients. Details of these parameters can be found in the references listed above which describe the basic sea-ice models of the various groups.

Component coupling and coupled model evaluation

We describe in the following some of the key aspects of the model development process at the three U.S. groups that contributed models to the Fourth Assessment of the IPCC, with particular focus on those aspects most relevant for simulation of the 20th century global mean temperature record on the one hand, and the model's climate sensitivity on the other hand. We begin with some general comments on the model development process.

The complexity of the climate system, and our inability to resolve all relevant processes in our models, result in a host of choices for development teams to make. Differing expertise, experience, and interests result in distinct development pathways for each climate model. While we eventually expect to see model convergence, forced by increasing insights into the working of the climate system, we are still far from that limit today in several important aspects of the models. Given this level of uncertainty, multiple modeling approaches are clearly needed. Models differ in their details primarily because development teams have differing ideas concerning the underlying physical mechanisms relevant for the less well-understood aspects of the system.

The NOAA Geophysical Fluid Dynamics Laboratory Model Development Path

The Geophysical Fluid Dynamics Laboratory of NOAA conducted a thorough restructuring of its atmospheric and climate models over more than five years prior to its delivery of a model to the CMIP-3/IPCC database in 2004. This was performed partly in response to need for modernizing the software engineering, and partly in response to new ideas in modeling the atmosphere, ocean, and sea ice. The differences between the resulting models and the previous generation of climate models at GFDL are sufficiently varied and substantial, that mapping out exactly why climate sensitivity and other aspects of the climate simulations differ between these two generations of models would

be very difficult and has not been attempted. Unlike the earlier generation, the new models do not use flux adjustments.

The new atmospheric models developed at GFDL for global warming studies are referred to as AM2.0 and AM2.1 (GFDL Atmospheric Model Development Team, 2006). A key point of departure from previous models at GFDL was the adoption of a new numerical core for solving the fluid dynamical equations for the atmosphere. Much of the atmospheric development was based on running the model over observed seas surface temperature and sea ice boundary conditions over the period 1980-2000, with a focus on both the mean climate and the response of the atmosphere to ENSO variability in the tropical Pacific. Given the basic model configuration, several subgrid closures were varied to optimize aspects of the climate. Modest improvements in the midlatitude wind field were obtained by adjusting a part of the model referred to as “orographic gravity wave drag” which accounts for the effects of the force exerted on the atmosphere by unresolved topographic features ("hills"). Substantial improvements in tropical rainfall and its response to ENSO resulted from an optimization of parameters as well, especially the treatment of vertical transport of horizontal momentum by moist convection.

The ocean model chosen for this development was the latest version of the Modular Ocean Model developed over several decades at GFDL, notable new features in this version being a grid structure better suited to simulating the Arctic ocean and a framework, that has been nearly universally accepted by ocean modelers in recent years, for sub-gridscale mixing that avoids unphysical mixing between oceanic layers of differing densities (Gent and McWilliams, 1990). A new sea ice model includes the large-scale effective rheology that has proven itself in the past decade in several models, and multiple ice thickness/lead classes in each grid box. The land model chosen was relatively simple, with vertically resolved soil temperature but retaining the “bucket hydrology” from the earlier generation of models.

The resulting climate model was studied, restructured, and tuned for an extended period, with particular interest in optimizing the structure and frequency of the model’s spontaneously generated EL Nino events, minimizing surface temperature biases, and maintaining an Atlantic overturning

circulation of sufficient strength. During this development phase, climate sensitivity was monitored by integrating the model to
equilibrium with doubled CO2 when coupled to a "flux-adjusted slab" ocean
model A single model modification reduced the model's sensitivity from a value of 4.0–4.5 K to values between 2.5 and 3.0 K. The change responsible for this reduction was the inclusion of a new model of mixing in the planetary boundary near the Earth's surface. It was selected for inclusion in the model because it generated more realistic boundary layer depths and near surface relative humidities. The reduction in sensitivity resulted from modifications to the low level cloud field; the size of this reduction was not anticipated.

Aerosol distributions used by the model were computed off-line from the MOZART-II model as described in Horowitz, *et al*., (2003). No attempt was made to simulate the indirect aerosol effects (interactions between clouds and aerosols) as the confidence in the schemes tested was deemed insufficient for inclusion in the model. In the 20th century simulations, solar variations followed the prescription of Lean *et al*., (1995), while volcanic forcing was estimated from obervations. Stratospheric ozone was prescribed, with the Southern Hemisphere ozone hole prescribed, in particular, in the 20th century simulations. A new detailed land-use history provided a time-history of vegetation-types.

Final tuning of the global energy balance of the model, using two parameters in the cloud prediction scheme, was conducted by examining control simulations of the fully coupled model using fixed 1860 and 1990 forcings. The IPCC-relevant runs of the resulting model (CM2.0) were provided to the CMIP-3/IPCC archive under considerable time pressure.

The simulations of the 20th century with time-varying forcings provided to the database were the first simulations of this kind generated with this model. There was no retuning of the model, and no iteration of the aerosol or any other time-varying forcings, at this point.

Model development efforts proceeded in the interim, and a new version of the model emerged rather quickly in which the numerical core of the atmospheric model was replaced by a "finite-volume" code (Lin and Rood, 1996), substantially improving the wind fields near the surface. These

improved winds in turn resulted in improved extratropical ocean circulation and temperatures. ENSO variability increased in this model, to unrealistically large values. But the efficiency of the ocean code was also improved substantially, and with a retuning of the clouds for global energy balance, the new model, CM2.1, was deemed to be a substantial enough improvement to warrant generating a new set of runs for the database. CM2.1 when run with a slab ocean model was found to have a somewhat increased sensitivity, (3.3K). However, the transient climate sensitivity, the global mean warming at the time of CO2 doubling in a fully-coupled model with 1%/yr increasing CO2, is actually slightly smaller than in CM2.0.
The solar, aerosol, volcanic, and greenhouse gas forcings are identical in the two models.

The Community Climate System Model Development Path

A new version of the Community Climate System Model, version 3 (CCSM3) has been developed, and was released to the climate community in June, 2004. CCSM3 is a coupled climate model with components representing the atmosphere, ocean, sea ice, and land surface connected by a flux coupler. CCSM3 is designed to produce realistic
simulations over a wide range of spatial resolutions, enabling inexpensive simulations lasting several millennia or detailed studies of continental-scale dynamics, variability, and climate change. Twenty six papers documenting all aspects of the CCSM3, and runs performed with it, were published is a *Journal of Climate Special Issue*, Vol 19, No 11, June 2006. Three different resolutions of the model are supported. The highest resolution is the configuration used for climate-change simulations, with a T85 grid for the atmosphere and land, and a grid with approximately 1º resolution for the ocean and sea-ice, but finer meridional resolution near the equator. The second resolution is a T42 grid for the atmosphere and land, with the 1ºocean and sea-ice resolution. There is also a lower resolution version, designed for Paleoclimate studies, that has T31 resolution for the atmosphere and land, and a 3ºversion of the ocean and sea ice.

The new version of the CCSM3 incorporates several significant improvements in the physical parameterizations. The enhancements in the model physics are designed to reduce or eliminate several systematic biases in the mean climate produced by previous versions of CCSM. These include new treatments of cloud processes, aerosol radiative forcing, land-atmosphere fluxes, ocean

mixed-layer processes, and sea-ice dynamics. There are significant improvements in the sea-ice thickness, polar radiation budgets, tropical sea-surface temperatures, and cloud radiative effects. CCSM3 produces stable
climate simulations of millennial duration without ad hoc adjustments to the fluxes exchanged among the component models. Nonetheless, there are still systematic biases in the ocean-atmosphere fluxes in coastal regions west of continents, the spectrum of ENSO variability, the spatial distribution of precipitation in the tropical oceans, and continental precipitation and surface air temperatures. Work is underway to produce the next version of the CCSM, which will reduce these biases further, and to extend the CCSM to a more accurate and comprehensive model of the complete Earth's climate system.

The climate sensitivity of the CCSM3 has a weak dependence on the resolution used.
The equilibrium temperature increase due to a doubling of carbon dioxide, using a slab ocean model, is 2.71C, 2.47C, and 2.32C, respectively, for the T85, T42, and T31 atmosphere resolutions. The transient climate response to doubling carbon dioxide in fully coupled integrations is much less dependent on resolution, being 1.50C, 1.48C, and 1.43C, respectively, for the T85, T42, and T31 atmosphere resolutions, see the Kiehl *et al*. paper in the *Journal of Climate Special Issue*, Vol 19, No 11, June 2006, 2584–2596.

For the IPCC Fourth Assessment Report, the following CCSM3 runs were submitted for evaluation, and to PCMDI for dissemination to the climate scientific community. Long, present day and 1870 control runs, an ensemble of eight 20th century runs, and smaller ensembles of future scenario runs for the A2, A1B, and B1 scenarios, and for the 20th century commitment run, where the carbon dioxide levels were kept at their 2000 values.
The control and 20th century runs are documented and analysed in several papers in the *Journal of Climate Special Issue*, and the future climate change projections using the CCSM3 are documented by Meehl *et al* (2006).

The GISS Development Path

The most recent version of the GISS atmospheric GCM, modelE, resulted from a substantial reworking of the previous version, model II'. While the model physics has become more sophisticated, execution by the user is simplified as a result of modern software engineeering and improved model documentation embedded within the code and accompanying web pages. The model can be downloaded from the GISS website by outside users, and is designed to run on myriad platforms ranging from laptops to a variety of multi-processor computers, partly as the result of the rapidly shifting computing environment at NASA. The most recent (post-AR4) version can be run on an arbitrarily large number of processors.

Historically, GISS has eschewed flux adjustment. Nonetheless, the net energy flux at the top of atmosphere and surface have been reduced to near zero, by adjusting the threshold relative humidity for water and ice cloud formation, two parameters that are otherwise weakly constrained by observations. Near-zero fluxes at these levels are necessary to minimize drift of either the ocean or the coupled climate.

To assess the sensitivity of the climate response to the treatment of the ocean, modelE has been coupled to a slab-ocean model with prescribed horizontal heat transport, along with two ocean GCMs. One GCM, the Russell ocean (Russell *et al.*,1995), has 13 vertical layers and horizontal resolution of 4º latitude by 5º longitude, and is mass conserving (rather than volume conserving like the GFDL MOM). Alternatively, ModelE is coupled to the Hybrid Coordinate Ocean Model (HYCOM), an isopycnal model developed originally at the University of Miami (Sun and Bleck, 2006). HYCOM has 2º latitude by 2º longitude resolution at the equator, with the latitudinal spacing decreasing poleward with the cosine of latitude. A separate rectilinear grid is used in the Arctic to avoid the polar singularity, and joins the spherical grid around 60 N.

Climate sensitivity to doubling of CO_2 depends upon the ocean model due to differences in sea-ice. For the slab-ocean model, the climate sensitivity is 2.7 C, and 2.9 C for the Russell ocean (Hansen et *al* 2005). As at GFDL and CCSM, no effort is made to match a particular sensitivity, nor is the sensitivity or forcing adjusted to match 20^{th} century climate trends (Hansen et *al* 2007). Aerosol forcing is calculated from prescribed concentration, computed offline by a physical model of the aerosol life cycle. In contrast to the GFDL and NCAR models, modelE includes a representation of

the aerosol indirect effect. Cloud droplet formation is related empirically to the availability of cloud condensation nuclei, which depends upon the prescribed aerosol concentration (Menon and Del Genio 2005).

Flexability is emphasized in model development (Schmidt *et al.,* 2006). ModelE is designed for a variety of applications, ranging from simulation of stratospheric dynamics and the middle atmosphere response to solar forcing, to projection of twenty-first century trends in surface climate. Horizontal resolution is typically 4º latitude by 5º longitude, although twice the resolution is more often used for studies of cloud processes. The model top has been raised from 10 mb (as in the previous model II') to 0.1 mb, so that the top has less influence upon the stratospheric circulation. Coding emphasizes "plug-and-play" structure, so that the model can be easily adapted for future needs, such as fully interactive carbon and nitrogen cycles.

Model development is devoted to improving the realism of individual model parameterizations, such as the planetary boundary layer, or sea ice dynamics. Because of the variety of applications, relatively little emphasis is placed upon optimizing the simulation of specific phenomena such as El Nino or the Atlantic thermohaline circulation; as noted above, successful reproduction of one phenomena usually results in a sub-optimal simulation of another. Nonetheless, some effort was made to reduce biases in previous versions of the model that emerged from the interaction of various features of the model, such as subtropical low clouds, tropical rainfall, and variability of the stratospheric winds. Some of the model adjustments were structural, as opposed to the adjustment of a particular parameter: for example, the introduction of a new planetary boundary layer parameterization that reduced the unrealistic formation of clouds in the lowest model level (Schmidt *et al.,* 2006).

Because of their uniform horizontal coverage, satellite retrievals are emphasized for model evaluation, like Earth Radiation Budget Experiment fluxes at TOA, Microwave Sounding Unit channels 2 (troposphere) and 4 (stratosphere) temperatures, and International Satellite Cloud Climatology Project (ISCCP) diagnostics. Comparison to ISCCP is through a special algorithm that samples the GCM output to mimic data collection by an orbiting satellite. For example, high clouds may include contributions from lower levels in both the model and the downward looking satellite

instrument. This satellite perspective within the model allows a rigorous comparison to observations. In addition to satellite retrievals, some GCM fields like zonal wind are compared to in situ observations adjusted by the ERA-40 reanalyses. Surface air temperature is taken from the Climate Research Unit (Jones *et al.*, 1999).

Common problems

The CCSM and GFDL Development Teams met several times during this period to compare experiences and discuss common biases in the two models. A topic of considerable discussion and concern, for example, was the tendency for too strong an equatorial cold tongue in the Eastern Equatorial Pacific and associated problems with the pattern of precipitation (often referred to as the "double ITCZ problem"). It was noted in these meetings that the climate sensitivities of the two models had converged to some extent from an earlier generation in which the NCAR model was on the low end of the canonical sensitivity range of 1.5–4.5K, while the GFDL model had been near the high end. This convergence in the global mean was considered by the teams to be coincidental; it was not a consequence of any specific actions taken so as to engineer convergence, and did not reflect convergence either in the specifics of the cloud feedback processes that resulted in these sensitivity changes, nor in the regional temperature changes than make up these global mean values.

A procedure common to each of these three models, and to all other comprehensive climate models, is a tuning of the global mean energy balance. A climate model must be in balance at the top of the atmosphere and globally averaged, to within a few tenths of a W/m^2 in its control (pre-1860) climate if it is to avoid temperature drifts in 20^{th} and 21^{st} century simulations that would obscure the response to the imposed changes in greenhouse, aerosol, volcanic, and solar forcings. Especially because of the difficulty in modeling clouds, but even in the clear sky, untuned models do not currently possess this level of accuracy in their radiative fluxes. The imbalances are more typically range up to 5 W/m^2 or more. Parameters in the cloud scheme are then altered to create a balanced state, often taking care that the individual components of this balance, the absorbed solar flux and emitted infrared flux, are individually in agreement with observations, since these help insure the correct distribution of the heating between atmosphere and ocean. This is occasionally referred to as

the "final tuning" of the model, to distinguish it from the various choices made with other motivations while one is configuring the model.

The need for this final tuning does not preclude the use of these models for global warming simulations, in which the radiative forcing is itself of the order of several W/m^2. Consider for example, the study of Ramaswamy *et al*., (2001) of the effects of modifying the treatment of the "water vapor continuum" in a climate model. This is an aspect of the radiative transfer algorithm in which there is significant uncertainty. While modifying the treatment of the continuum can change the top-of-atmosphere balance by more than 1 W/m^2, the effect on climate sensitivity is found to be insignificant. The change in radiative transfer in this instance alters the outgoing infrared flux by roughly 1% , and it affects the sensitivity (by altering the derivative of the flux with respect to temperature) by roughly the same percentage. But a change in sensitivity of this magnitude, say from 3K to 3.03K, is of little consequence given uncertainties in the cloud feedbacks. It is some aspects of the models that affect the strengths of temperature-dependent feedbacks that are of particular concern, not errors in mean fluxes *per se*.

Reductive vs. holistic evaluation of models*:*

In order to evaluate models, appreciation is needed of their structure. For example, the discussion of the climatic response to increasing greenhouse gases is intimately related to the question of how the infrared radiation escaping to space is controlled. When summarizing the results from climate models, one often speaks and thinks in terms of a simple energy balance model in which the global mean infrared energy escaping to space is a single number that has a simple dependence on global mean surface temperature. Water vapor or cloud feedbacks are often incorporated into such global mean energy balance models with simple empirical relationships that can easily be tailored to generate a desired result. In contrast, Figure II D shows a snapshot at an instant in time of the infrared radiation escaping to space in the kind of atmospheric general circulation model discussed in this report. The detailed distributions of clouds and water vapor simulated by the model, transported by the model's evolving wind fields, create complex patterns in space and time that, if the simulation is sufficiently realistic, resemble the images seen from satellites viewing the Earth at infrared wavelengths.

Figure II D

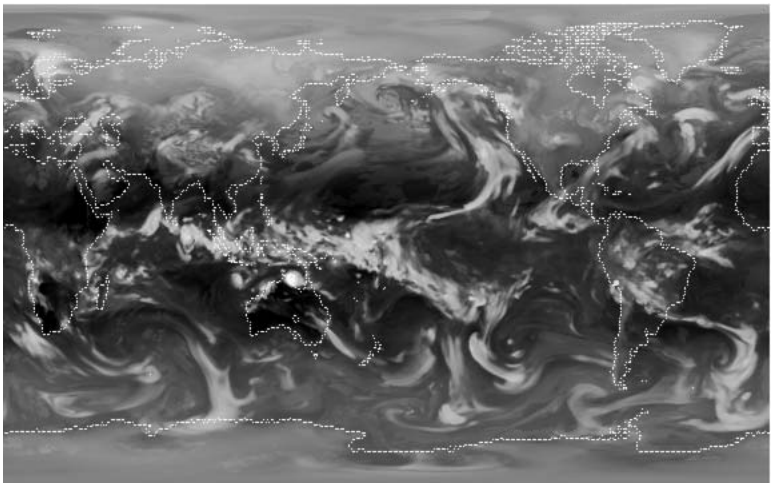

A snapshot in time of the infrared radiation escaping to space in a version of the atmospheric model AM2 (GAMDT, 2004) constructed at NOAA's Geophysical Fluid Dynamics Laboratory. The energy emitted is largest in the darkest areas and smallest in the brightest areas. (This version of the atmospheric model has higher resolution than that used for the simulations in the CMIP3 archive (50 km rtrher than 200km)but other than resolution it uses the same numerical algorithm.)

This class of model evolves the state of the atmosphere/land system forward in time, starting from some initial condition. It consists of rules that generate this state (temperature, winds, water vapor, clouds, rainfall rate, water storage in the land, land surface temperature) from the preceding state, in this case one half hour earlier. By this process it evolves the "weather" over the Earth. To change the way in which this model's infrared radiation reacts to increasing temperatures, one would need to modify these rules.

The goal of the climate modeling enterprise is to decrease the level of empiricism and to base models as much a possible on well-established physical principles. This goal is pursued primarily by decomposing the climate system into a number of relatively simple processes and interactions, and by focusing on the rules governing the evolution of these individual processes, rather than working with more holistic concepts such as the global mean infrared radiation escaping to space, the average summertime rainfall over Africa, or the average wintertime surface pressure over the Arctic. These are all outcomes of the model, determined by the set of reductive rules that govern the model's evolution.

Suppose one is interested in how ocean temperatures affect rainfall over Africa. One can develop an empirical, holistic, model, using observations and standard statistical techniques, in which one "fits" the model to these observations. Alternatively, one can try to use a general circulation model of the sort pictured above, which does not deal directly with a high level climate output such as African rainfall averaged over some period, but rather attempts to simulate the inner workings, or dynamics, of the climate system at a much finer level of granularity. To the extent that the simulation is successful and convincing, with analysis and manipulation of the model one can hope to uncover the detailed physical mechanisms underlying this causal connection. The resulting fit may or may not be as good as the fit obtained with the explicitly tuned statistical model, but a reductive model ideally provides a different level of confidence in its explanatory and predictive power. See, for example, Hoerling, et al 2006 for an analysis of African rainfall/ocean temperature relationships in a set of atmospheric GCMs.

Our confidence in the explanatory and predictive power of climate models grows based on their ability to simulate many aspects of the climate system *simultaneously* with the same set of

physically based rules. When one evaluates a models ability to simulate the evolution of the global mean temperature evolution over the 20th century, it is important to try to make this evaluation in the context of the model's simultaneous capacity to simulate the seasonal cycle of the Asian monsoons, for example, and it ability to generate the poleward shift of the jet stream in the Southern hemisphere over the past 30 years that has impacted rainfall over southern Australia, and its ability to spontaneously generate El-Nino's of the correct frequency and spatial structure and to capture the effects of El Nino on rainfall and clouds. The quality of the simulation in all of these respects adds confidence in the reductive rules being used to generate the simultaneous simulation of all of these phenomena.

A difficulty that we will return to frequently in this report is that of relating the qualities of a climate simulation to a level of confidence in the model's ability to predict climate change.

The use of model metrics

Recently, objective evaluation of models has exploded with the wide availability of model simulation results in the CMIP3 model database (Meehl, et al, 2006). One important area of research is in the design of of metrics to test the ability of models to simulate well observed climate features (Reichler and Kim, 2007; Gleckler, et al,, 2007). It is unclear which aspects of observed climate must be simulated to ensure reliable future predictions. For example, it is not clear that the most realiable climate projections for temperature over North America are obtained from models that simulate the most realistic present-day temperatures for North America. The projected climate changes in North America may depend strongly on the changes in ocean temperature in the tropical Pacific Ocean, and the manner in which the jet stream over the Pacific responds to these changes in temperature. The quality of a models simulation of atmosphere-ocean cpoupling over the Pacific could potentially be a more relevant metric of quality in this instance. However, metrics can provide guidance about the overall strength and weaknesses of individual models as well as the general state of modeling.

The use of metrics can also inform the community as why it is impossible at this time to determine which is the "best" climate model. In Figure II E below, each of the colored triangles represents a

different metric for which each model was evaluated, for example, “ts” represents surface temperature. The figure displays the relative error value for a variety of metrics, for each model, represented by a vertical column above each tick mark on the horizontal axis. Values less than zero represent a better than average simulation of a particular field measured by the metric, while values greater than zero show models with errors greater than the average. The black triangles connected by the dashed line represent the normalized sum from the errors of all 23 fields. The models were then ranked from left to right based on the value of this total error. As can be seen, the models with the lowest total error, tend to also score better than average in most individual metrics, however, the “best” models do not score the best for every metric. For an individual application, the model with the lowest total error may not be the best choice.

Figure II E – Model metrics for 23 different climate fields. Values less than 0 indicate an error less than the average CMIP3 model, while values greater than 0 show values greater than the average. The black triangles connected by the black line is a total score obtained by averaging all 23 fields.

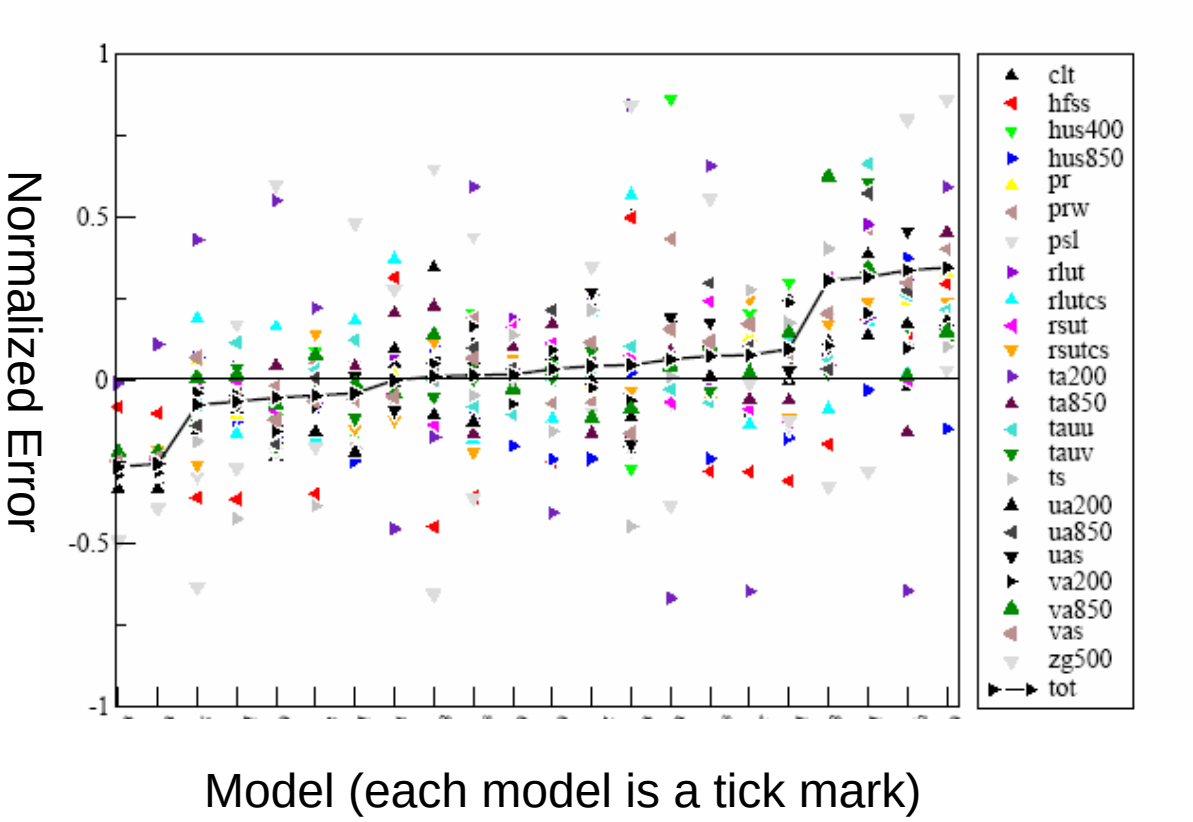

Climate simulations discussed in this report

Three types of climate simulation are discussed in this report. They differ according to the climate forcing factors used as input to the models:

Control runs use constant forcing. (The name "control runs" originated in comparing them with the other simulation types discussed below.) The Sun's energy output and the atmospheric concentrations of carbon dioxide and other gases and aerosols do not change in control runs. As with the other types of climate simulation, day-night and seasonal variations occur, as well as internal "oscillations" such as ENSO (see below). Other than these variations, the control run of a well-behaved climate model is expected to reach a steady state eventually.

Values of control-run forcing factors are typically set to match present-day conditions, and model output is then compared with present-day observations. Actually, the present climate is affected not only by current forcing but also by the history of forcing over time—in particular past emissions of greenhouse gases—but present-day control run output and observations are expected to agree fairly closely if models are reasonably accurate. We compare model control runs with observations in Chapter V below.

Idealized climate simulations are aimed at understanding important processes in models and in the real world. They include experiments in which the amount of atmospheric carbon dioxide increases at precisely 1% per year (about twice the present rate of increase) or doubles instantaneously. The carbon dioxide doubling experiments are typically run until the simulated climate reaches a steady state in equilibrium with the enhanced greenhouse effect. Until the mid-1990's, idealized simulations were often employed to assess possible future climate changes including human-induced global warming. Recently, however, the more realistic time-evolving simulations defined immediately below have been used for making climate predictions. We discuss idealized simulations and their implications for climate sensitivity in Chapter IV below.

Time-dependent climate forcing simulations are the most realistic, especially for eras in which climate forcing is changing rapidly such as the 20th and 21st centuries. Input for the 20th century simulations includes observed time-varying values of solar energy output, atmospheric carbon dioxide, and other climate-relevant gases and aerosols including those produced in volcanic eruptions. Each modeling group uses its own best estimate of these factors. There are significant uncertainties in many of them, especially atmospheric aerosols, so that different models use somewhat different input for their 20th century simulations. We discuss these simulations in Chapter V after comparing control runs with observations.

Time-evolving climate forcing is also used as input for modeling future climate change. This subject is discussed in CCSP Synthesis and Assessment Product 3.2. Finally, we mention for the record simulations of the distant past (various time periods ranging from the early Earth up to the 19th century). These simulations are not discussed in this report, but some of them have been used to loosely "paleocalibrate" simulations of the more recent past and the future (Hoffert and Covey, 1992; Hansen *et al*., 2006; Hegerl *et al*., 2006).

Chapter III – The Added Value of Regional Climate Model Simulations

Types of downscaling simulations

This section focuses on downscaling using three-dimensional models based on fundamental conservation laws, i.e., numerical models with a similar basis as GCMs. A later section of the chapter discusses an alternative approach, statistical downscaling. There are three primary approaches to numerical downscaling: limited-area models (Giorgi and Mearns, 1991; McGregor, 1997; Giorgi and Mearns, 1999; Wang *et al*., 2004), stretched grid models (e.g., Deque *et al*.,1995; Fox-Rabinovitz *et al*., 2001, 2006) and uniformly high-resolution atmospheric GCMs (AGCMs) (e.g., Brankovic and Gregory, 2001; May and Roeckner, 2001; Duffy *et al*., 2003; Coppola and Giorgi, 2005). The last approach is sometimes called "time-slice" climate simulation because the AGCM simulates a portion of the period simulated by the parent, coarser resolution GCM that supplies boundary conditions to it. The limited-area models, also known as regional climate models (RCMs), have the most widespread use. All three approaches use interactive land models, but sea-surface temperatures and sea ice are generally specified from observations or an atmosphere-ocean GCM. All three approaches are also used for purposes beyond downscaling global simulations, most especially to study climatic processes and interactions on scales too fine for typical GCM resolutions.

RCMs, as limited-area models, cover only a portion of the planet, typical a continental domain or smaller. They require lateral boundary conditions from observations, such as atmospheric analyses (e.g., Kanamitsu *et al*. 2002, Uppala *et al*. 2005), or a global simulation. There has been limited two-way coupling wherein an RCM to supplies part of its output back to the parent GCM (Lorenz and Jacob, 2005). Simulations with observation-based boundary conditions are used not only for studying fine scale climatic behavior, but also to help segregate GCM error from error intrinsic to the RCM when performing climate-change simulations (Pan et al., 2001). RCMs may also use grids nested inside a coarser RCM simulation to achieve higher resolution in subregions (e.g. Liang *et al*., 2001; Hay *et al*., 2006). Stretched-grid models, like the high-resolution AGCMs, simulate the

globe, but with spatial resolution varying horizontally. Highest resolution may focus on one (e.g. Deque and Piedelievre, 1995; Hope *et al*., 2004) or a few regions (e.g., Fox-Rabinovitz *et al*., 2002). In some sense, high-resolution AGCMs are a limiting case of stretched-grid simulations where the grid is uniformly high everywhere.

Highest spatial resolutions are most often several tens of kilometers, though some (e.g., Grell *et al*., 2000a,b; Hay *et al*., 2006) have simulated climate with resolutions as small as a few kilometers using multiply nested grids. Duffy *et al*. (2003) have performed multiple AGCM time-slice computations using the same model to simulate resolutions from 310 km down to 55 km. Such approaches expose changes in climate with resolution. Higher resolution generally yields improved climate, especially for fields with high spatial variability, such as precipitation. For example, some studies show that higher resolution does not have a statistically significant advantage in simulating large-scale circulation patterns but it does yield better monsoon precipitation forecasts and interannual variability (Mo *et al*., 2005) and precipitation intensity (Roads *et al*., 2003).

However, improvement is not guaranteed: Hay *et al*. (2006) find deteriorating timing and intensity of simulated precipitation versus observations in their inner, high-resolution nests, even though the inner nest improves resolution of topography. Extratropical storm tracks in a time-slice AGCM may shift poleward relative to the parent, coarser GCM (Stratton, 1999; Roeckner *et al*., 2006) or lower resolution versions of the same AGCM (Brankovic and Gregory, 2001), thus yielding an altered climate with the same sea-surface temperature distribution as the parent model.

Spatial resolution affects the length of simulation periods because higher resolution requires shorter time steps for numerical stability and accuracy. Required time steps scale with the inverse of resolution and can be one or two orders of magnitude smaller than AOGCM time steps. Since increases in resolution are most often applied to both horizontal directions, this means that computation demand varies inversely with the cube of resolution. Although several RCM simulations have lasted 20 to 30 years (Christensen *et al*., 2002; Leung *et al*., 2004; Plummer *et al*., 2006) and even as long as 140 years (McGregor, 1999) with no serious drift away from reality, stretched-grid, time-slice AGCM and RCM simulations typically last from months to a few years. Vertical resolution usually does not change with horizontal resolution, though Lindzen and Fox-

Rabinovitz (1989) and Fox-Rabinovitz and Lindzen (1993) have expressed concerns about the adequacy of vertical resolution relative to horizontal resolution in climate models.

Higher resolution in RCMs and stretched-grid models must also satisfy numerical constraints. Stretched-grid models whose ratio of coarsest to finest resolution exceeds a factor of roughly three are likely to produce inaccurate simulation due to truncation error (Qian *et al*., 1999). Similarly, RCMs will suffer from incompletely simulated energy spectra and thus loss of accuracy if their resolution is roughly 12 times or more finer than the resolution of the source of lateral boundary conditions, which may be coarser RCM grids (Denis *et al*., 2002, 2003; Laprise, 2003; Antic *et al*., 2004, 2006; Dimitrijevic and Laprise 2005). In addition, these same studies indicate that lateral boundary conditions should be updated more frequently than twice per day.

Additional factors also govern ingestion of lateral boundary conditions (LBCs) by RCMs. LBCs are most often ingested in RCMs by damping of the model's state toward the LBC fields in a buffer zone surrounding the domain of interest (Davies, 1976; Davies and Turner, 1977). If the buffer zone is only a few grid points wide, the interior region may suffer phase errors in simulating synoptic-scale waves (storm systems), with resulting error in the overall regional simulation (Giorgi et *al*.,1993). Spurious reflections may also occur in at boundary regions (e.g., Miquez-Macho et *al*., 2005). RCM boundaries should be where the driving data are of optimum accuracy (Liang et *al*., 2001), but placing the buffer zone in a region of rapidly varying topography can induce surface pressure errors due to mismatch between the smooth topography implicit in the coarse resolution driving data and the varying topography resolved by the model (Hong and Juang 1998). Domain size may also influence RCM results. If a domain is too large, the model's interior flow may drift from the large-scale flow of the driving data set (Jones et *al*., 1995). However, too small a domain overly constrains interior dynamics, preventing the model from generating appropriate response to interior mesoscale-circulation and surface conditions (Seth and Giorgi, 1998). RCMs appear to perform well for domains roughly the size of the contiguous United States. **Figure III.A** shows that the daily, root-mean-square difference (RMSD) between simulated and observed (reanalysis) 500 hPa heights is generally within observational noise levels (roughly 20 m).

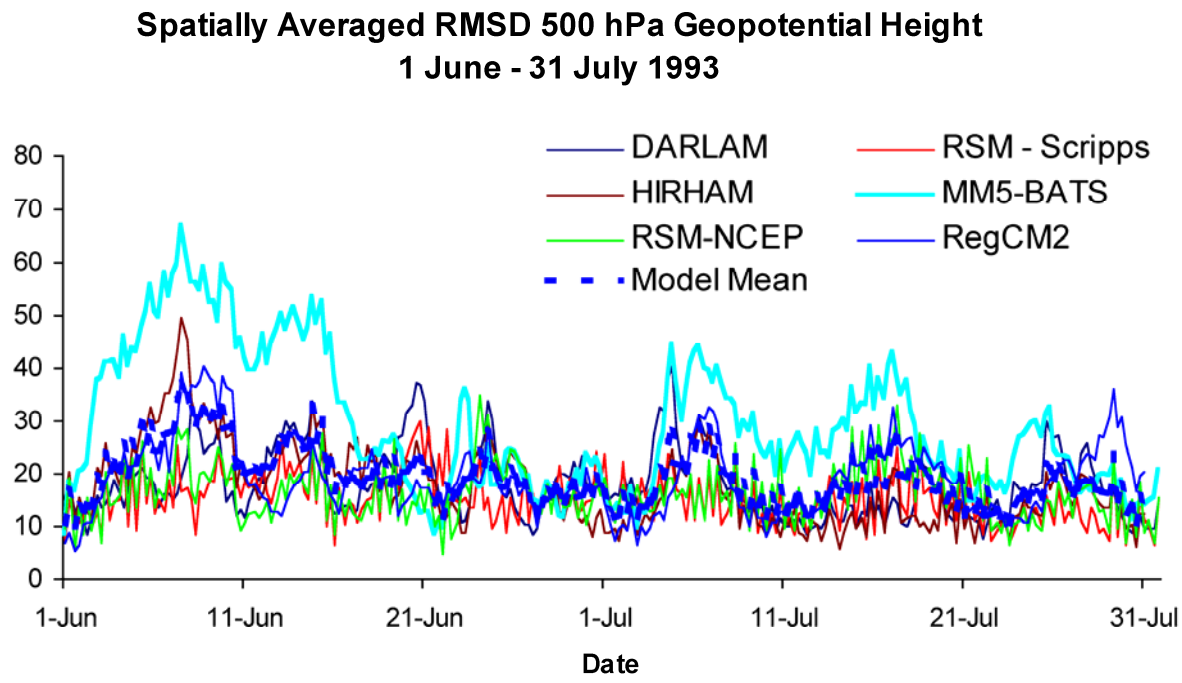

Figure III. A. Daily root-mean-square differences (RMSD) in 500 hPa height between observations (reanalysis) and 6 models participating in the PIRCS 1b experiment (Anderson *et al*., 2003). RMSD values averaged over the simulation domain inside the boundary-forcing zone. Also shown is the mean curve for the 6 models. (y-axis scale: meters).

Because simulations from the downscaling models may be analyzed for periods as short as a month, model spin-up is important (e.g., Giorgi and Bi, 2000). During spin-up the model evolves to conditions representative of its own climatology, which may differ from the sources of initial conditions. The atmosphere spins up in a matter of days, so the key factor is spin-up of soil moisture and temperature, which evolve more slowly. Equally important, data for initial conditions is often lacking or has low spatial resolution, so that initial conditions may be only a poor approximation to the model's climatology. Spin-up is especially relevant for downscaling because these models are presumably resolving finer surface features than coarser models, with the expectation that the downscaling models are providing added value through proper representation of these surface features. Deep soil temperature and moisture, at depths of 1–2 meters, may require several years of spin up. However, these deep layers generally interact weakly with the rest of the model, so shorter spin-up times are used. For multi-year simulations, 3–4 years appears to be a minimal requirement (Christensen, 1999; Roads *et al*., 1999). This ensures that the upper meter of soil has a climatology in further simulation that is consistent with the evolving atmosphere.

Many downscaling simulations, especially with RCMs, are for periods much shorter than two years. Such simulations likely will not use multi-year spin up. Rather, these studies may focus on more rapidly evolving atmospheric behavior that is governed by lateral boundary conditions, including extreme periods like drought (Takle *et al*.,1999) or flood (Giorgi *et al*., 1996; Liang *et al*., 2001; Anderson *et al*., 2003). Thus, they assume that the interaction with the surface, while not negligible, is not strong enough to skew the atmospheric behavior studied. Alternatively, relatively short regional simulations may specify, for sensitivity study, substantial changes in surface evaporation (e.g., Paegle et *al*., 1996), soil moisture (e.g., Xue et *al*., 2001) or horizontal moisture flux at lateral boundaries (e.g., Qian *et al*., 2004).

Even with higher resolution than standard GCMs, models simulating regional climate still need parameterizations for subgrid-scale processes, most notably boundary-layer dynamics, surface-atmosphere coupling, radiative transfer and cloud microphysics. . Most regional simulations also require a convection parameterization, though a few have used sufficiently fine grid-spacing, a few kilometers, to allow acceptable simulation without one (e.g., Grell et al., 2000). Often, these

parameterizations are the same or nearly the same as used in GCMs. However, all parameterizations make assumptions that they are representing the statistics of subgrid processes, and so implicitly or explicitly they require that the grid box's area in the real world would have sufficient samples to justify the stochastic modeling. For some parameterizations, such as convection, this assumption becomes doubtful when grid boxes become only a few kilometers in size (Emanuel 1994). In addition, models simulating regional climate may include circulation characteristics, such as rapid mesoscale circulations (jets) whose interaction with subgrid processes like convection and cloud cover differs from the larger scale circulations resolved by typical GCMs. This factor is part of a larger issue, that parameterizations may have regime dependence, performing better for some conditions than others. For example, the Grell (1993) convection scheme is responsive to large-scale tropospheric forcing, whereas the Kain and Fritsch (1993) scheme is heavily influenced by boundary-layer forcing. As a result, the Grell scheme simulates better the propagation of precipitation over the U.S. Great Plains that is controlled by the large-scale tropospheric forcing, while the Kain–Fritsch scheme simulates better late afternoon convection peaks in the southeastern U.S. that are governed by boundary-layer processes (Liang et *al*., 2004). As a consequence, parameterizations for regional simulation may differ from their GCM counterparts, especially for convection and cloud microphysics. As noted earlier, the regional simulation in some cases may have resolution of only a few kilometers and the convection parameterization may be discarded (Grell *et al*., 2000). A variety of parameterizations exist for each of these phenomena, with multiple choices often available in a single model (e.g., Grell *et al*., 1994; Skamarock *et al*., 2005).

The chief reason for performing regional simulation, whether by an RCM, a stretched-grid model or a time-slice AGCM, is to resolve behavior considered important for a region's climate that a global model does not resolve. Thus, regional simulation should have clearly defined regional-scale (mesoscale) phenomena targeted for simulation. These include, for example, tropical storms (e.g., Oouchi *et al.*, 2006), effects of mountains (e.g., Leung and Wigmosta, 1999; Grell *et al*., 2000; Zhu and Liang, 2007), jet circulations (e.g., Takle *et al*., 1999; Anderson *et al*., 2001; Anderson *et al*., 2003; Byerle and Paegle, 2003; Pan *et al.*, 2004) and regional ocean-land interaction (e.g., Kim *et al*., 2005; Diffenbaugh *et al*. 2004). The most immediate value, then, of regional simulation is to explore how such phenomena operate in the climate system, which becomes a justification for the expense of performing regional simulation. Phenomena and computational costs together influence

the design of regional simulations. Simulation periods and resolution are balances between sufficient length and number of simulations for climate statistics versus computational cost. For RCMs and stretched-grid models, the sizes of regions targeted for high-resolution simulation are determined in part by where the phenomenon occurs.

In the context of downscaling, regional simulation offers the potential to include phenomena affecting regional climate change that are not explicitly resolved in the global simulation. When given boundary conditions corresponding to future climate, regional simulation can then indicate how these phenomena contribute to climate change. Results, of course, are dependent on the quality of the source of the boundary conditions (Pan *et al*., 2001; de Elía *et al*., 2002), though use of multiple sources of future climate may lessen this vulnerability and offer opportunity for probabilistic estimates of regional climate change (Raisanen and Palmer, 2001; Giorgi and Mearns, 2003; Tebaldi et *al*., 2005). Results also depend on the physical parameterizations used in the simulation (Yang and Arritt, 200; Vidale *et al*., 2003; Déqué *et al*., 2005; Liang et *al*., 2006). Advances in computing power suggest that typical GCMs will eventually operate at resolutions of most current regional simulations (a few tens of kilometers), so that understanding and modeling improvements gained for regional simulation can promote appropriate adaptation of GCMs to higher resolution. For example, interaction between mesoscale jets and convection appears to require parameterized representation of convective downdrafts and their influence on the jets (Anderson *et al*., 2007), behavior not required for resolutions that do not resolve mesoscale circulations.

Because of the variety of numerical techniques and parameterizations employed in regional simulation, many models and versions of models exist. Side-by-side comparison (e.g., Takle *et al*., 1999; Anderson *et al*., 2003; Fu *et al*., 2005; Frei *et al*., 2006; Rinke *et al*., 2006) generally shows no single model appearing as best versus observations, with different models showing superior performance depending on the field examined. Indeed, the best results for downscaling climate simulations and estimating climate-change uncertainty may come from assessing an ensemble of simulations (Giorgi and Bi, 2000; Yang and Arritt, 2002; Vidale *et al*., 2003; Déqué *et al*., 2005). Such an ensemble may capture much of the uncertainty in climate simulation, offering an opportunity for physically based analysis of the climate changes and also the uncertainty of the

changes. Several regional models have performed simulations of climate change for parts of North America, but at present, there have been no regional projections using an ensemble of regional models simulating the same time periods with the same boundary conditions. Such systematic evaluation has occurred in Europe [PRUDENCE (Christensen *et al*., 2002) and ENSEMBLES (Hewitt and Griggs 2007) projects] and is starting in North America with the North American Regional Climate Change Assessment Program (NARCCAP 2007).

Empirical downscaling

Empirical, or statistical, downscaling is an alternative approach to obtaining regional-scale climate information (Kettenberg *et al*.,1996; Hewitson and Crane, 1996; Giorgi *et al*., 2001; Wilby *et al*., 2004, and references therein). It uses statistical relationships to link resolved behavior in GCMs with climate in a targeted area. The size of the targeted area can be as small as a single point. So long as significant statistical relationships occur, empirical downscaling can yield regional information for any desired variable, such as precipitation and temperature, as well as variables not typically simulated in climate models, such as zooplankton populations (Heyen *et al*.,1998) and initiation of flowering (Maak and von Storch, 1997). The approach encompasses a range of statistical techniques from simple linear regression (e.g., Wilby *et al*., 2000) to more complex applications, such as those based on weather generators (Wilks and Wilby, 1999), canonical correlation analysis (e.g., von Storch *et al*.,1993) or artificial neural networks (e.g., Crane and Hewitson, 1998). Empirical downscaling can be very inexpensive compared to numerical simulation when applied to just a few locations or using simple techniques. This together with the flexibility in targeted variables has led to a wide variety of applications for assessing impacts of climate change.

There has been some side-by-side comparison of methods (Wilby and Wigley, 1997; Wilby *et al*., 1998; Zorita and von Storch 1999; Widman *et al*., 2003). These studies have tended to show fairly good performance of relatively simple versus more complex techniques and to highlight the importance of including moisture as well as circulation variables when assessing climate change. There also has been comparison of statistical downscaling and regional climate simulation (Kidson and Thompson, 1998; Mearns *et al*.,1999; Wilby *et al*., 2000; Hellstrom *et al*., 2001; Wood *et al*.,

2004; Haylock *et al*., 2006), with neither approach distinctly better or worse than the other. Statistical methods, though computationally efficient, are completely dependent on the accuracy of regional temperature, humidity and circulation patterns produced by their parent global models. In contrast, regional climate simulation, though computationally more demanding, can improve the physical realism of simulated regional climate through higher resolution and better representation of important regional processes. The strengths and weaknesses of statistical downscaling and regional modeling are thus complementary.

Strengths and limitations of regional models

We focus here on numerical models simulating regional climate without discussing empirical downscaling because the wide range of applications using the latter undermines making a general assessment of strengths and limitations.

The higher resolution in regional-scale simulations provides quantitative value to climate simulation. With finer resolution, one can resolve mesoscale phenomena contributing to intense precipitation, such as stronger upward motions (Jones *et al*.,1995) and coupling between regional circulations and convection (e.g., Anderson *et al*., 2007). Time-slice AGCMs show intensified storm-tracks relative to their parent model (Solman *et al*., 2003, Roeckner *et al*., 2006). Thus, although regional models may still miss the most extreme precipitation (Gutowski *et al*., 2003, 2007), they can give more intense events that will be smoothed in coarser resolution GCMs. The higher resolution also includes other types of scale-dependent variability, especially short-term variability such as extreme winds and locally extreme temperature that coarser resolution models will smooth and thus inhibit.

Mean fields also appear to be simulated somewhat better on average versus coarser GCMs because spatial variations are potentially better resolved. Thus, Giorgi *et al*., (2001) report typical errors in RCMs of less than 2˚C temperature and 50% for precipitation for regions 10^5–10^6 km^2. Large-scale circulation fields tend to be well simulated, at least in the extratropics.

As alluded to above, regional-scale simulations also have phenomenological value, simulating processes that GCMs either cannot resolve or can resolve only poorly. These include internal circulation features such as the nocturnal jet that imports substantial moisture to the center of the United States and couples with convection (e.g., Byerle and Paegle, 2003; Anderson *et al*., 2007). These processes often have substantial diurnal variation and are thus important to proper simulation of regional diurnal cycles of energy fluxes and precipitation. Some processes require resolving surface features too coarse for typical GCM resolution, such as rapid topographic variation and its influence on precipitation (e.g., Leung and Wigmosta, 1999; Hay *et al*., 2006) and climatic influences of bodies of water like the Gulf of California (e.g., Anderson *et al*., 2001) and the North American Great Lakes (Lofgren, 2004) and their downstream influences. In addition, regional simulations resolve land-surface features that may be important for climate-change impacts assessment, such as distributions of crops and other vegetation (Mearns, 2003; Mearns *et al*., 2003), though care is needed to obtain useful information at higher resolution (Adams *et al*., 2003).

An important limitation for regional simulations is that they are dependent on boundary conditions supplied from some other source. This applies to all three forms of numerical simulation (RCMs, stretched-grid models, time-slice AGCMs), since they all typically require input sea-surface temperature and ocean ice. Some RCM simulations have been coupled to a regional ocean-ice model, with mixed-layer ocean (Lynch *et al*.,1995, 2001) and a regional ocean-circulation model (Rummukainen *et al*., 2004) but this is not common. In addition, of course, RCMs require lateral boundary conditions. Thus, regional simulations by these models are dependent on the quality of the model or observations supplying the boundary conditions. This is especially true for projections of future climate, suggesting that there is value in performing an ensemble of simulations using multiple atmosphere-ocean global models to supply boundary conditions.

Careful evaluation is also necessary to show differences, if any, between the large-scale circulation of the regional simulation and its driving data set. Generally, any tendency for the regional simulation to alter biases in the parent GCM's large-scale circulation should be viewed with caution (Jones *et al*., 1995). RCM should not normally be expected to correct large-scale circulation problems of parent model, unless there is a clearly understood physical basis for the improvement. Clear physical reasons for the correction due to higher resolution, such as better rendition of physical processes like topographic circulation (e.g., Leung and Qian, 2003), surface-

atmosphere interaction (Han and Roads, 2004) and convection (Liang *et al*., 2006), must be established. Otherwise, the regional simulation may simply have errors that counteract the parent GCM's errors, which undermines confidence of projected future climate.

RCMs may also exhibit difficulty in outflow regions of the domain, especially for domains with relatively strong cross-boundary flow, such as extratropical domains covering a single continent or less. The difficulty appears to arise because storm systems may track across the RCM's domain at a different speed than in the driving-data source, resulting in a mismatch of circulations at boundaries where storms would be moving out of the domain. Also, there are always unresolved scales of behavior, so the regional simulations are still dependent on the quality of their parameterizations for the scales explicitly resolved. Finally, the higher computational demand due to shorter time steps limits the length of typical simulations to two to three decades or less (e.g., Christensen *et al*., 2002; NARCCAP, 2007), with few ensemble simulations to date.

Chapter IV – Model Climate Sensitivity

The response of climate to a perturbation, like a change in carbon dioxide concentration, or in the flux of energy from the sun, can be divided into two parts; the “radiative forcing” due to the perturbation in question; and the ”climate sensitivity”, characterizing the response of the climate per unit change in the radiative forcing. The climate response is then the product of the radiative forcing and the climate sensitivity. While it is not always perfectly clear, this distinction is useful in analyzing and discussing climate change. The utility of this decomposition is based on several considerations: radiative forcing can often be usefully considered as external to the climate system; climate sensitivity can often be thought of as independent of the agent responsible for the forcing; and when two or more factors are simultaneously present, one can approximate their cumulative effect by adding their respective radiative forcings.

Radiative forcing is typically calculated by changing the atmospheric composition or external forcing very quickly and computing the net trapping of heat that occurs before the climate system has had time to adjust. In the case of carbon dioxide, it has become standard to use the surface-plus-troposphere heating (encompassing both the surface and the altitude range of about 0-10 km in the atmosphere) in the definition of radiative forcing. The direct heat-trapping properties are very well characterized for the most significant greenhouse gases. As a result, uncertainty in climate responses to the greenhouse gases are typically dominated by uncertainties in climate sensitivity rather than in radiative forcing (Ramaswamy et al. 2001). For example, suddenly doubling the atmospheric amount of carbon dioxide would add energy to the surface and the troposphere at the rate of about 4 Watts per square meter for the first few months after the doubling, according to the most recent estimates (Forster and Ramaswamy, 2007). Eventually temperatures would increase (and climate would change in other ways) in response to this forcing, Earth would radiate more heat to space, and the imbalance would be redressed as the system returned to equilibrium.

The idea of encapsulating global climate sensitivity in a single number appeared early in the development of climate models (Schneider and Mass 1975). Today, two different numbers are in common use. Both involve changes in global and annual mean surface or near-surface temperature. (The global and annual mean is obtained by averaging over both Earth’s total area and the cycle of

the seasons.) *Equilibrium warming* is defined as the long-term surface warming after atmospheric carbon dioxide has been doubled but thereafter held constant, and the climate is allowed to reach a new steady state, as described in the preceding paragraph. *Transient climate response* or TCR is defined by assuming that carbon dioxide increases by 1% per year and recording the increase in temperature at the time that carbon dioxide doubles (about 70 years after the increase begins).

Equilibrium warming is difficult to obtain from AOGCMs because the deep ocean takes thousands of years to fully respond to changes in climate forcing. To avoid unacceptably lengthy computer simulations, equilibrium warming is usually estimated from a modified climate model in which the ocean component is replaced by a simplified, fast-responding "slab ocean model." This procedure makes the assumption that ocean heat transports do not change as the climate changes. The equilibrium response is of greatest interest when comparing climate models with paleoclimatic data, while the transient climate response is of more direct relevance to the attribution of recent warming and projections for the next century.

US models exemplify the climate sensitivity of modern AOGCMs. Kiehl et al. (2006) examined the sensitivity of three successive versions of the Community Climate System Model developed over a period of a decade: CSM1.4, CCSM2 and CCSM3. Stouffer et al. (2006) and Hansen et al. (2006) similarly studied the most recent GFDL and GISS models, respectively. As discussed above, these (and other) models differ in their details because development teams have differing ideas concerning the underlying physical mechanisms relevant for the less well-understood aspects of the system.

Climate sensitivity is an emergent, or holistic, property of the models – it is not input into the model. None of the U.S development teams engineered their models to produce a desired value of climate sensitivity.

Climate sensitivity values for the US models are shown in Table IV(1). Only the higher number associated with GISS Model E used a full OGCM as a part of the climate model. All other values of equilibrium warming in the table are obtained with the OGCM replaced by a slab ocean model.

Table IV 1 Model sensitivity values for US CMIP3 models

Model	**TCR**	**Equilib. warming***
CSM1.4	1.4°C	2.0°C
CCSM2	1.1°C	2.3°C
CCSM3	1.5°C	2.5°C
GFDL CM2.0	1.6°C	2.9°C
GFDL CM2.1	1.5°C	3.4°C
GISS Model E		2.7-2.9°C

Note that equilibrium warming is greater than TCR for any given model. This is because TCR is measured before the deep ocean, with its large thermal inertia, has had time to warm fully in response to doubled atmospheric carbon dioxide. Comparing different rows within any single column, it is apparent that a wide range of equilibrium sensitivity values are obtained by different models. Nearly three decades ago, Charney (1979) judged the range of equilibrium warming due to doubled atmospheric carbon dioxide, based on the few model calculations then available, to be 1.5-4.5°C, a three-fold range of uncertainty. The table might suggest a reduction in this range, but including other models in the CMIP3 archive expands the upper end; the full CMIP3 range is 2.1 to 4.4°C with a median of 3.2°C. Furthermore, a systematic exploration of plausible input parameters for a single (Hadley Centre) model gives a 5-95 percentile range of ~2-6°C, again a three-fold span (Piani et al. 2005, Knutti et al. 2006). The low end of the equilibrium sensitivity range is thought to be more certain than the high end (Bierbaum et al. 2003,Randall and Wood, 2007.) It is difficult to reconcile a very low sensitivity value with the climate changes observed during the past century (Andronova and Schlesinger 2001, Forest et al. 2001) and inferred for the more distant past (Hansen et al. 1993, Covey et al. 1996).

The variation among models is less for TCR than for equilibrium warming because enhanced equilibrium sensitivity correlates with enhanced heat transport to the deep ocean, and these two effects cancel to some extent in transient simulations (Covey et al. 2003). Apart from CCSM2, model TCR varies by less than 15% in the table above. Systematic exploration of model input parameters in one Hadley Centre model gives a wider range, 1.5-2.6°C (Collins et al. 2006). The full range in the CMIP3 archive is 1.3-2.6°C, with a median of 1.6°C and with the half of the models within the 25%-75% quartiles of the distribution lying within the relatively small range of 1.5-2.0°C (Randall and Wood, 2007).

Climate sensitivity can be altered in a model by modifying aspects of the models that are relatively poorly constrained by observations or theory. In an influential early paper, Senior and Mitchell (1993, 1996) demonstrated how a seemingly minor modification to the cloud prediction scheme can alter climate sensitivity. In the standard version of the model, the effective size of cloud drops is fixed. In two other versions, this cloud drop size is tied to the total amount of liquid water in the

cloud through two different empirical relationships. The equilibrium global mean warming ranged from from 1.9^{o}C to 5.5^{o}C in response to doubling CO_2 in the atmosphere in these three models.

Studies of the CCSM family of models provide another example of this problem. Kiehl et al. (2006) found that a variety of factors are responsible for differences in climate sensitivity among the models of this family. Most notably, the generally lower sensitivity of CCSM2 (evident in Table IV(1)) is mainly due to a single change (relative to CSM1.4 and CCSM3) in the model's algorithm for simulating convective clouds. CCSM3's formulation reflects intensive efforts to represent climate processes more accurately than its predecessors CSM1.4 and CCSM2, but it is not clear whether the resulting global climate sensitivity is closer to reality.

Fig. IV A below shows how equilibrium warming due to doubled atmospheric carbon dioxide varied during the development of the most recent GFDL models. The dramatic drop in sensitivity between model versions p10 and p12.5.1 was unexpected. It followed a reformulation of the model's treatment of processes in the lower atmospheric boundary layer which, in turn, affected how low level clouds in the model respond to climate change.

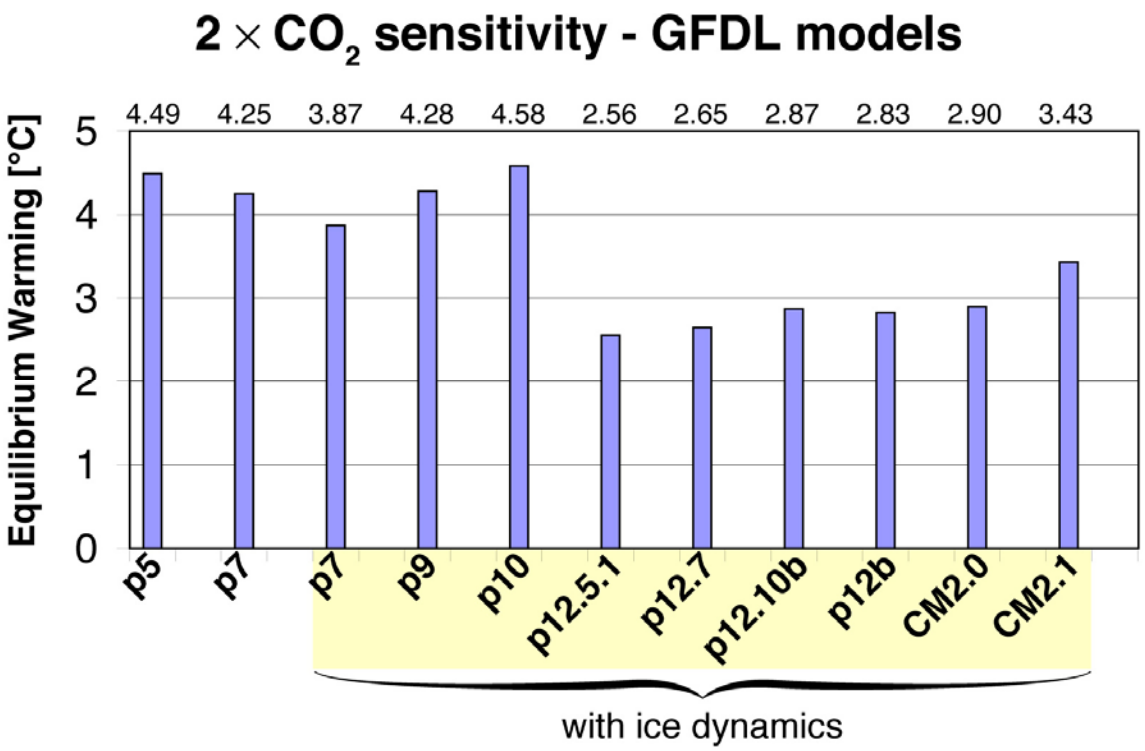

Figure IV A: Equilibrium global mean near-surface warming due to doubled atmospheric carbon dioxide from intermediate ("p") model versions leading to GFDL's CM2.0 and CM2.1. Equilibrium warming was assessed by joining a simplified slab ocean model to the atmosphere, land and sea ice AOGCM components. The later versions include sea ice motion (dynamics) as well as sea ice thermodynamics.

Better understanding of Earth's climate sensitivity, with potential reduction in its uncertainty, will require better understanding of a multitude of climate feedback processes (Bony et al. 2006). We discuss two of the most important of these feedback effects below. The strengths of these feedbacks are most frequently described by the resulting change in the heating of the troposphere-plus-surface per degree warming of global mean temperature, in units of W/m2/K.

Cloud Feedbacks

Clouds reflect solar radiation to space, cooling the Earth-atmosphere system. Clouds also trap infrared radiation, keeping the Earth warm. The net effect depends on the height, location, microphysical and radiative properties of clouds, and their appearance in time with respect to the seasonal and diurnal cycles of the incoming solar radiation. Cloud feedback refers to the changes in cloud amounts and properties that can either amplify or moderate a climate change. Uncertainties of cloud feedbacks in climate models have repeatedly been identified as the leading source of uncertainty in model-derived estimates of climate sensitivity (e.g., Cess et al 1990; Randall et al. 2000; Zhang 2004; Stephens 2005; Bony et al. 2006; Soden and Held 2006). The fidelity of cloud feedbacks in climate models is therefore important to the reliability of their prediction of future climate change.

Several diagnostic methods have been used to evaluate and understand cloud feedbacks in AGCMs. One method is referred to as partial radiative perturbation (PRP) (e.g., Hansen et al. 1984; Wetherald and Manabe 1988; Zhang et al. 1994; Soden et al. 2004; Soden and Held 2006). A second method uses the changes in cloud radiative forcing (CRF) (Cess and Potter 1988). The CRF approach is more commonly used because of convenience of calculation and, most importantly, the availability of satellite data for comparison. There are significant differences between the diagnosed feedbacks from the two methodologies (Zhang et al. 1994; Coleman 2003; Soden et al. 2004), with the PRP estimates, considered to be more appropriate for feedback analyses, producing cloud feedbacks that are more positive by roughly 0.6 $W/m^2/K$, causing some confusion in the literature on cloud feedbacks. The differences between models are similar using either technique, and both correlate well with the climate sensitivity across models.

Early GCM cloud feedback studies diagnosed positive cloud feedbacks (Hansen et al. (1984); Wetherald and Manabe (1988)) using the PRP approach. In an influential work, Cess et al. (1990) used the response of models to a simple warming or cooling of the oceans by 2^oK as a surrogate climate change and diagnosed the cloud feedbacks in 19 GCMs using the CRF approach, showing a wide range of values from negative to strongly positive. Many subsequent studies with other GCMs also showed large sensitivity of cloud feedbacks to the formulation of model physics (e.g., Le Treut et al. 1994; Yao and Del Genio, 2002; Soden et al. 2004; Yokohata et al., 2005).

Many recent studies have focused on categorizing and decomposing the model cloud feedbacks according to the simulated meteorological conditions, rather than lumping them into a single global number. Williams et al. (2003), Bony et al. (2004), and Wyant et al. (2006) showed that in the tropical region, the CRF response differs most between models in subsidence regimes in which deep convection is suppressed, and not primarily in the regions of deep convection, suggesting a dominant role for low-level clouds in the diversity of modelled tropical cloud feedbacks. Others have also diagnosed errors in the simulation of particular cloud regimes or in specific dynamical conditions (Klein and Jakob, 1999; Tselioudis et al., 2000;; Webb et al., 2001, Norris and Weaver, 2001; Jakob and Tselioudis, 2003; Williams et al., 2003; Bony et al., 2004; Lin and Zhang, 2004; Ringer and Allan, 2004; Bony and Dufresne, 2005; Del Genio et al., 2005; Williams et al., 2006; Wyant et al., 2006). Zhang et al. (2005) evaluated clouds in ten AGCMs and showed that even though they simulate reasonable radiation balance at the top of the atmosphere, models have systematic compensatory cloud biases. Common among them are overestimation of optical thick clouds and underestimation of middle and low clouds. The biases are large enough to affect the ability to simulate cloud feedback in a climate change.

Soden and Held (2006) evaluated cloud feedbacks in 12 CMIP3 coupled models using simplified PRP calculations. They showed positive cloud feedback in all models, ranging from 0.14 $W/m^2/K$ to 1.18 $W/m^2/K$. The highest values raise the equilibrium climate sensitivity from typical values of 2K for CO_2 doubling, a typical value in the absence of cloud feedback, to roughly 4K. Comparing with the earlier studies of Cess (1990) and Coleman (2003), the spread among GCMs has become somewhat smaller over the years, but it is still very substantial.

Results are beginning to emerge from a new class of much higher resolution atmospheric simulations. Using the surrogate climate change framework of Cess (1990) in which ocean temperatures are warmed uniformly, Miura et al. (2005) carried out experiments with a global model with 7 km resolution, obtaining a climate sensitivity that is significantly reduced by strong negative (CRF) feedback outside of the tropics. A multi-grid technique in which high resolution cloud models are embedded in each grid box of a traditional GCM was utilized by Wyant et al. (2006) and generated a negative CRF response of -0.9 $W/m^2/K$ in the same Cess framework (corresponding to roughly neutral PRP cloud feedbacks). Much work will be required with these new types of models before they can be given substantial weight in discussions of the most probable value for cloud feedbacks, but they are hinting that the feedback may be less positive than is typical in the CMIP3 AGCMs. Results from this new generation of models will be of considerable interest in the coming years.

Several questions remain to be answered about cloud feedbacks in GCMs. The physical mechanisms underlying cloud feedbacks in different models must be better characterized, so that we can better appreciate which features and mechanisms in these models are robust across the models and which are not. It is not clear how best to judge the importance of model biases in simulations of the current climate, and in the simulations of cloud changes in different modes of observed variability. In particular, it is unclear how to translate these biases into levels of confidence in the simulations of cloud feedback processes in climate change scenarios. New satellite products such as those from active radar and lidar systems will undoubtedly play vital role in cloud research in the coming years, and are providing more confidence that progress on these difficult questions can be achieved.

Water Vapor Feedback

Analysis of the radiative feedbacks in the CMIP3 models (Soden and Held, 2006) reaffirms that water vapor feedback, the increase in heat trapping due to the increase in water vapor as the climate warms, is fundamental to their climate sensitivity. The strength of the water vapor feedback in these

models is typically close in magnitude but slightly weaker than that obtained by assuming that relative humidity remains unchanged as the climate warms.

A trend towards increasing column water vapor in the atmosphere consistent with model predictions has been documented from microwave satellite measurements (Trenberth, et al 2005) and excellent agreement has been found between satellite observations and climate models constrained by the observed ocean surface temperatures (Soden, 2000). These studies increase confidence in the model's vapor distributions more generally, but they are dominated by changes in the lower troposphere and do not directly address the bulk of the water vapor feedback issue. This feedback is primarily a consequence of increases in water vapor in the tropical upper troposphere. Studies of vapor trends in this region are therefore of central importance. Soden (2006) presents analysis of radiance measurements (from the infrared sounder on NOAA satellites) that relative humidity has remained unchanged in the upper tropical troposphere over the past few years, which combined with temperature measurements provides evidence that water vapor in this region is increasing.

One can use observations of interannual variability in water vapor to help judge the quality of model simulations. Recently, Minchswaner, et al (2006) have compared the interannual variability in humidities in the highest altitudes of the tropical troposphere, as measured by infrared limb sounding satellites, with CMIP3 20th century simulations. Both models and observations show a small negative correlation between relative humidity and tropical temperatures, due to in large part to a tendency for lower relative humidity in warm El-Nino years and higher values in cold La Nina years. However, there is a suggestion that the magnitude of this co-variation is underestimated in most of the models. Looking across the models, there is also a tendency for models with larger interannual variations in relative humidity to produce larger reductions in this region in response to global warming, suggesting that this deficiency in interannual variability might be relevant for climate sensitivity. Thus, this study provides indirect evidence suggesting that the feedback for the very highest levels of the tropical troposphere may be overestimated somewhat in models.

The potential for the uncertainties in cloud feedbacks to impact water vapor feedbacks in the tropics, through evaporation of condensate, remains a possibility. But analyses examining the

extent to which tropical humidities can be understood without considering sources from condensate, such as Dessler and Sherwood (2000) continue to suggest that effects of this kind are small.

The CMIP3 simulations of the water vapor climatology has also been critically analyzed (e.g., Pierce et al, 2006). Despite uncertainties in the observations, some systematic deficiencies are clear, but just as for clouds, it is not straightforward to judge which kinds of deficiencies in the models are of most concern for estimating feedback strength.

The strength of water vapor feedback varies somewhat across models, but its strength is inversely correlated with the lapse rate feedback (Zhang et al, 1994; Soden and Held, 2006). The latter is a way of accounting for the fact that temperatures do not warm uniformly in response to greenhouse gas increases. In particular, models generally predict that that the tropical upper troposphere warms more rapidly than the surface. Due to the increased infrared emission to space from the warm upper troposphere, the surface need warm less for the system to come to energy balance with the radiative forcing, providing a negative feedback on surface temperatures. Since much of the water vapor feedback comes from the tropical upper troposphere as well, there is some cancellation between these two effects, resulting in a net feedback ranging from 0.8-1.2 $W/m^2/C$ in the CMIP3 study of Soden and Held (2006). There is considerably less scatter among the models when one sums the water vapor and lapse rate feedbacks than in either of these individual contributions in isolation.

Disparities In Imposed Radiative Forcing

While increases in the concentration of greenhouse gases provide the largest change in radiative forcing during the twentieth century (IPCC AR4), other forcings must be considered to account for the observed change in surface air temperature. The burning of fossil fuels that releases greenhouse gases into the atmosphere can also create aerosols (small liquid droplets or solid particles that are temporarily suspended in the atmosphere) that cool the planet by reflecting sunlight back to space. In addition, there are changes in land use that change the reflectivity of the earth's surface, as well as variations in sunlight impinging on the earth, among other forcings. In this section, we briefly discuss the extent to which twentieth century radiative forcing is known. Further information is provided in Forster and Ramaswamy (2007).

The radiative forcing can be quantified in different ways, as outlined by Hansen, et al 2005. The radiative response to CO_2 doubling at the top of the atmosphere can be computed for example, by holding all atmospheric and surface temperatures fixed, by allowing the stratospheric temperatures to adjust to the new CO_2 levels, by fixing surface temperatures over both land and ocean and allowing the atmosphere to equilibrate, and fixing ocean temperatures only and allowing the atmosphere and land to equilibrate. Comparing model forcings in the literature is made more complex because of differing definitions in different papers. Compared to the pre-industrial, present-day forcing in GISS modelE is 1.77 W/m^2 when computed with fixed ocean temperatures (Hansen et al. 2007), but it is 2.1 W/m^2 in the GFDL CM2.1 model (I. Held, personal communication) using the same definition, while it is 2.6 W/m^2 if only the stratosphere is allowed to adjust (D. Schwarzkopf, personal communication). Variations in radiative forcing among models introduce uncertainty in the simulation and attribution of twentieth century climate change.

Greenhouse gases like carbon dioxide and methane have atmospheric lifetimes that are long compared to the time required for these gases to be thoroughly mixed throughout the atmosphere. Trends in concentration are consistent throughout the world, and have been measured routinely since the International Geophysical Year in 1958. Measurements of the gas bubbles trapped in ice cores give the concentration prior to that date with less time resolution. While changes in greenhouse gas concentration are accurately known, the associated radiative forcing varies among climate models. This is partly because GCM radiative calculations need to be computationally efficient, necessitating various approximations to calculations based upon the most accurate laboratory spectroscopic data and radiation algorithms. Using changes in well-mixed greenhouse gases, including carbon dioxide, methane, nitrous oxide and chlorofluorocarbons, measured between 1860 and 2000, Collins et al (2006) compared the radiative forcing computed by climate models (including CCSM, GFDL, and GISS) for clear sky conditions in midlatitude summer. The GCM values were further compared to line-by-line (LBL) calculations, where fewer approximations are made, and small differences result mainly from the omission of particular absorption bands (Collins et al 2006). The median LBL forcing at the top of the model by greenhouse gases is 2.1 W/m2, and the corresponding median among the climate models is higher by only 0.1 W/m2. However, the standard deviation among model estimates is 0.30 W/m2 (compared to 0.13 for the

LBL models). In general, forcing calculated by the CCSM and GISS models is on the high side of estimates, while the GFDL model is on the low side. For a doubling of greenhouse gas concentration, CCSM and GISS calculate forcing at the top of the atmosphere of 3.95 and 4.06 W/m2, respectively, while the GFDL model calculates 3.50 W/m2 compared to the all-model average of 3.67 +/- 0.28 W/m2 (W. Collins, personal communication), for this particular atmospheric profile. LBL calculations are not available for the entire globe, and uncertainties in the observed 3-dimensional cloud distribution create additional uncertainties in the forcing computations. But based on these most recent comparisons with LBL computations, it is reasonable to assume that radiative forcing due to carbon dioxide doubling in individual climate models, including the US models, may be in error by roughly 10 percent.

Aerosols have short lifetimes, on the order of a week or so, that prevents them from dispersing uniformly throughout the atmosphere, in contrast to well-mixed greenhouse gases. Consequently, aerosol concentrations have large spatial variations, which are currently not measured with sufficient detail. Global radiative forcing by aerosols has historically been estimated using physical models of aerosol creation and dispersal constrained by the available observations. Recent estimates center around -1.5 W/m2 (Anderson et al., 2003). Satellite retrievals are increasingly used to provide direct observational estimates, which range from 0.35-0.25 W/m2 (Chung et al 2005) to -0.5-0.33 W/m2 (Yu et al 2006) to -0.8-0.1 W/m2 (Bellouin et al 2005) (??). That these estimates do not overlap suggests that there are assumptions that are not represented in the formal uncertainty analysis of each study. In particular, each calculation must decide how to extract the anthropogenic fraction of aerosol within each column. Because aerosol species are not retrieved directly, and the instruments cannot identify the original source region, this extraction is uncertain. In the absence of species identification, the optical properties used in the calculation of radiative forcing are also imprecisely known. Future satellite instruments will identify aerosol type with greater accuracy, improving the forcing estimates.

Global forcing by aerosols is estimated by the IPCC AR4 as -0.2 +/- 0.2 W/m2, according to models, and -0.5 +/- 0.4 W/m2, based upon satellite estimates. This represents decreased uncertainty compared to the 2001 IPCC estimate of -0.9 +/- 0.5 W/m2. However, this represents only the direct radiative forcing by aerosols: that is, the change in the radiative fluxes through

scattering and absorption of photons by aerosol droplets or particles. Aerosols also act as cloud condensation nuclei, and alter radiative forcing by clouds. For example, an increase in aerosol number increases the condensation nuclei available for cloud droplet formation, which has the potential to increase cloud droplet number. If the total cloud water is unchanged by the aerosols, the cloud will nonetheless be brighter because a larger number of smaller cloud droplets have a larger cross-sectional area for reflection of sunlight. This is the first aerosol indirect effect (Twomey 1977). Smaller cloud droplets are also thought to slow the coalescence and growth of rain droplets, reducing precipitation efficiency and extending the cloud lifetime: the second aerosol indirect effect (Albrecht 1989). Aerosol changes to cloud droplet density can also alter dynamical mixing within the cloud, affecting cloud cover and lifetime (Ackerman et al, 2004). Because of the complex interactions between aerosols and dynamics along with cloud microphysics, the aerosol indirect effect is very difficult to measure directly, and model estimates vary widely. This effect was generally omitted from the IPCC AR4 models, although it was included in GISS modelE where increased cloud cover due to aerosols results in a twentieth century forcing of -0.87 W/m2 (Hansen et al 2007).

Other model forcings include variability of solar irradiance and volcanic aerosols. Satellites provide the only measurements of these quantities at the top of the atmosphere. Prior to the satellite era in the 1970's, solar variations are inferred using records of sunspot area and number and cosmic ray-generated isotopes in ice cores (Foukal et al 2006), which are converted into irradiance variations using empirical relations. The US CMIP3 models all use the solar reconstruction by Lean et al (1995) with subsequent updates. Prior to the satellite era, volcanic aerosols are inferred from surface estimates of aerosol optical depth. The radiative calculation requires aerosol amount and particle size, which is inferred using empirical relations with optical depth derived from recent eruptions. The GFDL and GISS models use updated versions of the Sato et al (1993) eruption history, while CCSM uses Ammann et al (2003).

Land use changes are also uncertain, and can be of considerable signficance locally, but global models typically show very modest global responses, as discussed in Hegerl and Zwiers, 2007.

Studies attributing 20th century global warming to various natural and human-induced forcing changes are clearly hindered by these uncertainties in radiative forcing, especially in the solar and aerosol components. Recent satellite measurements of solar irradiance are of vital importance because they show that the Sun's contribution to the rapid warming of the past several decades is small. The relevance of solar energy output changes for the warming earlier in the 20th century is more uncertain. Given the solar reconstructions in use in the CMIP3 models, much of the early 20th century warming is driven by solar variations in these models, but uncertainties in these reconstructions do not allow confident attribution statements concerning this early century warming. The large uncertainties in aerosol forcing are the most important reason that one cannot use the observed late 20th century warming to provide a sharp constraint on climate sensitivity. We do not have good estimates of the fraction of the greenhouse gas forcing that has been cancelled by aerosols.

Ocean heat uptake/content related to climate sensitivity

The uncertainties associated with modeling of the uptake of heat by the ocean are significant in our understanding of the robustness of the estimates of the Earth's future global temperature. The degree to which the ocean takes up heat inversely affects the earth's surface temperature (e.g. Sun and Hansen 2003). Studies show (e.g. Volker et al. 2002) that CO_2 uptake by the ocean is also linked in complicated ways to the ocean's temperature. In an AOGCM, the ocean component's ability to take up heat is dependent upon how a model defines the physics to handle the mixing of heat and salt and how it transports heat between the low latitudes (where heat is taken up by the ocean) and high latitudes (where heat is given up by the ocean). The processes involved make use of several parameterizations (see section describing the ocean component of an AOGCM) and these parameterizations have their own uncertainties. Hansen et al. (1985) and Wigley and Schlesinger (1985) explored, early on, the important role of the ocean in moderating global temperatures and associated uncertainties in mixing parameters. Thus, as part of understanding any given model's climate sensitivity value, it is necessary to also understand its ability to accurately represent the ocean's mixing processes and the transport of the ocean's heat as well as feedbacks between the ocean, ice, and atmosphere.

Unfortunately, the relative importance of the uptake rate as compared to other processes, including feedbacks between the ocean and atmosphere, is still an open research topic. The uncertainties in the estimates of ocean uptake are not well understood. Comparisons of ocean heat uptake with respect to climate sensitivity mostly compare a few runs of the same model and runs between different AOGCMs. Raper et al. (2002) examined climate sensitivity and ocean heat uptake in a suite of recent AOGCMs. They calculated the ratio of the change in heat flux to the change in temperature (defined as the "ocean heat uptake efficiency": **k** by Gregory and Mitchell 1997) and found a general trend in the models that lower ocean uptake efficiency values were associated with lower climate sensitivity values. In an example that compares a current generation of AOGCM to previous generation AOGCMs, Kiehl et al. (2006) demonstrate that the atmospheric component of the models is the primary reason for different climate sensitivities and the ocean component's ability to uptake heat is of secondary importance. How the atmosphere affects the ocean's surface density is the important factor, rather than the particular aspects of the ocean component that is being used. The ocean heat uptake efficiency values calculated, in this second study, are not consistent with Raper et al. (2002), in that the model with the highest ocean heat update efficiency has the lowest climate sensitivity and the reasons for the differences are not understood. In a related study, Stouffer et al. (2006), using a different current AOGCM, conclude that a more realistic Southern Hemisphere atmospheric jet may produce a more realistic representation of the ocean's heat uptake in this region.

Impact of climate sensitivity on using model projections of future climates

This chapter -- and most investigations -- emphasize the global and annual mean of surface temperature change, even though practical applications of climate change science involve particular seasons and locations. The underlying assumption is that local climate impacts scale with changes in global surface temperature. Results of idealized simulations (the transient climate response experiments discussed above) indicate that this assumption may indeed be a reasonable first approximation to model behavior. Figure IV-B-1 shows, for North America, the ratio of the warming near the time of atmospheric carbon dioxide doubling (TCR as defined above) to its global mean value for the "average" CMIP3 model and each of the three US models. In all cases, the warming generally increases with latitude, and interior regions warm more than coastal areas. The

similarity of the four maps indicates a rough agreement of "scaled" regional warming among the models. The agreement occurs despite ~50% differences in globally averaged surface temperature change among the US models (Table IV.1).

Figure IV-B-2 shows the analogous results for precipitation change. Here the changes are generally positive in the Eastern US and negative in the Western US, consistent with the general finding that wet areas become wetter and dry areas become drier in global warming scenarios. The ratios of local to global mean precipitation change (which in turn scales with global mean temperature change) are again quite similar among the three US models as well as the "average" CMIP3 model.

Figure IV B 1 Ratio of annual local surface temperature change to annual global surface temperature change in mean CMIP3 model and three US CMIP3 models for idealized CO_2 doubling.

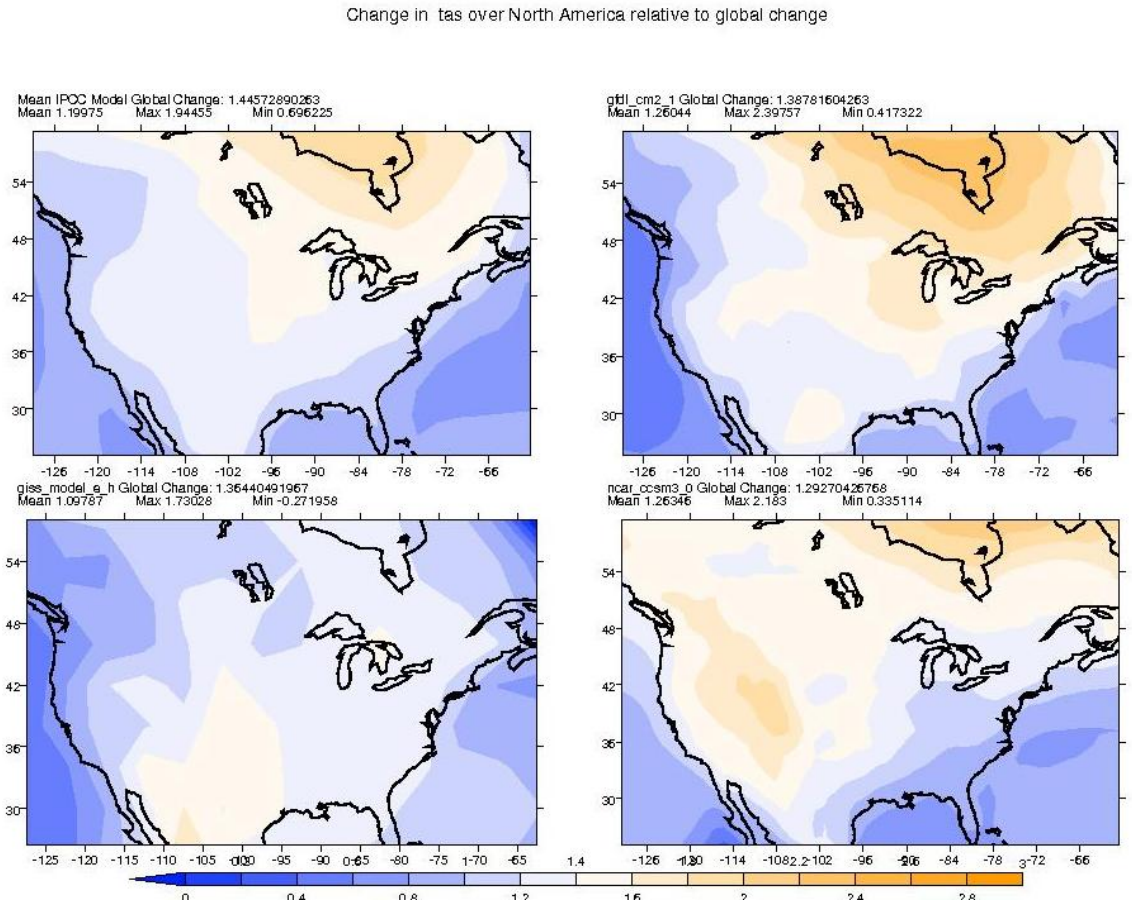

Figure IV B 2 Ratio of annual local precipitation change to global annual precipitation change in mean CMIP3 model and three US CMIP3 models for idealized CO_2 doubling.

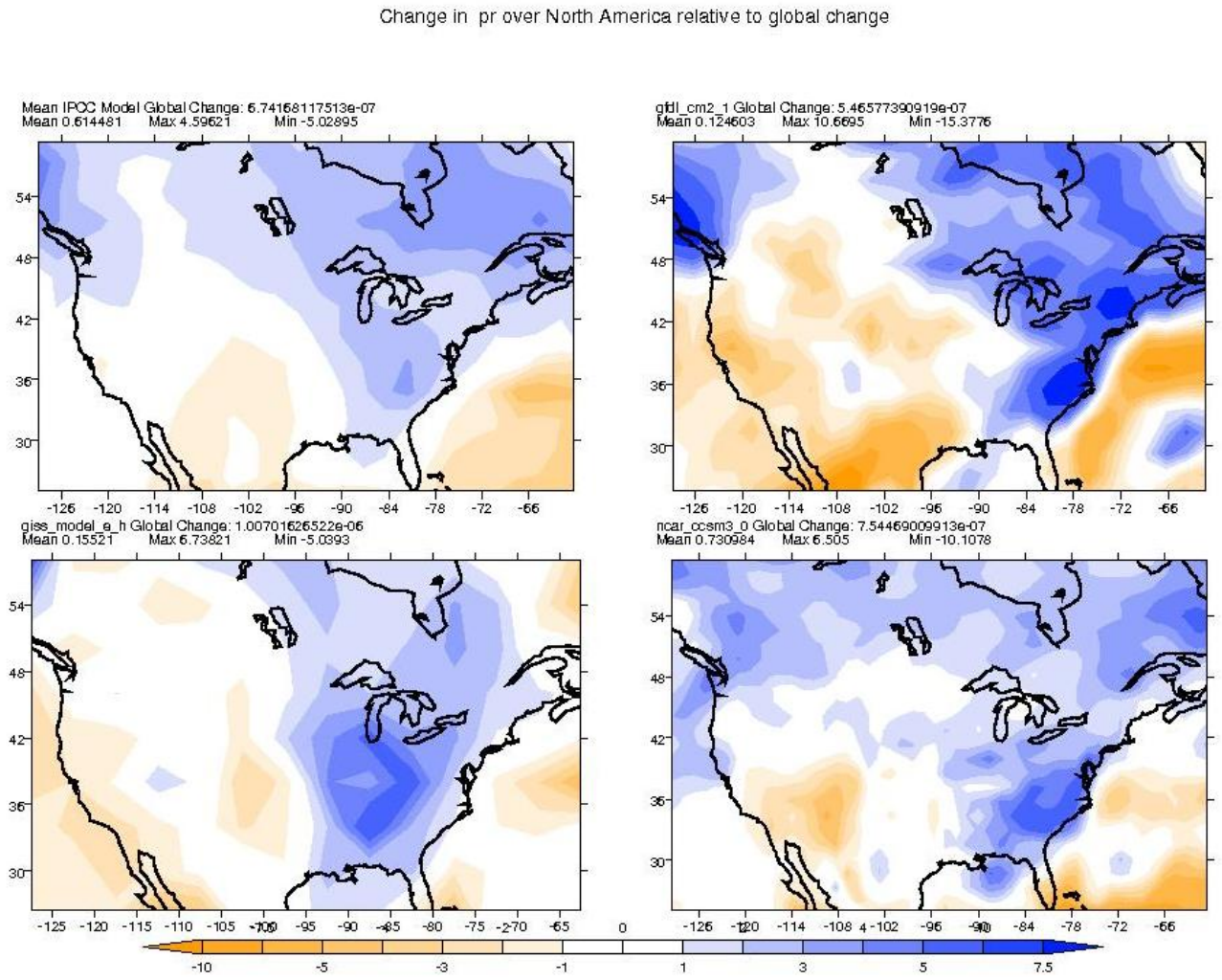

Chapter V: Model simulation of major climate features

Mean climate

Monthly mean near-surface temperature is well simulated by modern AOGCMs. This success occurs despite the fact that nearly all models now allow the ocean and atmosphere to exchange heat and water without explicitly forcing agreement with observation by artificial adjustment to air-sea fluxes. Figure V A quantifies the extent of agreement between simulations by several models and observations for both temperature and precipitation (the triangular points will be discussed in Chapter VI below). Each model's temperature or precipitation simulation produces a single point on the diagram, but in the figure, the ranges of results from all the models are shown as shaded areas.

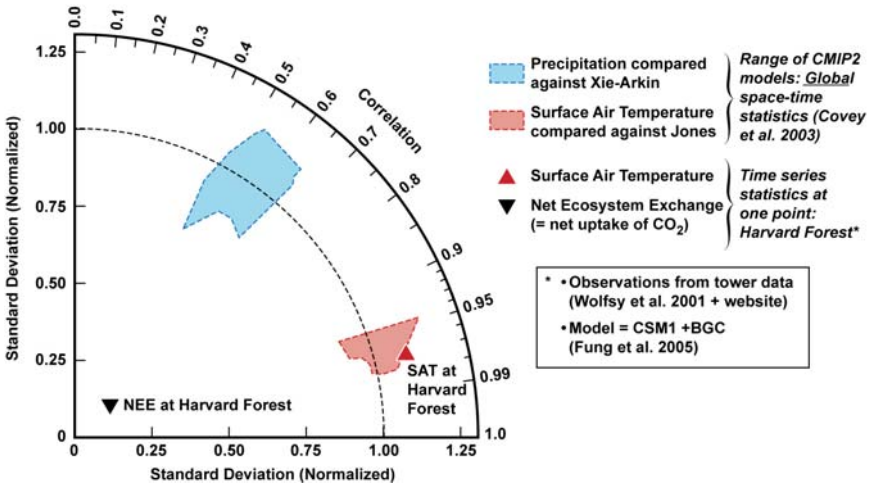

Figure V. A. Taylor Diagram of CMIP3 models

This type of diagram (Taylor 2001) displays the overall space-time correlation between simulated and observed variables as an angular coordinate. A 100% perfect correlation would place a point along the horizontal direction to the right, while zero correlation would place a point along the upward vertical direction. Looking at the red-shaded area that depicts the range of near-surface temperature simulations, one sees a remarkable 95–98% correlation with observations. The second independent (radial) coordinate in the diagram gives the ratio of simulated to observed amplitude for the variations that are being correlated. A value of 1.0 indicates perfect agreement of the amplitudes. In this coordinate system, complete agreement between simulation and observation in both dimensions would place a point where the dashed semicircle and the horizontal line intersect. The distance from this point to the actual point for any given model is proportional to the combined root-mean-square model error in both space and time dimensions. Temperature points for all of the models lie very close to complete agreement with observation—indeed nearly within the uncertainty range of the observations themselves (Covey *et al*., 2003).

For monthly mean precipitation, AOGCM simulations are considerably less precise than for temperature. The figure shows that overall space-time correlation between models and observations is ~50–60%. Qualitative examination of latitude-longitude maps shows that AOGCMs generally reproduce the observed broad patterns of precipitation amount and year-to-year variability (A. Dai, 2006: Precipitation characteristics in eighteen coupled climate models, J. Climate, in press). The most prominent error is that models without flux adjustment fail to simulate the observed northwest-to-southeast orientation of a large region of particularly heavy cloudiness and precipitation in the Southwest Pacific Ocean (the Southwest Pacific Convergence Zone or SPCZ). Instead, these models produce an unrealistic set of Inter-Tropical Convergence Zones in two parallel lines straddling the Equator: a “double ITCZ” pattern. The double-ITCZ error has been frustratingly persistent in climate models despite much effort to correct it. The average day-night cycle of temperature and precipitation in AOGCMs exhibits general agreement with observations, although simulated cloud formation tends to start too early in the day. Another discrepancy between models and observations appears upon sorting precipitation into light, moderate and heavy categories. Models reproduce the observed extent of moderate precipitation (10-20 mm/day) but underestimate the extent of heavy precipitation and overestimate the extent of light precipitation

(Dai 2006). Additional model errors appear when precipitation is studied in detail for particular regions, e.g. within the US (Ruiz-Barradas, A., and S. Nigam, 2007).

Taking examples from two of the US model families discussed in Chapter IV, one finds that AOGCM-simulated and observed maps of surface temperature and even precipitation appear rather similar at first sight. Constructing simulated-minus-observed "difference maps," however, reveals monthly and seasonal mean temperature and precipitation errors up to ~10°C and 7 mm / day respectively at some points (Figs V B, W. Collins *et al*., 2006; and V C Dellworth *et al*., 2006).

Figure V.B 1–4. CCSM3 annual mean simulated-minus-observed sea surface temperature [°C]

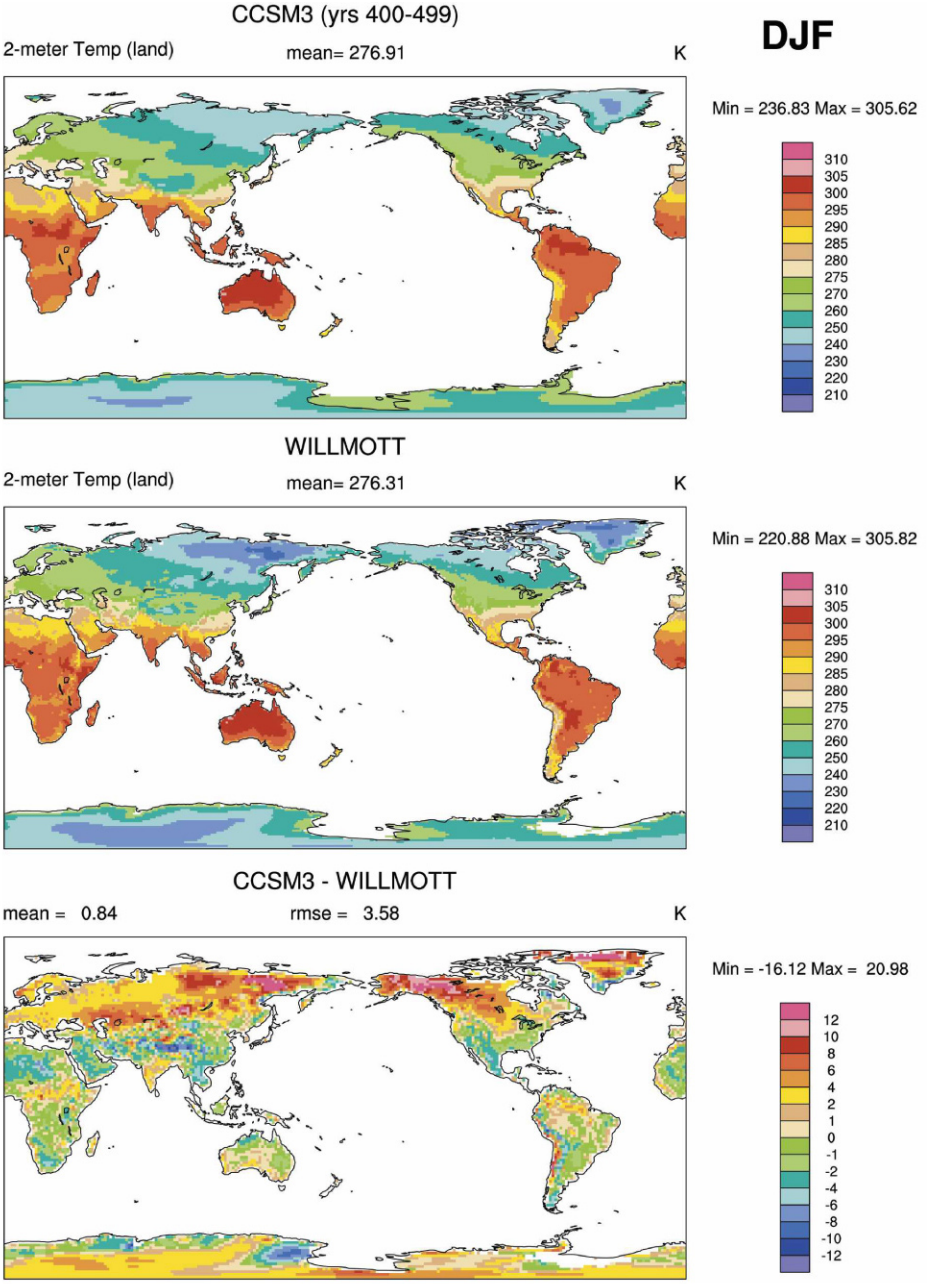

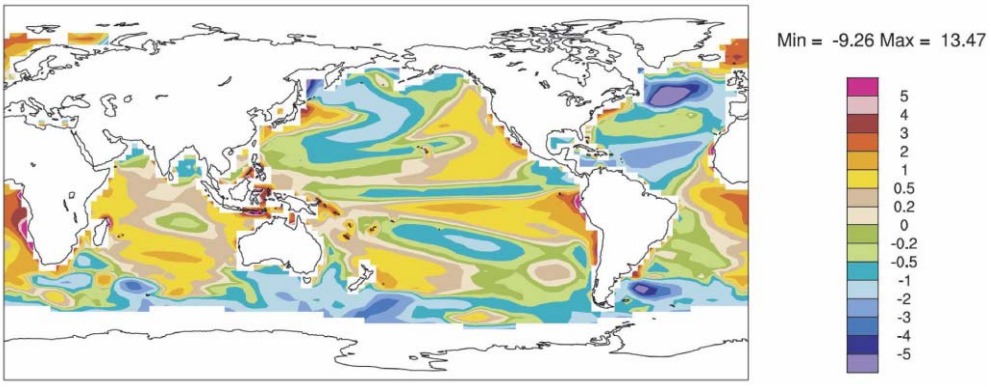

1

The CCSM3 temperature difference maps exhibit the largest errors in the Arctic (note scale change in last frame), where continental wintertime near-surface temperature is overestimated. AOGCMs find this quantity particularly difficult to simulate because, for land areas near the poles in winter, models must resolve a strong temperature inversion (warm air overlying cold air).

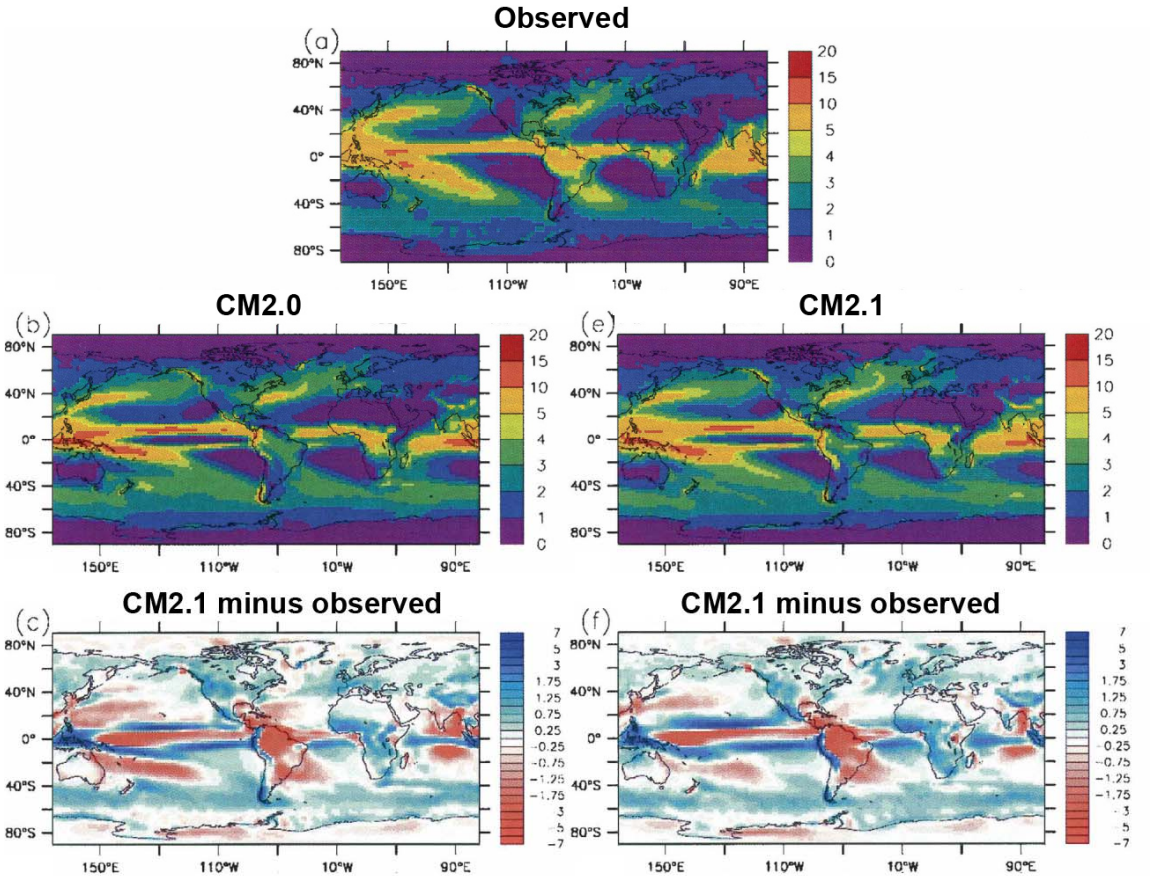

Figure V. C 1-5. **Observed and model-simulated precipitation [mm/day]**

The GFDL precipitation difference maps reveal significant widespread errors in the tropics, most notably in the ITCZ region discussed above and in the Amazon River basin, where precipitation is underestimated by several millimeters per day.

Similar precipitation errors appear in the following table of CCSM3 results Table V 1.

Table V 1 CCSM3 Precipitation by region(Collins, et al, 2006)

Region	CCSM3-simulated precip	Error
Southeast USA (30-40°N, 80-100°W)	2.4 mm/day	–24%
Amazon basin (10°S-10°N, 60-80°W)	4.5 mm/day	–28%
Southeast Asia (10-30°N, 80-110°E)	3.1 mm/day	–24%

AOGCM precipitation errors have serious implications for "Earth system" models with interactive vegetation, because such models use the simulated precipitation to calculate plant growth (see Chapter VI below). Errors of the magnitude shown above would produce an unrealistic distribution of vegetation in an Earth system model, e.g. by spuriously deforesting the Amazon basin.

In summary, modern AOGCMs generally simulate large-scale mean climate with considerable accuracy, but the models are not reliable for aspects of mean climate in some regions, especially precipitation.

20th century trends

Modern AOGCMs are able to simulate not only the time-average climate but also changes (trends) of climate during over the past century or more. For example, Figure V D shows results from the three US models and "average" CMIP3 models. All parts of the figure display the same curves of annual mean globally averaged near-surface temperature as observed by the UK Climatic Research Unit (CRU), as well as simulated by the average over all CMIP3 models and the average over only those CMIP3 models that included the effects of volcanic eruptions. Results from individual US models are shown both for separate ensemble members (dotted lines) and for the average over all ensemble members (continuous lines). Separate ensemble members were run under a variety of initial conditions. The precise initial conditions, especially deep ocean temperature and salinity, are not known for 1860; the spread among the dotted-line curves thus indicates uncertainty in model-simulated temperature arising from our lack of knowledge of initial conditions.

These results demonstrate that modern climate models typically exhibit good agreement with observed near-surface temperature trends for the global mean (Min and Hense, 2006). Global warming during the past few decades is successfully simulated by the models only if they include anthropogenic emissions of greenhouse gases and aerosols. Min and Hense, (in press) show the same is true for most individual continents. Observed trends in climate extremes such as heat-wave frequency and frost-day occurrence are also simulated with basic reliability by the latest generation of AOGCMs (Tebaldi et al., in press).

Figure V D 1. Twentieth century globally averaged surface temperature simulation from GFLD CM2.1

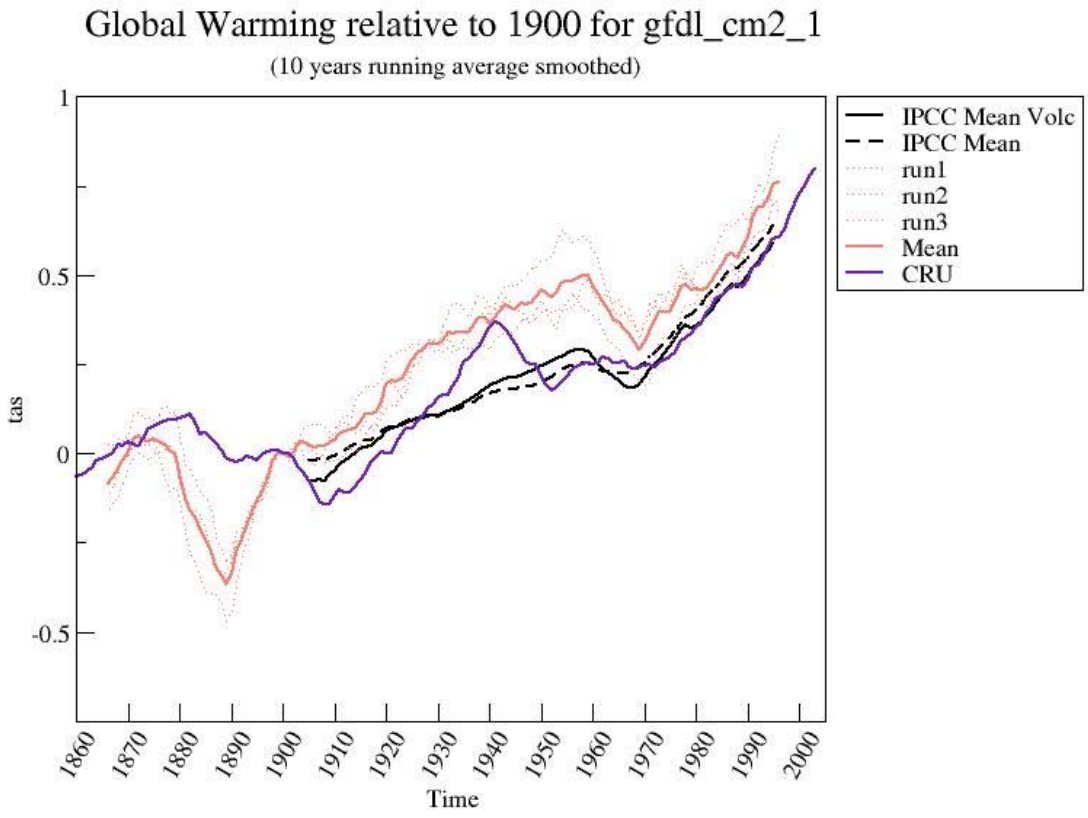

Figure V D 2 Twentieth century globally averaged surface temperature simulation from GISS Model E-r

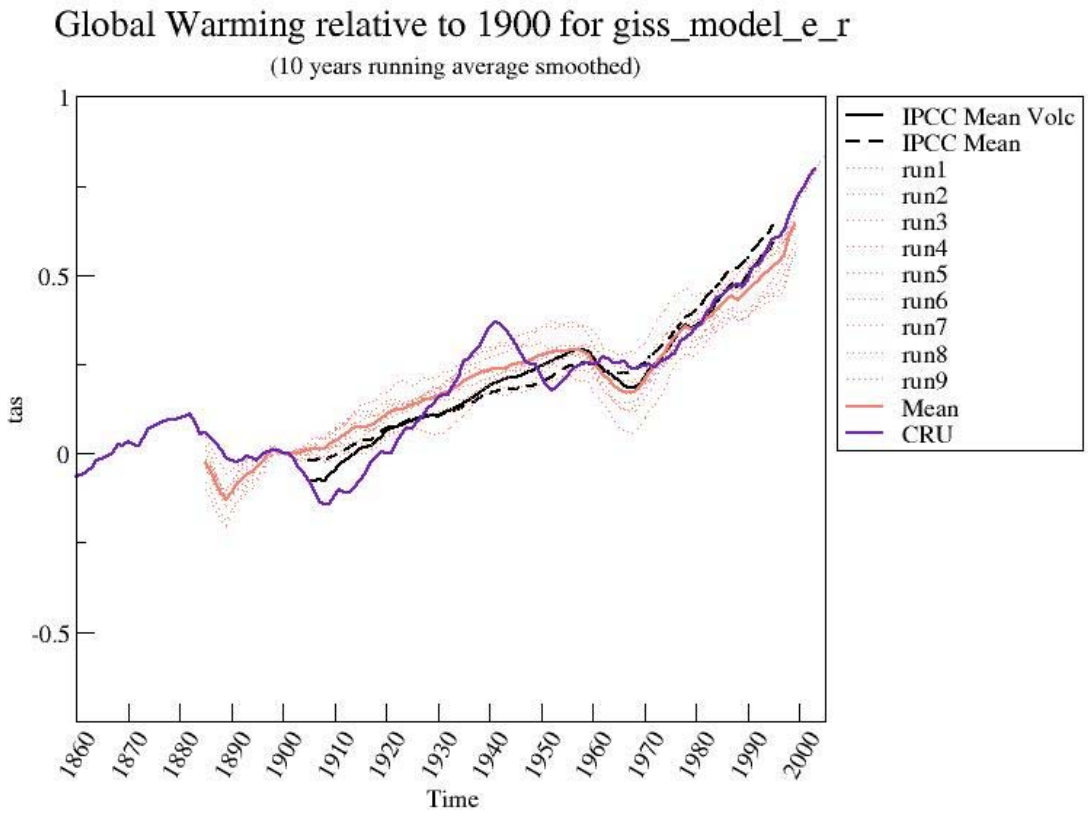

Figure V D 3 Twentieth century globally averaged surface temperature simulation from CCSM3

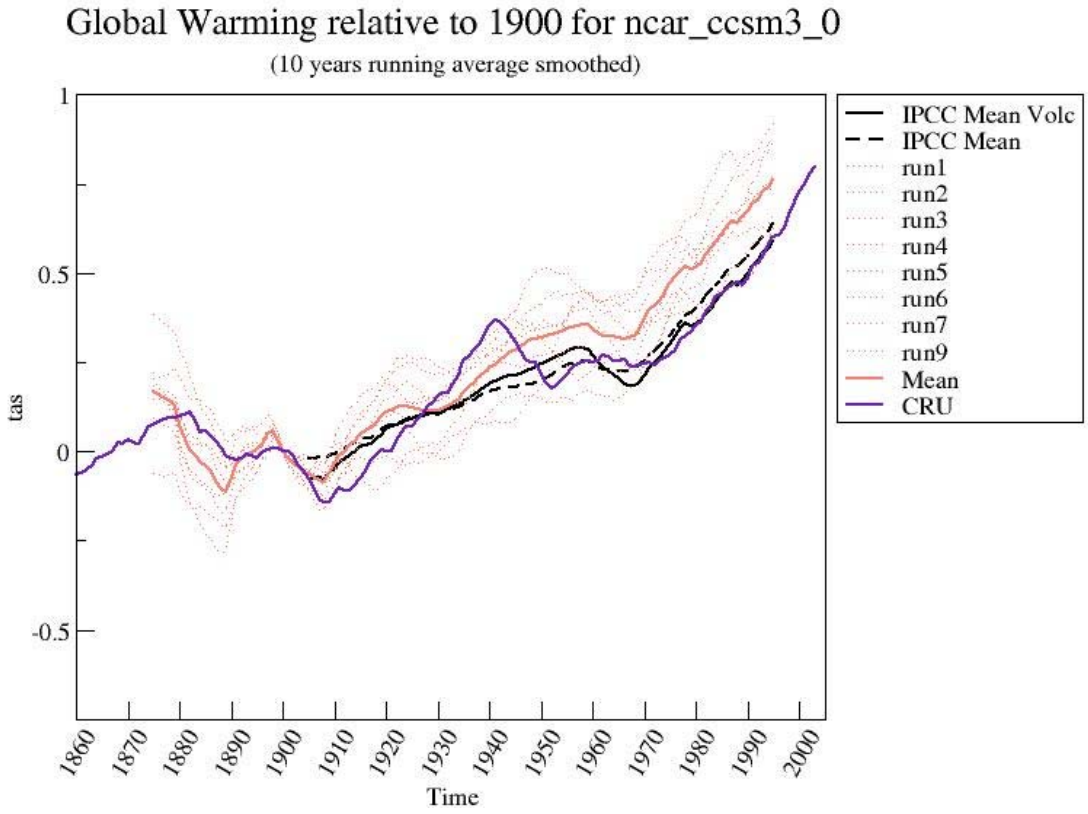

Figure V D 4 Twentieth century globally averaged surface temperature simulation from the three US CMIP3 models and the average of all CMIP3 models that include4d volcanic effects

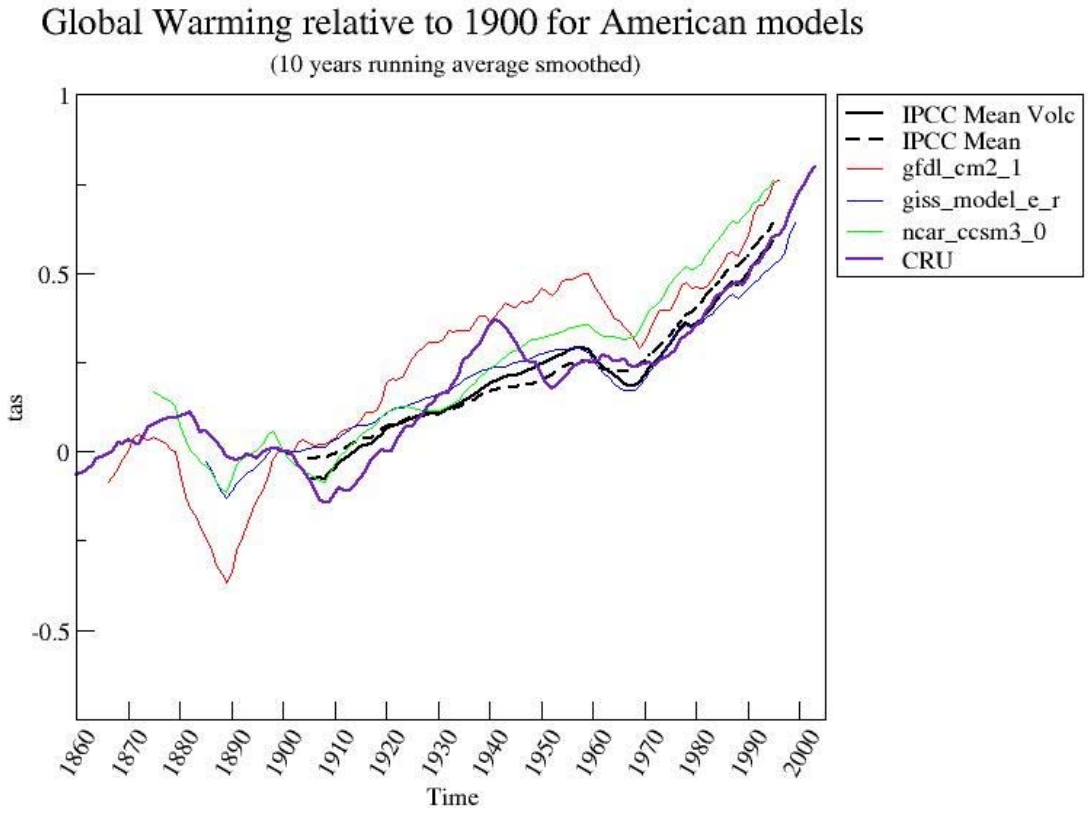

At smaller scales the model simulation of trends can be less accurate. For example, model-simulated trends do not consistently match the observed lack of 20th century warming in the Central US **(**Kunkel et al., in press). The evolution of large-scale patterns, however, can be simulated with fair detail by modern climate models. For example, the longitude-latitude map of trends from GISS modelE agrees reasonably well with the observed spatial distribution Fig V E (Hansen *et al*., 2006) .

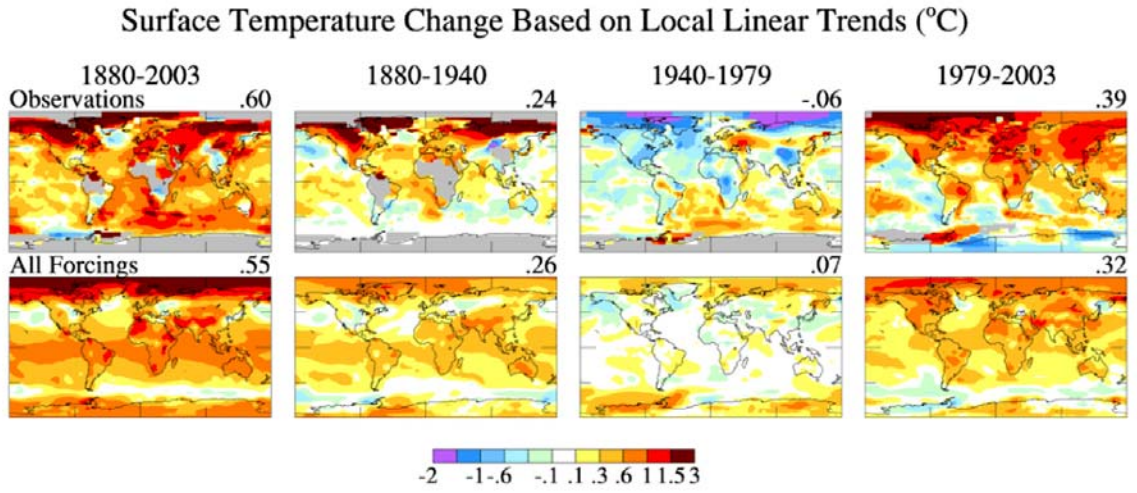

Figure V. E. The figure shows general agreement between the model and observations not only for the overall period 1880-2003, but also for the segments 1880–1940 and 1979–2003, which encompass periods of early and late 20th century warming.

Amplification of warming and cooling at high northern latitudes is the most obvious feature in the observations. For the period 1940–1979, the model simulates only a small change in global mean temperature in agreement with observations, but it fails to simulate the strong north polar cooling observed for this period. As a result, the model-simulated global mean temperature change (upper right corner of each frame) for 1940–1979 is slightly positive rather than slightly negative as observed. For both 20th century warming periods, the model simulates but underestimates the high-latitude amplification of global warming.

Finally, the CCSM3 simulates 4.7 cm of global mean sea level rise during the 20th century (Meehl *et al*. 2006). The actual value of sea level rise is 3–5 times as large, but the model does not include melting glaciers and ice sheets, and therefore it simulates only the part of sea level rise due to expansion of ocean water from heating.

A number of specific climate phenomena in addition to near-surface temperature, precipitation and sea level are discussed in the following sections. These are important for practical applications of climate models because they directly affect near-surface temperature and precipitation patterns (and thereby indirectly affect the evolution of sea level, together with many other features of climate).

Annular Modes

The primary mode of Arctic interannual variability is the Arctic Oscillation (Thompson and Wallace 1998), which is also referred to as the Northern Annual Mode (NAM) and which is related to the North Atlantic Oscillation (Hurrell 1995). The primary mode of Antarctic interannual variability is the Southern Annular mode (SAM) (Thompson and Wallace 2000), also known as Antarctic Oscillation. Coupled global climate models have shown skill in simulating the NAM (Fyfe et al. 1999, Shindell et al. 1999, Miller et al. 2006), although in some cases too much of the variability in sea level pressure is associated with the NAM in these models (Miller et al. 2006). Global climate models also realistically simulate the SAM (Fyfe et al. 1999, Cai et al. 2003, Miller et al. 2006), although some details of the SAM (e.g. amplitude and zonal structure) show

disagreement between global climate model simulations and reanalysis data (Raphael and Holland 2006; Miller et al. 2006).

In response to increasing concentrations of greenhouse gases and tropospheric sulfate aerosols in the 20th century, the multi-model average exhibits a positive annular trend in both hemispheres, with decreasing sea-level pressure (SLP) over the poles and a compensating increase in mid-latitudes (Miller et al. 2006). However, the models underestimate the coupling of stratospheric changes (from volcanic aerosols) to annular variations at the surface, and may not simulate the appropriate response to increasing GHGs (Miller et al. 2006)) and changes in stratospheric ozone (Arblaster and Meehl, 2006).

.

Ocean structure and circulation

A set of ocean characteristics or metrics (sea surface temperature, ocean heat uptake, meridional overturning and ventilation, sea level variability and global sea level rise) is used to describe the realism of the ocean in the climate models.

Sea surface temperature: The sea surface temperature (SST) plays a critical role in the determination of the climate and the predictability of the changes. In general, when the simulated fields of SST are compared to observational fields there is improvement in the models' representation of the mean SST Figure V F(Delworth *et al*., 2006) compares the CM2.0 and CM2.1 mean SST field averaged over a period of 100 years to the Reynolds SST observational climatology. With an improved atmospheric core and a different viscosity parameter value, the later version (CM2.1) of the GFDL climate model produces a reduced cold bias in the northern hemisphere.

Figure V F Maps of errors in simulation of annual mean sea-surface temperature (SST). Units are K. The errors are computed as model minus observations, where the observations are from the ReynoldsSST data (provided by the NOAA-CIRES Climate Diagnostics Center, Boulder, Colorado, USA, from their Web site at http://www.cdc.noaa.gov/). (a) CM2.0 (using model years 101-200). (b) CM2.1 (using model years 101-200). Contour interval is 1K, except that there is no shading for values between 1 K and +1 K.

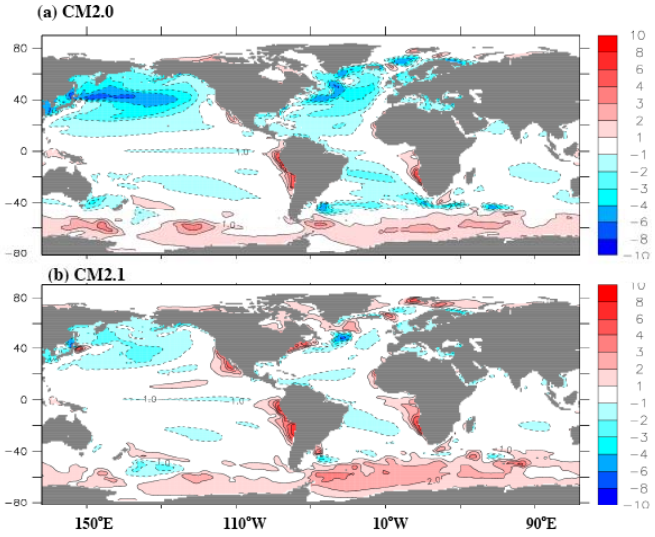

The CCSM3.0 model also has improved its simulation of SST primarily in the handling of the processes associated with the mixed layer of the upper ocean waters (Danabasoglu *et al*., 2005). The improvement in the representation of the SST is apparent especially in the eastern tropical Pacific (see Figure V G). An inter-model comparison of the 50 year global SST trend for each model is shown in Figure V H. The SST trends range from a low of 0.1°C/50yrs to a high of about 0.6°C/50yrs, with the observational trend estimate given as about 0.43°C/50yrs. The figure also shows that within a group, the estimates significantly vary. This distribution of values in SST trends shows that improvements in any model's representation of SST are dependent on both advances in the ocean and atmospheric components.

Figure V G Differences in annual-mean surface temperature between CCSM2 and the HadISST data set (Rayner *et al*. 2003) (top); corresponding differences for CCSM3 (bottom) (Collins, et al, 2005).

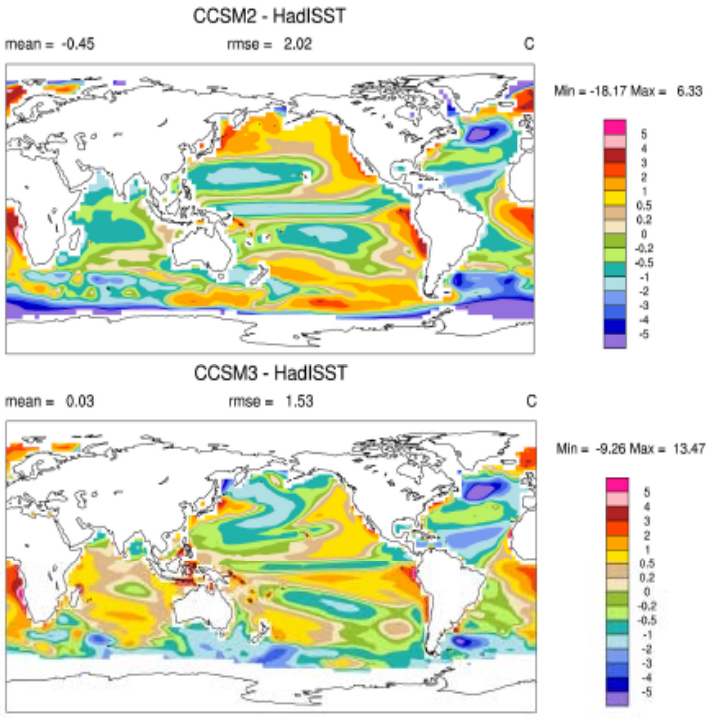

Figure V H Scatter plot of the SST trends averaged in the central and eastern tropical Pacific (9 S–9 N and 90–180 W), and global mean surface temperature trends. Correlation of the model results is 0.58, of higher magnitude than the 95% significance level of 0.46. The 1:1 line is drawn for clarity. The red boxes denote US Climate models and the black box is the relationship computed from observations. (**Zhang & McPhaden, 2006)**

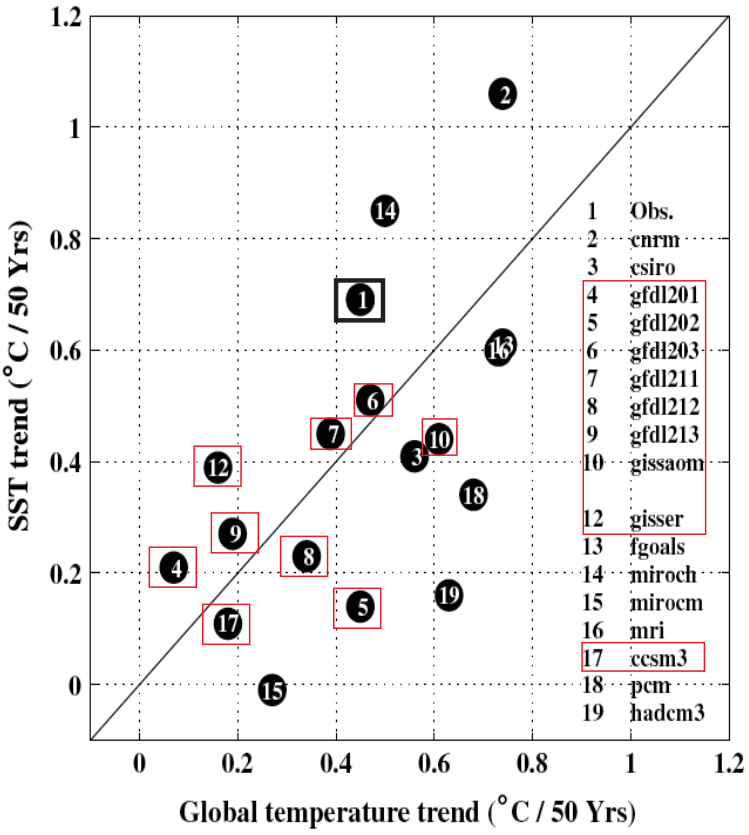

Meridional overturning circulation and ventilation: The circulation process related to the transportation heat and freshwater throughout the global oceans is referred to as thermohaline circulation. The Atlantic portion of this process is called the Atlantic meridional overturning circulation (AMOC). Tropical and warm waters flow northward via the Gulf Stream and North Atlantic Current. The southward flow occurs when water is sub-ducted in the regions of the Labrador Sea and Greenland Seas and occurs when the freshening of the surface waters become denser and flow down the slope to deeper depths. Similar processes occur at locations in the Southern Ocean. Ventilation is the process by which these dense surface waters are carried into the interior of the ocean. The important climate parameter is the rate at which this process occurs, the so-called "ventilation rate". It has been suggested that this pattern of circulation if it becomes weaker (i.e. less warmer water flowing towards Europe) will impact the climate. It is thus important to understand how well the ocean component simulates the observed estimates of these overturning processes.

Schmittner et al. [2005] examined the performance of the models in reproducing the observed meridional overturning in 4 of the 5 US models. The authors examined a small ensemble set of simulations to quantify the uncertainty in the models' representation of 20^{th} century AMOC transports. To make their estimate, they evaluated the global temperature (T), the global salinity (S), the pycnocline depth (D), the surface temperature and surface salinity in the Atlantic (SST, SSS), and calculations of the overturning at 3 locations ~in the Atlantic. Their results suggest that temperature is simulated the most successfully on the large scale and that the overturning transports at 24°N are close (~18Sv) to the observed measurements (~15.8Sv). However, the maximum mean overturning transports in these models are too high (23.2, 31.7, 27.7, and 30.9 Sv: *Schmittner et al*. [2005] and 21.2 Sv from *Bryan et al.* [2006]) than the observed value (17.7 Sv). Table V 2 shows a reduced version of Table 1 from *Schmittner et al*. [2005] that shows the root mean errors (RMS) for the various quantities as compared to observations. The authors do not attempt to explain why the models are different from each other and from observations, rather, that there is a broad range in the value of these metrics for a set of climate models.

Table V 2 Model Errors

Model	T_{global}	S_{global}	D_{global}	SST_{NAtl}	SSS_{NAtl}	D_{NAtl}	$AMOC_{24N}$ (15.8) (SV)
GFDL-2.0	0.20	0.43	0.57	0.34	0.53	0.75	0.16 (18.3)
GISS-AOM	0.66	0.75	2.29	0.43	0.79	3.48	0.22 (19.2)
GISS-EH	0.31	0.76	1.57	0.61	1.12	1.85	0.34 (21.1)
GISS-ER	0.69	0.82	2.06	0.65	1.11	2.40	0.13 (17.9)

From Schmittner et al. [2005] Table 1. RMS Errors for the Individual Models; RMS errors are normalized by the standard deviation of the observations unless otherwise stated. *Schmittner et al.* 2005; "Observation-based estimates of the AMOC at 24 N from *Ganachaud and Wunsch* [2000] *and Lumpkin and Speer* [2003], at 48 N from *Ganachaud* [2003], and its maximum value in the North Atlantic from *Smethie and Fine* [2001] *and Talley et al.* [2003], as well as temperature, salinity, and pycnocline depth observations from the World Ocean Atlas 2001 [*Conkright et al.*, 2002] are used to evaluate the climate models."

The global overturning circulation can also be quantified by also examining the realism of the transports through the Drake Passage. The passage, between the tip of South America and the Antarctic Peninsula provides a constrained passage to measure the flow between two large ocean basins. The observed mean transport is around 135 Sv. *Russell et al.* [2006] estimate the flow in the passage for a subset of the climate models (Table V 3). There is a wide range in the simulated mean values. The interaction between the atmospheric and ocean component models appears to be important in reproducing the observed transport. The strength and location of the zonal wind stress correlates with how well the transport reflects observed values.

TABLE V 3

Model	ACC (Sv)	$d\rho/dy$ (kg m^{-3})	Total τ_x 10^{12} N	Max τ_x (N m^{-2})	Lat of max τ_x
Observational estimate	135	0.58	6.5	0.161	52.4
GISS-ER	266	0.62	4.3	0.107	46.0
GISS-AOM	202	0.38	2.9	0.166	43.5
GFDL-CM2.1	135	0.58	6.1	0.162	51.0
GFDL-CM2.0	113	0.56	4.5	0.149	46.0
GISS-EH	-6	0.43	3.6	0.096	46.0

Reduced From Table 1 *Russell et al.* [2006] Various parameters related to the strength of the ACC. The ACC transport is the integral of the zonal velocity across the Drake Passage at 69°W. The density gradient (dρ/dy) is the zonally averaged density difference between 65° and 45°S. The total ACC-related wind stress (τ_x total) is the integral of the zonal wind stress over the Drake Passage channel (54°–64°S). The maximum westerly wind stress (τ max) is the maximum of the zonally averaged wind stress that is located at the latitude given by Lat τ max. The observed ACC strength is from *Cunningham et al.* (2003). The observed density gradient is calculated from the World Ocean Atlas 2001 (*Conkright et al.* 2002). The observed wind data are from the NCEP long-term mean *(Kistler et al.* 2001). NA indicates data not archived at PCMDI

Northward Heat Transport: A common metric used to quantify the realism in ocean models is the northward transport of heat. This integrated quantity (from top to bottom and across latitude bands) gives an estimate of how heat moves within the ocean and is important in balancing the overall heat budget of the Earth. The calculations for the ocean's northward heat transport in the current generation of climate models show that the models reasonably represent the observations (*Delworth et al*. 2006, *Collins et al*. 2006, and *Schmidt et al*. 2006). The current models have significantly improved over the last generation in the Northern Hemisphere. Comparisons of the simulated values to the observed values for the North Atlantic are within the uncertainty of the observations. In the Southern Hemisphere, the comparisons in all the models are not as good, with the Indian Ocean transport estimates contributing to a significant part of the mismatch.

Heat Content: Related to the heat transport is the ocean's heat content itself. This can be thought of how realistically the models reproduce the uptake of heat. An evaluation of the temporally evolving ocean heat content in the suite of climate models for the AR4 shows the models abilities to simulate the zonally integrated annual and semi-annual cycle in heat content. In the middle latitudes [*Gleckler et al.* 2006], the models do a reasonable job while there is a broad spread of values for the tropical and polar regions. This analysis showed that the models replicate the dominant amplitude of the annual cycle along with its phasing in the mid-latitudes **[**Fig V I]. At high latitudes, the comparisons with observations are not as consistent. While the annual cycle and global trend are reproduced, analyses of the models [e.g. *Hansen et al.* 2005] show that they do not simulate the decadal changes in estimates made from observations [*Levitus et al.* 2001]. Part of the difficulty of comparisons at high latitudes and at long periods is the paucity of observational data [*Gregory et al.* 2004].

Figure V I 1

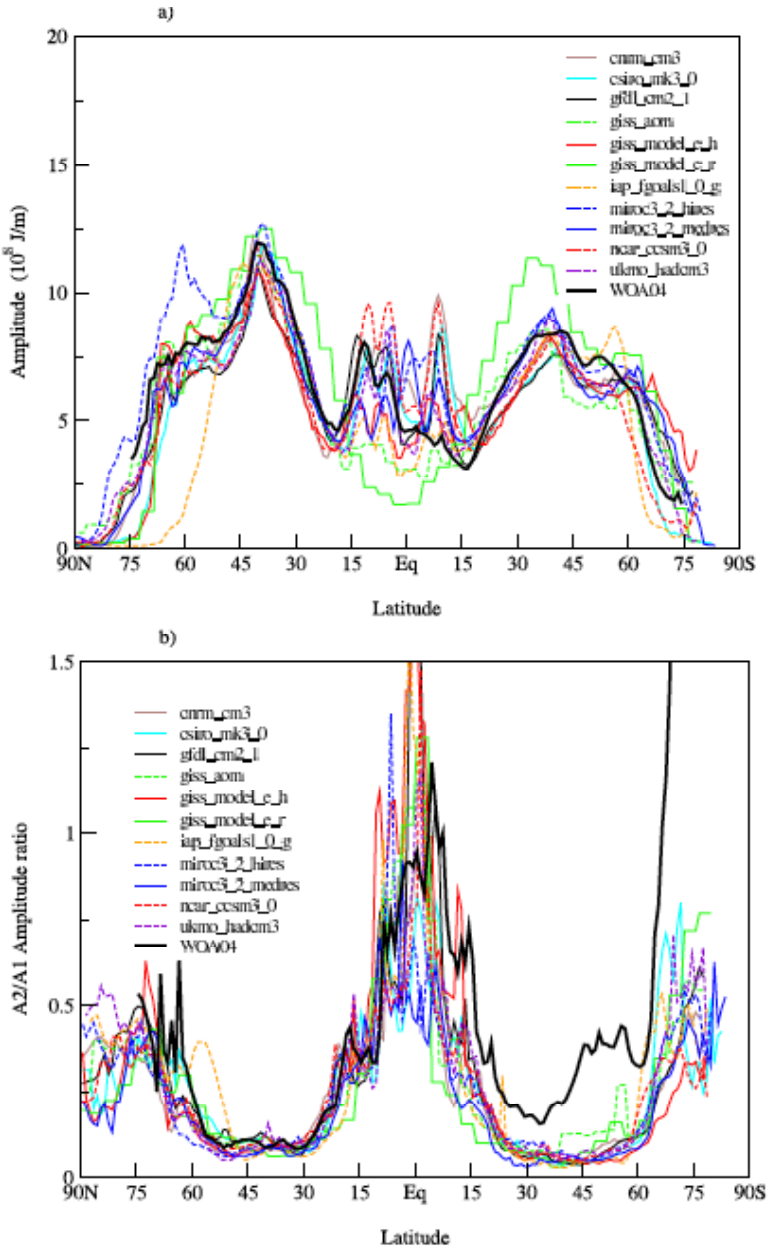

From Glecker *et al.* 2006 .**Figure 1.** Observed (WOA04) and simulated zonally integrated ocean heat content (0–250 m): (a) annual cycle amplitude (10^8J/ m^2) and (b) semiannual/annual (A2/A1).

Figure V I 2

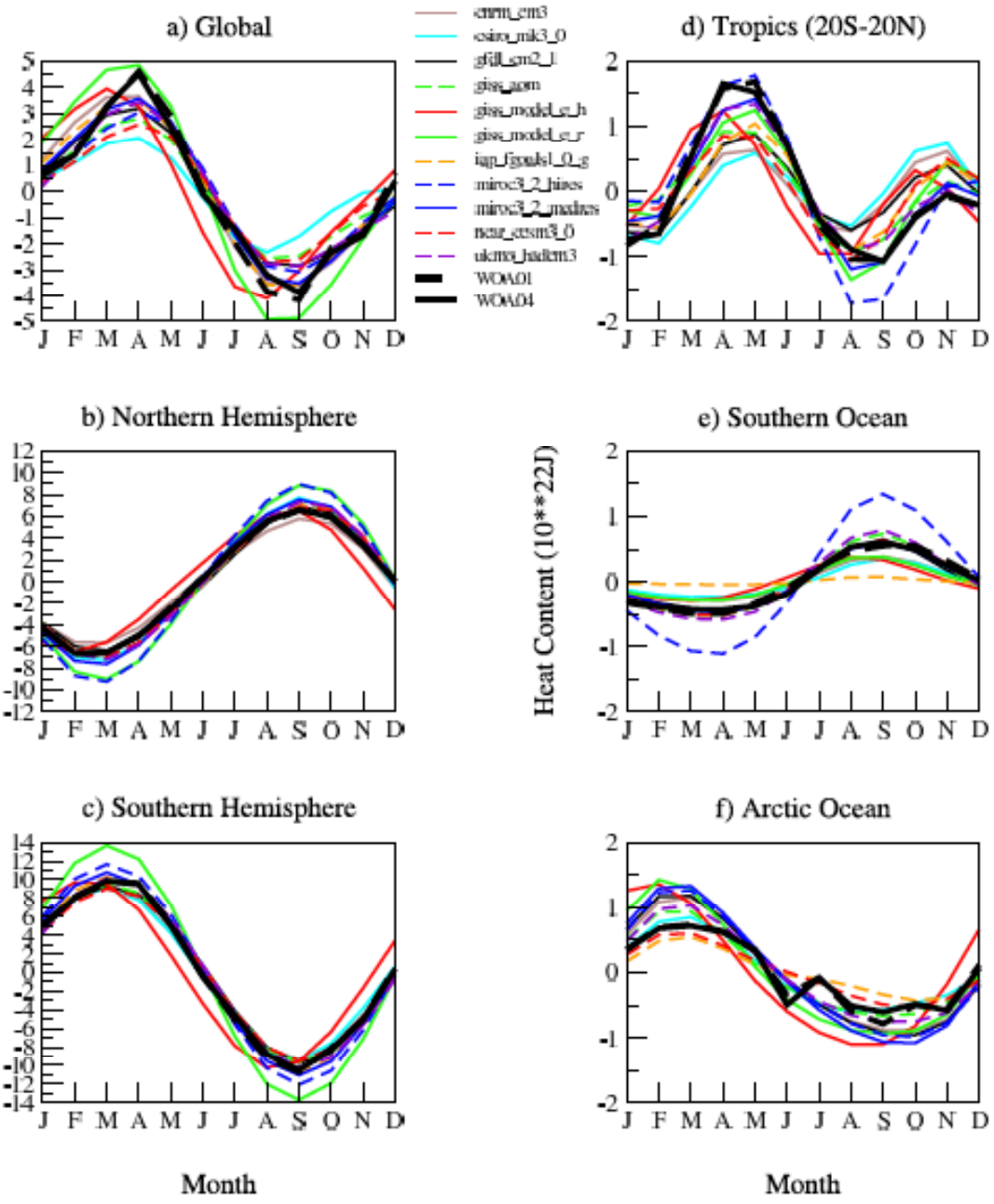

From Glecker *et al.*, 2006, **Figure 3**. Annual cycle of observed (WOA04) and simulated basin average global ocean heat content (0–250 m). Units are 10^{22}J. Arctic Ocean is defined as north of 60 N, and Southern Ocean is south of 60 S.

Global mean sea level rise: Two separate physical processes contribute to the sea level rising: 1) the thermal expansion of the ocean from an increase in the heat uptake by the ocean (steric component) and 2) the addition of freshwater from precipitation, continental ice melt, and/or river runoff (the eustatic component). The current ocean component of all the models except the GISS models, conserve volume. In practice, the first component can be easily computed from a model's primary variables. The second contribution maybe considered as a freshwater flux into the ocean. The various ocean models handle the process in different ways. With the addition of a free surface in the current generation of ocean models, the freshwater flux into the oceans can be included directly [*Griffies et al*. 2001]. In other cases, the mass or freshwater contribution is computed by quantities estimated by land/ice sheet components of the climate model [e.g. *Church et al.*, 2005, *Gregory et al.*, 2006]. In general, the state-of-the-art climate models underestimate the combined global mean sea level rise as compared to tide gauge and satellite altimeter estimates while the rise for each of the separate components is within the uncertainty of the observed values. The reason for this is an open research question and may relate to either observational sampling or not correctly accounting for the all the eustatic contributions. The steric component to the global mean sea level rise is estimated to be 0.40+/-0.05mm/yr from observations [*Antonov et al.* 2005]. The models simulate a similar, but somewhat smaller rise [*Gregory et al.*, 2006, *Meehl et al.* 2005]. There are also significant differences in the magnitudes of the decadal variability between the observed and the simulated sea level or SSH. It most be noted, however, that progress is been made over the previous generation of climate models. When atmospheric volcanic contributions are included, for example, ocean models of the current generation capture the observed impact on the ocean (a decrease in the global mean sea level). Figure V J from *Church et al*. 2006 gives an example of a few models and their de-trended estimate of the historic global mean sea level that shows the influence of including the additional atmospheric constituents in changing the steric height of the ocean.

Figure V J

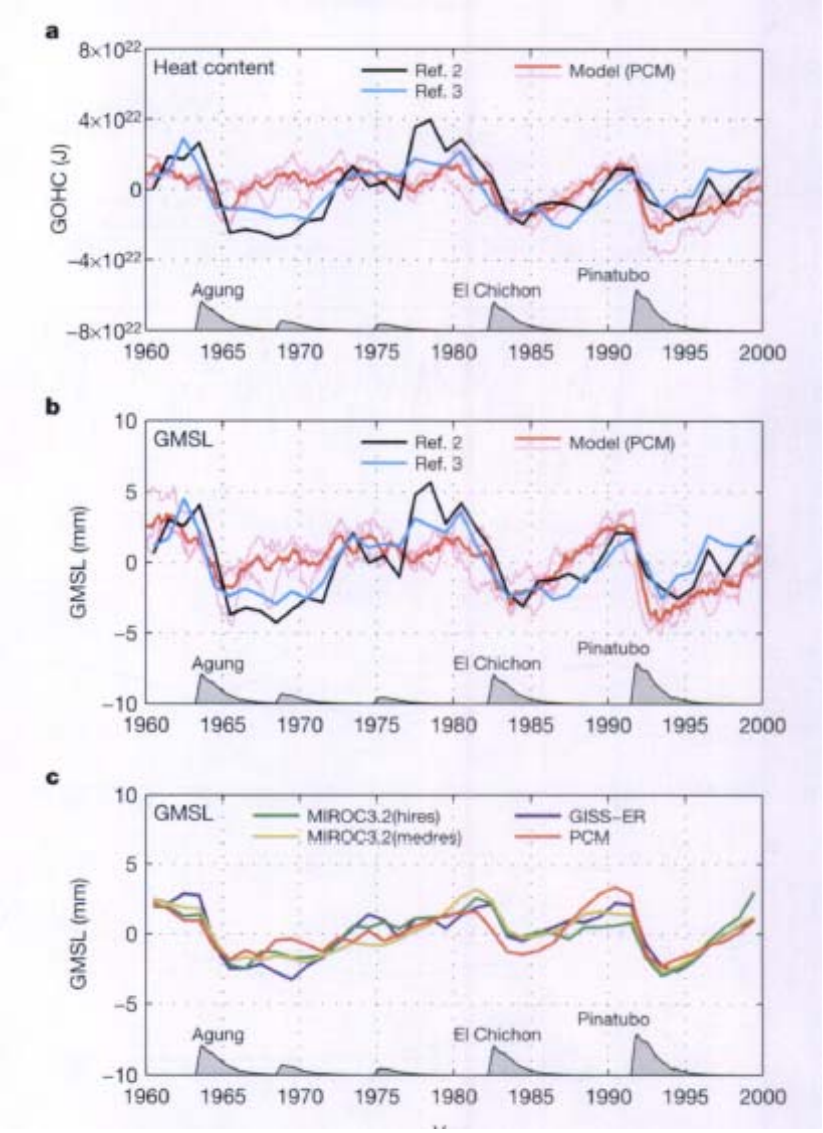

Figure 2 | Observed and modelled GOHC and GMSL for the period 1960–2000. The response to volcanic forcing, as indicated by the differences between the pairs of PCM simulations for GOHC (**a**) and the GMSL (**b**) is shown for the ensemble mean (bold line) and the three ensemble members (light lines). The observational estimates[2,3] of GOHC and GMSL are shown by the black and blue bold lines. For **a** and **b**, all results are for the upper 300 m only and have been detrended over the period 1960–2000. **c**, The ensemble mean (full depth) GMSL for the GISS-ER, MIROC3.2(hires), MIROC3.2(medres) and the PCM models (after subtracting a quadratic) are shown.

C. Simulation of specific climate dynamical features

Extratropical storms

Climate models have developed from numerical weather prediction models whose performance has been primarily judged on their ability to forecast mid-latitude weather. The success of these models in their simulation of midlatitude cyclones and anticyclones has resulted in the continuous growth in the value of numerical weather prediction. The ability of general circulation models to generate realistic statistics of midlatitude weather has also been central in the development of climate modeling. This is not only because midlatitude weather is important in its own right, but also because these storms are the primary mechanism by which heat, momentum, and water vapor are transported by the atmosphere, making their simulation crucial for the simulation of the atmospheric climate.

Indeed, it can be thought of as the defining feature of Atmospheric General Circulation Models (AGCMs) that they compute midlatitude eddy statistics and the associated eddy fluxes through explicit computation of the life cycles of individual weather systems and not through some turbulence or closure theory. It may seem very inefficient to compute the evolution of individual eddies when primarily interested in the long term statistics of the eddies, but it is has been the clear judgment of the community for decades that the explicit simulation of these eddies in climate models is far superior to the attempts that have been made to date in developing closure theories for the eddy statistics. The latter theories typically form the basis for EMICs (Earth System Models of Intermediate Complexity), which are far more efficient computationally than GCMs, but provide less convincing simulations.

Two figures illustrate the quality of the simulations of midlatitude eddy statistics that coupled AOGCMs of the horizontal resolution used in AR4 are capable of generating. Shown for the GFDL CM2.1 in Fig. V K 1 is the wintertime variance of the north-south component of velocity at 300 hPa (in the upper troposphere) and in Fig. V K 2 the wintertime poleward eddy heat flux, or the covariance between temperature and north-south velocity, at 850mb (in the lower troposphere). When analyzing eddy statistics it is often useful to filter the flow fields to retain only those time scales, roughly 2-10 days, associated with midlatitude weather systems, but the two quantities

chosen here are dominated by these time scales to a sufficient degree that they are relatively insensitive to filtering. Here we have simply removed the monthly means before computing variances. In each case, the eddy statistics are compared to the estimates of the observed statistics obtained from the NCEP-NCAR reanalysis (B.Wyman, personal communication).

In winter, Northern Hemisphere storms are organized into two major oceanic storm tracks over the Pacific and Atlantic oceans. Historically, it has been found that atmospheric models of resolutions of about 200-300 kms are typically capable of simulating the midlatitude storm tracks with comparable realism to that shown in the figure. The eddy amplitudes are often a bit weak and often displaced slightly equatorward, especially in Southern hemisphere summer (although the model shown here has a weaker Southern hemisphere bias than most models). In models with resolution coarser than 200-300kms, the simulation of the midlatitude storm tracks typically deteriorates significantly (see for example, Boyle 1993). It is thought to be important for the general improvement in model simulations described in Chapter 1 that most of the models in the CMIP3 database are now utilizing this 200-300km resolution. While finer resolution results in better simulations of the structure of midlatitude storms, including the structure of warm and cold fronts as well as the interaction between these storms and coastlines and mountain ranges, the improvements in the midlatitude climate on large scales tend to be less dramatic and systematic. Other factors besides horizontal resolution are considered to be important for the details of storm track structure, including the distribution of tropical rainfall, which is sensitive to the closure schemes utilized for moist convection, interactions between the stratosphere and the troposphere, which are sensitive to vertical resolution. Roeckner *et al* (2006) illustrate the importance of vertical resolution for the midlatitude circulation and storm track simulation.

A more detailed look at the ability of the AR4 models to simulate the space-time spectra of the observed eddy statistics is provided by Lucarini, *et* al,(2006). These authors view the deficiencies noted, which vary in detail from model to model, as serious limitations to the credibility of the models. But, as indicated in Chapter 1, our ability to translate measures of model biases into useful measures of model credibility is limited, and the implications of these biases in the space-time spectra of the eddies is not self-evident. Indeed, in the context of the simulation of the eddy characteristics generated in complex turbulent flows in the laboratory (e.g., Dimotakis , 2005) the

quality of these atmospheric simulations, closely based on fluid dynamical first principles, should probably be thought of as one of the most impressive characteristics of current models.

As an example of a significant model deficiency that can plausibly be linked to limitations in the credibility of the climate projections, note that the Atlantic storm track, as indicated by the maximum in velocity variance in Fig 5.1, is too zonally oriented, the observed stormtrack having more of an southwest-northeast tilt. This particular deficiency is common in the CMIP-3 models (van Ulden and van Oldenborgh, 2006) and is related to the difficulty in simulating the phenomenon of blocking in the North Atlantic with the correct frequency and amplitude. Van Ulden and van Oldenborgh make the case that this bias is significant for the quality of regional climate projections over Europe.

.

Figure V K 1: Top: variance of north-south velocity at 300hPa as simulated by the GFDL CM2.1 model in years 1981-2000 of one realization of the 20C3M simulation, as contributed to the CMIP3 database. Units are m^2/s^2. Middle: The same quantity as obtained from the NCEP-NCAR reanalysis (ref). Bottom: model minus observations.

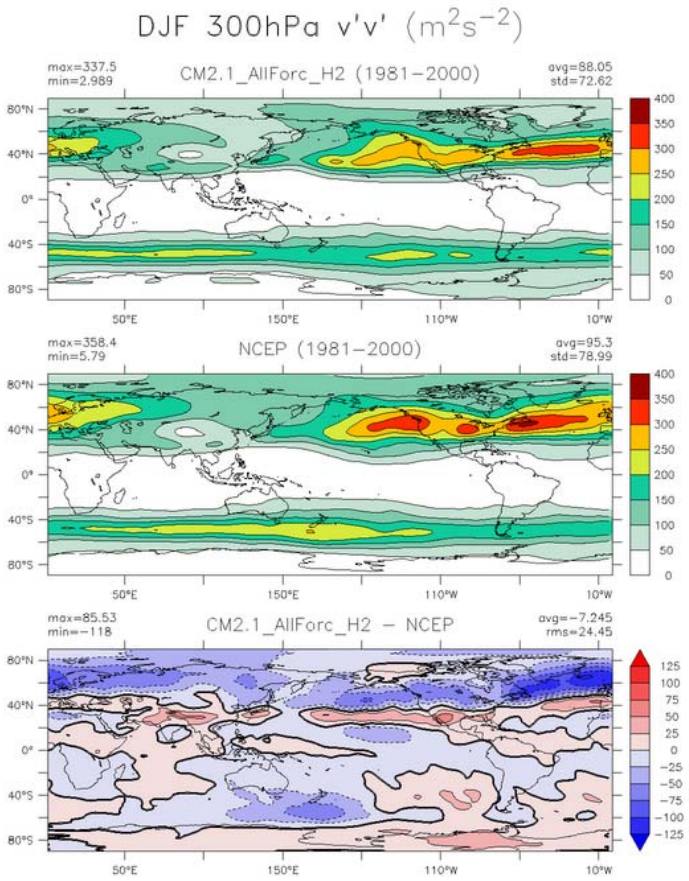

Figure V K 2: Top: covariance of north-south velocity and temperature at 850hPa as simulated by the GFDL CM2.1 model in years 1981-2000 of one realization of the 20C3M simulation, as contributed to the CMIP3 database. Units are Km/s. Middle: The same quantity as obtained from the NCEP-NCAR reanalysis (ref). Bottom: model minus observations.

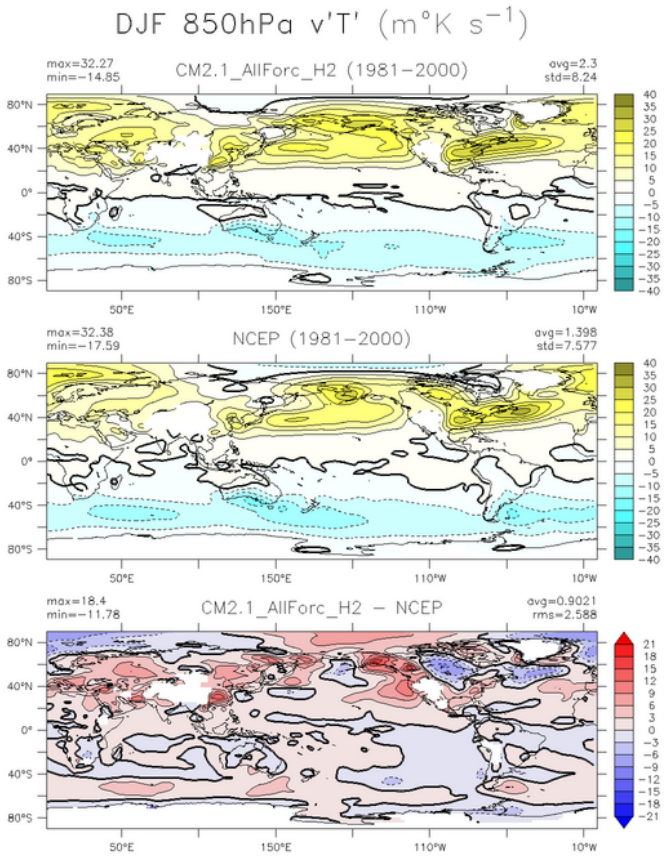

Monsoons

The word `monsoon' derives from the Arabic word for season, and a monsoonal circulation is distinguished by its seasonal reversal after the sun crosses the equator into the new summer hemisphere. Rain is largest, if not entirely restricted, to the summer within monsoonal climates, when continental rainfall is supplied mainly by evaporation from the nearby ocean. This limits the reach of monsoon rains to the distance over which moisture can be transported onshore (Prive and Plumb 2007). Variations in the spatial extent of the monsoon from year to year determine which inland regions experience a drought.

Historical theories for the monsoon emphasize the influence of the contrast between land and ocean (Webster et al. 1998). Land responds more quickly to solar heating than the ocean, where heating is mixed over a deeper layer. Air is driven by this temperature contrast toward the warm land, where it ascends and precipitates moisture before returning offshore. Conversely, land cools more rapidly during winter when the sun is in the opposite hemisphere, and this drives air offshore toward the warmer ocean where it rises. While a coastal sea breeze is also driven by the temperature contrast between land and ocean, the monsoon is distinguished by its continental scale. The onshore flow is so extensive that it is deflected by the earth's rotation. Over the Arabian Sea, for example, surface air flows toward the east and northeast during the Northern Hemisphere summer, rather than traveling directly north toward the Asian continent.

While the monsoon takes its name from a language spoken by traders

around the Arabian Sea, this circulation reaches far beyond the periphery of the Indian Ocean, and local cultures have their own words for the monsoon: for example, Mei-yu in China, Chang-ma in Korea, and Bai-yu in Japan. Over a billion people are dependent upon the arrival of the monsoon rains for water and irrigation for agriculture. The Asian monsoon during NH summer is the most prominent example of the monsoon circulation, dominating global rainfall during this season. However, the seasonal reversal of winds and summer rainfall maximum also indicate monsoon circulations in West Africa and the Amazon basin. In addition, during NH summer, air flows off the eastern Pacific Ocean toward Mexico and the American southwest, while over the Great Plains of the United States, moisture from the Gulf of Mexico brings an annual peak in rainfall. Thus, the climate in these regions is also described as monsoonal.

Because of the geographic extent of the Asian monsoon, the fidelity of climate model simulations is weighed according to metrics from a variety of regions. Kripalani et al. (2007) judged that three-quarters of the eighteen analyzed coupled models (including the GFDL CM2.0 and 2.1 models, along with the NCAR PCM and GISS modelE-R) match the timing and magnitude of the summertime peak in precipitation over East Asia between 100 and 145E and 20 to 40N that is evident in the NOAA NCEP Climate Prediction Center Merged Analysis of Precipitation (CMAP, Xie and Arkin 1997). However, only half of these models (including both GFDL CGCMs) were able to reproduce the observed spatial distribution of monsoon rainfall, and its extension along the coast of China toward the Korean peninsula and Japan. Considering a broader range of longitude (40-180E) that includes the Indian subcontinent, Annamalai et al. (2007) found that only six of eighteen CGCMs (including both GFDL models) were significantly correlated with the observed spatial pattern of CMAP precipitation during June through

September. These six models also included a realistic simulation of ENSO variability, which is known to influence interannual variations in the Asian summer monsoon. Kitoh and Uchiyama (2007) computed the spatial correlation and root-mean-square error of simulated precipitation over a similar region and found the GFDL models in the top tercile with a spatial correlation exceeding 0.8, while the GISS modelE-R correlation was just under 0.5.

During NH winter, the Asian surface winds are directed offshore: from the northeast over India, and the northwest over East Asia. The two American models included in the comparison of the simulated East Asian winter monsoon by Hori and Ueda (2006), GFDL CM2.0 and GISS modelE-R, generally reproduce the observed spatial distribution of sea level pressure and 850 mb zonal wind.

In response to increasing greenhouse gases, models project increasing summer precipitation during the 21st century (Kripalani et al. 2007 Kimoto 2005). However, the circulation strength in both winter and summer is expected to weaken (Kimoto 2005, Ueda et al. 2006), consistent with simple physical arguments by Held and Soden (2006). The latter is also consistent with a study of previous generation models where interannual fluctuations in low-latitude rainfall increased, indicating increasingly severe seasonal departures from the mean (R\"ais\"anen 2002).

Observed variability of the West African monsoon is related to variations of ocean temperature in the Gulf of Guinea. The drying of the Sahel during the late 20th century, and the attendant societal impacts, is related to the inland extent of the monsoonal circulation. Cook and Vizy (2006) found that slightly over half of the 18 analyzed coupled models reproduced the observed maximum in

precipitation over land during June through August. Of these models, only six reproduced the anti-correlation between Gulf of Guinea ocean temperature and Sahel rainfall. The GISS modelE-H and both GFDL models were among the most realistic.

It is unresolved whether the late-20th century Sahel drought is due to natural or human influences. Hoerling et al. (2006) surveyed the average response of eighteen coupled model to conclude that anthropogenic forcings during this period account for only a small fraction of rainfall variations observed in the Sahel. In contrast, Biasutti and Giannini (2006), contrast Sahel rainfall between simulations with observed 20th century forcings (such as greenhouse gas and aerosol concentrations), nineteenth century (pre-industrial) conditions, and increasing greenhouse gases. They suggest that the observed late 20th century trend was externally forced, predominately by anthropogenic aerosols. This conclusion is based upon the average behavior of the models considered. It is supported in particular by the GFDL and GISS models. It is currently unclear how to resolve these contrasting conclusions, because they are based upon different methods and comparisons of models. Both studies agree that the Sahel drought is the result of ocean warming in the Gulf of Guinea, compared to the NH subtropical Atlantic. What remains unresolved is whether forcing by greenhouse gases and aerosols has changed the contrast in ocean temperature between these two regions.

Rainfall over the Sahel and Amazon are anti-correlated: when the Gulf of Guinea warms, rainfall is generally reduced over the Sahel but increases over South America. Amazon rainfall also depends upon the eastern equatorial Pacific, and during an El Nino, rainfall is reduced in the Nordeste region of the Amazon. Li et al. (2006) compare the hydrological cycle of eleven CGCMs over the Amazon during the

late 20th and twenty-first centuries. Based upon a comparison to CMAP rainfall, the GISS modelE-R is among the best, with the GFDL CM2.1 and NCAR CCSM3 models similarly ranked. Despite this fidelity, the models make disparate predictions for the 21st century. In the GISS modelE-R, the equatorial Pacific warms more in the west, resembling a La Nina event. This, together with warming in the Gulf of Guinea, is associated with an increase in Amazon rainfall. While the NCAR CCSM3 predicts a comparable increase, the GFDL CM2.1 exhibits a decrease and lengthening of the Amazon dry season.

The studies of Li et al. (2006) along with Ammamalai et al. (2007) note that future changes in the South American and Asian monsoons are intimately tied to the response of El Nino in the 21st century. Expected temperature changes in the eastern equatorial Pacific are discussed in ENSO section. Here, we note that a consensus is yet to emerge, adding to uncertainty in monsoon projections.

The ability of climate models to simulate NH summer rainfall over the US Great Plains and Mexico was summarized by Ruiz-Barradas and Nigam (2006). Among the American models, the GISS modelE-H matches the annual cycle of precipitation over the Great Plains and Mexico most closely. It is also one of two models to simulate interannual variations in precipitation that are significantly correlated with observed variability during the second half of the 20th century. The observed predominance of moisture import from the Gulf of Mexico compared to local evaporation is most closely reproduced by the NCAR PCM. Moisture import is excessive in the GISS modelE-H, whereas as evaporation contributes too large a fraction in the GFDL CM2.1.

Initial evaluations of the monsoon simulated by the most recent generation of climate models have emphasized the seasonal time scale.

However, subseasonal variations, such as break periods when the monsoon rains are temporarily interrupted, are crucial to forecasts and the impact of the monsoon upon water supply. Simulation of the diurnal cycle, and the local hour of rainfall, is also important to the partitioning of rainfall between runoff and transpiration, and these are important topics for future model evaluation. Transports of moisture by regional circulations beneath the resolution of the model (such as low-level jets along the Rockies and Andes and tropical cyclones) contribute to the onshore transport of moisture. In general, the models show success at simulating the gross seasonal features of the various monsoon circulations, but variations on smaller spatial and time scales that are important to specific watersheds and hydrological projections need to be evaluated.

Tropical storms

Tropical storms (hurricanes in the Atlantic and typhoons in the Pacific and Indian Oceans) are of too small a scale to be reliably simulated in the class of global climate models currently used for climate projections. There is hope for qualitatively useful simulations of the climatology of incipient tropical depressions, however. The work of Vitart and Anderson (2001) is an example of evidence for signficant information content concerning tropical storm-like vortices in simulations with models of this type, using the model's ability to simulate the effects of El Nino on Atlantic storm frequency as a guide.

The recent 20km resolution simulation with an atmospheric model over prescribed ocean temperatures by Oouchi et al (2006) is indicative of the kinds of modeling that will be brought to bear on this problem in the next few years. Experience with tropical storm forecasting suggests that this resolution should be adequate for describing many aspects of the evolution of nature tropical storms, and possibly the generation of storms from incipient disturbances, but probably not tropical storm intensity.

An alternative very promising approach is described by Knutson et al (2007), in which a regional model of comparable resolution (18 km) is used in a downscaling framework to simulate the Atlantic hurricane season. Given the observed year-to year variations in the large-scale structure of the atmosphere over the Atlantic ocean, the model is capable of simulating the year-to-year variations in hurricane frequency over a 30-year period with a correlation of 0.7-0.8 and also captures the observed trend towards greater hurricane frequency over this period in the Atlantic. These results suggest that models of this resolution may be able to provide a convincing downscaling capability for tropical storm frequency projections into the future, although these projections will still rely on the quality of the global model projections for changes in sea surface temperature, atmospheric stability, and vertical shear. The behavior of the El Nino Southern Oscillation into the future will be a key element affecting changes in those aspects of the large-scale structure of the atmosphere over the Atlantic that control tropical storm formation and tracks.

Polar climates

Changes in polar snow and ice cover affect the Earth's albedo and thus the amount of insolation heating the planet (e.g., Holland and Bitz 2003, Hall 2004, Dethloff *et al*. 2006). Concern has also emerged about potential melting of glaciers and ice sheets in Greenland and Antarctica that could produce substantial sea-level rise (Arendt *et al*. 2002, Braithwaite and Raper 2002, Alley *et al*. 2005). Polar regions thus require accurate simulation for projecting future climate change and its impacts.

Polar regions present unique environments and, consequently, challenges for climate modeling. The obvious are processes involving frozen water. While not unique to polar regions, they are more pervasive there. These processes include seasonally frozen ground and permafrost (Lawrence and Slater 2005, Yamaguchi *et* al. 2005) and seasonal snow cover (Slater *et al*. 2001), which can have significant sub-grid heterogeneity (Liston 2004), and clear-sky precipitation, especially in the Antarctic (King and Turner 1997, Guo *et al*. 2003). Polar radiation also has important characteristics that test the ability of models to handle extreme geophysical behavior,

such as longwave radiation in clear, cold environments (Hines *et al*. 1999, Chiacchio *et al*. 2002, Pavolonis *et al*. 2004) and cloud microphysics in the relatively clean polar atmosphere (Curry *et al*. 1996, Pinto *et al*. 2001, Morrison and Pinto 2005). In addition, polar atmospheric boundary layers can be very stable (Duynkerke and de Roode 2001, Tjernström *et al*. 2004, Mirocha *et al*. 2005), and stable boundary layers remain an important area for model improvement.

Confidence in climate model projections of future climate is greatly increased if it can be shown that climate models can accurately simulate the current climate state, and much effort has gone into this type of analysis (e.g. Collins et al. 2006, Delworth et al. 2006). In particular climate models should be able to reproduce both long-term and short-term variations in climate including daily, seasonal, interannual, and decadal variability. For polar regions, much of the assessment of simulated interannual variability has focused on the primary modes of polar interannual variability, the Northern and Southern Annular Modes. Assessment of simulated annular modes appears in Section B. of this chapter.

Less attention has been given to the ability of global climate system models to simulate shorter-duration climate and weather variability in polar regions. Uotila *et al*. (2007) and Cassano *et al*. (2007) evaluated the ability of an ensemble of 15 global climate-system models to simulate the daily variability in sea level pressure in the Antarctic and Arctic. In both polar regions, it was found that the 15-model ensemble was not able to reproduce the daily synoptic climatology, with only a small subset of the models accurately simulating the frequency of the primary synoptic weather patterns identified in global reanalysis data sets. The U.S. models discussed in detail in Chapter 2 of this report spanned the same range of accuracy as non-U.S. models, with GFDL and NCAR GCM versions part of the small, accurate subset. Vavrus *et al*. (2006) assessed the ability of seven global climate models to simulate extreme cold-air outbreaks in the Northern Hemisphere, and found that the spatial pattern of the outbreaks was accurately reproduced in the models, although some details differed.

Attention has also been given to the ability of regional climate models to simulate polar climate. In particular, the Arctic Regional Climate Model Intercomparison Project (ARCMIP) (Curry and Lynch 2002) engaged a suite of Arctic regional atmospheric models to simulate a common domain and period over the western Arctic. Rinke *et al*. (2006) evaluated the spatial and temporal patterns simulated by 8 ARCMIP models, and found that the model ensemble agreed well with global reanalyses, despite some large errors for individual models. Tjernstrom *et al*. (2005)

evaluated near-surface properties simulated by 6 ARCMP models. In general surface pressure, air temperature, humidity, and wind speed were all well simulated, as were radiative fluxes and turbulent momentum flux. Tjernstrom *et al*. (2005) found that turbulent heat flux was poorly simulated, and that over an entire annual cycle the accumulated turbulent heat flux simulated by the models was an order of magnitude larger than the observed turbulent heat flux (Fig. PA-1). In both Tjernstrom *et al.* (2005) and Rinke *et al.* (2006), the U.S. models performed about the same as their European counterparts.

Although simulations of polar climate display agreement with observed behavior, as indicated above, there remains room for improvement. In global models, polar simulation may be affected by errors in simulating other regions of the planet, but much of the difference from observations and uncertainty about projected climate change stems from current limitations in polar simulation. These limitations include missing or incompletely represented processes and poor resolution of spatial distributions.

As with other regions, model resolution affects simulation of important processes. In the polar regions, surface distributions of snow depth vary markedly, especially when snow drifting occurs. Improved snow models are needed to represent such spatial heterogeneity (e.g., Liston 2004), which will continue to involve scales smaller than resolved for the foreseeable future. Frozen ground, whether seasonally frozen or occurring as permafrost, presents additional challenges. Models for permafrost and seasonal freezing and thawing of soil are being implemented in land surface models (see Chapter 2, Land Surface Models). Modeling soil freeze and thaw continues to be a challenging problem as characteristics of energy and water flow through the soil affect temperature changes, and such fluxes are poorly understood (Yamaguchi *et al*. 2005**)**.

Frozen soil affects surface and subsurface hydrology, which influences the spatial distribution of surface water with attendant effects on other parts of the polar climate system such as carbon cycling (e.g., Gorham 1991, Aurela *et al*. 2004), surface temperature (Krinner 2003), and atmospheric circulation (Gutowski *et al*. 2007). The flow of fresh water into polar oceans potentially alters their circulation, too. Surface hydrology modeling typically includes limited, at best, representation of subsurface water reservoirs (aquifers) and horizontal flow of water at both the surface and below surface. These features limit the ability of climate models to represent changes in polar hydrology, especially in the Arctic.

Vegetation has been changing in the Arctic (Callaghan *et al*. 2004) and projected warming, which may be largest in regions where snow and ice cover retreat, may produce further changes in vegetation (e.g., Lawrence and Slater 2005). Current models use static distributions of vegetation, but dynamic vegetation models will be needed to account for changes in land-atmosphere interactions influenced by vegetation.

A key concern in climate simulations is how projected anthropogenic warming may alter ice sheets on land, whose melting could raise sea levels substantially. At present, climate models do not include ice-sheet dynamics and thus cannot account directly for how ice sheets might change, possibly changing heat absorption from the sun and atmospheric circulation in the vicinity of the ice sheets.

How well each of the processes above is represented in climate simulation depends in part on model resolution. Distributions of snow, ice sheets, surface water, frozen ground and vegetation have important spatial variation on scales smaller than the resolutions of typical contemporary climate models. Finer resolution is thus needed. Part of this need may be satisfied by regional models simulating just a polar region. Because both the northern and southern polar regions are within circumpolar atmospheric circulations, their synoptic coupling with other regions is more limited than is the case with midlatitude regions, where the westerlies rapidly move synoptic systems in and out of a region (e.g., Wei *et al*. 2002), which could allow polar-specific models that focus on ant/arctic processes, in part to improve modeling of surface-atmosphere exchange processes (Fig. V L). While each of the above processes have been simulated in finer scale, stand-alone models, their interactions as part of a climate system also need to be simulated and understood.

Fig. V L. Cumulative fluxes of surface sensible heat (top panel) and latent heat (bottom) at the SHEBA site from six models simulating a western Arctic domain for Sept. 1997 – Sept. 1998 for ARCMIP. SHEBA observations are the gray vertical bars; model identifications are given by the key in the upper panel. Adapted from Tjernstrom *et al*. (2005).

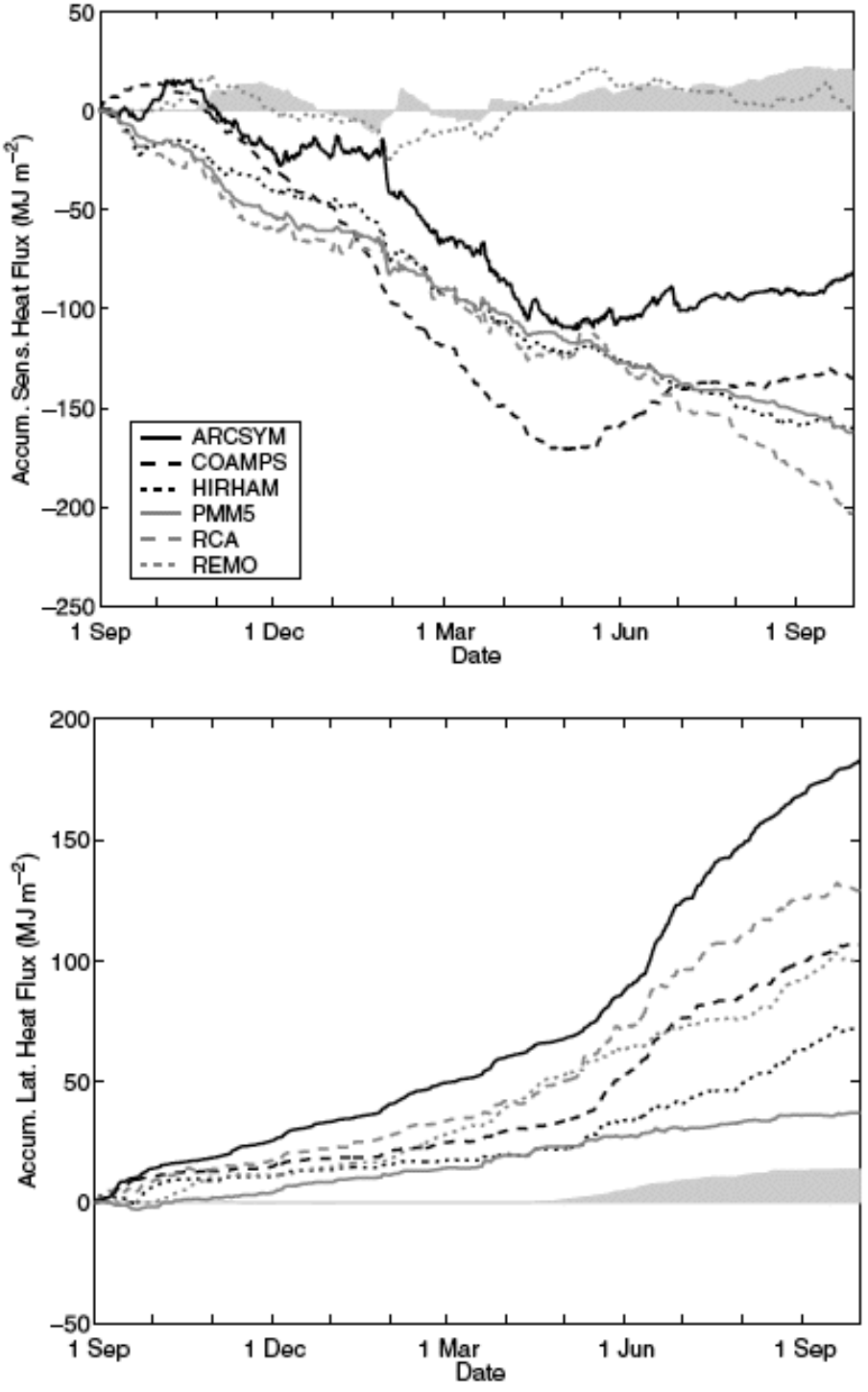

Sea ice plays a critical role in the exchange of heat, mass, and momentum between the ocean and atmosphere and any errors in the sea-ice system will contribute to errors in the other components. Two recent papers [*Holland and Raphael* 2006 and *Parkinson et al.* 2006] quantify how the current models simulate the sea-ice process of the climate system. Very limited observations make any evaluation of sea ice difficult. The primary observation available is sea ice concentration. In some comparisons, sea ice extent (ice concentration greater than 15%), is used. Satellites have made it possible for a more complete data set of observations for the past few decades. Prior to satellite measurements becoming available, observations of ice extent were fewer. Other quantities that might be evaluated include ice thickness. Such comparisons are difficult because of the limited number of observations and will not be discussed.

Ice Concentration and extent: Both of these studies indicate that the seasonal pattern in ice growth and decay in the polar regions for all the models is reasonable [*Holland and Raphael* 2006] (**Figure V M**). However, there is a large amount of variability between the models in their representation of the sea ice extent in both the northern and southern hemispheres. Generally, the models do better in simulating the Arctic region than in their simulation of the Antarctic region as shown with **Figure V N].** An example of the complex nature of reproducing the ice field is given in *Parkinson et al.* [2006]. They found that all the models showed an ice-free region in winter to the west of Norway, as seen in observational data, but all the models also produced too much ice north of Norway. They suggest that this is because the North Atlantic Current is not being simulated correctly. In a qualitative comparison, Hudson Bay is ice covered in winter in all the models correctly reproducing the observations. The set of models are not consistent in their "fidelity" between the Northern and Southern regions and maybe due, partly, to how the parameters are defined in the sea ice models.

Holland and Raphael [2006] examined the variability in the Southern Ocean sea ice extent extensively. As an indicator of the ice response to large scale atmospheric events, they compared a set of IPCC AR4 climate models sea ice response to the atmospheric index, the Southern Annular Mode (SAM) for the April-June (AMJ) period (Table V 4). The models show that the ice variability does respond modestly to the large scale atmosphere forcing but less than limited observations show. Two of the models also exhibit the out-of-phase buildup of ice between the Atlantic and Pacific sectors (the Antarctic Dipole) to some degree.

Table V 4

MODIFIED FROM Table 1 *Holland and Raphael* [2006] Correlations of the leading mode of sea ice variability and the southern annular mode (SAM) for the observations and model simulations

	AMJ SAM and high-pass filtered fields	AMJ SAM and detrended fields
Observations	**0.47**	**0.47**
CCSM3	**0.40**	**0.44**
GFDL-CM2.1	**0.39**	0.19
GISS-ER	0.30	0.20

Bold values are significant at the 95% level accounting for the autocorrelation of the timeseries

Figure V M

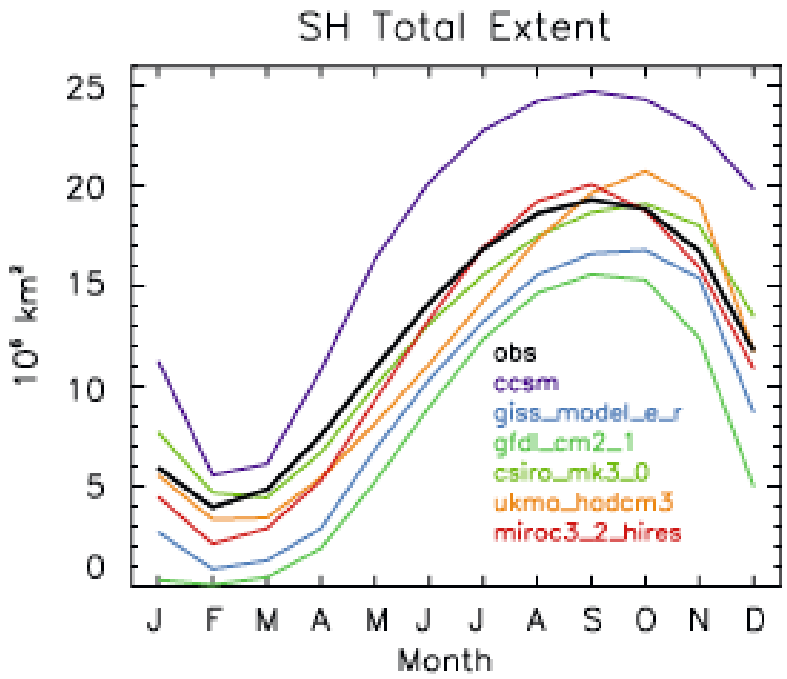

From *Holland and Raphael* 2006. Fig. 1 The annual cycle of southern hemisphere ice extent defined to be the area of ice with concentrations greater than 15%

Figure V N

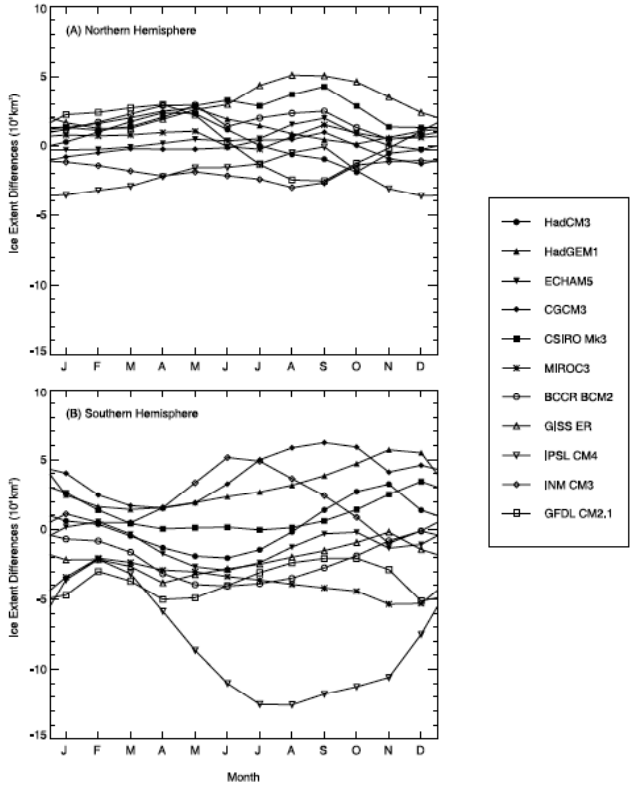

From Parkinson *et al*. 2006: Figure 4. Difference between the modeled 1979–2004 monthly average sea ice extents and the satellite-based observations (modeled minus observed), for each of 11 major GCMs, for both the (a) Northern Hemisphere and (b) Southern Hemisphere.

Modes of variability

The Madden-Julian Oscillation: (MJO) is a characteristic pattern in the tropical atmosphere. It has taken on special prominence in research on simulating the tropical atmosphere. This phenomenon consists of large-scale eastward propagating patterns in humidity, temperature, and atmospheric circulation which strengthen and weaken tropical rainfall as they propagate around the Earth in roughly 30-60 days. This pattern often dominates intraseasonal (within season) variability of tropical precipitation on time scales longer than a few days, creating such phenomena as 1-2 week breaks in Asian monsoonal rainfall and weeks with enhanced hurricane activity in the Eastern North Pacific and the Gulf of Mexico. Inadequate prediction of the evolution of these propagating structures is considered one the main impediments to more useful extended-range weather forecasts in the tropics, and improved simulation of this phenomenon is considered by some a litmus test for the credibility of climate models in the tropics

Recent surveys of model performance indicate that simulations of the MJO remain inadequate. For example, Lin *et al* (2006), in a study of many of the models in the CMIP-3 models, conclude that "… current GCMs still have significant problems and display a wide range of skill in simulating the tropical intraseasonal variability", while Zhang *et al*. (2005) in another multi-model comparison study, state that "… commendable progress has been made in MJO simulations in the past decade, but the models still suffer from severe deficiencies …" Nearly all models do capture the essential feature of the pattern, with large-scale eastward propagation and with roughly the correct vertical structure. But the propagation is often too rapid and the amplitudes too weak. As an example of recent work, Klein (2007?) studies whether two of the US IPCC models can maintain a pre-existing strong MJO pattern when initialized with observations (from the TOGA-COARE field experiment), with limited success. Controlled experiments have suggested that for models to simulate MJO, the instability of the atmospehre must be allowed to accumulate to a certain amount before convective storms are triggered, and sufficient mesoscale statiform heating from convective systems should exist in the upper troposphere (Wang and Schlesinger 1999). These processes are however poorly understood in current climate models.

The difficulty in simulation of the MJO is related to the multi-scale nature of the phenomenon: the propagating pattern is itself of large enough scale that it should be resolvable by climate models, but the convection and rainfall modulated by this pattern, and feeding back and energizing it, occur on much smaller, unresolved, scales. In addition to this dependence on the parameterization of tropical convection, a long list of other effects has been shown by models and/or observational studies to be important for the MJO. These include the pattern of evaporation generated as the MJO propagates through convecting regions, feedback from cloud-radiative interactions, intraseasonal ocean temperature changes, the diurnal cycle of convection over the ocean, as well as the vertical structure of the latent heating, including especially the proportion of shallow cumulus congestus clouds and deep convective cores in the different phases of the oscillation (Lin *et al*. 2004).

A picture seems to be emerging that the difficulty in simulation may not be due to a single model deficiency but a result of the complexity of the phenomenon, given this long list of factors thought to be significant. In several of the multi-model studies, such as Lin *et al* (2006) a few of the models do perform well, but without a clearer understanding of how these factors combine to generate the observed characteristics of the MJO, it is difficult to maintain a good simulation as the model is modified for other reasons, and it is difficult to transfer one model's successful simulation to other models. It also remains unclear whether the models with superior MJO simulations should be given extra weight in multi-model studies of climate change in the tropics.

The El Nino – Southern Oscillation (ENSO) El Nino was named originally in the 19th century by Peruvian sailors to note the early arrival of a warm current from equatorial latitudes (Philander 1990). Every few years, a springtime northerly current arrives prematurely around Christmas (Yu and McPhaden 1999), bringing heavy rains to coastal Peru and a temporary decline in the anchovy harvest. By the mid 20th century, scientists recognized that this local anomaly was in fact part of a disruption to the atmospheric circulation across the entire Pacific basin. During El Niño, atmospheric mass migrates west of the dateline as part of the Southern Oscillation, reducing surface pressure and drawing rainfall into the central and eastern Pacific (Rasmussen and Wallace 1983).

Together, El Niño and the Southern Oscillation, often abbreviated in combination as ENSO, are the largest source of tropical variability observed during recent decades.

Changes along the equatorial Pacific have been linked to global disruptions of climate (Ropelewski and Halpert 1987). During an El Niño event, the Asian monsoon is typically weakened, along with rainfall over eastern Africa, while precipitation increases over the American southwest. El Niño raises the surface temperature as far poleward as Canada, while changes in the North Pacific Ocean are linked to decadal variations in ENSO (Trenberth and Hurrell 1994). In many regions far from the eastern equatorial Pacific, accurate projections of climate change in the twenty-first century depend upon the accurate projection of changes to El Niño. Moreover, the demonstration that ENSO alters climate across the globe indicates that even changes to the *time-averaged* equatorial Pacific during the 21st century will influence climate far beyond the tropical ocean. For example, a long-term warming of the eastern equatorial Pacific relative to the surrounding ocean will favor a weaker Asian monsoon, even in the absence of changes to the size and frequency of El Niño events.

Incident sunlight is largest on the equator, but in the eastern Pacific, the ocean is colder than at neighboring latitudes. Because of the Earth's rotation, easterly winds along the equator cool the surface by raising cold water from below, which offsets heating by the absorption of sunlight (e.g. Clement *et al* 1996). In contrast, warm water extends deeper to the west so upwelling has little effect upon the surface temperature of the West Pacific, where the warmer ocean is consistent with the strong, equatorial solar heating. The westward increase of temperature along the equator is associated with a decrease in atmospheric pressure, reinforcing the easterly Trade winds.

Theoretical arguments offer conflicting projections of tropical Pacific climate during the twenty-first century. One projection is for the equatorial temperature contrast to increase, so that the average state more closely resembles La Niña, marked by unusually cold ocean temperatures and enhanced upwelling in the East Pacific, the opposite to El Niño (Clement *et al* 1996; Cane *et al* 1997). According to this argument, an increase in net radiation into the ocean resulting from an increase in greenhouse gas concentration is partially offset by the upwelling of cold water. This compensation is stronger in the east than in the west, where the surface layer of warm water extends to greater depth. There is evidence for an observed trend toward a La Niña state (Cane *et al* 1997),

but the trend remains ambiguous because of the large decadal variations in the ENSO cycle. Another theory is based upon the origin of upwelling water along the equator within descending surface water in higher latitudes. Liu *et al* (1998) suggest that as these higher latitudes warm, the temperature of the upwelling water will increase, reducing its ability to offset radiative warming at the surface. A third theory suggests that as the tropical atmosphere becomes more stable in response to surface warming, the tropical circulation will weaken (Knutsen and Manabe 1998; see also Meehl and Washington 1996). This will draw less cold water to the surface, preferentially warming the East Pacific. Until recently, many coupled ocean-atmosphere models projected larger warming of the East Pacific and a drift of mean conditions toward an ENSO state.

Below, we summarize the most recent model comparisons, emphasizing those studies carried out as part of the IPCC AR4. Our conclusions are based upon model behavior from a worldwide collection of coupled ocean-atmosphere models, although we illustrate many of the scientific issues using models from American laboratories. The coupled models are designed for prediction of global climate over decades and centuries and are not tuned to optimize their simulation of ENSO *per se,* unlike many of the more simple dynamical and statistical models currently used for operational forecasts of ENSO over a period of several months. Nonetheless, we find that the global models as a group exhibit realistic simulations of present-day seasonal variations and ENSO variability, and represent a marked improvement compared to previous generations of coupled models. However, among the most realistic models, there is little consensus on the anticipated change to either the mean state of the tropical Pacific (particularly the east-west difference in ocean temperature along the equator) or the amplitude and frequency of ENSO variability. This introduces uncertainty in the projected climate response within regions throughout the globe influenced by El Niño.

In general, coupled models developed for the CMIP3 are far more realistic than those of a decade ago, when ENSO variability was comparatively weak, and some models lapsed into permanent El Niño states (Neelin *et al.,* 1992). Even compared to the models assessed more recently by ENSIP and CMIP2 (Latif *et al.,* 2001; AchutaRao and Sperber 2002), ENSO variability of ocean surface temperature is more realistic, although sea level pressure and precipitation anomalies show little recent improvement (AchutaRao and Sperber 2006). Part of this progress is the result of increased resolution of the equatorial ocean circulation that has accompanied inevitable increases in

computing speed. Table V 5 shows the horizontal and vertical resolution of the seven American coupled models whose output was submitted to AR4.

Table V 5

Spacing of grid points at the equator in the American coupled models developed for AR4. Except for the GISS models, spacing of grid points generally increases away from the equator outside of the domain of ENSO, so that resolution is highest on the equator.

Model:	Longitude	Latitude	Vertical Levels
GFDL CM2.0	1	1/3	50
GFDL CM2.1	1	1/3	50
GISS AOM	5	4	13
GISS modelE-H	2	2	16
GISS modelE-R	5	4	13
NCAR CCSM3	1.125	0.27	27
NCAR PCM	0.94	0.5	32

.....

Along the equator, oceanic waves that adjust the equatorial temperature and currents to changes in the wind are tightly confined to within a few degrees of latitude. To simulate this adjustment, the ocean state is calculated at points as closely spaced as 0.27 degrees of latitude in the NCAR CCSM3. NCAR PCM has half degree resolution, while both GFDL models have equatorial resolution of one-third of a degree. This degree of detail is a substantial improvement compared to previous generations of models. In contrast, the GISS AOM and modelE-R calculate equatorial temperatures at grid points separated by four degrees of latitude. This is broad compared to the latitudinal extent of cold temperatures observed within the eastern Pacific (the `cold tongue' region), which are the result of a narrow band of cold water rising to the surface along the equator. In the coarse resolution models, changes to the upward flow are spread over the dimensions of the grid

box, which is broader than the observed upwelling. The cooling effect of this rising water is spread over a larger area, so that the amplitude of the resulting temperature fluctuation at the surface is weakened. In fact, both the GISS AOM and modelE-R models have unrealistic ENSO variations that are much smaller than observed (Hansen *et al* 2007). This minimizes the influence of their simulated El Nino and La Nina events on climate outside the equatorial Pacific, and we will not discuss these two models further in this section.

In comparison to previous generations of global models, where ENSO variability was typically weak, the AR4 coupled models generally simulate El Nino near the observed amplitude, or even above (Neelin *et al* 1992; AchutaRao and Sperber 2006). The latter study compared sea surface temperature (SST) variability within the tropical Pacific calculated under pre-industrial conditions. Despite its comparatively low two-degree latitudinal grid spacing, the GISS modelE-H among the American models most closely matches observed SST variability since the mid-19th century, according to the HadISST v1.1 data set (Rayner *et al* 2003). The NCAR PCM also exhibits El Niño warming close to the observed magnitude. This comparison is based upon spatial averages within three longitudinal bands, and GISS modelE-H along with the NCAR models exhibit their largest variability in the eastern band as observed. However, GISS modelE-H underestimates variability since 1950, when the NCAR CCSM3 is closest to observations (Joseph and Nigam 2006). While the fidelity of each model's ENSO variability depends upon the specific data set and period of comparison (c.f. Capotondi *et al.*, 2006; Merryfield 2006, van Oldenborgh *et al.*, 2005), the general consensus is that the GISS modelE-H, both NCAR models, and GFDL CM2.0 have roughly the correct amplitude, while variability is too large by roughly one-third in the GFDL CM2.1. While most models (including GISS modelE-H and both NCAR models, but excluding the GFDL models) exhibit the largest variability in the eastern band of longitude, none of the AR4 models match the observed variability at the South American coast, where El Nino was originally identified (AchutaRao and Sperber 2006; Capotondi *et al.*, 2006). This is possibly because the longitudinal spacing of the model grids is too large to resolve coastal upwelling, and its interruption during El Niño (Philander and Pacanowski 1981). Biases in the atmospheric model, including underestimate of the persistent stratus cloud decks along the coast, may also contribute (Mechoso *et al.*, 1995).

El Niño occurs every few years, albeit irregularly. The spectrum of anomalous ocean temperature

shows a broad peak between two and seven years, and there are multi-decadal variations in event frequency and amplitude. Almost all of the AR4 models have spectral peaks within this range of time scales. Interannual power is broadly distributed within the American models, as observed, with the exception of the NCAR CCSM3 which exhibits strong biennial oscillations.

While the models generally simulate the observed magnitude and frequency of events, reproduction of their seasonality is more elusive. Anomalous warming typically peaks late in the calendar year, as originally noted by South American fisherman. Among American models, this seasonal dependence is simulated only by the NCAR CCSM3 (Joseph and Nigam 2006). Warming in the GFDL CM2.1 and GISS modelE-H are nearly uniform throughout the year, while warming in the NCAR PCM is largest in December but exhibits a secondary peak in early summer. The mean seasonal cycle along the equatorial Pacific also remains a challenge for the models. Each year, the east Pacific cold tongue is observed to warm during NH spring and cool again late in the calendar year. The GFDL CM2.1 and NCAR PCM1 have the weakest seasonal cycle among the American models, while GISS modelE-H, GFDL 2.0 and NCAR CCSM3 are closest to the observed amplitude (Guilyardi 2006). Among the worldwide suite of AR4 models, the amplitude of the seasonal cycle of equatorial ocean temperature generally varies inversely with the strength of the ENSO cycle.

Anticipation of twenty-first changes to El Nino remains uncertain, because of a lack of consensus among the models. Among fifteen models forcecd by increasing carbon dioxide, three exhibit statistically significant increases in amplitude, while five exhibit a decrease, compared to their variability under pre-industrial conditions (Merryfield, 2006). Even when only the most realistic models are surveyed (including the GFDL CM2.1), identified according to a detailed examination of their mechanisms of variability (described below), no consensus emerges. No significant change in event period is found either (Guilyardi 2006). These trends are inferred based upon the response to a doubling or quadrupling of carbon dioxide, compared to a pre-industrial climate. This forcing is strong compared to forcing over the 20th century in which one might hope to infer trends in El Nino from the observational record. The occurrence of the two largest El Nino events late in the 20th century has been attributed to increasing greenhouse gas concentrations (Trenberth and Hoar 1997; Knutsen and Manabe 1998), although this remains unsettled because of large variations in the

tropical Pacific within the multi-decadal instrument record (Rajagopalan *et al.,* 1997).

Changes in the climate of the tropical Pacific (as opposed to trends in El Nino variability) are also inconsistent (van Oldenborgh *et al* 2006). Of particular interest is the relative warming along the equator, because this is related to the strength of the tropical circulation, which creates regional changes throughout the globe. The ostensible consensus among the most recent generation of models (including both American and international modeling centers) is that the eastern Pacific will warm by about a half degree Celsius more compared to the west (see Figure 10.16 of Meehl et al. 2007).
This is small compared to the currently observed difference of a few degress. When only the most realistic models are surveyed (including the two GFDL models), the warming is nearly uniform across the Pacific (van Oldenborgh et al. 2005). This behavior is consistent with a previous generation of global models, surveyed as part of CMIP2 (Collins et al. 2005). When the model predictions were weighted by the realism of each model, the multi-model average warming was nearly uniform, with only a small probability of greater warming in the east. In summary, warming along the equatorial Pacific is expected to be uniform or slightly larger to the east, but this contrast is on the order of differences among the models. This translates into an uncertainty in the climate in regions outside the tropical Pacific affected by ENSO.

The lack of consensus among model projections for the 21st century may result from the combination of physical mechanisms contributing to observed variability, and the difficulty of simulating them individually along with their relative importance. There is evidence that the importance of certain mechanisms changed in the middle of the 1970's (Wang 1995), so it is unclear what the correct emphasis should be. In addition, positive feedbacks, inferred from the observations, may exacerbate unrealistic features in the models, contributing further to model error.

Several studies have assessed the mechanisms contributing to variability among the AR4 models. Confidence in the models' projection of climate within the tropical Pacific during the twenty-first century depends upon accurate simulation of mechanisms of variability observed at present. El Niño occurs when the upwelling of cold water to the surface is interrupted within the equatorial eastern Pacific and South American coast. This can occur because the rate of upwelling decreases, or

alternatively because the temperature of the upwelling water increases. This subsurface temperature is related to the depth of the thermocline, within which the water temperature falls off sharply with depth. During El Niño, the thermocline deepens, so that upwelling water originating in the cold water below now begins its rise within the relatively warm layer above (Wyrtki 1975). In addition, the slowing of the easterly Trade winds reduces the rate of upwelling (Bjerknes 1969), which at the surface reduces the export of water from the cold tongue toward the West Pacific. Within the weaker surface current, water has more time to be warmed by the sun and overlying atmosphere. El Niño is a coupled phenomenon because the winds that change the upwelling of cold water to the surface depend upon the ocean temperature itself. Because the easterlies are driven partly by the temperature contrast between the cold east Pacific and the warmer ocean west of the dateline, warming in the east reinforces the slackening of the easterly Trade winds.

The coupling between ocean temperature and equatorial winds is typically inferred by regressing wind stress upon temperature averaged within the ENSO domain. The observed wind anomaly is westerly and strongest slightly to the west of a warm ocean anomaly, as expected based upon simple theoretical models (Gill 1980; Lindzen and Nigam 1987, Yu and Neelin 1997). The model wind anomalies are typically displaced farther west than observed, and are excessively confined to the equator (Capotondi *et al.,* 1987). The NCAR PCM regression is roughly half the observed strength, while among the American models, the NCAR CCSM3 and GFDL CM2.1 come closest to observations (Van Oldenborgh *et al.,* 2005). The GISS modelE-H exhibits reasonable coupling in the Central Pacific, but almost no coupling toward South America.

The converse response of SST to wind anomalies is diagnosed by evaluating various terms in the equation for the evolution of ocean temperature (van Oldenborgh 2005; Capotondi *et al.,* 2006). Changes in the temperature of upwelling water are observed to be important in the eastern Pacific (Capotondi *et al.,* 2006). This feedback is reproduced by the GFDL CM2.0 and NCAR CCSM3 models, although with somewhat low amplitude, possibly because the climatological upwelling is weak. (The model output necessary for this diagnosis was not available for the GFDL CM2.1, NCAR PCM, and GISS modelE-H.) While a decrease in the rate of upwelling is crucial to observed warming in the Central Pacific, this feedback is weak in the GFDL CM2.0, and absent in the NCAR CCSM3. The ocean feedback to wind anomalies is also diagnosed by regressing the evolution of

ocean temperature upon various mechanisms represented within the ocean heat budget (van Oldenborgh *et al.*,2005). The NCAR PCM has very strong feedbacks of upwelling rate and temperature in response to wind anomalies, which compensate for its weak wind response to anomalous SST. The GFDL CM2.1 generally reproduces the observed regression relations. In contrast, van Oldenborgh *et al.* (2005) note that regression analysis of GISS modelE-H is noisy and difficult to interpret. It is not clear at this point how GISS modelE-H compensates for its weak wind response to ocean temperature anomalies in order to create ENSO temperature variability near the observed magnitude and location. This lack of transparency calls its projection of future changes into question.

In general, GFDL2.1 is consistently ranked among American models as the most realistic simulation of El Nino (van Oldenborgh *et al.,* 2005; Guilyardi 2006; Merryfield 2006). This is based not only on its surface temperature variability (which in fact is slightly too high), but on its faithful simulation of the observed relationship between ocean temperature and surface wind, along with the wind-driven ocean response. While SST in many models is consistently dominated either by anomalies of upwelling strength or else temperature, these processes alternate in importance over several decades within the GFDL CM2.1 as observed (Guilyardi 2006). Since the 1970's, the upwelling temperature has been the predominant feedback (Wang 1995).

While GFDL CM2.1 predicts a reduced ENSO amplitude in response to increased greenhouse forcing, there is no consensus even among the most highly regarded models. Philip and Van Oldenborgh (2006) find that while both upwelling feedbacks amplify as the greenhouse gas concentration increases, damping processes (due to cloud radiation, for example) also become more effective. A robust prediction of future El Niño amplitudes requires both the upwelling feedback and damping along with their relative amplitude to be simulated consistently, which remains a challenge.

El Niño events are related to climate anomalies throughout the globe. Models with more realistic ENSO variability generally exhibit an anti-correlation with the strength of the Asian summer monsoon (e.g. Annamalai *et al.,* 2006), while 21st century changes to Amazon rainfall have been shown to depend upon projected trends in the tropical Pacific (Li *et al.,* 2006). El Niño has a long-

established relation to North American climate (Horel and Wallace 1981), assessed in the AR4 models by Joseph and Nigam (2006). This relation is strongest during NH winter, when the tropical anomalies are largest. Anomalous circulations driven by rainfall over the warming equatorial Central Pacific radiate atmospheric disturbances into mid-latitudes that are amplified within the North Pacific storm track (Sardeshmukh and Hoskins 1988; Held *et al.*, 1989; Trenberth *et al.*, 1998). To simulate the influence of ENSO upon North America, the models must simulate realistic rainfall anomalies and in the correct season in order that the connection is amplified by the wintertime storm tracks. The connection between equatorial Pacific and North American climate is simulated most accurately by the NCAR PCM model (Joseph and Nigam 2006). In the GFDL CM2.1, North American anomalies are too large, consistent with the model's excessive El Niño variability within the equatorial Pacific. The connection between the two regions is realistic if the model's tropical amplitude is accounted for. In the GISS model, anomalous rainfall during ENSO is small, consistent with the weak tropical wind stress anomaly cited above. The influence of El Nino over North America is nearly negligible in this model. The weak rainfall anomaly is presumably a result of unrealistic coupling between the atmospheric and ocean physics. When SST is instead prescribed in this model, rainfall calculated by the GISS modelE AGCM over the American southwest is significantly correlated with El Niño as observed.

Realistic simulation of El Niño, and its global influence, remains a challenge for coupled models, because of the myriad processes contributing and their changing importance in the observational record. Key aspects of the coupling between the ocean and atmosphere, the relation between SST and wind stress anomalies, for example, are the result of complicated interactions between the resolved model circulations, along with parameterizations of the ocean and atmospheric boundary layers and moist convection. Simple models identify parameters controlling the magnitude and frequency of El Niño, such as the wind anomaly resulting from a change in SST (e.g., Zebiak and Cane 1987; Fedorov and Philander 2000), offering guidance to improve the realism of fully coupled GCM's. However, in a GCM, the coupling strength is emergent rather than prescribed, and it is often unclear *a priori* how to change the coupling. Nonetheless, the improved simulations of the ENSO cycle compared to previous generations (AchutaRao and Sperber 2006) suggest that additional realism can be expected in the future. This optimism arises in part from the extensive and

unprecedented model comparisons carried out as part of the AR4, where the flaws identified in current models may point toward future solutions.

Multi-decadal variability

The Earth's climate varies naturally on multi-decadal scales due to the internal dynamics of the system. These changes are apparent from accurate measurements taken over decades to centuries. From the 1950s onward, an unprecedented volume of observations has been collected that contributes to the understanding of the changes to our climate. The satellite era, beginning in the late 1960's has further expanded the available data and contributed greatly to the set of measurements that are used in this area of research. Further, retrospective research efforts are able to deduce earlier changes to the climate through the analyses of climate indicators such as tree rings and ice cores.

To understand the long period changes in the Earth's climate system, scientists primarily use a set of indices that reduce a large amount of data to a small set of time series. For example, in the tropical Pacific, an index referred to as "Nino 3" is the average sea surface temperature (SST) between 5°N-5°S and150°W-90°W, and indicates variations associated with El Nino and the climate of the tropical Pacific. Other indices, such as the North American Oscillation Index, use sea surface pressure differences at two locations, one in Iceland and one near the Azores (Jones et al. 1997, Hurrell 1995) to examine large-scale shifts in atmospheric pressure systems. Long period measurements of precipitation, such as over the Sahel (20°N-10°N, 20°W-10°E) (Janowiak 1988) also are used understand decadal variability. These analyses can be used to assess the realism of internal or natural variability of the climate models. In addition to whether actual events have been modeled correctly, the climate models are evaluated also in terms of whether the statistical properties of the observed variability are well represented. Previous sections have described some of the low frequency behavior of the climate models (e.g. ENSO, annular modes, polar climates, ice models).

All the models have their own unique intrinsic or natural variability due to the various model design decisions that have been made. The models also tend to differ regionally in their simulation skill.

For example, some are better at simulating the North Atlantic, while others have more skill in the tropics. Often, this regional skill is serendipitous and emerges unexpectedly from attempts to improve simulation of processes that operate globally. A set of examples are given to provide an overview of the general abilities of the current climate models to reproduce decadal and longer variability.

In the Arctic, during the last century, there have been two long period warm events, one between 1920 and 1950 and another beginning after 1979. Wang et al. (2007) evaluated a set of IPCC Fourth Assessment models as to the models' ability are to reproduce the amplitudes of air temperature variability of the mid-century. The CCSM3 and GFDL-CM2 models contain similar variance with the observational variance in the Arctic region. Other models under-represented the natural variability.

Multi-decadal variability in the North Atlantic is characterized by the Atlantic Multidecadal Oscillation (AMO) index which represents a spatial average of SST (Enfield et al. 2001). Kravtsov and Spannagle (2007) analyzed SST from a set of current generation climate models. Their analysis attempts to separate the variability that is associated with internal fluctuations of the ocean from that associated with changes in the atmospheric component due to anthropogenic contributions. By isolating the multi-decadal period of several regions in the ensemble SST series through statistical methods, they found that models, on average, correlate well with the AMO (Figure 7, 8 from Kravtsov and Spannagle, 2007).

In the mid-latitude Pacific region, the decadal variability is generally under-represented in the ocean (e.g. volume transports as described by Zhang and McPhaden, 2006, Figure 3), with some of the models approaching the amplitudes seen in the observations. Examination of complicated feedbacks between the atmosphere and ocean at the decadal and longer scales show that the while the climate models generally reproduce the pattern in SST related to the Pacific Decadal Oscillation (PDO), observed correlations between the PDO and tropical SST are not seen in the models (e.g. Alexander et al. 2006).

One of the most difficult areas to simulate is the Indian Ocean, because of competing effects of warm water inflow through the Indonesian archipelago, ENSO, monsoons, etc). The processes interact to varying degrees, challenging a model's ability to simulate all aspects of the system with the observed relative emphasis. An index used to understand the Indian Ocean's variability is the Indian Ocean Dipole pattern that combines information about the SST and wind stress fields of the Indian Ocean (Saji et al., 1999). While most of the models evaluated by Saji et al. (2006) were able to simulate the Indian's Ocean response to local atmospheric forcing on short time periods (semi-annual), the longer period events such as the ocean's response to ENSO changes in the Pacific, were not simulated well.

Extreme events

Flood-producing precipitation, drought, heat waves, and cold waves have severe impacts on North America. Flooding resulted in average annual losses of $3.7 billion during 1983-2003 (**http://www.flooddamagedata.org/**). Losses from the 1988 drought were estimated at $40 billion and the 2002 drought at $11 billion. The heat waves in 1995 resulted in 739 excess deaths in Chicago alone (Whitman *et al*., 1997). It is probable that a large component of the overall impacts of climate change will arise from changes in the intensity and frequency of extreme events.

The modeling of extreme events poses special challenges since they are, by definition, rare in nature. Although the intensity and frequency of occurrence of extreme events are modulated by the state of the ocean and land surface and by trends in the mean climate state, internal variability of the atmosphere plays a very large role and the most extreme events arise from the chance confluence of unlikely conditions. Their very rarity makes statistical evaluation of model performance less robust than for the mean climate. For example, if one wanted to evaluate the ability of a model to simulate heat waves as intense as the 1995 event in Chicago, there are only a few episodes in the entire 20th century that approach or exceed that intensity (Kunkel *et al*., 1996). For such rare events, there is substantial uncertainty in the real risk, varying from once every 30 years to once every 100 years or more. Thus, a model that simulates such events at a frequency of once every 30 years may be

performing adequately, but it cannot be distinguished in its performance from a model simulating such an event at a frequency of once every 100 years.

Although one might expect that a change in mean climate conditions will apply equally to changes in the extremes, this is not necessarily the case. Using as an example the 50 state record low temperatures, the decade with the largest number of records is the 1930's, yet winters during this decade averaged as the third warmest since 1890; in fact, there is no significant correlation between the number of records and U.S. wintertime temperature (Vavrus *et al*., 2006). Thus, the severest cold air outbreaks in the past have not necessarily been coincident with cold winters. Another examination of model data showed that the future changes in extreme temperatures differed from changes in the mean temperature in many regions (Hegerl *et al*., 2004). This means that climate model output must be analyzed explicitly for extremes by examining daily (or even finer) resolution data, a resource-intensive effort.

The evaluation of model performance with respect to extremes is hampered by incomplete data on the historical frequency and severity of extremes. A study by Frich *et al*., (2002) described a set of indices suitable for performing global analyses of extremes and presented global results. However, many areas were missing due to lack of suitable station data, particularly in the tropics. It has become common to use some of these indices for comparisons between models and observations. Another challenge for model evaluation is the spatially-averaged nature of model data, representing an entire grid cell, while station data represent point observations. For some comparisons, it is necessary to average the station data over areas representing a grid cell.

There are several approaches toward the evaluation of model performance of simulation of extremes. One approach examines whether a model reproduces the magnitude of extremes. For example, a daily rainfall amount of 100 mm or more is expected to occur about once every year in Miami, once every 6 years in New York City, once every 13 years in Chicago, and once every 200 years in Phoenix. To what extent is a model able to reproduce the absolute magnitudes and spatial variations of such extremes? A second approach examines whether a model reproduces observed trends in extremes. Perhaps the most prominent observed trend in the U.S. is an increase in the

frequency and intensity of heavy precipitation, particularly during the last 20–30 years of the 20th century. Another notable observed trend is an increase in the length of the frost-free season.

In some key respects, it is likely that the model simulation of temperature extremes is less challenging than of precipitation extremes, in large part due to the scales of these phenomena. The typical heat wave or cold wave covers a relatively large region, of the order of several hundred miles or more, or a number of grid cells in a modern climate model. By contrast, heavy precipitation can be much more localized, often extending over regions of much less than 150 km, or less than the size of a grid cell. Thus, the modern climate model can directly simulate the major processes causing temperature extremes while heavy precipitation is sensitive to the parameterization of subgrid scale processes, particularly convection (Chapter 2; Emori *et al*., 2005; Iorio *et al*., 2004).

Droughts, particularly over North America and Africa

Recent analysis indicates that there has been a globally-averaged trend toward greater areal coverage of drought since 1972 (Dai *et al*., 2004). A simulation by the HadCM3 model reproduces this dry trend (Burke *et al*., 2006) only if anthropogenic forcing is included. A control simulation indicates that the observed drying trend is outside the range of natural variability. The model, however, does not always correctly simulate the regional distributions of areas of increasing wetness and dryness.

The simulation of specific regional features remains a major challenge for models. Globally, one of the most significant observed changes is the shift to more frequent and more severe droughts in the Sahel region of Africa since about 1970. Lau *et al*., (2006) find that only eight CGCMs produce a reasonable Sahel drought signal, while seven CGCMs produce excessive rainfall over the Sahel during the observed drought period. Even the model with the highest prediction skill of the Sahel drought could only predict the increasing trend of severe drought events but not the beginning and duration of the events. Hoerling *et al*. (2006) also finds that the AR4 models fail to simulate the drying and furthermore uses the model results to suggest that the observed drying was not due to anthropogenic forcing. However, two GFDL models are successful in reproducing the drying and analysis of those models suggests that the drying is of anthropogenic origin (Held *et al*. 2005).

Biasutti and Giannini (2006) interpret these results as an indication that the drying was a combination of decadal-scale internal variability superimposed on longer timescale changes associated with anthropogenic forcing. The differences between modeled and observed regional patterns may then be due to the randomness of natural variability, but may also result from inadequate representation of regional processes and feedbacks.

Excessive rainfall leading to floods Several different measures of excessive rainfall have been used in analyses of model simulations. A common one is the annual maximum 5-day precipitation amount, one of the Frich *et al*. (2002) indices. This has been analyzed in several recent studies (Kiktev *et al*. 2003; Hegerl *et al*. 2004; Tebaldi *et al*. 2006). Other analyses have examined thresholds of daily precipitation, either absolute (e.g. 50 mm per day in Dai 2006) or percentile (e.g. 4th largest precipitation event equivalent to 99th percentile of the 365 daily values as in Emori *et al*. 2005). Recent studies of model simulations produced for the IPCC AR4 provide information on the performance of the latest generation of models.

There is a general tendency for models to underestimate very heavy precipitation. This is shown in a comparison between satellite (TRMM) estimates of daily precipitation and model-simulated values within the 50S-50N latitude belt (Dai 2006). The TRMM observations derive 7% of the total precipitation from very heavy rainfall of 50 mm or more per day, in contrast to only 0-2% for the models. For the frequency of very heavy precipitation of 50 or more mm per day, the TRMM data show a frequency of 0.35% (about once every 300 days), whereas it is 0.02-0.11% (once every 900 to 5000 days) for the models. A global analysis of model simulations showed that the models produced too little precipitation in events exceeding 10 mm per day (Sun *et al*. 2006). Examining how many days it takes to accumulate 2/3's of the annual precipitation, the models generally show too many days compared to observations over North America, although a few models are close to reality. In contrast to the general finding of a tendency toward underestimation, a study (Hegerl *et al*. 2004) of two models (HadCM3 and CGCM2) indicates generally good agreement with the observed annual maximum 5-day precipitation amount over North America for HadCM3 and even somewhat of an overestimation for CGCM2.

This model tendency to produce rainfall events less intense than observed appears to be due in part to the low spatial resolution of global models. Experiments with individual models show that increasing the resolution improves the simulation of heavy events. For example, the 4th largest precipitation event in a model simulation with a resolution of approximately 300 km averaged 40 mm over the conterminous U.S., compared to an observed value of about 80 mm. When the resolution was increased to 75 km and 50 km, the 4th largest event was still smaller than observed, but by a much smaller amount (Iorio *et al*. 2004). A second factor that is important is the parameterization of convection. Thunderstorms are responsible for many intense events, but their scale is smaller than the size of model grids and thus they must be indirectly represented in models (Chapter 2). One experiment showed that changes to this representation improves model performance and, when combined with high resolution of about 1.1 deg latitude, can produce quite accurate simulations of the 4th largest precipitation event on a globally-averaged basis (Emori 2005). Another experiment found that the use of a cloud-resolving model imbedded in a global model eliminated the underestimation of heavy events (Iorio *et al*. 2004). A cloud-resolving model eliminates the need for a parameterization of convection, but is very expensive to run. These sets of experiments indicate that the problem of heavy event underestimation may be significantly reduced in the future as increases in the computer power allows simulations at higher spatial resolution and perhaps eventually the use of cloud-resolving models.

The improved model performance at higher spatial resolutions provide motivation for use of regional climate models when only a limited area is of interest, such as North America. The spatial resolution of these models is sufficient to resolve the major mountain chains; some of these models thus display considerable skill in areas where topography plays a major role in the spatial patterns. For example, they are able to reproduce rather well the spatial distribution of the magnitude of the 95th percentile of precipitation (Leung *et al*. 2003), the frequency of days with more than 50 mm and 100 mm (Kim and Lee 2003), the frequency of days over 25 mm (Bell *et al*. 2004), and the annual maximum daily precipitation amount (Bell *et al*. 2004) over the western U.S. Kunkel *et al*. (2002) found that an RCM's simulation of the magnitude of extreme events over the U.S. varied spatially and depended on the duration of the event being examined; there was a tendency for overestimation in the western U.S. and good agreement or underestimation in the central and eastern U.S.

Most studies of observed precipitation extremes suggest that such extremes have increased in frequency and intensity during the latter half of the 20th century. A study by Tebaldi *et al*., (2006) indicates that models generally simulate a trend towards a world characterized by intensified precipitation, with a greater frequency of heavy-precipitation and high-quantile events, although with substantial geographical variability. This is in agreement with observations. Wang and Lau (2006) find that the CGCMs simulate an increasing trend in heavy rain over the tropical ocean.

Heat and cold waves

Analysis of simulations produced for the IPCC AR4 by seven climate models indicates that they reproduce the primary features of cold air outbreaks (CAOs), with respect to location and magnitude (Vavrus *et al*., 2006). In their analysis, a CAO is an episode of at least 2 days duration during which the daily mean winter (December-January-February) surface temperature at a gridpoint is 2 standard deviations below the gridpoint's winter mean temperature. Maximum frequencies of about four CAO days/winter are simulated over western North America and Europe, while minimal occurrences of less than one day/winter exist over the Arctic, northern Africa, and parts of the North Pacific. The GCMs are generally accurate in their simulation of primary features, with a high pattern correlation with observations and the maximum number of days meeting the CAO criteria around 4 per winter. One favored region for CAOs is in western North America, extending from southern Alaska into the upper Midwest. Here, the models simulate a frequency of about 4 CAO days per year, in general agreement with the observed values of 3-4 days. The models underestimate the frequency in the southeastern United States: mean simulated values range from 0.5 to 2 days *versus* 2 to 2.5 days in observations. This regional bias occurs in all the models and reflects the inability of GCMs to penetrate Arctic air masses far enough southeastward over North America.

The IPCC AR4 model simulations show a positive trend for growing season, heat waves and warm nights and a negative trend for frost days and daily temperature range (maximum minus minimum) (Tebaldi *et al*. 2006). They indicate that this is in general agreement with observations, except that there is no observed trend in heat waves. The modeled spatial patterns have generally larger positive trends in western North America than in eastern sections. For the U.S., this is in qualitative agreement with observations which show that the decreases in frost-free season and frost days are largest in the western U.S. (Kunkel *et al*. 2004; Easterling *et al*. 2002).

Analysis of individual models provides a more detailed picture of model performance. In a simulation from the PCM (Meehl *et al*. 2004), the largest trends for decreasing frost days occurs in the western and southwestern USA (values greater than –2 days per decade), and trends near zero in the upper Midwest and northeastern USA, in good agreement with observations. The biggest discrepancy between model and observations is over parts of the southeastern USA where the model shows trends for decreasing frost days and the observations show slight increases. This is thought to be a partial consequence of the two large El Nino events in the observations during this time period (1982–83 and 1997–98) where anomalously cool and wet conditions occurred over the southeastern USA and contributed to slight increases of frost days. The ensemble mean from the model averages out effects from individual El Nino events, and thus the frost day trends reflect a more general response to the forcings that occurred during the latter part of the 20^{th} century. An analysis of short-duration heat waves simulated by the PCM (Meehl and Tebaldi, 2004) indicates good agreement with observed heat waves for North America. In that study, heat waves were defined by daily minimum temperature. The most intense events occurred in the southeast U.S. for both the model simulation and observations. The overall spatial pattern of heat wave intensity in the model matched closely with the observed pattern. In a four-member ensemble of simulations from the HadCM3 (Christidis *et al*. 2005), the model shows a rather uniform pattern of increases in the warmest night for 1950-1999. The observations also show a global mean increase, but with considerable regional variations. In North America, the observed trends in the warmest night vary from negative in the south-central sections to strongly positive in Alaska and western Canada, compared to a rather uniform pattern in the model. However, this discrepancy might be expected, since the observations probably reflect a strong imprint of internal climate variability that is reduced by ensemble averaging of the model simulations.

An analysis of the magnitude of temperature extremes for California in a regional climate model simulation (Bell *et al*. 2004) show mixed results. The hottest maximum in model is 4°C less than observations, while coldest min is 2.3°C warmer. The number of days >32°C is 44 in the model compared to an observed value of 71. This could result from the lower diurnal temperature range in the model (15.4°C observed vs. 9.7°C simulated). While these results are better than the driving GCM, the RCM results are still somewhat deficient, perhaps reflecting the very complex topography of the region of study.

Models display some capability to simulate extreme temperature and precipitation events, but there are differences from observed characteristics. They typically produce global increases in extreme precipitation and severe drought, and decreases in extreme minimum temperatures and frost days, in general agreement with observations. There is a general, though not universal, tendency to underestimate the magnitude of heavy precipitation events. Regional trend features are not always captured. Since the causes of observed regional trend variations are not known in general and such trends could be due in part to stochastic variability of the climate system, it is difficult to assess the significance of these discrepancies.

Chapter VI – Future Model Development

Cloud-resolved models

Cloud resolving models (CRMs) have spatial resolutions of less than a few kilometers. CRMs can therefore explicitly calculate many atmospheric systems that are on sub-grid scales of AGCMs (Randall *et al*. 2005). These include the mesoscale organizations in squall lines, updrafts and downdrafts, and cirrus anvils. The CRMs also allow calculation of cloud properties and cloud amount with more realistic dynamical conditions, and thus their impact on radiative transfer. Because of improved resolution, CRMs can also better simulate the spatial distribution of precipitation and convective enhancement of the surface fluxes, which are important to describe the interaction of the atmosphere with the land and ocean surfaces.

CRMs are variations of models designed for mesoscale storm and cumulus convection simulations. At CRM scales, hydrostatic balance is no longer universally valid. CRMs are therefore formulated with non-hydrostatic equations in which vertical accelerations are calculated. Tripoli (1992) contains a good review of the various model formulations used to simulate non-hydrostatic meteorological dynamics.

Similar to AGCMs, CRMs also contain empirical relationships to calculate the impact of sub-grid scale processes. These relationships however have different roles from those in AGCMs. First, because CRMs capture a larger portion of the size spectrum of the meteorological systems, the impact of the empiricism is less important in CRMs. For example, cumulus parameterizations for deep tropical convection are no longer needed in CRMs. Second, since CRMs better resolve atmospheric dynamics, cloud processes can be formulated based on more realistic physical conditions.

CRMs can therefore accommodate more sophisticated microphysical and precipitation processes than AGCMs. One-moment bulk microphysical schemes (mass concentration only) with two-class liquid (cloud water and rain) and three-class ice (cloud ice, snow and graupel/hail) are commonly used in CRMs. This level of sophistication is rare in AGCMs and, in any case, unlikely to be useful

given the absence of the needed detail in the small scale flow field. Some CRMs have started to use explicit bin-microphysical schemes. These schemes solve the stochastic kinetic equations for the size distribution functions of water droplets (both cloud droplets and raindrops) and different ice particle habitats (i.e., columnar, plate-like, dendrites, snowflakes, graupel and frozen drops). Because of better size information, these schemes can more realistically calculate the nucleation or activation processes of clouds, along with more accurate calculation of conversion processes among different cloud habitats (Tao 2007).

Subgrid scale processes in CRMs are calculated by using turbulence models. The majority of CRMs use either simple first-order closure to diagnostically compute the turbulent diffusion strength, or the one-and-a-half order closure to prognostically calculate the turbulent kinetic energy which is then used to determine turbulent diffusion coefficients. Prognostic methods typically take into account the thermodynamic stability, deformation, shear stability, diffusion, dissipation, moist processes and transport of sub-grid energy (Klemp and Wilhelmson 1978). Other CRMs use higher order turbulence closures (Krueger 1988).

Radiative transfer in the atmosphere and surface fluxes of heat and moisture in CRMs are computed using algorithms similar those in AGCMs. Because of better spatial resolution atmospheric fields such as clouds and precipitation, CRMs calculate these parameters more accurately than AGCMs.

High resolution of CRMs, however, is at the expense of model domain size and integration length. Current computing infrastructure, with the exception of the Japanese Earth Simulator, only allows CRMs to simulate the atmosphere of less than a few thousand kilometers. Most previous CRM studies were carried out only for two-dimensional slices of the atmosphere, an assumption that somewhat compromises the fidelity of three-dimensional convective cloud simulations. Few CRM simulations are carried out for longer than a year. CRMs with explicit bin-microphysics or high order turbulence closures have been integrated only for a few days.

Research with CRM falls into two categories. In the first one, CRMs are used to investigate the time evolution of cloud systems by specifying realistic initial conditions. This type of study enables deterministic understanding of convection initiation, cold pools, surface fluxes and their direct

comparison with aircraft and other high resolution observation. The simulations are however only valid for a few hours. In the second category, CRMs are used to study the properties of cloud ensembles by specifying external forcing fields. This approach allows statistical description of multiple cloud types with different life cycles (Tao 2007).

Although CRMs are advantageous over ACGMs in describing moist processes, they also face unique challenges when utilized in forecasting mode. CRM results are often very sensitive to the specification of initial conditions and external forcing conditions. They are also sensitive to the physical algorithms in themit. There are still large uncertainties in the CRM cloud microphysics, including prediction of ice particle concentrations, falling speed calculation of cloud habitats, initial broadening of cloud droplet spectra in warm clouds, details of hydrometeor spectra evolution, quantitative simulations of entrainment rates (Cotton 2003). The high sensitivity of model results makes it difficult to rigorously validate CRMs.

Several field programs, such as the DOE ARM program, have enabled collection of observational data that are essential to evaluate CRMs (Zhang *et al*. 2001; Tao *et al*. 2004). Results from these programs will facilitate the improvement of model physics. On the other hand, a global model approaching CRM resolution has been developed and has been integrated on the Earth Simulator with spatial resolution of 7 kilometers (Miura *et al*. 2005). There is another paradigm for multiscale problems that will be likely attempted in the next decade. This is the nesting of coupled regional models of the atmosphere and the ocean within global coupled GCMs. Progress on these fronts will guide where climate models should go in the future.

Biogeochemistry

The Carbon Cycle *Libes* [1992] defined biogeochemistry as "the science that studies the biological, chemical, and geological aspects of environmental processes". At present, three-dimensional climate models are usually limited to the physical climate system: atmosphere, land, ocean, and sea ice. However, the physical climate system and biogeochemical processes are tightly coupled. For example, changes in climate affect the exchange of atmospheric CO_2 with the land

surface and ocean, and changes in CO_2 fluxes affect Earth's radiative forcing and thus the physical climate system. Some recently developed AOGCMs have included the carbon cycle and confirmed the potential for strong feedback between it and global climate (Cox *et al.*, 2001; Friedlingstein *et al.*, 2001; Govindasamy *et al.*, 2005). The next generation of AOGCMs is expected to include the carbon cycle and possibly interactive atmospheric aerosols and chemistry. Such models would predict time-evolving atmospheric concentrations of CO_2, etc., using anthropogenic emissions rather than assumed concentrations as input.

Models that include the global carbon cycle must account for the processes shown in **Figure VI.1**. Boxes represent the carbon reservoirs and arrows show the direction and magnitude of the fluxes. The present-day atmosphere holds about 750 Petagrams of carbon atoms in the form of CO_2. ("Petagrams of carbon" is abbreviated PgC; note that 1 Petagram $=10^{15}$ grams $= 10^9$ metric tons.) A roughly equal amount of carbon is contained in land vegetation and about twice as much in soils. The ocean is by far the largest reservoir of carbon with about 40,000 PgC. The largest flows of carbon in the system are photosynthetic uptake of ~120 PgC / year by terrestrial ecosystems (gross primary productivity or GPP), plant respiration which releases ~60 PgC / year back to the atmosphere (hence the remainder—net primary production or NPP—is ~60 PgC / year), and heterotrophic (soil) respiration which releases ~60 PgC / year. In the upper ocean, photosynthesis by marine organisms incorporates carbon at the rate of ~50 PgC / year, about 4/5 of which is reconverted to CO_2 and related inorganic carbon molecules by respiration. The remaining ~10 PgC / yr of organic matter sinks into deep ocean, a process sometimes called the "biological pump." This organic matter is oxidized and eventually returns to the surface ocean via a combination of both convective / turbulent mixing and the "solubility pump" (the latter so named because it involves sinking of cold water, with high levels of dissolved inorganic carbon, near the poles).

The present-day global carbon cycle is not in equilibrium because of fossil fuel burning and other anthropogenic carbon emissions. These must of course be included in models of climate change, but such a calculation is not easy because human-induced changes to the carbon cycle are small compared to the large natural fluxes discussed above. Fossil fuels are estimated to contain about 4,000 PgC. During the 1990's, fossil fuel emissions averaged ~6 PgC / year and carbon release from land cover change (e.g. deforestation) averaged ~2 PgC / year, providing a net anthropogenic source

of ~8 PgC / year to the atmosphere. Terrestrial and ocean ecosystems together absorbed about half of this flux, i.e. ~4 PgC / year, with the net uptake of carbon by the terrestrial biosphere and the net flux of CO_2 into the ocean each estimated as ~2 PgC / year. The rest (~ 4 PgC/ year) accumulated in the atmosphere, appearing as an increasing concentration of atmospheric CO_2.

The globally averaged carbon reservoirs and fluxes shown in **Figure VI .1** are consistent with estimates from a variety of sources, but substantial uncertainties attach to the numbers (e.g. often a factor > 2 uncertainty for fluxes; see Prentice *et al*. 2001). Additional uncertainty applies to regional, seasonal and interannual variations in the carbon cycle. Evaluation of climate-carbon cycle models is therefore problematic: for many aspects of a simulation it is not clear what the "right answer" is.

Recent three-dimensional climate-carbon modeling studies

The feedbacks between the physical climate system and the carbon cycle are represented plausibly, but with substantial differences, in different AOGCM / carbon-cycle models. Cox *et al*. (2000) obtained a very large positive feedback, with global warming reducing the fraction of anthropogenic carbon absorbed by the biosphere and thus boosting the model's simulated atmospheric CO_2; Friedlingstein *et al*. (2001) obtained a much weaker feedback. Thompson *et al*. (2004) demonstrated that making different assumptions about the land biosphere within a single model gave markedly different feedback values. Using the same model, Govindasamy *et al*. (2005) noted a positive correlation between the magnitude of carbon cycle feedback and the sensitivity (q.v.) of the physical climate system.

A recent study examined carbon cycle feedbacks in eleven coupled AOGCM / carbon-cycle models using the same forcing (Friedlingstein *et al*., 2006). There was unanimous agreement among the models that global warming will reduce the fraction of anthropogenic carbon absorbed by the biosphere, but the magnitude of this feedback varied widely among the models (Fig VI .2), leading to additional global warming (when the models included an interactive carbon cycle) ranging between 0.1 to 1.5 °C. Eight models attributed most of the feedback to the land biosphere, while three attributed it to the ocean.

These results demonstrate extreme sensitivity of climate model output to assumptions about carbon-cycle processes. To reduce the consequent uncertainties in model predictions of the future, it will be necessary to thoroughly compare model output with real-world observations for present day conditions. Studies that span a broad range of ecosystems and climate regimes, including both and global remote sensing by satellites and local in situ measurements, are beginning to be integrated with diagnosis and improvements of the models. For example, the CCSM Biogeochemistry Working Group has recently begun intercomparison of three different biogeochemistry sub-models within the CCSM (climate.ornl.gov/bgcmip).

Other biogeochemical cycles Methane (CH_4) is a potent greenhouse gas and part of the carbon cycle. Also, CO_2-fertilized ecosystems are limited by the availability of nutrients such as nitrogen and phosphorous, so changes in their availability are important to the carbon cycle through changes in plant nutrient availability (Field *et al*. 1995; Schimel 1998; Nadelhoffer *et al*. 1999; Shaw *et al*. 2002; Hungate *et al*. 2003). Future climate-carbon models will probably represent these variables. The few models that do so now show less plant growth in response to increasing atmospheric CO_2 (Cramer *et al*. 2001, Oren *et al*. 2001, Nowak *et al*. 2004). Incorporation of other known limiting factors such as acclimation of soil microbiology to the higher temperatures (Kirschbaum, 2000; Tjoelker, *et al*., 2001), and other elemental cycles such as the sulfur cycle (which affects aerosol and cloud properties), will also be important in developing comprehensive Earth system models.

Land Cover and land management practice changes

Generally, climate-carbon models do not include the effects land cover and land management changes on natural ecosystems. Land cover change is often accounted for simply by prescribing estimates for the historical period (e.g., Houghton, 2003) and the IPCC SRES scenarios for the future. These estimates do not include practices such as crop irrigation and fertilization. Many models with “dynamic vegetation” do not actually simulate crops; they allow only natural vegetation to grow. Deforestation, land cultivation and related human activities will probably be included in at least some future AOGCMs, enabling assessment of total anthropogenic effects on the global climate and environment (Ramankutty *et al*. 2002, Root and Schneider 1993).

Ocean Biogeochemistry

With respect to the ocean, we are concerned with how global warming impacts the marine environment including changes in the carbon content of the ocean and feedbacks to the atmosphere. Also of importance are the effects of modified ocean temperature, salinity and circulation patterns on the ocean's biota. Implementation of ocean biogeochemistry processes into AOGCMs is still in the development stage (e.g. CCSM Biogeochemistry Working Group Meeting Report, Mar. 2006, and GFDL Earth System Model, *http://gfdl.noaa.gov/~jpd/esmdt.html*) but is expected to proceed rapidly (*Doney et al.* 2004) to improve simulation of the ocean carbon cycle under various scenarios.

One challenge to this effort is the complexity of the ocean's ecosystems. Complexity is added with each organism that fixes nitrogen, denitrifies, calcifies, or silicifies because each adds additional parameterizations and variables to the system (*Hood et al*. 2006). There needs to be sufficient complexity in the biological models to capture the variability of the system as observed. In addition, models should include processes that are important over time periods substantially greater than a year (*Rothstein et al.* 2006) in addition to much shorter periods. However, Earth system models cannot be so complex that their computational cost precludes their actual use, and adding complexity to the biogeochemistry models may lead to a decrease in their predictive ability because the inability to constrain the model with the available data (*Hood et al*. 2006). Thus, as with other component models such as those simulating clouds and convection, the development of ocean (and land) BGC models for incorporation into physical climate models involves a trade-off between realism and tractability.

The current strategy of climate modeling groups to address ocean carbon and biogeochemistry includes systematic comparison of different models in the Ocean Carbon-Cycle Model Intercomparison Project (OCMIP) under auspices of the International Geosphere-Biosphere Programme (IGBP). The most recent phase of OCMIP involved 13 groups—including several from the USA—implementing a common biological model in their different GCMs (*Najjar et al.* 2006). The common biological model includes five prognostic variables: inorganic phosphate (PO_4^{2-}),

dissolved organic phosphorus (DOP), dissolved oxygen (O_2), dissolved inorganic carbon (CO_2 + HCO_3^- + CO_3^{2-}) and total alkalinity (the acid / base buffering capacity of the system). Intercomparison of the models revealed significant differences in simulated biogeochemical fluxes and reservoirs. A biogeochemistry model's realism of any particular simulation is closely tied to the dynamics of the simulation's circulation model. The US climate modeling groups are building upon this community effort to incorporate biogeochemistry into the ocean component of the models.

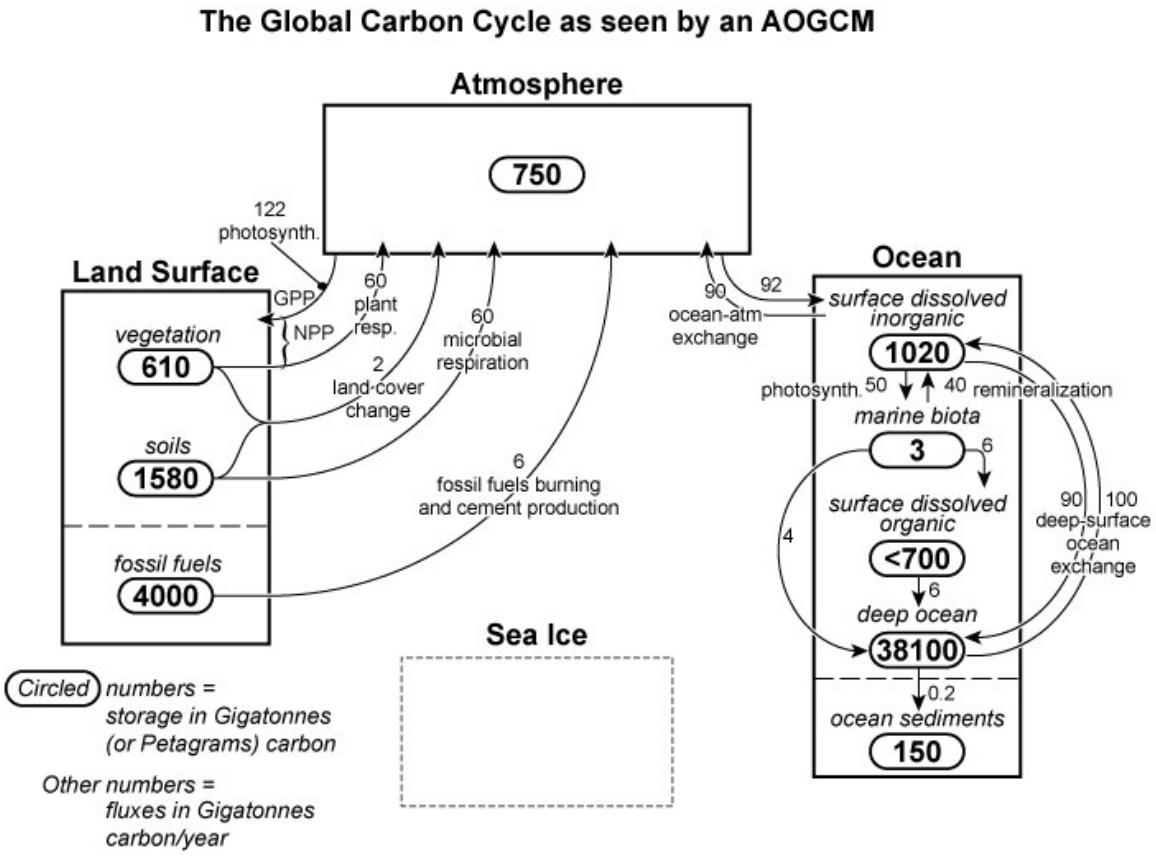

Figure VI 1: *The global carbon cycle from the point of view of existing physical climate system models (coupled AOGCMs). The four boxes represent atmosphere, land-surface, ocean and sea-ice—the major components of AOGCMS. Earth System Models will evolve from AOGCMS by incorporating the relevant biogeochemical cycles into the four-box framework (with the sea-ice component not being a reservoir of carbon). Numbers shown are average values for the 1990s. Small (≤ 1 PgC / year) fluxes such as carbon runoff from land to ocean and methane fluxes are not shown, except for burial of ~0.2 PgC / year in ocean bottom sediments. Burial in ocean sediments removes carbon from the AOGCM four-box domain;*

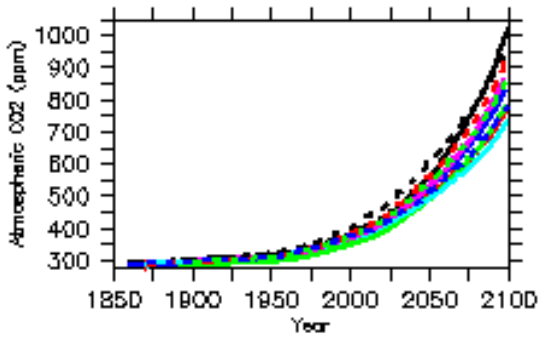

Figure VI .2: *Time series of atmospheric CO_2 temperature from eleven different AOGCM / carbon cycle models (from Friedlingstein et al. 2006, Figure 1(a))*

Chapter VII - Example Applications of Climate Model Results

Dryland Crop Yields

The effects of weather and climate on crops are complicated and not fully understood. Numerous models that simulate crop growth have been developed. These models parameterize many physiological processes. The present generation of state-of-the-art crop models typically steps through the growth process at a daily resolution and utilizes as input a number of meteorological variables that usually include maximum and minimum temperature, precipitation, solar radiation, and potential evapotranspiration. A key characteristic of these models is that they have been developed for application to a point location and have been validated based on point data, including meteorological inputs. Thus, the use of these models for assessment of climate change impacts on crop yields confronts a mismatch between the spatially-averaged climate model grid box data and the point data expected by the crop models. Also, biases in climate model data can have unknown effects on crop model results because the dependence of crop yields on meteorological variables is highly non-linear. The typical applications study circumvents these difficulties by avoiding the direct use of climate model output using some form of statistical downscaling. One approach developed during the early days of climate change assessments is still used today. In this approach, sometimes dubbed the “delta” method, the climate model output is used to determine the future change in climate with respect to the present-day climate, typically a difference for temperature and a percentage change for precipitation. Then, these change functions are applied to historical daily climate data for input to the crop model. In a second approach, the climate model data is used to adjust statistical characteristics of the observed data. Then, daily weather data for future periods are artificially produced using weather generators. In a recent study, Zhang (2005) used this approach to estimate Oklahoma wheat yields for a future simulation from HadCM3. These methods do not transmit certain climate model-simulated changes that do not affect basic statistical characteristics but might affect yields (a change to longer wet and dry spells without a change in total precipitation). Thus, additional uncertainty is introduced by such downscaling.

Small watershed flooding

This application faces many of the same issues as for dryland crop yields. For example, the models used for simulating runoff in small watersheds have been validated using point station data. In addition, runoff is a highly non-linear function of precipitation and the occurrence of flooding is particularly sensitive to the exact frequency and amount of precipitation for the most extreme events. As noted in Section V.H, climate models often under-estimate the magnitude of extremes. The ubiquitous "delta" method is also often used in such applications. Recently, Cameron (2006) determined percentage changes in precipitation from climate model simulations and applied these to a stochastic rainfall model to produce precipitation time series for input to a hydrologic model.

Urban heat waves

This estimation of changes in heat wave frequency and intensity can be accomplished using only near-surface temperature, a state variable. In addition, heat waves are large-scale phenomena and near-surface temperature is rather highly correlated over the scale of grid box size. Biases remain an issue, but that can be circumvented by using percentile-based definitions of heat waves. Meehl and Tebaldi (2004) used output from the National Center for Atmospheric Research/U.S. Department of Energy Parallel Climate Model (PCM) for 2080-2099 to calculate percentile-based measures of extreme heat; they found that heat waves will increase in intensity, frequency, and duration. If mortality estimates are desired, then biases are an issue because existing models (Kalkstein and Green 1997) used location-specific absolute magnitudes of temperature to estimate mortality. However, in this case, there are other factors that should be considered, such as adaptation (e.g. Davis et al. 2002).

Water Resources in the Western U.S.

The possibility that climate change may adversely affect the limited water resources of the mostly arid and semi-arid western U.S. poses a threat to the prosperity of that region. A group of university and government scientists, under the auspices of the Accelerated Climate Prediction Initiative (ACPI), conducted a coordinated set of studies that represented an end-to-end assessment of this issue (Barnett et al. 2004). A suite of carefully selected climate simulations were performed by the Parallel Climate Model (Dai et al. 2004; Pierce et al. 2004). These were then used to drive a

regional climate model to provide higher resolution data (Leung et al. 2004), both for direct assessment of effects on water resources and for use in impacts models. Finally, time series of model data at a daily resolution were used in a set of studies to assess water resources impacts (Steward et al. 2004; Payne et al. 2004; VanRheenen et al. 2004; Dettinger et al. 2004; Knowles and Cayan 2004; Christensen et al. 2004) and other environmental impacts (Brown et al. 2004; Pierce 2004). This project is noteworthy because of the close coordination between the production of the model simulations and the needs of the impacts modeling. Those performing the impacts studies had the opportunity of influence the model simulations and the type of model output that was made available. It is also a good example of the use of very detailed, high temporal resolution model data, rather than simple change functions between the present and the future. Overall, this assessment indicated that future climate change will likely create major challenges for water resource management, even under the rather modest changes produced by the low climate sensitivity PCM.

REFERENCES:

AchutaRao, K.M., B.D. Santer, P.J. Gleckler, K.E. Taylor, D.W. Pierce, T.P. Barnett, and T.M.L. Wigley, 2006: Variability of ocean heat uptake: Reconciling observations and models. *J. Geophys. Res.*, **111**, doi:10.1029/2005JC003136.

AchutaRao, K. and K.R. Sperber, 2006: ENSO simulation in coupled ocean-atmosphere models: Are the current models better? *Climate Dynamics*, doi:10.1007/s00382-006-0119-7.

Ackerman, A.S., M.P. Kirkpatrick, D.E. Stevens, and O.B. Toon, 2004: The impact of humidity above stratiform clouds on indirect aerosol climate forcing. *Nature*, **432**, 1014–1017.

Adams, R.M., B.A. McCarl, L.O. Mearns, 2003: The effects of spatial scale Climate scenarios on economic assessments: An example from U.S. agriculture. *Climate Change,* **60**, 131–148.

Albrecht, B.A., 1989: Aerosols, cloud microphysics, and fractional cloudiness. *Science,***245**, 1227–1230.

Alexander, M., J. Yin, G. Branstator, A. Capotondi, C. Cassou, R. Cullather, Y.-O. Kwon, J. Norris, J. Scott, and I. Wainer, 2006: Extratropical atmosphere-ocean variability in CCSM3. *J. Climate,* **19**, 2496–2525.

Alley, R.B., R.U. Clark, P. Huybrechts, and I. Joughin, 2005: Ice-sheet and sea-level changes. *Science,***310**, 456–460.

Ammann, C.M., G.A. Meehl, W.M. Washington, and C.S. Zender, 2003: A Mon. and latitudinally varying volcanic forcing dataset in simulations of 20th century climate. *Geophys. Res. Letts.*, **30**(12), 1657.

Anderson, B.T., J.O. Roads, S.C. Chen, and H.M.H. Juang, 2001: Model dynamics of summertime low-level jets over northwestern Mexico. *J. Geophys. Res.*, **106**(D4), 3401–3413.

Anderson, C.J., R.W. Arritt, and J.S. Kain, 2007: An alternative mass flux profile in the Kain-Fritsch Convective Parameterization and its effects in seasonal precipitation. *J. Hydrometeorology*, in press.

Anderson, C.J., R.W. Arritt, E.S. Takle, Z. Pan, W.J. Gutowski, R. da Silva, and PIRCS modelers, 2003: Hydrologic processes in regional climate model simulations of the central United States flood of June–July 1993. *J. Hydrometeorology*, **4**, 584–598.

Anderson, T.L., R.J. Charlson, S. Schwartz, R. Knutti, O. Boucher, H. Rodhe, and J. Heintzenberg, 2003: Climate forcing by aerosols—a hazy picture. *Science*, **300**, 1103–1104.

Andersson, L., J.J. Wilk, M.C. Todd, D.A. Hughes, A. Earle, D. Kniverton, R. Layberry, and H.H.G. Savenije, 2006: Impact Climate change and development scenarios on flow patterns in the Okavango River. *J. Hydrology,* **331**, 43–57.

Annamalai, H., K. Hamilton, and K.R. Sperber, 2007: South Asian summer monsoon and its relationship with ENSO in the IPCC AR4 simulations. *J. Climate*, in press.

Antic, S., R. Laprise, B. Denis, and R. de Elia, 2006: Testing the downscaling ability of a one-way nested regional climate model in regions of complex topography. *Climate Dynamics,* **26**, 305–325.

Antonov, J.I., S. Levitus, and T.P. Boyer, 2005: Thermosteric sea level rise, 1955–2003. *Geophys. Res. Lett.*, **32**, L12602.

Arakawa, A. and W.H. Schubert, 1974: Interaction of a cumulus cloud ensemble with the large-scale environment. Part I. *J. Atmos. Sci.,* **31**, 674–701.

Arblaster J.M., and G.A. Meehl, 2006: Contribution of various external forcings to trends in the Southern Annular Mode. *J. Climate,* **19**, 2896–2905.

Arendt, A.A., K.A. Echelmeyer, W.D. Harrison, C.S. Lingle, and V.B. Valentine, 2002: Rapid wastage of Alaska glaciers and their contribution to rising sea level. *Science,* **297**, 382–386.

Arora, V.K. and G.J. Boer, 2003: A representation of variable root distribution in dynamic vegetation models. *Earth Interactions,* **7**, 1–19.

Arzel, O., T. Fichefet and H. Goosse, 2006: Sea ice evolution over the 20th and 21st centuries as simulated by current AOGCMs. *Ocean Modelling*, **12**, 401–415.

Aurela, M., T. Laurila, and J.P. Tuovinen, 2004: The timing of snow melt controls the annual CO2 balance in a subarctic fen. *Geophys. Res. Lett.,* **31**, L16119.

Avissar, R.and R.A. Pielke, 1989: A parameterization of heterogeneous land-surface for Atmos. numerical models and its impact on regional meteorology. *Mon. Weather Rev.,***117**, 2113–2136.

Baldocchi, D. and P. Harley, 1995: Scaling carbon dioxide and water vapour exchange from leaf to canopy in a deciduous forest. I. Leaf model parameterization. *Plant, Cell and Environment,* **18**, 1146–1156.

Bard, E., B. Hamelin, and R.G. Fairbanks, 1990: U-Th ages obtained by mass spectrometry in corals from Barbados: sea level during the past 130,000 years. *Nature,* **346,** 456–458.

Barnett, T., R. Malone, W. Pennell, D, Stammer, B. Semtner, and W. Washington, 2004: The effects of climate change on water resources in the west: Introduction and overview. *Climatic Change*, **62**, 1–11.

Barnett, T.P., D.W. Pierce, K.M. AchutaRao, P.J. Gleckler, B.D.Santer, J.M. Gregory, and W.M. Washington, 2005: Penetration of human-induced warming into the world's oceans. *Science*, **309**, 284.

Beckman, A. and R. Doscher, 1997: A method for improved representation of dense water spreading over topography in geopotential-coordinate models. *J. Phys.Oceanography*, **27**, 581–591.

Bell, J.L., L.C. Sloan, and M.A. Snyder, 2004: Regional changes in extreme climatic events: a future climate scenario. *J. Climate*, **17**(**1**), 81–87.

Bellouin, N., O. Boucher, J. Haywood, and M.S. Reddy, 2005: Global estimate of aerosol direct radiative forcing from satellite measurements. *Nature*, **438**, 1138–1141.

Beringer, J., A.H. Lynch, F.S. Chapin, M. Mack, and G.B. Bonan, 2001: The representation of arctic soils in the land surface model: The importance of mosses. *J. Climate*, **14**, 3324–3335.

Betts, A.K. and J.H. Ball, 1997: Albedo over the boreal forest. *J. Geophys. Research-Atmospheres*, **102,** 28901–28909.

Biasutti, M. and A. Giannini, 2006: Robust Sahel drying in response to late 20th century forcings. *Geophys. Res. Lett*., **33**, L11706.

Bierbaum, R.M., M.J. Prather, E.M. Rasmusson and A.J. Weaver, 2003: *Estimating Climate Sensitivity: Report of a Workshop.* Ntl. Academy of Sci., Washington, D.C. (http://books.nap.edu/catalog/10787.html).

Bitz, C.M. and W.H. Lipscomb, 1999: An energy-conserving thermodynamic model of sea ice. *J. Geophys. Res.*, **104**, 15 669–15 677.

Bjerknes, Jacob, 1969: Atmos. teleconnections from the equatorial Pacific. *Mon. Weather Rev.*, **97**, 163172.

Bleck, R., 2002: An oceanic general circulation model framed in hybrid isopycnic-Cartesian coordinates. *Ocean Modelling*, **4**, 55–88.

Boisserie, M., D.W. Shin, T.E. Larow, and S. Cocke, 2006: Evaluation of soil moisture in the Florida State University climate model: Ntl. Center for Atmos. Research community land

model (FSU-CLM) using two reanalyses (R2 and ERA40) and *in situ* observations. *J. Geophys. Res.*, **111**(D8), Art. No. D08103.

Bonan, G.B., D. Pollard, and S.L. Thompson, 1992: Effects of Boreal Forest Vegetation on Global Climate. *Nature*, **359,** 716–718.

Bonan, G.B., 1995: Sensitivity of a GCM simulation to inclusion of inland water surfaces. *J. Climate*, **8**, 2691–2704.

Bony, S., R. Colman, V.M. Kattsov, R.P. Allan, C.S. Bretherton, J.-L. Dufresne, A. Hall, S. Hallegatte, M.M. Holland, W. Ingram, D.A. Randall, B.J. Soden, G.Tselioudis and M. J. Webb, 2006: How well do we understand and evaluate climate change feedback processes? *J. Climate,* **19**, 3445–3482.

Bony, S., and J.-L. Dufresne, 2005: Marine boundary layer clouds at the heart of tropical cloud feedback uncertainties in climate models. *Geophys. Res. Lett*., **32**, L20806.

Bony, S., J.-L. Dufresne, H. LeTreut, J.-J. Morcrette, and C. Senior, 2004: On dynamic and thermodynamic components of cloud changes. *Climate Dynamics,* **22**, 71–86.

Bony, S., and K.A. Emanuel, 2001: A parameterization of the cloudiness associated with cumulus convection: Evaluation using TOGA COARE data, *J. Atmos. Sci*., **58**, 3158–3183.

Boone, A., V. Masson, T. Meyers, and J. Noilhan, 2000: The influence of the inclusion of soil freezing on simulations by a soil-vegetation-atmosphere transfer scheme. *J. Ap. Meteorology*, **39**, 1544–1569.

Boyle, J.S., 1993: Sensitivity of dynamical quantities to horizontal resolution for a climate simulation using the ECMWF (cycle 33) model. *J. Climate,* **6,** 796–815.

Braithwaite, R.J. and S.C.B. Raper, 2002: Glaciers and their contribution to sea level change. *Physics and Chemistry of the Earth.*, **27**, 1445–1454.

Brankovic, T.and D. Gregory, 2001: Impact of horizontal resolution on seasonal integrations. *Climate Dynamics*, **18**, 123–143.

Breugem, W.-P., W. Hazeleger, and R.J. Haarsma, 2006: Multi-model study of tropical Atlantic variability and change. *Geophys. Res. Lett*., submitted.

Briegleb, B.P., E.C. Hunke, C.M. Bitz, W.H. Lipscomb, and J.L. Schramm, 2002: *Description of the Community Climate System Model Version 2 Sea Ice Model*, 60 pp. (available at http://www.ccsm.ucar.edu/models/ccsm2.0/csim/).

Brinkop, S. and Roeckner, E., 1995: Sensitivity of a general circulation model to parameterizations of cloud-turbulence interactions in the Atmos. boundary layer. *Tellus*, **47A**, 197–220.

Brown, T.J., B.L. Hall, and A.L. Westerling, 2004: The impact of twenty-first century climate change on wildland fire danger in the western United States: An applications perspective. *Climatic Change*, **62**, 365–388.

Bryan, F. O., G. Danabasoglu, P. R. Gent, K. Lindsay, 2006: Changes in ocean ventilation during the 21st Century in the CCSM3. *Ocean Modelling*, **15**, 141–156.

Bryan, K., 1969a: A numerical method for the study of the circulation of the world ocean. *J. Comp. Phys.*, **4**, 347–376.

Bryan, K., 1969b: Climate and the ocean circulation. III: The ocean model, *Mon. Weather Rev.*, **97**, 806–824.

Bryan, K. and Cox, M. D., 1967: A numerical investigation of the oceanic general circulation. *Tellus*, **19**, 54–80.

Bryden and Imawaki, 2000 p. 109

Burke, E. J., S.J. Brown, and N. Christidis, 2006: Modelling the recent evolution of global drought and projections for the 21st century with the Hadley Centre climate model. *J. Hydrometeorology*, **7**, 1113–1125.

Byerle, L.A.and J. Paegle, 2003: Modulation of the Great Plains low-level jet and moisture transports by orography and large-scale circulations. *J. Geophys. Res.*, **108(D16)**, Art. No. 8611.

Cai, W.J., P.H. Whetton, and D.J. Karoly, 2003: The response of the Antarctic Oscillation to increasing and stabilitzed Atmos. CO_2. *J. Climate*, **16**, 1525–1538.

Callaghan, T.V., *et al.*, 2004: Responses to projected changes in climate and UV-B at the species level. *Ambio*, **33**, 418–435.

Cameron, D., 2006: An application of the UKCIP02 climate change scenarios to flood estimation by continuous simulation for a gauged catchment in the northeast of Scotland, UK (with uncertainty). *J. Hydrology*, **328**, 212–226

Cane, M.A., A.C. Clement, A. Kaplan, Y. Kushnir, R. Murtugudde, D. Pozdnyakov, R. Seager, and S.E. Zebiak, 1997: Twentieth century sea surface temperature trends. *Science*,**275**, 957–960.

Capotondi, et al, 1987 p. 139

Capotondi, A., A. Wittenber, S. Masina, 2006: Spatial and temporal structure of ENSO in 20th century coupled simulations. *Ocean Modelling*, **15**, 274–298.

Carril, A.F., C.G. Menéndez, and A. Navarra, 2005: Climate response associated with the Southern Annular Mode in the surroundings of Antarctic Peninsula: A multimodel ensemble analysis. *Geophys. Res. Lett*., **32**.

Cassano, J.J., P. Uotila, A.H. Lynch, and E.N. Cassano, 2007: Predicted changes in synoptic forcing of net precipitation in large Arctic river basins during the 21st century. *J. Geophys. Res*., in press.

Cassano, J.J., P. Uotilla, and A.H. Lynch, 2006: Changes in synoptic weather patterns in the polar regions in the 20th and 21st centuries, Part 1: Arctic. *Intl.l J. Climatology*, in press.

Cazenave, A. and R.S. Nerem, 2004: Present-day sea level change: observations and causes. *Rev. of Geophysics*, **42**(3), RG3001.

Cess, R. D., and G. L. Potter, 1988: Exploratory studies of cloud radiative forcing with ageneral circulation model. *Tellus*, **39A**, 460–473.

Cess, R.D., *et al.,* 1990: Intercomparison and interpretation Climate feedback processes in 19 Atmos. general circulation models. *J. Geophys. Res.,* **95**,16 601–16 615.

Charney, J.G., 1979: *Carbon Dioxide and Climate: A Scientific Assessment.* Ntl. Academy of Sci., Washington, D.C., 22 pp.

Chen, F. and J. Dudhia, 2001: Coupling an advanced land surface–hydrology model with the Penn State–NCAR MM5 modeling system. Part I: Model implementation and sensitivity. *Mon. Weather Rev.*,**129**, 569–585.

Cheng, A. and K.-M. Xu, 2006: Simulation of shallow cumuli and their transition to deep convective clouds by cloud-resolving models with different third-order turbulence closures. *Quarterly J. of the Royal Meterological Soc.*, **132**, 359–382.

Cheng, Y., V.M. Canuto, and A.M. Howard, 2002: An improved model for the turbulent PBL. *J. Atmos. Sci.*, **59**, 1550–1565.

Chiacchio, M., J. Francis, and P. Stackhouse, Jr., 2002: Evaluation of methods to estimate the surface downwelling longwave flux during Arctic winter. *J. Ap. Meteorology*, **41**, 306–318.

Choi, H.I., P. Kumar, and X.-Z. Liang, 2007: 3-D volume averaged soil-moisture transport model with a scalable parameterization of subgrid topographic variability. *Water Resources Research*, in press.

Christensen, J.H., T. Carter, and F. Giorgi, 2002: PRUDENCE employs new methods to assess European climate change. *Eos*, **83**, 147.

Christensen, N.S., A.W. Wood, N. Voisin, D.P. Lettenmaier, and R.N. Palmer, 2004: The effects of climate change on the hydrology and water resources of the Colorado River basin. *Climatic Change*, **62**, 337–363.

Christensen, O.B, 1999: Relaxation of soil variables in a regional climate model. *Tellus*, **51A**, 674–685.

Christidis, N., P.A. Stott, S. Brown, G.C. Hegerl, 2005: Detection of changes in temperature extremes during the second half of the 20th century. *Geophys. Res. Lett*., **32**, L20716.

Chung, C.E., V. Ramanathan, D. Kim, and I. Podgorny, 2005: Global anthropogenic aerosol direct forcing derived from satellite and ground-based observations. *J. Geophys. Res.*, **110**, D24207.

Church, J.A.and N.J. White, 2006: A 20th century acceleration in global sea-level rise. *Geophys. Res. Lett*., **33**, L01602.

Clement, A.C., R. Seager, M.A. Cane, and S.E. Zebiak, 1996: An ocean dynamical thermostat. *J. Climate*, **9**, 2190–2196.

Clement, A.C. and B. Soden, 2005: The sensitivity of the tropical-mean radiation budget. *J. Climate*, **18**, 3189–3203.

Collins, M., B.B.B. Booth, G. Harris, J.M. Murphy, D.M.H. Sexton, M. Webb, 2006: Towards quantifying uncertainty in transient climate change. *Climate Dynamics*, in press.

Collins, W., *et al.*, 2004, Description of the NCAR Community Atmos. Model (CAM3). *NCAR Technical Report*. Ntl. Center for Atmos. Research, P.O. Box 3000, Boulder, CO, USA 80305, in preparation.

Collins, W.D., C.M. Bitz, M.L. Blackmon, G.B. Bonan, C.S. Bretherton, J.A. Carton, P. Chang, S.C. Doney, J.J. Hack, T.B. Henderson, J.T. Kiehl, W.G. Large, D.S. McKenna, B.D. Santer, and R.D. Smith, 2006: The community climate system model: CCSM3. *J. Climate*, in press.

Collins, W.D., *et al.*, 2006: Radiative forcing by well-mixed greenhouse gases: Estimates from climate models in the Intergovernmental Panel on Climate Change (IPCC) Fourth Assessment Report (AR4), *J. Geophys. Res.*, **111**, D14317.

Collins, W.D., C.M. Bitz, M.L. Blackmon, G.B. Bonan, C.S. Bretherton, J.A. Carton, P. Chang, S.C. Doney, J.J. Hack, T.B. Henderson, J.T. Kiehl, W.G. Large, D.S. McKenna, B.D. Santer, and R.D. Smith, 2005: The Community Climate System Model: CCSM3. *J. Climate*, **18**.

Colman, R., 2003: A comparison Climate feedbacks in general circulation models. *Climate Dynamics*, **20**, 865–873.

Conkright, M.E., *et al.*, 2002: *World Ocean Atlas 2001:* Objective Analyses, Data Statistics, and Figures, CD-ROM documentation. NOAA, Silver Spring, MD. 17 pp.

Cook, K.H. and E.K. Vizy, 2006: Coupled model simulations of the West African monsoon system: 20th century simulations and 21st century predictions. *J. Climate*, **19**, 3681–3703.

Cotton, W.R., 2003: Cloud modeling from days of EML to the present—Have we made progress? In: *AMS Meteorological Monographs—Symposium on Cloud Systems, Hurricanes and TRMM*, 95–106.

Covey, C., L.C. Sloan, and M.I. Hoffert, 1996: Paleoclimate data constraints on climate sensitivity: The paleocalibration method. *Climatic Change,* **32**,165–184.

Cox, P. M., R.A. Betts, C.D Jones, S.A. Spall, and I.J. Totterdell, 2000: Acceleration of global warming due to carbon-cycle feedbacks in a coupled model. *Nature*, **408**, 184–187.

Cramer, W., A. Bondeau, F.I. Woodward, *et al.*, 2001: Global response of terrestrial ecosystem and function to CO_2 and climate change: Results from six dynamic global vegetation models. *Global Change Biology*, **7**, 357373.

Crane, R.G.and B.C. Hewitson, 1998: Doubled CO_2 precipitation changes for the Susquehanna basin: Down-scaling from the GENESIS general circulation model. *Intl. J. Climatology*, **18**, 65–76.

Cubasch, U., G.A. Meehl, G. Boer, R.J. Stouffer, M. Dix, A. Noda, C.A. Senior, S. Raper, and K.S. Yap, 2001: Projections of future climate change. In: *Climate Change 2001: The Scientific Basis.* [Houghton, J.T., Y. Ding, D.J. Griggs, M. Noguer, P.J. van der Linden, X. Dai, K. Maskell, and C.A. Johnson (eds.)], Cambridge University Press, Cambridge, UK, 525–582.

Curry, J.A. and A.H. Lynch, 2002: Comparing Arctic regional climate models. *Eos,* **83**, 87.

Curry, J.A., J. Schramm, and E.E. Ebert, 1995: On the sea ice albedo climate feedback mechanism. *J. Climate*, **8**, 240–247.

Curry, J.A., W.B. Rossow, D. Randall, and J.L. Schramm, 1996: Overview of Arctic cloud and radiation characteristics. *J. Climate*, **9**, 1731–1764.

Cusack, S., J.M. Edwards, and R. Kershaw, 1999: Estimating subgrid variance of saturation and its parametrization for use in a GCM cloud scheme. *Quarterly J. Royal Meteorological Soc.*, **125**, 3057–3076.

Dai, A., 2006: Precipitation characteristics in eighteen coupled climate models. *J. Climate*, in press.

Dai, A., W.M. Washington, G.A. Meehl, T.W. Bettge, and W.G. Strand, 2004: The ACPI climate change simulations. *Climatic Change*, **62**, 29–43.

Dai, A., K.E. Trenberth, and T. Qian, 2004: A global data set of Palmer Drought Severity Index for 1870–2002: Relationship with soil moisture and effects of surface warming. *J. Hydrometeorology*, **5**, 1117–1130.

Danabasoglu, G., W.G. Large, J.J. Tribbia, P.R. Gent, and B.P. Briegleb, 2006: Diurnal ocean-atmosphere coupling. *J. Climate*, doi: 10.1175/JCLI3739.1.

Davies, H.C., 1976: Lateral boundary formulation for multilevel prediction models. *Quarterly J. of the Royal Meteorological Soc.*, **102**, 405–418.

Davies, H.C. and R.E. Turner, 1977: Updating prediction models by dynamical relaxation: An examination of the technique. *Intl. J. Climatology*, **103**, 225–245.

Davis, R.E., P.C. Knappenberger, W.M. Novicoff, and P.J. Michaels, 2002: Decadal changes in heat-related human mortality in the eastern United States. *Climate Research*, **22**, 175–184.

DeCaria, A.J., K.E. Pickering, G.L. Stenchikov, and L.E. Ott, 2005: Lightning-generated NOx and its impact on tropospheric ozone production: A three-dimensional modeling study of a Stratosphere–Troposphere Experiment: Radiation, Aerosols and Ozone (STERAO-A) thunderstorm. *J. Geophys. Res.*, **110**, D14303.

de Elía, R., R. Laprise, and B. Denis, 2002: Forcasting skill limits of nested, limited-area models: A perfect-model approach. *Mon. Weather Rev.*, **130**, 2006–2023.

Dehtloff, K. *et al.*, 2006: A dynamical link between the Arctic and the global climate system. *Geophys. Res. Lett.*, **33**, L03703.

Del Genio, A.D. and M.-S. Yao, 1993: Efficient cumulus parameterization for long-term climate studies: The GISS scheme. *The Representation of Culumus Convection in Numeric Models. Meteoroogical Monograph*, No. 46, Am. Meteorological Soc., 181–184.

Del Genio, A.D., W. Kovari, M.-S. Yao, and J. Jonas, 2004: Cumulus microphysics and climate sensitivity. *J. Climate*.

Del Genio, A.D., A. Wolf, and M.-S. Yao, 2005b: Evaluation of regional cloud feedbacks using single-column models. *J. Geophys. Res.*, **110**.

Del Genio, A.D., M.-S. Yao, W. Kovari, and K.-W. Lo, 1996: A prognostic cloud water parameterization for global climate models. *J. Climate*, **9**, 270–304.

Delworth, T.L., *et al.*, 2006: GFDL's CM2 global coupled climate models—Part 1: Formulation and simulation characteristics. *J. Climate*, **19**, 643–674.

Denis, B., R. Laprise, D. Caya, and J. Cote, 2002: Downscaling ability of one-way , nested regional climate models: The big-brother experiments. *Climate Dynamics*, **18**, 627–646.

Denis, B., R. Laprise, and D. Caya, 2003: Sensitivity of a regional climate model to the resolution of the lateral boundary conditions. *Climate Dynamics*, **20**,107–126.

Déqué, M. and J.P. Piedelievre, 1995: High-resolution climate simulation over Europe. *Climate Dynamics*, **11**, 321–339.

Déqué, M., R.G. Jones, M. Wild, F. Giorgi, J.H. Christensen, D.C. Hassell, P.L. Vidale, B. Rockel, D. Jacob, E. Kjellström, M. de Castro, F. Kucharski, and B. van den Hurk, 2005: Global high resolution versus Limited Area Model climate change projections over Europe: quantifying confidence level from PRUDENCE results. *Climate Dynamics*, **25**, 653–670.

Dettinger, M.D., D.R. Cayan, M.K. Meyer, and A.E. Jeton, 2004: Simulated hydrologic responses to climate variations and change in the Merced, Carson, and American River basins, Sierra Nevada, California, 1900–2099. *Climatic Change*, **62**, 283–317.

Dickinson, R.E., A. Henderson-Sellers, and P.J. Kennedy, 1993: Biosphere-Atmosphere Transfer Scheme (BATS) version 1e as coupled to the NCAR Community Climate Model. *NCAR Technical Note*, NCAR/TN-387+STR, Ntl. Center for Atmos. Research, Boulder, CO, USA, 72 pp. [Available from Ntl. Center for Atmos. Research, P.O. Box 3000, Boulder, CO, USA 80305.]

Diffenbaugh, N.S., M.A. Snyder, L.C. Sloan, 2004: Could CO_2-induced land-cover feedbacks alter near-shore upwelling regimes? *Proc. Ntl. Academy Sci.*, **101**, 27–32.

Dimotakis, P.E., 2005: *Turbulent mixing. Annual Rev. of Fluid Mechanics.*Volume 37:, pp. 329–356.

Doney, S.C., R. Anderson, J. Bishop, K. Caldeira, C. Carlson, M.-E. Carr, R. Feely, M. Hood, C. Hopkinson, R. Jahnke, D. Karl, J. Kleypas, C. Lee, R. Letelier, C. McClain, C. Sabine, J. Sarmiento, B. Stephens, and R. Weller, 2004: *Ocean Carbon and Climate Change (OCCC): An implementation strategy for U.S. ocean carbon cycle Science.*. University Corporation for Atmos. Research, Boulder, CO, 108 pp.

Ducharne, A., C. Golaz, E. Leblois, K. Laval, J. Polcher, E. Ledoux, and G. de Marsily, 2003: Development of a high resolution runoff routing model, calibration and application to assess runoff from the LMD GCM. *J. Hydrology,* **280**, 207–228.

Duffy, P.B., B. Govindasamy, J.P. Iorio, J. Milovich, K.R. Sperber, K.E. Taylor, M.F. Wehner, and S.L. Thompson, 2003: High-resolution simulations of global climate, Part 1: Present climate. *Climate Dynamics,* **21**, 371–390.

Duynkerke, P.G. and S.R. de Roode, 2001: Surface energy balance and turbulence characteristics observed at the SHEBA Ice Camp during FIRE III. *J. Geophys. Res.,* **106**, 15 313–15 322.

Easterling, D.R., 2002: Recent changes in frost days and the frost-free season in the United States. *Bulletin of the Am. Meteorological Soc.,* **83**, 1327–1332.

Ebert, E.E., J.L. Schramm, and J.A. Curry, 1995: Disposition of solar radiation in sea ice and the upper ocean. *J. Geophys. Res.,* **100**, 15 965–15 975.

Emanuel, K.A., 1991: A scheme for representing cumulus convection in large-scale models. *J. Atmos. Science,***48**, 2313–2335.

Emanuel, K.A., 1994: *Atmos. Convection*. Oxford University Press, Oxford, UK, 580 pp.

Emori, S. and S.J. Brown, 2005: Dynamic and thermodynamic changes in mean and extreme precipitation under changed climate. *Geophys. Res. Lett*., **32**, L17706.

Enfield, D.B., A.M. Mestas-Nuñez, and P.J. Trimble, 2001: The Atlantic Multidecadal Oscillation and its relationship to rainfall and river flows in the continental U.S., *Geophys. Res. Lett.*, **28**, 2077–2080.

Essery, R. and J. Pomeroy, 2004: Implications of spatial distributions of snow mass and melt rate for snow-cover depletion: theoretical considerations. *Annals of Glaciology*, **38**, 261–265.

Fedorov, A. and S.G. Philander, 2000: Is El Niño changing? *Science*, **288,** 1997–2002.

Field, C., R. Jackson, and H. Mooney, 1995: Stomatal responses to increased CO_2: Implications from the plant to the global scale. *Plant, Cell and Environment*, **18**, 1214–1225.

Forest, C.E., P.H. Stone, and A.P. Sokolov , 2006: Estimated PDFs of climate system properties including natural and anthropogenic forcings, *Geophys. Res. Lett.*, **33**, L01705, doi:10.1029/2005GL023977.

Foukal, P. and C. Fröhlich, H. Spruit and T.M.L. Wigley, 2006: Variations in solar luminosity and their effect on the Earth's climate. *Nature*, **443**,161–166.

Fox-Rabinovitz, M.S. and R.S. Lindzen, 1993: Numerical experiments on consistent horizontal and vertical resolution for Atmos. models and observing systems. *Mon. Weather Rev.*, **121**, 264–271.

Fox-Rabinovitz, M.S., L. Takacs, R.C. Govindaraju, and M.J. Suarez, 2001: A variable-resolution stretched-grid general circulation model: Regional climate simulation. *Mon. Weather Rev.*,**129**, 453–469.

Fox-Rabinovitz, M.S., L.L. Takacs, and R.C. Govindaraju, 2002: A variable-resolution stretched-grid general circulation model and data assimilation system with multiple areas of interest: Studying the anomalous regional climate events of 1998. *J. Geophys. Res.*, **107**(D24), Art. No. 4768.

Fox-Rabinovitz, M.S., J. Cote, B. Dugas, M. Deque, and J.L. McGregor, 2006: Variable resolution general circulation models: Stretched-grid model intercomparison project (SGMIP). *J. Geophys. Res.*, **111**(D16), Art. No. D16104.

Frei, C., R. Schöll, S. Fukutome, J. Schmidli, and P.L. Vidale, 2006: Future change of precipitation extremes in Europe: An intercomparison of scenarios from regional climate models. *J. Geophys. Res.*, **111**(D6), Art. No. D06105.

Frich, P., *et al.*, 2002: Observed coherent changes in climatic extremes during the second half of the twentieth century. *Climate Research*, **19**,193–212.

Fridlind, A.M., *et al.*, 2004: Evidence for the predominance of mid-tropospheric aerosols as subtropical anvil cloud nuclei. *Science*,**304**, 718–722.

Friedlingstein, P., L. Bopp, P. Clais, *et al.*, 2001: Positive feedback between future climate change and the carbon cycle. *Geophys. Res. Lett.*, **28**,1543–1546.

Friedlingstein, P., P. Cox, R. Betts, *et al.*, 2006: Climate-carbon cycle feedback analysis: Results from the C^4MIP model intercomparison. *J. Climate*, **19**, 3337–3353.

Fu, C B., S. Wang, Z. Xiong, W.J. Gutowski, D.-K. Lee, J.L. McGregor, Y. Sato, H. Kato, J.-W. Kim, and M.-S. Su, 2005: Regional climate model intercomparison project for Asia. *Bulletin Am. Meteorological Soc.*, **86**, 257–266.

Fyfe, J.C., G.J. Boer, and G.M. Flato, 1999: The Arctic and Antarctic oscillations and their projected changes under global warming. *Geophys. Res. Lett.*, **11**,1601–1604.

Ganachaud, A., 2003: Large-scale mass transports, water mass formation, and diffusivities estimated from World Ocean Circulation Experiment (WOCE) hydrographic data, *J. Geophys. Res.*,**108**(C7), 3213.

Ganachaud, A. and C. Wunsch, 2000: Improved estimates of global ocean circulation, heat transport and mixing from hydrographic data. *Nature*, **408**, 453–457.

Gao, S., L. Ran, and X. Li, 2006: Impacts of ice microphysics on rainfall and thermodynamic processes in the tropical deep convective regime: A 2D cloud-resolving modeling study. *Mon. Weather Rev.*, in press.

Gates, W.L., A. Henderson-Sellers, G.J. Boer, C.K. Folland, A. Kitoh, B.J. McAvaney, F. Semazzi, N. Smith, A.J. Weaver and Q.-C. Zeng,1996: Climate models—Evaluation. In: *Climate Change 1995: The Science. Climate Change. Contribution of Working Group I to the Second Assessment Report of the Intergovernmental Panel on Climate Change* [Houghton, J.T., L.G. Meira Filho, B.A. Callander, N. Harris, A. Kattenberg, and K. Maskell (eds.)]. Cambridge University Press, Cambridge, UK, and New York, NY, USA, 228–284.

Gent, P. and J.C. McWilliams, 1990: Isopycnal mixing in ocean circulation models. *J. Phys. Oceanography*, **20**,150–155.

GFDL Global Atmos. Model Development Team (GAMDT), 2004: The new GFDL global atmosphere and land model AM2/LM2: evaluation with prescribed SST conditions. *J. Climate*, submitted.

Ghan, S. J., *et al.*, 2000: An intercomparison of single column model simulations of summertime midlatitude continental convection. *J. Geophys. Res.*, **105**, 2091–2124.

Giorgi, F. and X. Bi, 2000: A study of internal variability of a regional climate model. *J. Geophys. Res.*, **105,** 29503–29521.

Giorgi, F., B. Hewitson, J. Christensen, M. Hulme, H. Von Storch, P. Whetton, R. Jones, L. Mearns, and C. Fu, 2001: Chapter 10. Regional climate change information—Evaluation and projections. In: *Climate Change 2001: The Scientific Basis*. [Houghton, J.T., Y. Ding,

D.J. Griggs, M. Noguer, P.J. vad der Linden, X. Dai, K. Maskell, and C.A. Johnson (eds.)]. Cambridge University Press, Cambridge, UK, 583–638.

Giorgi, F., M.R. Marinucci, and G.T. Bates, 1993: Development of a second-generation regional climate model (RegCM2). Part II: Convective processes and assimilation of lateral boundary conditions. *Mon. Weather Rev.*,**121,** 2814–2832.

Giorgi, F. and L.O. Mearns, 1991: Approaches to the simulation of regional climate change—A Rev.. *Rev. of Geophysics,* **29**,191–216.

Giorgi, F. and L.O. Mearns, 1999: Introduction to special section: Regional climate modeling revisited. *J. Geophys. Res.*, **104**(D6), 6335–6352.

Giorgi, F. and L.O. Mearns, 2003: Probability of regional climate change based on the Reliability Ensemble Averaging (REA) method. *Geophys. Res. Lett*., **30**, Art. No. 1629.

Giorgi, F., L.O. Mearns, C. Shields, and L. Mayer, 1996: A regional model study of the importance of local versus remote controls of the 1988 drought and the 1993 flood over the central United States. *J. Climate*, **9**, 1150–1162.

Gleckler, P.J., K.R. Sperber, and K. AchutaRao, 2006: Annual cycle of global ocean heat content: Observed and simulated. *J. Geophys. Res.,* **111**, C06008.

Gnanadesikan, A., K.W. Dixon, S.M. Griffies, V. Balaji, M. Barreiro, J.A. Beesley, W.F. Cooke, T.L. Delworth, R. Gerdes, M.J. Harrison, I.M. Held, W.J. Hurlin, H.-C. Lee, Z. Liang, G. Nong, R.C. Pacanowski, A. Rosati, J. Russell, B.L. Samuels, Q. Song, M.J. Spelman, R.J. Stouffer, C.O. Sweeney, G. Vecchi, M. Winton, A.T. Wittenberg, F. Zeng, R. Zhang, and J.P. Dunne, 2006: GFDL's CM2 global coupled climate models. Part II: The baseline ocean simulation. *J. Climate*, **19**, 675–697.

Gorham, E., 1991: Northern peatlands—role in the carbon-cycle and probable responses to climatic warming. *Ecological Applications*, **1**,182–195.

Govindasamy, B., S. Thompson, A. Mirin, M. Wickett, K. Caldeira, and C. Delire, 2005: Increase of carbon cycle feedback with climate sensitivity: Results from a coupled climate and carbon cycle model. *Tellus*, **57B**,153–163.

Grabowski, W.W. and M. W. Moncrieff, 2001: Large-scale organization of tropical convection in two-dimensional explicit numerical simulations. *Intl. J. Climatology*, **127**, 445–468.

Grabowski, W.W., 2003: MJO-like coherent structures: Sensitivity simulations using the cloud-resolving convection parameterization (CRCP). *J. Atmos. Sci.,* **60**, 847–864.

Gregory, D. and S. Allen, 1991: The effect of convective scale downdrafts upon NWP and climate simulations. *9th Conf. Numerical Weather Prediction*. Am. Meteorological Soc., Denver, CO,122–123.

Gregory, D. and P.R. Rowntree, 1990: A mass flux convection scheme with representation of cloud ensemble characteristics and stability dependent closure. *Mon. Weather Rev.*, **118**, 1483–1506.

Gregory, J.M., 1999: Representation of the radiative effect of convective anvils. *Hadley Centre Technical Note 7*, Hadley Centre for Climate Prediction and Research, Met Office, Fitzroy Road, Exeter, EX1 3BP, UK.

Gregory, J.M., H.T. Banks, P.A. Stott, J.A. Lowe, and M.D. Palmer, 2004: Simulated and observed decadal variability in ocean heat content. *Geophys. Res. Lett.*, **31**(15), L15312.

Gregory, J.M., J.A. Lowe, and S.F.B. Tett, 2006: simulated global-mean sea level changes over the last half-millennium. *J. Climate*, **19,** 4576–4592.

Gregory, J.M. and J.F.B. Mitchell, 1997: The climate response to CO_2 of the Hadley Centre coupled AOGCM with and without flux adjustment. *Geophys. Res. Lett.*, **24**, 1943–1946.

Grell, G.A., 1993: Prognostic evaluation of assumptions used by cumulus parameterizations. *Mon. Weather Rev.*, **121**, 764–787.

Grell, G.A., H. Dudhia, and D. S. Stanfler, 1994: A description of the fifth generation Penn State–NCAR Mesoscale Model (MM5). *NCAR Technical Note.* NCAR/TN-3981STR, Ntl. Center for Atmos. Research, Boulder, CO, 122 pp. [Available from Ntl. Center for Atmos. Research, P.O. Box 3000, Boulder, CO 80305.]

Grell, G.A., L. Schade, R. Knoche, A. Pfeiffer, and J. Egger, 2000: Nonhydrostatic climate simulations of precipitation over complex terrain. *J. Geophys. Res.*, **105** (D24), 29595–29608.

Griffies, S.M., 1998: The Gent-McWilliams skew-flux. *J. Phys. Oceanography*, **28**, 831–841.

Griffies, S.M., A. Gnanadesikan, K.W. Dixon, J.P. Dunne1, R. Gerdes, M.J. Harrison, A. Rosati1, J.L. Russell, B.L. Samuels, M.J. Spelman, M. Winton, and R. Zhang, 2005: Formulation of an ocean model for global climate simulations, *Ocean Science*,**1,** 45–79.

Griffies, S.M., Pacanowski, R. Schmidt, and V. Balaji, 2001: Tracer conservation with an explicit free surface method for z coordinate ocean models. *Mon. Weather Rev.*, **129**,1081–1098.

Gu, L., H. Shugart, J. Fuentes, T. Black, and S. Shewchuk, 1999: Micrometeorology, bioPhys.exchanges and NEE decomposition in a two-storey boreal forest–development and test of an integrated model. *Agricultural and Forest Meteorology,* **94**,123–148.

Guilyardi, E., 2006: El Niño—mean state—seasonal cycle interactions in a multi–model ensemble. *Climate Dynamics*, **26**, 329–348.

Guo, Z., D.H. Bromwich, and J.J. Cassano, 2003: Evaluation of polar MM5 simulations of Antarctic Atmos. circulation. *Mon. Weather Rev.*, **131**, 384–411.

Gutowski, W.J., S.G. Decker, R.A. Donavon, Z. Pan, R.W. Arritt, and E.S. Takle, 2003: Temporal-spatial scales of observed and simulated precipitation in central U.S. climate. *J. Climate*, **16**, 3841–3847.

Gutowski, W.J., K.A. Kozak, R.W. Arritt, J.H. Christensen, J. Patton, and S. Takle, 2007: A possible constraint on regional precipitation intensity changes under global warming. *J. Hydrometeorology*, submitted.

Gutowski, W.J., Z. Ötles, and Y. Chen, 1998: Effect of ocean-surface heterogeneity on climate simulation. *Mon. Weather Rev.,* **126**, 1419–1429.

Gutowski, W., C. Vörösmarty, M. Person, Z. Ötles, B. Fekete, and J. York, 2002: A Coupled Land–Atmosphere Simulation Program (CLASP). *J. Geophys. Res.,* **107**(D16), 4283.

Gutowski, W.J., H. Wei, C.J. Vörösmarty, and B.M. Fekete, 2007: Influence of Arctic wetlands on Arctic Atmos. circulation. *J. Climate*, in press.

Hack, J. J., 1994: Parameterization of moist convection in the Ntl. Center for Atmos. Research Community Climate Model (CCM2). *J. Geophys. Res.,* **99**, 5551–5568.

Hagemann, S. and L. Dümenil, 1998: A parameterization of the lateral water flow for the global scale. *Climate Dynamics*, **14**,17–31.

Hall, A., 2004: The role of surface albedo feedback in climate. *J. Climate,* **17**, 1550–1568.

Han, J. and J.O. Roads, 2004: U.S. climate sensitivity simulated with the NCEP regional spectral model. *Climate Change,* **62**,115–154.

Hansen, J., *et al.,* 1984: Climate sensitivity: analysis of feedback mechanisms. In: *Climate Processes and Climate Sensitivity,* Maurice Ewing Series, 5 [Hansen, J.E. and T. Takahashi (eds.)]. Am. Geophys. Union, Washington, DC, pp. 130–163.

Hansen, J., D. Johnson, A. Lacis, S. Lebedeff, P. Lee, D. Rind, and G. Russell, 1981: Climate impact of increasing Atmos. carbon dioxide. *Science*, **213**, 957–966.

Hansen, J., A. Lacis, R. Ruedy, M. Sato, and W. Wilson, 1993: How sensitive is the world's climate? *Ntl. Geographic Research and Exploration*, **9**, 42–158.

Hansen, J., L. Nazarenko, R. Ruedy, M. Sato, J. Willis, A. Del Genio, D. Koch, A. Lacis, K. Lo, S. Menon, T. Novakov, J. Perlwitz, G. Russell, G.A. Schmidt, and N. Tausnev, 2005: Earth's energy imbalance: Confirmation and implications. *Science*, **308,**1431–1435.

Hansen, J., G. Russell, A. Lacis, I. Fung, D. Rind, and P. Stone, 1985: Climate response times: Dependence on climate sensitivity and ocean mixing. *Science*, **229,** 857–859.

Hansen, J., M. Sato, R. Ruedy, P. Kharecha, A. Lacis, R. Miller, L. Nazarenko, K. Lo, G.A. Schmidt, G. Russell, I. Aleinov, S. Bauer, E. Baum, B. Cairns, V. Canuto, M. Chandler, Y. Cheng, A. Cohen, A. Del Genio, G. Faluvegi, E. Fleming, A. Friend, T. Hall, C. Jackman, J. Jonas, M. Kelley, N.Y. Kiang, D. Koch, G. Labow, J. Lerner, S. Menon, T. Novakov, V. Oinas, Ja. Perlwitz, Ju. Perlwitz, D. Rind, A. Romanou, R. Schmunk, D. Shindell, P. Stone, S. Sun, D. Streets, N. Tausnev, D. Thresher, N. Unger, M. Yao, and S. Zhang, 2006: Climate simulations for 1880–2003 with GISS modelE. **http://arxiv.org/abs/physics/0610109** ; also submitted to *Climate Dynamics*.

Hansen, J., M. Sato, R. Ruedy, L. Nazarenko, A. Lacis, G.A. Schmidt, G. Russell, I. Aleinov, M. Bauer, S. Bauer, N. Bell, B. Cairns, V. Canuto, M. Chandler, Y. Cheng, A. Del Genio, G. Faluvegi, E. Fleming, A. Friend, T. Hall, C. Jackman, M. Kelley, N.Y. Kiang, D. Koch, J. Lean, J. Lerner, K. Lo, S. Menon, R.L. Miller, P. Minnis, T. Novakov, V. Oinas, Ja. Perlwitz, Ju. Perlwitz, D. Rind, A. Romanou, D. Shindell, P. Stone, S. Sun, N. Tausnev, D. Thresher, B. Wielicki, T. Wong, M. Yao, and S. Zhang, 2005: Efficacy Climate Forcings. *J. Geophys. Res.*, **110**, D18104.

Harries, J.E., H.E. Brindley, P.J. Sagoo, and R.J. Bantges, 2001: Increases in greenhouse forcing inferred from the outgoing longwave radiation spectra of the Earth in 1970 and 1997. *Nature*, **410**, 355–357.

Hartmann, D.L. and M.L. Michelsen, 2002: No evidence for iris. *Bulletin Am. Meteorological Soc.*, **83**:

Hay, L.E., M.P. Clark, M. Pagowski, G.H. Leavesley, G.A. Grell, and W.J. Gutowski, Jr., 2006: One-way coupling of an atmospheric and a hydrologic model in Colorado. *J. Hydrometeorology*, **7,** 569–589.

Haylock, M.R., G.C. Cawley, C. Harpham, R.L. Wilby, and C.M. Goodess, 2006: Downscaling heavy precipitation over the UK: A comparison of dynamical and statistical methods and their future scenarios. *Intl. J. of Climatology,* **26**, 1397–1415.

Hegerl, G.C., T.J. Crowley, W.T. Hyde and D.J. Frame, 2006: Climate sensitivity constrained by temperature reconstructions over the past seven centuries. *Nature*, **440**, 1029–1032.

Hegerl, G.C., F.W. Zwiers, P.A. Stott, and V.V. Kharin, 2004: Detectability of anthropogenic changes in annual temperature and precipitation extremes. *J. Climate*, **17**(19), 3683–3700.

Held, I and M.J. Suarez, 1994: A proposal for the intercomparison of the dynamical cores of Atmos. general circulation models. *Bulletin of the Am. Meteorological Soc.,* **75**(10), 1825–1830.

Held, I.M. and B.J. Soden, 2006: Robust Responses of the Hydrological Cycle to Global Warming. *J. Climate*, **19**, 5686–5699.

Held, I.M., S.W. Lyons, and S. Nigam, 1989: Transients and the extratropical response to El Niño. *J. of the Atmos. Sci.,* **46**(1), 163–174.

Held, I.M., R.S. Hemler, and V. Ramaswamy, 1993: Radiative-convective equilibrium with explicit two-dimensional moist convection. *J. Atmos. Sci.,* **50**, 3909–3927.

Held, I.M., T.L. Delworth, J. Lu, K.L. Findell, and T.R. Knutson, 2005: *Simulation of Sahel drought in the 20th and 21st centuries.* Proc. Ntl. Academy Sci., **102**, 17,891–17,896.

Helfand, H.M. and J.C. Labraga, 1988: Design of a non-singular level 2.5 second order closure model for the prediction of Atmos. turbulence. *J. Atmos. Sci.,* **45,** 113–132.

Hellstrom, C., D.L. Chen, C. Achberger, and J. Raisanen, 2001: Comparison Climate change scenarios for Sweden based on statistical and dynamical downscaling of Mon. precipitation. *Climate Research*, **19**, 45–55.

Henderson-Sellers, A., 2006: Improving land-surface parameterization schemes using stable water isotopes: Introducing the “iPILPS” initiative. *Global and Planetary Change*, **51**, 3–24.

Henderson-Sellers, A., P. Irannejad, K. McGuffie, and A.J. Pitman, 2003: Predicting land-surface climates—Better skill or moving targets? *Geophys. Res. Letts.,* **30**, 1777.

Henderson-Sellers, A., A.J. Pitman, P.K. Love, P. Irannejad, and T.H. Chen, 1995: The project for Intercomparison of Land-Surface Parameterization Schemes (PILPS) —Phase-2 and Phase-3. *Bulletin Am. Meteorological Soc.,* **76**, 489–503.

Hewitson, B.C. and R.G. Crane, 1996: Climate downscaling: Techniques and application. *Climate Research*, **7**, 85–95.

Hewitt, C.D and D.J. Griggs, 2004: Ensembles-based predictions Climate changes and their impacts. *Eos*, **85**, 566.

Heyen, H., H. Fock, and W. Greve, 1998: Detecting relationships between the interannual variability in ecological time series and climate using a multivariate statistical approach—A case study on Helgoland Roads zooplankton. *Climate Research,* **10**, 179–191.

Hibler, W.D., 1979: A dynamic thermodynamic sea ice model. *J. Phys. Oceanography,* **9**, 815–846.

Hines, K.M., R.W. Grumbine, D.H. Bromwich, and R.I. Cullather, 1999: Surface energy balance of the NCEP MRF and NCEP-NCAR reanalysis in Antarctic latitudes during FROST. *Weather Forecasting,* **14**, 851–866.

Hirano, A., R. Welch, and H. Lang, 2003: Mapping from ASTER stereo image data: DEM validation and accuracy assessment. *ISPRS J. of Photogrammetry and Remote Sensing,* **57**, 356–370.

Hoerling, M., J. Hurrell, J. Eischeid, and A. Phillips, 2006: Detection and attribution of 20th century northern and southern African rainfall change. *J. Climate*, **19**, 3989–4008.

Hoffert, M.I. and C. Covey, 1992: Deriving global climate sensitivity from paleoclimate reconstructions. *Nature*, **360**, 573–576.

Holland, M.M. and C.M. Bitz, 2003: Polar amplification Climate change in coupled models. *Climate Dynamics*, **21**, 221–232.

Holland, M.M. and M.N. Raphael, 2006: Twentieth century simulation of the southern hemisphere climate in coupled models. Part II: Sea ice conditions and variability. *Climate Dynamics*, **26**, 229–245.

Holtslag, A.A.M. and B.A. Boville, 1993: Local versus nonlocal boundary-layer diffusion in a global climate model, *J. Climate*, **6,** 1825–1842.

Hong, S.-Y. and H.-M.H. Juang, 1998: Orography blending in the lateral boundary of a regional model. *Mon. Weather Rev.*, **126**, 1714–1718.

Hoogenboom, G., J.W. Jones, and K.J. Boote, 1992: Modeling growth, development, and yield of grain legumes using SOYGRO, PNUTGRO, and BEANGRO—A Rev.. *Trans. ASAE,* **35**, 2043–2056.

Hood, R.R., E.A. Laws, R.A. Armstrong, N.R. Bates, C.W. Brown, C.A. Carlson, F. Chai, S.C. Doney, P.G. Falkowski, R.A. Feely, M.A.M. Friedrichs, M.R. Landry, J.K. Moore, D.M. Nelson, T. Richardson, B. Salihoglu, M. Schartau, D.A. Toole, and J.D. Wiggert, 2006: Pelagic functional group modeling: Progress, challenges and prospects. *Deep-Sea Research II*, **53**, 459–512.

Hope, P.K., N. Nicholls, and J.L. McGregor, 2004: The rainfall response to permanent inland water in Australia. *Australian Meteorological Magazine*, **53**, 251–262.

Horel, J.D. and J.M. Wallace, 1981: Planetary-scale atmospheric phenomena associated with the Southern Oscillation. *Mon. Weather Rev.*, **109**, 813–829.

Hori, M.E. and H. Ueda, 2006: Impact of global warming on the East Asian winter monsoon as revealed by nine coupled atmosphere–ocean GCMs. *Geophys. Res. Letts.,* **33**, doi:10.1029/2005GL024961.

Horowitz, L.W., *et al.,* 2003: A global simulation of tropospheric ozoneand related tracers: Description and evaluation of MOZART, version 2. *J. Geophys. Res.*, **108**(D24), 4784.

Houghton, R., 2003: Revised estimates of the annual net flux of carbon to the atmosphere from changes in land use and land management 1850–2000. *Tellus*, **55B**, 378–390.

Huang, B., P.H. Stone, and C. Hill, 2003: Sensitivities of deep-ocean heat uptake and heat content to surface fluxes and subgridscale parameters in an ocean general circulation model with idealized geometry, *J. Geophys. Res.*, **108**(C1), 3015, doi:10.1029/2001JC001218.

Hungate, B.A., J.S. Dukes, M.R. Shaw, Y. Luo, and C.B. Field, 2003: Nitrogen and climate change. *Science*, **302**, 1512–1513.

Hunke, E.C. and J.K. Dukowicz, 1997: An elastic-viscous-plastic model for sea ice dynamics. *J. Phys. Oceanography*, **27**,1849–1867.

Hunke, E.C. and Y. Zhang, 1999: A comparison of sea ice dynamics models at high resolution. *Mon. Weather Rev.*, **127**, 396–408.

Hurrell, J.W., 1995: Decadal trends in the North Atlantic Oscillation and relationships to regional temperature and precipitation. *Science,***269**, 676–679.

Iorio, J.P., P.B. Duffy, B. Govindasamy, S.L. Thompson, M. Khairoutdinov, and D. Randall, 2004: Effects of model resolution and subgrid-scale physics on the simulation of precipitation in the continental United States. *Climate Dynamics*, **23**, 243–258.

IPCC, Intergovernmental Panel on Climate Change, 2007: Working Group 1 *Fourth Assessment Report Summary for Policymakers*, **www.ipcc.ch**.

Irannejad, P., A. Henderson-Sellers, and S. Sharmeen, 2003: Importance of land-surface parameterization for latent heat simulation. *Geophys. Res. Letts.,* **30**, 1904.

Jakob, C. and G. Tselioudis, 2003: Objective identification of cloud regimes in the tropical western Pacific. *Geophys. Res. Letts.,* **30**, 2082.

Janowiak, J. E., 1988: An investigation of interannual rainfall variability in Africa. *J. Climate,* **1**, 240–255.

Jones, C.A. and J.R. Kiniry, 1986: *CERES-Maize: A simulation model of maize growth and development*. Texas A&M University Press, College Station, TX.

Jones, P.D., T. Jónsson, and D. Wheeler, 1997: Extension to the North Atlantic Oscillation using early instrumental pressure observations from Gibraltar and South-West Iceland. *Int. J. Climatol.* **17**,1433–1450.

Jones, R.G., J.M. Murphy, and M. Noguer, 1995: Simulation Climate change over Europe using a nested regional climate model. I: Assessment of control climate, including sensitivity to location of lateral boundaries. *Intl. J. Climatology,* **121**, 1413–1449.

Joseph, R. and S. Nigam, 2006: ENSO evolution and teleconnections in IPCC's 20th century climate simulations: Realistic representation? *J. Climate*. Accepted.

Kain, J.S. and J. M. Fritsch, 1993: Convective parameterization in mesoscale models: The Kain-Fritsch scheme. In: *The Representation of Cumulus Convection in Numerical Models, Meteorological Monographs,* Am. Meteorological Soc., **46**, 165–170.

Kalkstein, L.S. and J.S. Greene, 1997: An evaluation Climate/mortality relationships in larger U.S. cities and the possible impacts of a climate change. *Environmental Health Perspectives,* **105**, 84–93.

Kanamitsu, M., W. Ebisuzaki, J. Woollen, S.-K. Yang, J.J. Hnilo, M. Fiorino, and G.L. Potter, 2002: NCEP-DEO AMIP-II Reanalysis (R-2). *Bulletin Am. Meteorological Soc.,* **83**, 1631–1643.

Kattenberg, A., F. Giorgi, H. Grassl, G A. Meehl, J.F.B. Mitchell, R.J. Stouffer, Tokioka, A.J. Weaver, T.M.L. Wigley, 1996: Chapter 6. Climate Models Projections of Future Climate. In: *Climate Change 1995–The Science. Climate Change.* [Houghton, J.T., L.G. Miera Filho,

B.A. Chandler, N. Harris, A. Kattenberg, and K. Maskell (eds.)]. Cambridge University Press, Cambridge, UK, 285–358.

Kattsov, V.M., J.E. Walsh, A. Rinke, K. Dethloff, 2000: Atmos. climate models: simulation of the Arctic Ocean fresh water budget components. In: *The Freshwater Budget of the Arctic Ocean.* [Lewis, E.L. (ed.)]. Kluwer Academic Publishers, Dordrecht, The Netherlands, 209–247.

Kattsov, V. and E. Källén, 2005: Future changes Climate: Modelling and scenarios for the Arctic Region. In: *Arctic Climate Impact Assessment (ACIA).* Cambridge University Press, Cambridge, UK, 1042 pp.

Khain, A. and A. Pokrovsky, 2004: Simulation of effects of Atmos. aerosols on deep turbulent convective clouds using a spectral microphysics mixed-phase cumulus cloud model. Part II: Sensitivity study. *J. of Atmos. Sci.*, **61**, 2963–2982.

Kidson, J.W. and C.S. Thompson, 1998: Comparison of statistical and model-based downscaling techniques for estimating local climate variations. *J. Climate,* **11**, 35–753.

Kiehl, J.T., J. Hack, G. Bonan, B. Boville, B. Briegleb, D. Williamson, and P. Rasch, 1996: *Description of the NCAR Community Climate Model (CCM3). NCAR Technical Note.* NCAR/TN-420+STR, Ntl. Center for Atmos. Research, Boulder, CO, 152 pp. [Available Ntl. Cen. Atmos. Res., P.O. Box 3000, Boulder, CO, 80305.]

Kiehl, J.T., C.A. Shields, J.J. Hack, and W.D. Collins, 2006: The climate sensitivity of the Community Climate System Model: CCSM3. *J. Climate*, **19**, 2584–2596.

Kiktev, D., D.M.H. Sexton, L. Alexander, and C.K. Folland, 2003: Comparison of modeled and observed trends in indices of daily climate extremes. *J. Climate,* **16**, 3560–3571.

Kim, J., J. Kim, J.D. Farrara, and J.O. Roads, 2005: The effects of the Gulf of California SSTs on warm-season rainfall in the southwestern United States and northwestern Mexico: A regional model study. *J. Climate*, **18**, 4970–4992.

Kim, J. and J.E. Lee, 2003: A multiyear regional climate hindcast for the western United States using the mesoscale Atmos. simulation model. *J. Hydrometeorology*, **4(5),** 878–890.

Kimoto, M., 2005: Simulated change of the east Asian circulation under global warming scenario. *Geophys. Res. Letts.,* **32**, L16701.

King, J.C. and J. Turner, 1997: *Antarctic Meteorology and Climatology.* Cambridge University Press, Cambridge, UK, 256 pp.

Kirschbaum, M.U.F., 2000: Will changes in soil organic carbon act as a positive or negative feedback on global warming? *Biogeochemistry*, **48**, 21–51.

Kitoh, A. and T. Uchiyama, 2006: Changes in onset and withdrawal of the East Asian summer rainy season by multi-model global warming experiments. *J. Meteorological Soc. of Japan*, **84**, 247–258.

Kleidon, A., 2004: Global datasets of rooting zone depth inferred from inverse methods. *J. Climate*, **17**, 2714–2722.

Klein, S.A. and C. Jakob, 1999: Validation and sensitivities of frontal clouds simulated by the ECMWF model. *Mon. Weather Rev.*, **127**, 2514–2531.

Klemp, J.B. and R. Wilhelmson, 1978: The simulation of three-dimensional convective storm dynamics. *J. Atmos. Sci.*, **35**, 1070–1096.

Knowles, N. and D.R. Cayan, 2004: Elevational dependence of projected hydrologic changes in the San Francisco estuary and watershed. *Climatic Change*, **62**, 319–336.

Knutson, T.R., T.L. Delworth, K.W. Dixon, I.M. Held, J. Lu, V. Ramaswamy, M.D. Schwarzkopf, G. Stenchikov, and R J. Stouffer, 2006: Assessment of twentieth-century regional surface temperature trends using the GFDL CM2 coupled models. *J. Climate*, **19**(9), 1624–1651.

Knutson, T. and S. Manabe, 1998: Model assessment of decadal variability and trends in the tropical Pacific Ocean. *J. Climate*, **11**, 2273– 2296.

Knutson, T.R., J.J. Sirutis, S.T. Garner, I.M. Held, and R.E. Tuleya, 2007: Simulation of recent multi-decadal increase of Atlantic hurricane activity using an 18km regional model. *Bulletin Am. Meteorological Soc*., in press.

Knutti, R., G.A. Meehl, M.R. Allen, and D.A. Stainforth, 2006: Constraining climate sensitivity from the seasonal cycle in surface temperature. *J. Climate,* in press.

Koren, V., J. Schaake, K. Mitchell, Q.Y. Duan, F. Chen, and J.M. Baker, 1999: A parameterization of snowpack and frozen ground intended for NCEP weather and climate models. *J. Geophys. Res.*, **104**(D16), 19569–19585.

Kraus, E.B. and J.S. Turner, 1967: A one-dimensional model of the seasonal thermocline. II, The general theory and its consequences. *Tellus*, **19**, 98–105.

Kravtsov, S.V., and C. Spannagle, 2007: Multi-decadal climate variability in observed and modeled surface temperatures. *J. Climate*, submitted.

Krinner, G., 2003: Impact of lakes and wetlands on boreal climate. *J. Geophys. Res.*, **108**(D16), 4520.

Kripalani, R.H., J.H. Oh, and H.S. Chaudhari, 2007: Response of the East Asian summer monsoon to doubled Atmos. CO2: Coupled climate models simulations and projections under IPCC AR4. *Theoretical and Applied Climatology*, **87**, 1–28.

Kripalani, R.H., J.H. Oh, Ashwini Kulkarni, S.S. Sabade, and H.S. Chaudhari, 2006: South Asian summer monsoon precipitation variability: Coupled climate simulations and projections under IPCC AR4. *Theoretical and Applied Climatology*, in press.

Krueger, S.K., 1988: Numerical simulation of tropical cumulus clouds and their interaction with the subcloud layer. *J. of Atmos. Sci.*, **45**, 2221–2250.

Kunkel, K.E., K. Andsager, X.-Z. Liang, R.W. Arritt, E.S. Takle, W.J. Gutowski, Jr., and Z. Pan, 2002: Observations and regional climate model simulations of heavy precipitation events and seasonal anomalies: A comparison. *J. Hydrometeorology*, **3**, 322–334.

Kunkel, K.E., S.A. Changnon, B.C. Reinke, and R.W. Arritt, 1996: The July 1995 heat wave in the Midwest: A climatic perspective and critical weather factors. *Bulletin Am. Meteorological Soc.*, **77**, 1507–1518.

Kunkel, K.E., D.R. Easterling, K. Hubbard, and K. Redmond, 2004: Temporal variations in frost-free season in the United States: 1895–2000. *Geophys. Res. Letts.*, **31**, L03201.

Kunkel, K.E., X.-Z. Liang, J. Zhu, and Y. Lin, 2007: Can CGCMs simulate the Twentieth Century "warming hole" in the central United Sates *J. Climate*, in press.

Kuo, H.L., 1974: Further studies of the parameterization of the influence of cumulus convection on large-scale flow. *J. of Atmos. Sci.*, **31**, 1232–1240.

Laprise, R., 2003: Resolved scales and nonlinear interactions in limited-area models. *J. of Atmos. Sci.*, **60**, 768–779.

Large, W., J.C. McWilliams, and S.C. Doney, 1994: Oceanic vertical mixing: A Rev. and a model with a nonlocal boundary mixing parameterization. *Rev. Geophysics*, **32**, 363–403.

Latif, M., *et al.*, 2001: ENSIP: The El Nino simulation intercomparison project. *Climate Dynamics*, **18**, 255–272.

Lau, K.-M., S. Shen, K.-M. Kim, and H. Wang, 2006: A multi-model study of the 20th century simulations of Sahel drought from the 1970s to 1990s. *J. Geophys. Res.*, **111**(D0711), **need inclusive page numbers**.

Lawrence, D.M. and A.G. Slater, 2005: A projection of severe near-surface permafrost degradation during the 21st century. *Geophys. Res. Letts.*, **32**, L24401.

Le Treut, H. and Z.X. Li, 1991: Sensitivity of an Atmos. general circulation model to prescribed SST changes: Feedback effects associated with the simulation of cloud optical properties. *Climate Dynamics*, **5**,175–187.

Le Treut, H., Z.X. Li, and M. Forichon, 1994: Sensitivity of the LMD general circulation model to greenhouse forcing associated with two different cloud water parametrizations. *J. Climate*, **7**, 1827–1841.

Leung, L.R., Y. Qian, X. Bian, W.M. Washington, J. Han, and J.O. Roads, 2004: Mid-century ensemble regional climate change scenarios for the western United States. *Climatic Change*, **62**, 75–113.

Leaman, K., R. Molinari, and P. Vertes, 1987: Structure and variability of the Florida Current at 27N: April 1982–July 1984. *J. of Phys.Oceanography*, **17**, 565–583.

Lean, J., J. Beer, and R. Bradley, 1995: Reconstruction of solar irradiance since 1610: Implications for climate change. *Geophys. Res. Letts.*, **22**, 3195–3198.

Lee, H.-C., A. Rosati, M. Spelman, and T. Delworth, 2006: Barotropic tidal mixing effects in a coupled climate model: Ocean conditions in the northern Atlantic. *Ocean Modelling*, **11**, 464–477.

Leung, L.R. and Y. Qian, 2003: The sensitivity of precipitation and snowpack simulations to model resolution via nesting in regions of complex terrain. *J. Hydrometeorology*, **4**, 1025–1043.

Leung, L.R., Y. Qian, and X. Bian, 2003: Hydroclimate of the western United States based on observations and regional climate simulation of 1981–2000. Part I: Seasonal statistics. *J. Climate*, **16**(12), 1892–1911.

Leung, L.R., Y. Qian, X. Bian, W.M. Washington, J. Han, and J.O. Roads, 2004: Mid-century ensemble regional climate change scenarios for the western United States. *Climate Change*, **62**, 75–113.

Leung L.R. and M.S. Wigmosta, 1999: Potential climate chance impacts on mountain watersheds in the Pacific Northwest. *J. Am. Water Resources Assn.*, **35**, 1463–1471.

Levitus, S., J.I. Antonov, J. Wang, T.L. Delworth, K.W. Dixon, and A.J. Broccoli, 2001: Anthropogenic warming of Earth's climate system. *Science*, **292**, 267–270.

Li, K.Y., R. De Jong, M.T. Coe, and N. Ramankutty, 2006: Root-water-uptake based upon a new water stress reduction and an asymptotic root distribution function. *Earth Interactions*, **10**, Art. No. 14.

Li, W., R. Fu, and R.E. Dickinson, 2006: Rainfall and its seasonality over the Amazon in the 21st century as assessed by the coupled models for the IPCC AR4. *J. Geophys. Res.*, **11**, D02111.

Li, X., Y. Chao, J. McWilliams, and L-L. Fu, 2001: A comparison of two vertical-mixing schemes in a Pacific Ocean General Circulation Model. *J. Climate*, **14**, 1377–1398.

Li, X. and T. Koike, 2003: Frozen soil parameterization in SiB2 and its validation with GAME-Tibet observations. *Cold Regions Science. and Technology,* **36**, 165–182.

Li, Z.X., 1999: Ensemble Atmos. GCM simulation Climate interannual variability from 1979 to 1994. *J. Climate*, **12**, 986–1001.

Liang, X.-Z., K.E. Kunkel, and A.N. Samel, 2001: Development of a regional climate model for U.S. Midwest applications. Part 1: Sensitivity to buffer zone treatment. *J. Climate*, **14**, 4363–4378.

Liang, X.-Z., L. Li, A. Dai, and K.E. Kunkel, 2004: Regional climate model simulation of summer precipitation diurnal cycle over the United States. *Geophys. Res. Letts.*, **31**, L24208.

Liang, X.-Z., J. Pan, J. Zhu, K.E. Kunkel, J.X.L. Wang, and A. Dai, 2006: Regional climate model downscaling of the U.S. summer climate and future change. *J. Geophys. Res.*, **111**, D10108.

Liang, X., Z. Xie, and M. Huang, 2003: A new parameterization for surface and groundwater interactions and its impact on water budgets with the variable infiltration capacity (VIC) land surface model. *J. Geophys. Res.*, **108**, 8613.

Libes, S.M., 1992: *An Introduction to Marine Biogeochemistry.* Wiley, New York, New York, 734 pp.

Lin, J.L., B. Mapes, M.H. Zhang, and M. Newman, 2004: Stratiform precipitation, vertical heating profiles, and the Madden–Julian Oscillation. *J. Atmos. Sci.*, **61**, 296–309.

Lin, J.L., G.N. Kiladis, B.E. Mapes, K.M. Weickmann, K.R. Sperber, W.Y. Lin, M.Wheeler, S.D. Schubert, A. Del Genio, L.J. Donner, S. Emori, J.-F. Gueremy, F. Hourdin, P.J. Rasch, E. Roeckner, and J.F. Scinocca, 2006: Tropical intraseasonal variability in 14 IPCC AR4 climate models. Part I: Convective signals. *J. Climate*, in press.

Lin, S.J. and R.B. Rood, 1996: Multidimensional flux-form semi-lagrangian transport schemes. *Mon. Weather Rev.*, **124**, 2046–2070.

Lin, W.Y. and M.H. Zhang, 2004: Evaluation of clouds and their radiative effects simulated by the NCAR Community Atmos. Model CAM2 against satellite observations. *J. Climate*, **17**, 3302–3318.

Lindzen, R.S., M.-D. Chou, and A. Y. Hou, 2001: Does Earth have an adaptive infrared iris? *Bulletin Am. Meteorological Soc.*, **82**, 417–432.

Lindzen, R.S. and M.S. Fox-Rabinovitz, 1989: Consistent vertical and horizontal resolution. *Mon. Weather Rev.*, **117**, 2575–2583.

Liston, G.E., 2004: Representing subgrid snow cover heterogeneities in regional and global models. *J. Climate*, **17**, 1381–1397.

Liu, Z., 1998: On the role of ocean in the transient response of tropical climatology to global warming. *J. Climate*, **11**, 864–875.

Lock, A., 1998: The parametrization of entrainment in cloudy boundary layers. *Quarterly J. Royal Meterological Soc.*, **124**, 2729–2753.

Lock, A.P., A.R. Brown, M.R. Bush, G.M. Martin, and R.N.B. Smith, 2000: A new boundary layer mixing scheme. Part I: Scheme description and single-column model tests. *Mon. Weather Rev.*,**128**, 3187–3199.

Lofgren, B.M., 2004: A model for simulation of the climate and hydrology of the Great Lakes basin. *J. Geophys. Res.*, **109(D18),** Art. No. D18108.

Lohmann, U. and E. Roeckner, 1996: Design and performance of a new cloud microphysics scheme developed for the ECHAM4 general circulation model. *Climate Dynamics*, **12**, 557–572.

Lorenz, P., D. Jacob, 2005: Influence of regional scale information on the global circulation: A two-way nesting climate simulation. *Geophys. Res. Lett.*, **32,** Art. No. L18706.

Lucarini, V., S. Calmanti, A. dell'Aquila, P.M. Ruti, and A. Speranza, 2006: Intercomparison of the northern hemisphere winter mid-latitude Atmos. variability of the IPCC models. *Climate Dynamics*.

Lumpkin, R. and K. Speer, 2003: Large-scale vertical and horizontal circulation in the North Atlantic Ocean. *J. of Phys.Oceanography*, **33**, 1902–1920.

Luo, L.F., *et al.*, 2003: Effects of frozen soil on soil temperature, spring infiltration, and runoff: Results from the PILPS 2(d) experiment at Valdai, Russia. *J. Hydrometeorology*, **4**, 334-351.

Lynch, A.H., W.L. Chapman, J.E. Walsh, and G. Weller, 1995: Development of a regional climate model of the western Arctic. *J. Climate,* **8,** 1555–1570.

Lynch, A.H., J.A. Maslanik, and W.L. Wu, 2001: Mechanisms in the development of anomalous sea ice extent in the western Arctic: A case study. *J. Geophys. Res.*, **106**(D22), 28097–28105.

Lynn, B.H., A. Khain, J. Dudhia, D. Rosenfeld, A. Pokrovsky, and A. Seifert, 2005: Spectral (bin) microphysics coupled with a mesoscale model (MM5). Part II: Simulation of a CaPE rain event with a squall line. *Mon. Weather Rev.*, **133**, 59–71.

Maak, K. and H. von Storch, 1997: Statistical downscaling of Mon. mean temperature to the beginning of flowering of *Galanthus nivalis L.* in Northern Germany. *Intl. J. of Biometeor*ology, **41**, 5–12.

Malevsky–**Malevich**, S.P., E.D. Nadyozhina, V.V. Simonov, O.B. Shklyarevich, and E.K. Molkentin, 1999: The evaluation Climate change influence on the permafrost season soil thawing regime. *Contemporary Investigation at Main GeoPhysical Observatory*, **1**, 33–50 (in Russian).

Manabe, S., 1969: Climate and the ocean circulation. The Atmos. circulation and hydrology of the Earth's surface. *Mon. Weather Rev.*, **97**, 739–774.

Manabe, S., J. Smagorinsky, and R.F. Strickler, 1965: Simulated climatology of a general circulation model with a hydrological cycle. *Mon. Weather Rev.,* **93**, 769–798.

Manabe, S., R J. Stouffer, M.J. Spelman, and K. Bryan, 1991: Transient responses of a coupled ocean-atmosphere model to gradual changes of Atmos. CO2. Part I: Annual mean response. *J. Climate*, **4**, 785–818.

Martin, G.M., M.R. Bush, A.R. Brown, A.P. Lock, and R.N.B. Smith, 2000: A new boundary layer mixing scheme. Part II: Tests in climate and mesoscale models. *Mon. Weather Rev.*, **128**, 3200–3217.

Maxwell, R.M. and N.L. Miller, 2005: Development of a coupled land surface and groundwater model. *J. Hydrometeorology*, **6**, 233–247.

McCreary, J. and P. Lu, 1994: Interaction between the subtropical and equatorial ocean circulation—the subtropical cell. *J. of Phys.Oceanography*, **24**, 466–497.

McCulloch, M.T. and T. Ezat, 2000: The coral record of the last interglacial sea levels and sea surface temperatures. *Chem. Geol.*, **169**, 107–129.

McGregor, J.L., 1997: Regional climate modelling. *Meteorology and Atmos. Physics*, **63**, 105–117.

McGregor, J.L., 1999: Regional modelling at CAR: Recent developments. In *Parallel Computing in Meteorology and Oceanography*, BMRC Research Report No. 75, Bureau of Meteorology, Melbourne, Australia, 43–48.

McPhaden, M.J., A.J. Busalacchi, R. Cheney, J.R. Donguy, K.S. Gage, D. Halpern, M. Ji, P. Julian, G. Meyers, G.T. Mitchum, P.P. Niiler, J. Picaut, R.W. Reynolds, N. Smith, and K. Takeuchi, 1998: The Tropical Ocean Global Atmosphere (TOGA) observing system: A decade of progress. *J. Geophys. Res.*, **103**, 14 169–14 240.

Mearns, L.O., 2003: Issues in the impacts Climate variability and change on agriculture—Applications to the southeastern United States. *Climate Change*, **60**, 1–6.

Mearns, L.O., I. Bogardi, F. Giorgi, I. Matayasovszky, and M. Palecki, 1999: Comparison Climate change scenarios generated daily temperature and precipitation from regional climate model experiments and statistical downscaling. *J. Geophys. Res.*, **104**, 6603–6621.

Mearns, L.O., F. Giorgi, L. McDaniel, and C. Shields, 2003: Climate scenarios for the southeastern US based on GCM and regional model simulations. *Climate Change*, **60**, 7–35.

Mechoso, C.R., A.W. Robertson, N. Barth, M.K. Davey, P. Delecluse, P.R. Gent, S. Ineson, B. Kirtman, M. Latif, H. Le Treut, T. Nagai, J.D. Neelin, S.G.H. Philander, J. Polcher, P.S. Schopf, T. Stockdale, M.J. Suarez, L. Terray, O. Thual, and J.J. Tribbia, 1995: The seasonal cycle over the tropical Pacific in coupled ocean-atmosphere general circulation models. *Mon. Weather Rev.*, **123**, 2825–2838.

Meehl, G. and C. Tebaldi, 2004: More intense, more frequent, and longer lasting heat waves in the 21st Century. *Sci.*, **305**, 994–997.

Meehl, G.A., C. Tebaldi, and D. Nychka, 2004: Changes in frost days in simulations of twenty-first century climate. *Climate Dynamics*, **23**, 495–511.

Meehl, G.A., W.M. Washington, B.D. Santer, W.D. Collins, J.M. Arblaster, A. Hu, D.M. Lawrence, H. Teng, L.E. Buja, and W.G. Strand, 2006: Climate change projections for the

twenty-first century and climate change commitment in the CCSM3. *J. Climate*, **19**, 2597–2616.

Mellor, G.L. and T. Yamada, 1974: A hierarchy of turbulent closure models for planetary boundary layers. *J. of Atmos. Sci.*, **31**,1791–1806.

Mellor, G.L. and T. Yamada, 1982: Development of a tubulence closure model for geoPhys.fluid problems. *Rev.s of Geophysics and Space Physics*, **20**, 851–875.

Merryfield, W.J., 2006: Changes to ENSO under CO2 doubling in a multi-model ensemble. *J. Climate*, **19**, 4009–4027.

Miguez-Macho, G., G.L. Stenchikov, and A. Robock, 2005: Regional climate simulations over North America: Interaction of local processes with improved large-scale flow. *J. Climate*, **18**, 1227–1246.

Miller, D.A., and R.A. White, 1998: A conterminous United States multilayer soil characteristics dataset for regional climate and hydrology modeling. *Earth Interactions*, **2**,1–26.

Miller, R.L., G.A. Schmidt, and D.T. Shindell, 2006: Forced variations of annular modes in the 20th century IPCC AR4 simulations. *J. Geophys. Res.*, in press.

Min, S.-K. and A. Hense, 2006: A Bayesian assessment Climate change using multi-model ensembles. Part I: Global mean surface temperature. *J. Climate*, **19,** 3237–3256.

Min, S.-K. and A. Hense, 2006: A Bayesian assessment Climate change using multi-model ensembles. Part II: Regional and seasonal mean surface temperature. *J. Climate,*in press.

Mirocha, J.D., B. Kosovic, and J.A. Curry, 2005: Vertical heat transfer in the lower atmosphere over the Arctic Ocean during clear-sky periods. *Boundary-Layer Meterology*, **117**, 37–71.

Mitchell, J. F. B., C.A. Senior, and W. J. Ingram, 1989: CO2 and climate: A missing feedback? *Nature*, **341**, 132–134.

Miura, H., H. Tomita, T. Nasuno, S. Iga, M. Satoh, and T. Matsuno, 2005: A climate sensitivity test using a global cloud resolving model under an aqua planet condition. *Geophys. Res. Letts.*, **32**, L19717.

Mo, K.C., J.E. Schemm, H.M.H. Juang, R.W. Higgins, and Y. Song, 2005: Impact of model resolution on the prediction of summer precipitation over the United States and Mexico. *J. Climate*, **18**, 3910–3927.

Moorthi, S. and M.J. Suarez, 1992: Relaxed Arakawa-Schubert: A parameterization of moist convection for general circulation models. *Mon. Weather Rev.,* **120**, 978–1002.

Morel, A. and D. Antoine, 1994: Heating rate within the upper ocean in relation to its bio-optical state. *J. Phys.Oceanography*, **24**, 1652–1665.

Morrison, H. and J.O. Pinto, 2005: Mesoscale modeling of springtime Arctic mixed-phase stratiform clouds using two-moment bulk microphysics scheme. *J. Atmos. Sci.*, **62**, 3683–3704.

Murray, R.J., 1996: Explicit generation of orthogonal grids for ocean models. *J. Comp. Physics*, **126**, 251–273.

NARCCAP, cited as 2007: http://www.narccap.ucar.edu.

Nadelhoffer, K. J., B.A. Emmett, P. Gundersen, *et al.*, 1999: Nitrogen makes a minor contribution to carbon sequestration in temperate forests. *Nature*, **398**, 145–148.

Najjar, R.G., X. Jin, F. Louanchi, O. Aumont, K. Caldeira, S.C. Doney, J.-C. Dutay, M. Follows, N. Gruber, F. Joos, K. Lindsay, E. Maier-Reimer, R.J. Matear, K. Matsumoto, A. Mouchet, J.C. Orr, G.-K. Plattner, J.L. Sarmiento, R. Schlitzer, M.F. Weirig, Y. Yamanaka, and A. Yool, 2006: Impact of circulation on export production, dissolved organic matter and dissolved oxygen in the ocean: Results from OCMIP-2. *Global Biogeochemistry Cycles*, submitted.

Neelin, J.D., M. Latif, M.A.F. Allaart, M.A. Cane, U. Cubasch, W.L. Gates, P.R. Gent, M. Ghil, C. Gordon, N.C. Lau, C.R. Mechoso, G.A. Meehl, J.M. Oberhuber, S.G.H. Philander, P.S. Schopf, K.R. Sperber, A. Sterl, T. Tokioka, J. Tribbia, and S.E. Zebiak, 1992: Tropical air-sea interaction in general circulation models. *Climate Dynamics*, **7**, 73–104.

Niu, G.Y., and Z.L. Yang, 2006: Effects of frozen soil on snowmelt runoff and soil water storage at a continental scale. *J. Hydrometeorology*, **7**, 937–952.

Nordeng, T.E., 1994: Extended versions of the convective parameterization scheme at ECMWF and their impact on the mean and transient activity of the model in the tropics. *Technical Memorandum 206, European Center for Medium range Weather Forecasting (ECMWF)*, Reading, UK.

Norris, J. and C.P. Weaver, 2001: Improved techniques for evaluating GCM cloudiness applied to the NCAR CCM3. *J. Climate*, **14**, 2540–2550.

Nowak, R.S., D.S. Ellsworth, and S.D. Smith, 2004: Tansley Rev.: Functional responses of plants to elevated Atmos. CO_2—Do photosynthetic and productivity data from FACE experiments support early predictions? *New Phytologist*, **162**, 253–280.

Ohlmann, J.C., 2003: Ocean radiant heating in climate models. *J. Climate*, **16**, 1337–1351.

Oleson, K.W., Y. Dai, G. Bonan, M. Bosilovich, R. Dickinson, P. Dirmeyer, F. Hoffman, P. Houser, S. Levis, G.-Y. Niu, P. Thornton, M. Vertenstein, Z.-L. Yang, and X. Zeng, 2004: Technical Description of the Community Land Model (CLM). *NCAR Technical Note.* NCAR/TN-461+STR, Ntl. Cen. for Atmos. Research, Boulder, CO,173 pp. [Available from Ntl. Cen. for Atmos. Res., P.O. Box 3000, Boulder, CO 80305.]

Oouchi, K., J. Yoshimura, H. Yoshimura, R. Mizuta, S. Kusunoki, and A. Noda, 2006: Tropical cyclone climatology in a global-warming climate as simulated in a 20km-mesh global atmospheric model: Frequency and wind intensity analyses. *J. Meteorological Soc. Japan,* **84,** 259–276.

Oren, R., *et al.*, 2001: Soil fertility limits carbon sequestration by forest ecosystems in a CO_2-enriched atmosphere. *Nature*, **411**, 469–477.

Ott, L.E., K.E. Pickering, G.L. Stenchikov, and H. Huntrieser, 2006: The effects of lightning NOx production during the July 21 EULINOX storm studied with a 3-D cloud-scale chemical transport mode. *J.Geophys. Res.*, submitted.

Overgaard, J., D. Rosbjerg, and M.B. Butts, 2006: Land-surface modelling in hydrological perspective–A Rev. *Biogeoscience*,**3**, 229–241.

Pacanowski, R.C. and S.G.H. Philander, 1981: Parametrization of vertical mixing in numerical models of tropical oceans. *J. Phys.Oceanography*, **11**, 1443–1451.

Paegle, J., K.C. Mo., and J. Nogués-Paegle, 1996: Dependence of simulated precipitation on surface evaporation during the 1993 United States summer floods. *Mon. Weather Rev.*, **124**, 345–361.

Pan, Z., J.H. Christensen, R.W. Arritt, W.J. Gutowski, Jr., E.S. Takle, and F. Otieno, 2001: Evaluation of uncertainties in regional climate change simulations. *J. Geophys. Res.*, **106**, 17,735–17,752.

Pan, Z., R.W. Arritt, E.S. Takle, W. J. Gutowski, Jr., C. J. Anderson, and M. Segal, 2004: Altered hydrologic feedback in a warming climate introduces a "warming hole". *Geophys. Res. Lett.*, **31,** L17109, doi:10.1029/2004GL020528.

Parkinson, C.L., K.Y. Vinnikov, and D.J. Cavalieri, 2006: Evaluation of the Simulation of the Annual Cycle of Arctic and Antarctic. *J. Geophys. Res.*, **111**, C07012.

Paulson, C.A. and J.J. Simpson, 1977: Irradiance measurements in the upper ocean. *J. Ap. Oceanography,* **7**, 952–956.

Pavolonis, M., J.R. Key, and J.J. Cassano, 2004: Study of the Antarctic surface energy budget using a polar regional Atmos. model forced with satellite-derived cloud properties. *Mon. Weather Rev.*, **132**, 654–661.

Payne, A.J., A. Vieli, A.P. Shepherd, D.J. Wingham, and E. Rignot, 2004: Recent dramatic thinning of largest West Antarctic ice stream triggered by oceans. *Geophys. Res. Letts.,* **31**, L23401.

Payne, J.T., A.W. Wood, A.F. Hamlet, R.N. Palmer, and D.P. Lettenmaier, 2004: Mitigating the effects of climate change on the water resources of the Columbia River basin. *Climatic Change*, **62**, 233–256.

Peltier, W.R., 2004: Global glacial isostasy and the surface of the ice-age earth: The ice-5G (VM2) model and GRACE. *Annual Rev. of Earth Planetary Sci.,* **32**, 111–149.

Philander, S.G.H., 1990: *El Niño, La Niña, and the Southern Oscillation*. Academic Press, San Diego, CA, 293 pp.

Philander, S.G.H. and R.C. Pacanowski, 1981: The oceanic response to cross-equatorial winds (with application to coastal upwelling in low latitudes). *Tellus,* **33**, 201–210.

Philip, S.Y. and G.J. Van Oldenborgh, 2006: Shifts in ENSO coupling processes under global warming. *Geophys. Res. Letts.,* **33**, L11704.

Piani, C., D.J. Frame, D.A. Stainforth, and M.R. Allen, 2005: Constraints on climate change from a multi-thousand member ensemble of simulations. *Geophys. Res. Letts.,* **32**, L23825.

Pierce, D.W., 2004: Future change in biological activity in the north Pacific due to anthropogenic forcing of the physical environment. *Climatic Change*, **62**, 389–418.

Pierce, D.W, T.P. Barnett, E.J. Fetzer, P.J. Gleckler, 2006: Three-dimensional tropospheric water vapor in coupled climate models compared with observations from the AIRS satellite system, *Geophys. Res. Letts.*, **33,** L21701

Pincus, R., H.W. Barker, and J.J. Morcrette, 2003 : A fast, flexible, approximate technique for computing radiative transfer in inhomogeneous cloud fields. *J. Geophys. Res.,* doi:10.1209/2002JD003322,2003.

Pinto, J.O., J.A. Curry, and J.M. Intrieri, 2001: Cloud-aerosol interactions during autumn over Beaufort Sea. *J. Geophys. Res,* **106**, 15077–15097.

Pitman, A.J., A.G. Slater, C.E. Desborough, and M. Zhao, 1999: Uncertainty in the simulation of runoff due to the parameterization of frozen soil moisture using the GSWP methodology. *J. Geophys. Res.*, **104**, 16879–16888.

Plummer, D.A., D. Caya, A. Frigon, H. Côté, M. Giguère, D. Paquin, S. Biner, R. Harvey, and R. de Elía, 2006: Climate and climate change over North America as simulated by the Canadian Regional Climate Model. *J. Climate*, **19**, 3112–3132.

Pope, V.D., M. Gallani, P.R. Rowntree, and R.A. Stratton, 2000: The impact of new Phys.parametrizations in the Hadley Centre climate model—HadAM3. *Climate Dynamics*, **16**, 123–146.

Prentice, I.C., *et al.*, 2001: [IPCC 3rd Assessment Report, Working Group I, Chapter 3

Prive, N.C., and R.A. Plumb, 2007: Monsoon dynamics with interactive forcing. Part I: Axisymmetric studies. *J. Atmos. Sci*., in press.

Qian, J., F. Giorgi, and M.S. Fox–Rabinovitz, 1999: Regional stretched grid generation and its application to the NCAR RegCM. *J. Geophys. Res.*, **104**(D6), 6501–6514.

Qian, J.H., W.K. Tao, and K.M. Lau, 2004: Mechanisms for torrential rain associated with the mei-yu development during SCSMEX 1998. *Mon. Weather Rev.*, **132**, 3–27.

Raisanen, J., 2002: CO_2-Induced Changes in Interannual Temperature and Precipitation Variability in 19 CMIP Experiments, *J. Climate*, **15**, 2395–2411.

Raisanen, J. and T.N. Palmer, 2001: A probability and decision-model analysis of amultimodel ensemble Climate change simulations. *J. Climate*, **14**, 3212–3226.

Rajagopalan, B., U. Lall, and M.A. Cane, 1997: Anomalous ENSO occurrences: An alternate view. *J. Climate*, **10**(9), 2351–2357.

Ramankutty, N., J.A. Foley, J. Norman, and K. McSweeney, 2002: The global distribution of cultivable lands: current patterns and sensitivity to possible climate change. *Global Ecology and Biogeography*, **11**, 377–392.

Ramaswamy, V., D. Boucher, J. Haigh, D. Hauglustaine, J. Haywood, G. Myhre, T. Nakajima, G.Y. Shi, and S. Solomon, 2001: Radiative forcing Climate change. In: *Climate Change 2001: The Scientific Basis*, [Houghton, J.T., Y. Ding, D.J. Griggs, M. Noguer, P.J. van der Linden, X. Dai, K. Maskell, and C.A. Johnson (eds.)]. Cambridge University Press, Cambridge, UK, pp. 349–416.

Randall, D., M. Khairoutdinov, A. Arakawa, and W. Grabowski, 2003: Breaking the cloud parameterization deadlock. *Bulletin Am. Meteorological Soc.*, **84**, 1547–1564.

Randall, D., M. Khairoutdinov, A. Arakawa, and W. Grabowski, 2005: Breaking the Cloud Parameterization Deadlock, *Bulletin Am. Meteorological Soc.*, **84**, 1547–1564 , doi: 10.1175/BAMS-84-11-1547.

Randall, D.A., M.E. Schlesinger, V. Galin, V. Meleshko, J.-J. Morcrette, and R. Wetherald, 2000: Cloud feedbacks. In: *Frontiers in the Science. Climate Modeling* [Kiehl, J.T. and V. Ramanathan (eds.)]. Proceedings of a symposium in honor of Robert D. Cess..

Randall, D., R. A. Wood, S. Bony, R. Colman, T. Fichefet, J. Fyfe, V. Kattsov, A. Pitman, J. Shukla, J. Srinivasan, R. J. Stouffer, A. Sumi, K. Taylor, 2007: Chapter 8: Climate Models and Their Evaluation. In: *Climate Change 2007. The Fourth Scientific Assessment*, S. Solomon et al. (ed.), Intergovernmental Panel on Climate Change (IPCC), ***www.ipcc.ch***.

Raphael, M.N. and M.M. Holland, 2006: Twentieth century simulation of the Southern Hemisphere climate in coupled models. Part 1: Large-scale Circulation Variability. *Climate Dynamics,* **26**, 217–228.

Raper, S.C.B., J.M. Gregory, and R.J. Stouffer, 2002: The role of climate sensitivity and ocean heat uptake on AOGCM transient temperature response, *J. Climate*, **15**, 124–130.

Rasch, P.J. and J.E. Kristjánsson, 1998: A comparison of the CCM3 model climate using diagnosed and predicted condensate parameterizations. *J. Climate*, **11**, 1587–1614.

Rasmussen, E.M. and J.M. Wallace, 1983: Meteorological aspects of the El Nino/Southern Oscillation. *Science*, **222**, 1195–2002.

Rawlins, M.A., R.B. Lammers, S. Frolking, B.M. Fekete, and C.J. Vorosmarty, 2003: Simulating pan-Arctic runoff with a macro-scale terrestrial water balance model. *Hydrodrology Proceedings*, **17**, 2521–2539.

Rayner, N.A., D.E. Parker, E.B. Horton, C.K. Folland, L.V. Alexander, D.P. Rowell, E.C. Kent, and A. Kaplan, 2003: Global analyses of sea surface temperature, sea ice, and night marine air temperature since the late nineteenth century. *J. Geophys. Res.*, **108**(D14), 4407.

Rignot, E. and P. Kanagaratnam, 2006: Changes in the velocity structure of the Greenland ice sheet. *Science,* **311**, 986–990.

Ringer, M.A. and R.P. Allan, 2004: Evaluating climate model simulations of tropical clouds. *Tellus,* **56A,** 308–327.

Rinke, A., K. Dethloff, J. Cassano, J.H. Christensen, J.A. Curry, P. Du, E. Girard, J.-E. Haugen, D. Jacob, C.G. Jones, M. Koltzow, R. Laprise, A.H. Lynch, S. Pfeifer, M.C. Serreze, M.J. Shaw, M. Tjernstrom, K. Wyser, and M. Zagar, 2006: Evaluation of an ensemble of Arctic regional climate models: Spatiotemporal fields during the SHEBA year. *Climate Dynamics.* doi 10.1007/s00382-005-0095-3.

Roads, J.O., S.-C. Chen, M. Kanamitsu, and H. Juang, 1999: Surface water characteristics in the NCEP Global Spectral Model and reanalysis. *J. Geophys. Res.*, **4**(D16), 19307–19327.

Roads, J., S.C. Chen, and M. Kanamitsu, 2003: U.S. regional climate simulations and seasonal forecasts. *J. Geophys. Res.*, **108**(D16), Art. No. 8606.

Roberts, M.J. and R. Wood, 1997: Topographic sensitivity studies with a Bryan-Cox-type ocean model. *J. of Phys. Oceanography*, **27**, 823–836.

Roeckner, E., *et al.,* 1987: Cloud optical depth feedbacks and climate modelling. *Nature*, **329**, 138–140.

Roeckner, E. *et al.,* 1996: The Atmos. general circulation model ECHAM-4: Model description and simulation of present-day climate. Report 128, Max-Planck-Institut für Meteorologie, Hamburg, Germany.

Roeckner E., R. Brokopf, M. Esch, M. Giorgetta, S. Hagemann, L. Kornblueh, E. Manzini, U. Schlese, and U. Schulzweida, 2006: Sensitivity of simulated climate to horizontal and vertical resolution in the ECHAM5 atmosphere model. *J. Climate*, **19**, 3771–3791.

Root, T.L. and S.H. Schneider, 1993: Can large scale climatic models be linked with multiscale ecological studies? *Conservation Biology*, **7**(2), 256–270.

Ropelewski, C.F. and M.S. Halpert, 1987: Global and regional scale precipitation patterns associated with the El Nino Southern Oscillation. *Mon. Weather Rev.*, **115**, 1606–1626.

Rothstein, L.M., J.J. Cullen, M. Abbott, E.P.Chassignet, K. Denman, S.C. Doney, H. Ducklow, K. Fennel, M. Follows, D. Haidvogel, E. Hoffman, D.M. Karl, J. Kindle, I. Lima, M. Maltrud, C. McClain, D. McGillicuddy, M.J. Olascoaga, Y. Spitz, J. Wiggert, and J. Yoder, 2006: Modeling ocean ecosystems: The PARADIGM Program. *Oceanography*, **19**, 22–51.

Rotstayn, L.D., 1997: A physically based scheme for the treatment of stratiform clouds and precipitation in large-scale models. I: Description and evaluation of microPhys.processes. *Quarterly J.Royal Meterological Soc.,* **123**, 1227–1282.

Ruiz-Barradas, A. and S. Nigam, 2006: IPCC's twentieth-century climate simulations: Varied representations of North Am. hydroclimate variability. *J. Climate*, **19**, 4041–4058.

Rummukainen M., S. Bergstrom, G. Persson, J. Rodhe, and M. Tjernstrom, 2004: The Swedish Regional Climate Modelling Programme, SWECLIM: A Rev. *Ambio*, **33**, 176–182.

Russell, G.L., J.R. Miller, and D. Rind, 1995. A coupled atmosphere-ocean model for transient climate change studies. *Atmosphere-Ocean*, **33**(4), 683–730.

Russell, G.L., J.R. Miller, L.-C. Tsang, R.A. Ruedy, G.A. Schmidt, and S. Sheth, 2000: Comparison of model and observed regional temperature changes during the past 40 years. *J. Geophys. Res.*, **105**, 14 891–14 898.

Russell, J.L., R.J. Stouffer, and K.W. Dixon, 2006: Intercomparison of the southern ocean circulations control simulations. *J. Climate*, **19**, 4560–4575.

Ryan, B.F., J.J. Katzfey, D.J. Abbs, C. Jakob, U. Lohmann, B. Rockel, L.D. Rotstayn, R.E. Stewart, K.K. Szeto, G. Tselioudis, and M.K. Yau, 2000: Simulations of a cold front by cloud-resolving, limited-area, and large-scale models, and a model evaluation using *in situ* and satellite observations. *Mon. Weather Rev.*, **128,** 3218–3235.

Saji, N.H., S.-P. Xie, and T. Yamagata, 2005: Tropical Indian Ocean Variability in the IPCC Twentieth-Century Climate Simulations. *J. Climate*, **19**(17), 4397.

Saji, N.H., B.N. Goswami, P.N. Vinayachandran, and T. Yamagata, 1999: A dipole mode in the tropical Indian Ocean. *Nature*, **401,** 360–363.

Saraf, A.K., B.P. Mishra, S. Choudhury, and P. Ghosh, 2005: Digital Elevation Model (DEM) generation from NOAA-AVHRR night-time data and its comparison with USGS-DEM. *Intl. J. of Remote Sensing*, **26**, 3879–3887.

Sardeshmukh, P.D. and B.J. Hoskins, 1988: The generation of global rotational flow by steady idealized tropical divergence. *J. Atmos. Science*,**45**, 1228–1251.

Sato, M., J. Hansen, M.P. McCormick, and J. Pollack, 1993: Stratospheric aerosol optical depth, 1850–1990. *J. Geophys. Res.*, **98**, 22987–2299

Sausen, R., S. Schubert, and L. Dumenil, 1994: A model of the river-runoff for use in coupled atmosphere-ocean models. *J. of Hydrology*, **155**, 337352.

Schimel, D.S., 1998: The carbon equation. *Nature*, **393**, 208–209.

Schmidt, G.A., R. Ruedy, J.E. Hansen, I. Aleinov, N. Bell, M. Bauer, S. Bauer, B. Cairns, V. Canuto, Y. Cheng, A. Del Genio, G. Faluvegi, A.D. Friend, T.M. Hall, Y. Hu, M. Kelley,

N.Y. Kiang, D. Koch, A.A. Lacis, J. Lerner, K.K. Lo, R.L. Miller, L. Nazarenko, V. Oinas, J. Perlwitz, D. Rind, A. Romanou, G.L. Russell, M. Sato, D.T. Shindell, P.H. Stone, S. Sun, N. Tausnev, D. Thresher, and M.S. Yao, 2006: Present day Atmos. simulations using GISS ModelE: Comparison to *in-situ*, satellite and reanalysis data. **J. Clim., 19**, 153–192, doi:10.1175/JCLI3612.1.

Schmittner, A., M. Latif, and B. Schneider, 2005: Model projections of the North Atlantic thermohaline circulation for the 21st century assessed by observations. *Geophys. Res. Letts.*, **32**, doi:10.1029/2005GL024368.

Schneider, S.H. and C. Mass, 1975: Volcanic dust, sunspots, and temperature trends. *Science,***190**, 741–746

Schneider, S.H. and S.L. Thompson, 1981: Atmos. CO2 and climate: Importance of the transient response. *J. Geophys. Res.*, **86**, 3135–3147.

Schopf, P., M. Gregg, R. Ferrari, D. Haidvogel, R. Hallberg, W. Large, J. Ledwell, J. Marshall, J. McWilliams, R. Schmitt, E. Skyllingstad, K. Speer, K. Winters, 2003: *Coupling Process and Model Studies of Ocean Mixing to Improve Climate Models—A Pilot Climate Process Modeling and Science Team*.

Schramm, J.L., J.A. Curry, M.M. Holland, and E.E. Ebert, 1997: Modeling the thermodynamics of a sea ice thickness distribution. 1. Sensitivity to ice thickness resolution. *J. Geophys. Res.*, **102**, 23 079–23 091.

Schweitzer, L., 2006: Environmental justice and hazmat transport: A spatial analysis in southern California. *Transportation Research Part D–Transp. Environ.,* **11**, 408–421.

Segal, M. and R.W. Arritt, 1992: Nonclassical mesoscale circulations caused by surface sensible heat-flux gradients. *Bulletin Am. Meteorological Soc.,* **73**, 1593–1604.

Segal, M., M. Leuthold, R.W. Arritt, C. Anderson, and J. Shen, 1997: Small lake daytime breezes: Some observational and conceptual evaluations. *Bulletin Am. Meteorological Soc.*, **78**, 1135–1147.

Sellers, P.J., Y. Mintz, Y.C. Sud, and A. Dalcher, 1986: A Simple Biosphere Model (SiB) for use within general-circulation models. *J. of Atmos. Sci.,* **43**, 503–531.

Sellers, P.J., D.A. Randall, C.J. Collatz, J.A. Berry, C.B. Field, D.A. Dazlich, C. Zhang, G. Collelo, and L. Bounoua, 1996: A revised landsurface parameterization (SiB2) for Atmos. GCMs. Part 1: Model formulation. *J. Climate*, **9**, 676–705.

Semtner, A.J., 1976: A model for the thermodynamic growth of sea ice in numerical investigations Climate. *J. of Phys.Oceanography*, **6**, 27–37.

Seneviratne, S.I., D. Lüthi, M. Litschi, and C. Schär, 2006: Land-atmosphere coupling and climate change in Europe. *Nature*, **443**, 205–209.

Senior, C.A. and J.F.B. Mitchell, 1993: Carbon dioxide and climate: the impact of cloud parameterization. *J. Climate*, **6**, 5–21.

Senior, C.A. and J.F.B. Mitchell, 1996: Cloud feedbacks in the unified UKMO GCM. In: *Climate Sensitivity to Radiative Perturbations, Phys.Mechanism and Their Validation.* [Le Treut, H. (ed.)]., Springer, 331pp.

Shaw, M.R., *et al.*, 2002: Grassland responses to global environmental changes suppressed by elevated CO_2. *Science*, **298**, 1987–1990.

Shepherd, A. and D. Wingham, 2007: Recent sea-level contributions of the Antarctica and Greenland ice sheets. *Science*, **315**, 1529–1532.

Shindell, D.T., R.L. Miller, G.A. Schmidt, and L. Pandolfo, 1999: Simulation of recent northern winter climate trends by greenhouse-gas forcing. *Nature*, **399**, 452–455.

Siddall, M., E.J. Rohling, A. Almogi-Labin, Ch. Hemleben, D. Meischner, I. Schmelzer, and D.A. Smeed, 2003: Sea-level fluctuations during the last glacial cycle. *Nature*, **423**, 853–858.

Skamarock, W.C., J.B. Klemp, J. Dudhia, D.O. Gill, D.M. Barker, W. Wang, and J.G. Powers, 2005: A description of the advanced research WRF Version 2. *NCAR Technical Note.* NCAR/TN–468+STR, Ntl. Center for Atmos. Research, Boulder, CO, USA, 88 pp. [Available from Ntl. Cen. for Atmos. Res., P.O. Box 3000, Boulder, CO, 80305.]

Slater, A.G., *et al.*, 2001: The representation of snow in land surface schemes: Results from PILPS 2(d). *J. Hydrometeorology*, **2**, 7–25.

Small, C., V. Gornitz, and J.E. Cohen, 2000. Coastal hazards and the global distribution of population. *Environmental Geoscience*, **7**, 3–12.

Smethie, W.M., Jr., and R.A. Fine, 2001: Rates of North Atlantic Deep Water formation calculated from chlorofluorocarbon inventories. Deep Sea Research, Part I, **48**, 189– 215.

Smith, R.D. and P.R. Gent, 2002: *Reference manual for the Parallel Ocean Program (POP), ocean component of the Community Climate System Model (CCSM2.0 and 3.0).* Technical Report LA-UR-02-2484. Los Alamos Ntl. Laboratory, Los Alamos, NM. Available online at http://www.ccsm.ucar.edu/models/ccsm3.0/pop.

Smith, R.N.B., 1990: A scheme for predicting layer clouds and their water content in a general circulation model. *Quarterly J.Royal Meterological Soc.*, **116**, 435–460.

Soden, B.J., A.J. Broccoli, and R.S. Hemler, 2004: On the use of cloud forcing to estimate cloud feedback. *J. Climate*, **17**, 3661–3665.

Soden, B.J. and I.M. Held, 2006: An assessment Climate feedbacks in coupled ocean–atmosphere models. *J. Climate*, **19**, 3354–3360.

Sokolov, A.P., and P.H. Stone, 1998: A flexible climate model for use in integrated assessments, *Climate Dynamics*, **14**, 291–303.

Solman, S.A., M.N. Nunez, and P.R. Rowntree, 2003: On the evaluation of the representation of mid-latitude transients in the Southern Hemisphere by HadAM2B GCM and the impact of horizontal resolution. *Atmosfera*, **16**, 245–272.

Somerville, R.C.J. and L.A. Remer, 1984: Cloud optical thickness feedbacks in the CO2 climate problem. *J. Geophys. Res.*, **89**, 9668–9672.

Stephens, G.L., 2005: Cloud feedbacks in the climate system: a critical review. *J. Climate*, **18**, 237–273.

Stewart, I.T., D.R. Cayan, and M.D. Dettinger, 2004: Changes in snowmelt runoff timing in western North America under a 'Business as Usual' climate change scenario. *Climatic Change*, **62**, 217–232.

Stouffer, R.J., A.J. Broccoli, T.L. Delworth, K.W. Dixon, R. Gudgel, I. Held, R. Hemler, T. Knutson, Hyun-Chul Lee, M.D. Schwarzkopf, B. Soden, M.J. Spelman, M. Winton, and Fanrong Zeng, 2006: GFDL's CM2 global coupled climate models. Part IV: Idealized climate response. *J. Climate*, **19**, 723–740.

Stouffer, R.J., J. Russell, and M.J. Spelman, 2006: Importance of oceanic heat uptake in transient climate change. *Geophys. Res. Lett.*, **33**(17), L17704, doi:10.1029/2006GL027242.

Strack, J.E., R.A. Pielke, and J. Adegoke, 2003: Sensitivity of model-generated daytime surface heat fluxes over snow to land-cover changes. *J. Hydrometeorology.* **4,** 24–42.

Stratton, R.A., 1999: A high resolution AMIP integration using the Hadley Centre model HadAM2b. *Climate Dynamics*, **15**, 9–28.

Sturm, M., J.P. McFadden, G.E. Liston, F.S. Chapin, C.H. Racine, J. Holmgren, 2001: Snow-shrub interactions in Arctic tundra: A hypothesis with climatic implications. *J. Climate*, **14,** 336–344.

Sturm, M., T. Douglas, C. Racine, G.E. Liston, 2005: Changing snow and shrub conditions affect albedo with global implications. *J. Geophys. Res.-Biogeosciences,* **110,** Art. No. G01004.

Sud, Y.C. and G.K. Walker, 1999: Microphysics of clouds with the Relaxed Arakawa–Schubert Scheme (McRAS). Part II: Implementation and Performance in GEOS II GCM. *J. Atmos. Sci.*, **56(18)**, 3221–3240.

Sui, C.-H., X. Li, and K.-M. Lau, 1998: Radiative-convective processes in simulated diurnal variations of tropical oceanic convection. *J. Atmos. Sci.,* **55**, 2345–2359.

Sun, S. and R. Bleck, 2001: Atlantic thermohaline circulation and its response to increasing CO_2 in a coupled atmosphere-ocean model. *Geophys. Res. Letts.,* **28**, 4223–4226.

Sun, S. and J. Hansen, 2003: Climate simulations for 1951–2050 with a coupled atmosphere–ocean model. *J. Climate*, **16**, 2807–2826, doi:10.1175/1520–0442.

Sun, Y., S. Solomon, A. Dai, and R.W. Portmann, 2006: How often does it rain? *J. Climate,* **19**, 916–934.

Takle, E.S., W.J. Gutowski, R.A. Arritt, Z. Pan, C.J. Anderson, R.R. da Silva, D. Caya, S.-C. Chen, J.H. Christensen, S.-Y. Hong, H.-M.H. Juang, J. Katzfey, W.M. Lapenta, R. Laprise, P. Lopez, J. McGregor, and J.O. Roads, 1999: Project to Intercompare Regional Climate Simulations (PIRCS): Description and initial results. *J. Geophys. Res.,* **104**, 19,443–19,461.

Talley, L.D., J.L. Raid, and P.E. Robbins, 2003: Data-based meridional overturning streamfunctions for the global ocean. *J. Climate,* **16**, 3213–3226.

Tao, W., 2007: Cloud-resolving modeling. *J.Meteorological Soc. of Japan.* 125th Anniversary Special Issue, submitted.

Tao, W.-K., 2003: Goddard Cumulus Ensemble (GCE) model: Application for understanding precipitation processes. Cloud systems, hurricanes, and the Tropical Rainfall Measuring Mission (TRMM): A Tribute to Dr. Joanne Simpson, Meteorological Monograph. *Bulletin Am. Meteorological Soc.,* **51**, 107–138.

Tao, W.-K., D. Johnson, C.-L. Shie, and J. Simpson, 2004: Atmos. energy budget and large-scale precipitation efficiency of convective systems during TOGA COARE, GATE, SCSMEX and ARM: Cloud-resolving model simulations. *J. Atmos. Sci.,* **61**, 2405–2423.

Tao, W.-K., J. Simpson, C.-H. Sui, C.-L. Shie, B. Zhou, K. M. Lau, and M. Moncrieff, 1999: On equilibrium states simulated by Cloud-Resolving Models. *J. Atmos. Sci.,* **56**, 3128–3139.

Tebaldi, C., K. Hayhoe, J.M. Arblaster, and G.A. Meehl, 2006: Going to the extremes; An intercomparison of model-simulated historical and futre changes in extreme events. *Climate Change*. In press.

Tebaldi C., R.L. Smith, D. Nychka, and L.O. Mearns, 2005: Quantifying uncertainty in projections of regional climate change: A Bayesian approach to the analysis of multimodel ensembles. *J. Climate*, **18**, 1524–1540.

Tenhunen, J.D., R. Geyer, R. Valentini, W. Mauser, and A. Cernusca, 1999: Eco-system studies, land-use and resource management. In: *Integrating Hydrology, Ecosystems Dynamics and Biochemistry in Complex Landscapes*. [Tenhunen, J. D. and P. Kabat (eds.)]. Wiley, Chichester,1–19.

Thompson, D.W.J. and J.M. Wallace, 1998: The Arctic Oscillation signature in the wintertime geopotential height and temperature fields. *Geophys. Res. Letts.,* **25**, 1297–1300.

Thompson, D.W.J. and J.M. Wallace, 2000: Annual modes in the extratopical circulation. Part I: Month-to-month variability. *J. Climate,* **13**, 1000–1016.

Thompson, S., B. Govindasamy, A. Mirin, K. Caldeira, C. Delire, J. Milovich, M. Wickett, and D. Erickson, 2004: Quantifying the effects of CO_2-fertilized vegetation on future global climate and carbon dynamics. *Geophys. Res. Letts.,* **31**(23), L23211.

Tiedtke, M., 1989: A comprehensive mass flux scheme for cumulus parameterization in large scale models. *Mon. Weather Rev.*, **117**,1779–1800.

Tiedtke, M., 1993: Representation of clouds in large-scale models. *Mon. Weather Rev.*, **121**, 3040–3061.

Tjernström, M., M. Zagar, and G. Svensson, 2004: Model simulations of the Arctic Atmos. boundary layer from the SHEBA year. *Ambio*, **33**, 221–227.

Tjernstrom, M., M. Zagar, G. Svensson, J.J. Cassano, S. Pfeifer, A. Rinke, K. Wyser, K. Dethloff, C. Jones, T. Semmler, and M. Shaw, 2005: Modelling the Arctic boundary layer: An evaluation of six ARCMIP regional-scale models with data from the SHEBA project. *Boundary-Layer Meteorology*, **117**, 337–381.

Tjoelker, M.G., J. Oleksyn, and P.B. Reich, 2001: Modelling respiration of vegetation: Evidence for a general temperature-dependent Q(10). *Global Change Biology*, **7**, 223–230.

Tompkins, A., 2002: A prognostic parameterization for the subgrid-scale variability of water vapor and clouds in large-scale models and its use to diagnose cloud cover. *J. of Atmos. Sci.*, **59,** 1917–1942.

Trenberth, K.E. and J. Hurrell, 1994: Decadal atmosphere-ocean variations in the Pacific. *Climate Dynamics*, **9**, 303–319.

Trenberth K.E. and T.J. Hoar, 1997: El Niño and climate change. *Geophys. Res. Letts.,* **24**, 3057–3060.

Trenberth, K.E., G.W. Branstator, D. Karoly, A. Kumar, N.-C. Lau, and C. Ropelewski, 1998: Progress during TOGA in understanding and modeling global teleconnections associated with tropical sea surface temperatures. *J. Geophys. Res.,* **103** (special TOGA issue), 14291–14324.

Trenberth, K.E., J. Fasullo, and L. Smith, 2005: need article title. *Climate Dynamics*, doi**:**10.1007/s00382-005-0017-4.

Trier, S. B., W.C. Skamarock, M.A. LeMone, and D.B. Parsons, 1996: Structure and evolution of the 22 February 1993 TOGA COARE squall line: Numerical simulations. *J. of Atmos. Sci.,* **53**, 2861–2886.

Tripoli, G.J., 1992: A nonhydrostatic mesoscale model designed to simulate scale interaction. *Mon. Weather Rev.*, **120**, 1342–1359

Tripoli, G.J. and W.R. Cotton, 1989: Numerical study of an observed orogenic mesoscale convective system. Part 2: Analysis of governing dynamics. *Mon. Weather Rev.*, **117**, 305–328.

Tselioudis, G. and C. Jakob, 2002: Evaluation of midlatitude cloud properties in a weather and a climate model: Dependence on dynamic regime and spatial resolution. *J. Geophys. Res.,* **107**, 4781.

Tselioudis, G., Y.-C. Zhang, and W.R. Rossow, 2000: Cloud and radiation variations associated with northern midlatitude low and high sea level pressure regimes. *J. Climate*, **13**, 312–327, doi:10.1175/1520-0442(2000).

Tsushima, Y., A. Abe-Ouchi, and S. Manabe, 2005: Radiative damping of annual variation in global mean surface temperature: Comparison between observed and simulated feedback. *Climate Dynamics*, **24**, 591–597.

Twomey, S., 1977: The influence of pollution on the short wave albedo of clouds. *J. Atmos. Sci.*, **34**, 1149–1152.

Ueda, H., A. Iwai, K. Kuwako, and M.E. Hori, 2006: Impact of anthropogenic forcing on the Asian summer monsoon as simulated by 8 GCMs. *Geophys. Res. Letts.,* **33**, doi:10.1029/2005GL025336.

Uotila, P., A.H. Lynch, J.J. Cassano, and R.I. Cullather, 2007: Changes in Antarctic net precipitation in the 21st century based on IPCC model scenarios. *J. Geophys. Res.,* accepted pending revisions.

Uppala, S.M., *et al.*, 2005: The ERA-40 re-analysis. *Intl. J. of Climatology,* **131**, 2961–3012.

van Oldenborgh, G.J., S.Y. Philip, and M. Collins, 2005: El Niño in a changing climate: A multi-model study. *Ocean Science,* **1**, 81–95.

VanRheenen, N.T., A.W. Wood, R.N. Palmer, and D.P. Lettenmaier, 2004: Potential implications of PCM climate change scenarios for Sacramento-San Joaquin River basin hydrology and water resources. *Climatic Change*, **62**, 257–281.

van Ulden, A.P. and G.J. van Oldenborgh, 2006: Large-scale Atmos. circulation biases and changes in global climate model simulations and their importance for climate change in Central Europe. In: *Atmospheric Chemistry and Physics*, **6**(4), 863–881.

Vavrus, S., J.E. Walsh, W.L. Chapman, and D. Portis, 2006: The behavior of extreme cold air outbreaks under greenhouse warming. *Intl. J.Climatology*, **26**, 1133–1147.

Velicogna, I. and J. Wahr, 2006: Acceleration of Greenland ice mass loss in spring 2004. *Nature,* **443**(7109), 329–331.

Vidale, P.L., D. Lüthi, C. Frei, S.I. Seneviratne, and C. Schär, 2003: Predictability and uncertainty in a regional climate model. *J. Geophys. Res.*, **108**(D18), 4586.

Vinnikov, K.Y., D.J. Cavalieri, and C.L. Parkinson, 2006: A model assessment of satellite observed trends in polar sea ice extents. *Geophys. Res. Letts.,* **33**, L05704.

Vitart, F. and Anderson, J.L., 2001: Sensitivity of Atlantic Tropical Storm Frequency to ENSO and Interdecadal Variability of SSTs in an Ensemble of AGCM Integrations. *J. Climate*,**14**(4), 533–545.

Völker, C., D.W.R. Wallace, and D.A. Wolf-Gladrow, 2002: On the role of heat fluxes in the uptake of anthropogenic carbon in the North Atlantic, *Global Biogeochem. Cycles*, **16**(4), 1138, doi:10.1029/2002GB001897.

Von Storch, H., E. Zorita, and U. Cubasch, 1993: Downscaling of global climate change estimates to regional scales: An application to Iberian rainfall in wintertime. *J. Climate*, **6**, 1161–1171.

Wang, B., 1995: Interdecadal changes in El Niño onset in the last four decades. *J. Climate*, **8**, 267–284.

Wang, C., 2005: A model study of the response of tropical deep convection to the increase of CCN concentration. 1. Dynamics and microphysics. *J. Geophys. Res.*, **110**, D21211.

Wang, H. and K.-M. Lau, 2006: Atmos. hydrological cycle in the tropics in twentieth century coupled climate simulations. *J. Climate*, **26**, 655–678.

Wang, M., J.E. Overland, V. Kattsov, and J.E. Walsh, 2007: Intrinsic versus Forced Variation in Coupled Climate Model Simulations over the Arctic during the Twentieth Century, *J. Climate* **20**, 1093–1095 and 1097–1107.

Wang, M., J.E. Overland, V. Kattsov, J.E. Walsh, X. Zhang, and T. Pavlova, 2006: Intrinsic versus forced variation in coupled climate model simulations over the Arctic during the 20th Century. *J. Climate*, submitted.

Wang, W. and M.E. Schlesinger, 1999: The dependence on convection parameterization of the tropical intraseasonal oscillation simulated by the UIUC 11-Layer Atmos. GCM. *J. Climate*, **12**(5),1423–1457.

Warrach, K., H.T. Mengelkamp, and E. Raschke, 2001: Treatment of frozen soil and snow cover in the land surface model SEWAB. *Theoretical and Applied Climatology*, **69**, 23–37.

Webb, M., C. Senior, S. Bony, and J.J. Morcrette, 2001: Combining ERBE and ISCCP data to assess clouds in the Hadley Centre, ECMWF and LMD Atmos. climate models. *Climate Dynamics*, **17**, 905–922.

Webb, M.J., C.A. Senior, D.M.H. Sexton, W.J. Ingram, K.D. Williams, M.A. Ringer, B.J. McAvaney, R. Colman, B.J. Soden, R. Gudgel, T. Knutson, S. Emori, T. Ogura, Y. Tsushima, N. Andronova, B. Li, I. Musat, S. Bony and K. E. Taylor, 2006: On the contribution of local feedback mechanisms to the range of climate sensitivity in two GCM ensembles, *Climate Dynamics*, **27**, (1/July 2006), doi:10.1007/s00382-006-0111-2.

Webster, P.J., V.O. Maga, T.N. Palmer, J. Shukla, R.A. Thomas, M. Yanai, and T. Yasunari, 1998: Monsoons: Processes, predictability, and the prospects for prediction, *J. Geophys. Res*., **103**(C7), 14451–14510, 10.1029/97JC02719.

Wei, H., W.J. Gutowski Jr., C.J. Vorosmarty, and B.M. Fekete, 2002: Calibration and validation of a regional climate model for pan-Arctic hydrologic simulation. *J. Climate*, **15**, 3222–3236.

Wetherald, R.T. and S. Manabe, 1988: Cloud feedback processes in general circulation models. *J. Atmos. Sci.*, **45**, 1397–1415.

Whitman, S., G. Good, E.R. Donoghue, N. Benbow, W. Shou, and S. Mou, 1997: Mortality in Chicago attributed to the July 1995 heat wave. *Am. J. Public Health*, **87**, 1515–1518.

Wigley, T.M.L., and M.E. Schlesinger, 1985: Analytical solution for the effect of increasing CO_2 on global mean temperature. *Nature,* **315,** 649–652.

Wilby, R.L., L.E. Hay, W.J. Gutowski, Jr., R.W. Arritt, E.S. Takle, G.H. Leavesley, and M. Clark, 2000: Hydrological responses to dynamically and statistically downscaled general circulation model output. *Geophys. Res. Letts.*, **27**, 1199–1202.

Wilby, R.L., S.P. Charles, E. Zorita, B. Timbal, P. Whetton, and L.O. Mearns, 2004: *Guidelines for Use Climate Scenarios Developed from Statistical Downscaling Methods.* The IPCC Data Distribution Centre, University of East Anglia, UK, 27 pp. [Available online at http://ipcc-ddc.cru.uea.ac.uk/guidelines.]

Williams, K.D., M.A. Ringer, and C.A. Senior, 2003: Evaluating the cloud response to climate change and current climate variability. *Climate Dynamics*, **20**, 705–721.

Williams, K.D., *et al.*, 2006: Evaluation of a component of the cloud response to climate change in an intercomparison Climate models. *Climate Dynamics*, **145**, 145–165.

Wilks, D.S. and R.L. Wilby, 1999: The weather generation game: A Rev. of stochastic weather models. *Progress in Phys.Georaphy*, **23**, 329–357.

Wilson, D.R. and S.P. Ballard, 1999: A microphysics-based precipitation scheme for the UK Meteorological Office Numerical Weather Prediction Model. *Intl. J. Climatology*, **125,** 1607–1636.

Wilson, M.F., A. Henderson-Sellers, R.E. Dickinson, and P.J. Kennedy, 1987: Sensitivity of the Biosphere Atmosphere Transfer Scheme (BATS) to the inclusion of variable soil characteristics. *J. Climate and Applied Meteorology*, **26**, 341–362.

Wilson, T.B., J.M. Norman, W.L. Bland, and C.J. Kucharik, 2003: Evaluation of the importance of Lagrangian canopy turbulence formulations in a soil-plant-atmosphere model. *Agricultural and Forest Meteorology*, **115**, 51–69.

Winton, M., 2000: A reformulated three-layer sea ice model. *J. Atmos. and Oceanic Tech.*, **17**, 525 531.

Wittenberg, A.T., A. Rosati, N.-C. Lau, and J.J. Ploshay, 2006: GFDL's CM2 Global Coupled Climate Models, Part III: Tropical Pacific Climate and ENSO. *J. Climate,* **19**, 698–722.

Wood, A.W., L.R. Leung, V. Sridhar, and D.P. Lettenmaier, 2004: Hydrological implications of dynamical and statistical approaches to downscaling climate model outputs. *Climate Change*, **62**, 189–216.

Wu, X. and M.W. Moncrieff, 2001: Long-term behavior of cloud systems in TOGA COARE and their interactions with radiative and surface processes. Part III: Effects on the energy budget and SST. *J. Atmos. Sci.*, **58**, 1155–1168.

Wu, X., L. Deng, X. Song, and G.-J. Zhang, 2006: Coupling of convective momentum transport with convective heating in global climate simulations. *J. Atmos. Sci.*, in press.

Wyant, M.C., C.S. Bretherton, J.T. Bacmeister, J.T. Kiehl, I.M. Held, M.Z. Zhao, S.A. Klein, and B.J. Soden, 2006: A comparison of tropical cloud properties and responses in GCMs using mid-tropospheric vertical velocity. *Climate Dynamics*, **27**, 261–279.

Wyant, M.C., M. Khairoutdinov, and C.S. Bretherton, 2006: Climate sensitivity and cloud response of a GCM with a superparameterization, *Geophys. Res. Letts.,* **33**, L06714.

Wyrtki, K., 1975: El Nino—The dynamic response of the equatorial Pacific Ocean to Atmospheric Forcing. *J. Phys.Oceanography*, **5**, 572–584.

Xie and Arkin, 1997: Global precipitation: A 17-year Mon. analysis based on gauge observations, satellite estimates, and numerical model outputs. *Bulletin of the Am. Meteorological Soc.*, **78**, 2539–2558.

Xie, S.C., *et al.*, 2005: Simulations of midlatitude frontal clouds by single-column and cloud-resolving models during the Atmos. Radiation Measurement March 2000 cloud intensive operational period. *J. Geophys. Res.*, **110**, D15S03.

Xu, K.-M. and D.A. Randall, 1998: Influence of large-scale advective cooling and moistening effects on the quasi-equilibrium behavior of explicitly simulated cumulus ensembles. *J. of Atmos. Sci.*, **55**, 896–909.

Xu, K., M.H. Zhang, *et al.*, 2005: Modeling springtime shallow frontal clouds with cloud-resolving and single-column models. *J. Geophys. Res.*, **110**, D15S04, doi:10.1029/2004JD005153.

Xue, Y., F.J. Zeng, K.E. Mitchell, Z. Janjic, and E. Rogers, 2001: The impact of land surface processes on simulations of the U.S. hydrological cycle: A case study of the 1993 flood using the SSiB land surface model in the NCEP ETA regional model.

Yamaguchi, K., A. Noda, and A. Kitoh, 2005: The changes in permafrost induced by greenhouse warming: A numerical study applying multiple-layer ground model. *J. Meteorological Soc. of Japan*, **83**, 799–815.

Yang Z.W. and R. . Arritt, 2002: Tests of a perturbed physics ensemble approach for regional climate modeling. *J. Climate*, **15**, 2881–2896.

Yao, M.-S. and A.D. Del Genio, 2002: Effects of cloud parameterization on the simulation Climate changes in the GISS GCM. Part II: Sea surface temperature and cloud feedbacks. *J. Climate*, **15**, 2491–2503.

Yeh, P.J.-F. and E.A.B. Eltahir, 2005: Representation of water table dynamics in a land surface scheme. Part 1: Model development. *J. Climate*, 18, 1861–1880.

Yokohata, T., S. Emori, T. Nozawa, Y. Tsushima, T. Ogura, and M. Kimoto, 2005: Climate response to volcanic forcing: Validation Climate sensitivity of a coupled atmosphere-ocean general circulation model. *Geophys. Res. Letts.,* **32**, L21710.

York, J.P., M. Person, W.J. Gutowski, and T.C. Winter, 2002: Putting aquifers into Atmos. simulation models: An example from the Mill Creek Watershed, northeastern Kansas. *Advances in Water Resources*, **25**, 221–238.

Yu, H., Y.J. Kaufman, M. Chin, G. Feingold, L.A. Remer, T.L. Anderson, Y. Balkanski, N. Bellouin, O. Boucher, S. Christopher, P. DeCola, R. Kahn, D. Koch, N. Loeb, M.S. Reddy, M. Schulz, T. Takemura, and M. Zhou, 2006: A Rev. of measurement-based assessment of aerosol direct radiative effect and forcing. *Atmos. Chemistry and Physics*, **6**, 613–666.

Yu, X. and M.J. McPhaden, 1999: Seasonal variability in the equatorial Pacific. *J. of Phys.Oceanography*, **29**, 925–947.

Zebiak, S.E. and M.A. Cane, 1987: A model El Nino-Southern Oscillation. *Mon. Weather Rev.*, **115**, 2262–2278.

Zhang, C., M. Dong, H.H. Hendon, E.D. Maloney, and A. Marshall, 2006: Simulations of the Madden-Julian Oscillation by Global Weather Forecast and Climate Models. *Climate Dynamics*.

Zhang, D. and M.J. McPhaden, 2006: Decadal variability of the shallow Pacific meridional overturning circulation: Relation to tropical sea surface temperatures in observations and climate change models. *Ocean Modelling*, **15**, 250–273.

Zhang, G.J. and N.A. McFarlane, 1995: Sensitivity Climate simulations to the Parameterization of cumulus convection in the Canadian Climate Centre general circulation model. *Atmos.phere–Ocean*, **33**, 407–446.

Zhang, J. and D. Rothrock, 2000: Modeling Arctic sea ice with an efficient plastic solution, *J. Geophys. Res.*, **105**, 3325–3338.

Zhang, M.H., J.J. Hack, J.T. Kiehl, and R.D. Cess, 1994: Diagnostic study Climate feedback processes in Atmos. general circulation models. *J. Geophys. Res.*, **99**, 5525–5537.

Zhang, M., 2004: Cloud-climate feedback: How much do we know? In: *Observation, Theory, and Modeling of Atmos. Variability. World Scientific Series on Meteorology of East Asia*, Vol. 3 [Zhu, *et al.* (eds.)]. World Scientific Publishing Co., Singapore, 632 pp.

Zhang, M.H., *et al.*, 2005: Comparing clouds and their seasonal variations in 10 Atmos. general circulation models with satellite measurements. *J. Geophys. Res.*, **110**, D15S02, doi:10.1029/2004JD005021.

Zhang, M.H., J.L. Lin, R.T. Cederwall, J.J. Yio, and S.C. Xie, 2001: Objective analysis of the ARM IOP data: method and sensitivity. *Mon. Weather Rev.*, **129**, 295–311.

Zhang, X. and J.E. Walsh, 2006: Toward a seasonally ice-covered Arctic Ocean: Scenarios from the IPCC AR4 model simulations. *J. Climate*, **19**, 1730–1747.

Zhang, X.-C., 2005: Spatial downscaling of global climate model output for site-specific assessment of crop production and soil erosion. *Agricultural and Forest Meteorology*, **135**, 215–229.

Zhang, Y.C., A.N. Huang, and X.S. Zhu, 2006: Parameterization of the thermal impacts of sub-grid orography on numerical modeling of the surface energy budget over East Asia. *Theoretical and Applied Climatology*, **86**, 201–214.

Zhu, J. and X.-Z. Liang, 2007: Regional climate model simulations of U.S. precipitation and surface air temperature during 1982–2002: Interannual variation. *J. Climate*, in press.

1